PERFORMANCE BASED SEISMIC DESIGN OF STEEL FRAME BUILDING USING ENERGY BALANCE CRITERION

A THESIS

Submitted in partial fulfilment of the requirements for the award of the degree of

DOCTOR OF PHILOSOPHY

in

EARTHQUAKE ENGINEERING

by

PRAHLAD PRASAD

DEPARTMENT OF EARTHQUAKE ENGINEERING
INDIAN INSTITUTE OF TECHNOLOGY ROORKEE
ROORKEE-247 667 (INDIA)

JUNE, 2010

INDIAN INSTITUTE OF TECHNOLOGY ROORKEE
ROORKEE

CANDIDATE'S DECLARATION

I hereby certify that the work which is being presented in the thesis entitled **PERFORMANCE BASED SEISMIC DESIGN OF STEEL FRAME BUILDING USING ENERGY BALANCE CRITERION** in partial fulfilment of the requirements for the award of the degree of Doctor of Philosophy and submitted in the Department of Earthquake Engineering, Indian Institute of Technology Roorkee, Roorkee is an authentic record of my own work carried out during a period from July 2003 to June 2010 under the supervision of Dr. Manish Shrikhande, Associate Professor, Department of Earthquake Engineering, Indian Institute of Technology Roorkee, Roorkee and Dr. Pankaj Agarwal, Associate Professor, Department of Earthquake Engineering, Indian Institute of Technology Roorkee, Roorkee.

The matter presented in this thesis has not been submitted by me for the award of any other degree of this or any other Institute.

Prasad

(PRAHLAD PRASAD)

This is to certify that the above statement made by the candidate is correct to the best of our knowledge.

Shrikhande

(Manish Shrikhande)
Supervisor

(Pankaj Agarwal)
Supervisor

Date: June 30, 2010

The Ph.D. Viva-Voce Examination of **Mr. Prahlad Prasad**, Research Scholar, has been held on .....

Signature of Supervisors

Signature of External Examiner

Dedicated
to
My Parents
in
Their Loving Memory

ABSTRACT

The most fundamental problem in carrying out Performance Based Seismic Design (PBSD) is to grasp the nature of seismic loading on building structures. In this context, energy concept has been considered as the principal loading for seismic input and evaluation of capacity. For the present study, energy balance criterion for performance based seismic design is presented. Such criterion is promising for development of cumulative damage indices under seismic loading.

The study presented herein, aims at investigation of performance based seismic design of steel building frameworks using energy based evaluation. Energy based seismic design is based on the principle of balancing the input seismic energy through the energy absorbing/dissipating capacity of the structure. Using the energy balance equation, the amount of various energy capacities is quantified. Initial input seismic energy is consumed by the structure as elastic strain energy; a part of input seismic energy is dissipated as viscous damping energy, while the structure is elastic. Kinetic energy of the mass, along with elastic strain energy constitutes vibration energy. At the end of earthquake ground motion, this energy gets dissipated as viscous energy. Identification and quantification of inelastic energy in severe earthquake ground motions has been subject of the recent state of art, since earthquake resistant design allows damages for larger ground motions, because meeting corresponding demand through strength is not economically viable as well as higher strength does not warranty the better performance at the same time larger earthquake is rare to occur during the design life of a structure. In the study, the issue of performance based seismic design is reassessed for multi-performance objectives. The existing performance objective formats are discretized events on the possible damage spectrum under varying earthquake ground motions in space and time. Recent trend of research in this regard accepts the potentiality of energy based design as a better approach for further formulation and development of design aids, which are close to damages even better than displacement approach. Thus, energy based seismic design is viewed as an effective design approach for assessment of performance evaluation and further formulation of PBSD for new design decisions. Nonlinear static pushover analyses are popular for performance evaluation using force/displacement controlled/modal procedures. The aim of nonlinear static pushover analysis is to estimate the displacement in spite of the earthquake load imposes reversal of stresses due to its simplicity in comparison to the nonlinear dynamic loading. Input seismic energy has been investigated using the present state of art. An

algorithm of energy based capacity curve has been developed using the conventional pushover analysis procedures through some example building frames evaluated under varying earthquake ground motions. Energy based capacity curve is the plot of energy along ordinate and displacement along abscissa. Sequence of hinge formations are directly recorded through the variation of energy slope of energy capacity curve. Simplification of energy based capacity curve results into better damage assessment. Plotting conventional base shear and the corresponding energy capacity curve on the same ordinate and displacement on abscissa shows a clear relationship corresponding to various performance levels. Such a capacity curve for a particular structure is an index for its use under varying earthquake ground motions for evaluating capacity in terms of energy. Knowing the actual displacement, energy capacity may be evaluated using the developed capacity curve. In developing energy based design approach and assessing the damage potential of structures, distribution of input seismic energy among its components: strain energy, kinetic energy, damping energy and hysteretic energy, are required. This study is focused on the accuracy for input seismic energy evaluation and further distribution of the energy among its components in order to formulate some pattern of damage pattern as required for the performance assessment, during performance based seismic design.

The present performance levels are disctretized and are used in such way that one performance level has no relation with the other, however all performance levels are inherently associated with the each other. During this study it has been demonstrated through energy based relations under varying demands are related with each other in a definite fashion, which provide the support that the damage spectrum are continuous, and not discretized. In this regard a relation between elastic strain energy and inelastic energy has been established using suitable assumptions.

Elastic strain energy and the inelastic strain energy (hysteretic energy) have close relationship, since they represent the internal configuration of structure. A simple algorithm in between these two energy parameters has been developed as the content of this research program. Hysteretic energy, which is the outcome of the energy dissipated through yielding, depends upon the size and number of loops. Cumulative hysteretic energy under reversal of stresses due to varying earthquake ground motions, which is the major task of performance based design evaluation that can be viewed through the elastic strain energy since hysteretic energy is closely related.

Further, damage indices available in the literature are reassessed and extended using the energy response parameters as obtained during this research program. Interpretation of

ACKNOWLEDGEMENTS

First and foremost I wish to express my sincere sense of gratitude to my supervisors; Dr. Manish Shrikhande and Dr Pankaj Agarwal, whose valuable guidance, encouragement, moral support and inspiration led me to completion of my research study. I really feel privileged to have worked under their guidance.

I wish to express my thanks to Dr. D.K. Paul, Ex H.O.D., Earthquake Engineering, Dean and Faculty Affairs, IIT, Roorkee, Dr. Yogendra Singh, Earthquake Engineering, Dr. Pradeep Bhargava, Civil Engineering for their moral support and encouragement throughout my study.

I take this opportunity to thank Dr Ashwani Kumar, Head Earthquake Engineering Prof., A.D. Pandey, Earthquake Engineering for their moral support and encouragement.

I wish to extend my heartiest thanks to Dr. M.L Sharma, Earthquake Engineering, IIT, Rookee for his tremendous encouragement.

I am thankful to Dr. H.R. Wason, Dr G. I. Prajapati, Dr. A. K. Mathur, Dr. N.C. Singhal, Dr. B.K. Maheshwari, Dr. S. Mukerjee, R. N. Dubey, all from Earthquake Engineering for their affection during tenure of my research study.

Mr. Ratnesh Kumar, Research Scholar, Earthquake Engineering, deserves my special thanks for healthy discussions and his moral support. Thanks to Mr. V.V. Surya Kumar Dadi, and Mr. J.S.R. Prasad, Vijay Khose, Putul Haldhar research scholars, earthquake engineering for their co operation.

My heartfelt thanks to all the staff of Earthquake Engineering for their gentle behavior throughout my stay. A few of them I would like to mention their names are Shri.Rajendra Kumar Giri, Shri Satyendra Pal, Librarian, Shri Rajendra Sudan, P.A. to Head, Shri Laxman Singh, Shri Jabar Singh, Shri Narendra Kumar Sharma, Shri Sita Ram Sharma.

I am extremely thankful to Shri Muthuraman, Chairman, BOG, N.I.T., Jamshedpur, Dr. Debashish Bhattacharya, ex. Director, N.I.T., Jamshedpur, Late Dr. A.K.Jaiswal, ex. H.O.D. Applied Mechanics, NIT, Jamshedpur for granting me the study leave for the Ph.D. under QIP scheme.

I would like to thank to Dr. Rajneesh Srivastawa, Director, National Institute of Technology, Dr. S.B.L. Saksena, Prof & Registrar, NIT, Jamshedpur, Dr. B.N. Prasad Dean Faculty and Planning, N.I.T., Jamshedpur, Dr. A.K.L. Srivastawa, Head Civil Engineering, NIT, Jamshedpur for their kind permission to complete my research program.

I also thank to faculty members at NIT Jamshedpur for their moral support during tenure of my study at IIT Roorkee. Few of them are: Prof. Shambhu Sharan, Dr. Y. P. Yadav, Dr. M. M. Prasad, Dr. S. K. Singh, Dr. R. K Prasad, Dr. Ram Vinay Sharma, Dr. A. N. Thakur, Dr. R. N. Mahanty, Dr. Ramayan Singh, Dr. H. L. Yadav, Prof Ajay Kr. Singh, Prof. Virendra Kumar, and Prof. Ashok Kumar.

I wish to express my sincere sense of gratitude to my mother in law for her blessing. I also wish to extend my indebtedness to Shri Druv Prasad (bhaiya) and late bhabhi for their moral support. Special thanks to Mr. Kedar Nath, Mrs. Vineeta Priyambada, Mr. Alok Shreedhar, Mrs Swarn Suchi, Mr. Brajesh Kumar, and Mrs. Suchi Sushmita all my family members for their good wishes.

For their tremendous patience, sacrifice and love, the author is greatly indebted to his wife Dr. **Chetna Sumedha**, Daughter, **Charu Vatsala**, and Son **Sai Ishwaram.**

The job has not been possible without the blessings of my parents whom I lost during the period of this study.

My understanding of this study is greatly influenced by books, and publications. My heartiest thanks to the authors of these precious, invaluable books and publications without them nothing was possible.

Last but not the least I wish to thank all my loved ones, who helped me directly, indirectly during the period of my research program.

Prahlad Prasad

CONTENTS

Certificate i

Abstract iii

Acknowledgements vii

Contents ix

List of Figures xv

List of Tables xxii

List of Flow Charts xxv

List of Notations xxvi

Abbreviations xxvii

CHAPTER 1. INTRODUCTION

1.1 General 1

1.2 Performance-Based Seismic Design 3

1.2.1 Nonlinear Pushover Analysis for Performance Based Seismic 4

1.2.1.1 Conventional Pushover Analysis 5

1.2.1 2 Load And Displacement Control Pushover Analysis 5

1.2.1.3 Modal Pushover Analysis 6

1.2.1.4 Energy Based Pushover Analysis 6

1.3 Energy Based Seismic Design vs. Performance Based Seismic 6

1.3.1 Damage Indices 10

1.4 Motivation for the Present Work 10

1.5 Gap identified for the Present Study 12

1.6 Objectives of the Present Work 13

1.7 Scope and Organization of Thesis/Thesis Outline 13

CHAPTER 2 LITERATURE REVIEW

2.1 Introduction 19

2.2 Performance Based Seismic Design 25

2.2.1 Performance Objectives 25
2.2.1.1 Selection of Performance Objectives 27
2.2.1.2 Performance Levels 27
2.2.1.3 Seismic Hazard Levels 27
2.2.4 Development Of Performance Based Seismic Design 28
2.2.5 Comprehensive Approach of Performance-Based Seismic Design 29
2.3 Literature Review on Steel Moment Resistant Frame 30
2.3.1 Seismic Performance of Steel Buildings during Past Earthquakes 31
2.3.1.1 Michoacan Earthquake 31
2.3.1.2 Northridge Earthquake 32
2.3.1.3 Kobe Earthquake 32
2.4 Nonlinear Static Pushover Analysis for Performance Based Seismic Design 32
2.4.1 Nonlinear Analysis of Building Frameworks 33
2.4.1.1 Load-Displacement Control Pushover Analysis 34
2.4.1.2 Modal Pushover Analysis 35
2.4.1.3 N2 Method of Pushover Analysis 35
2.5 Seismic Loads for Pushover Analysis 36
2.6 Push-over Analysis 37
2.7 Damage-Based Seismic Design of Structures 37
2.8 Energy Concept of Seismic Design 39
2.8.1 Design Principle using Seismic Input Energy 39
2.8.2 Energy Concept of Seismic Design 40
2.8.3 Estimation of Strain Energy and Inelastic Energy 41
2.8.4 Energy Paths 42
2.9 Estimation of Input Seismic Energy 43
2.9.1 Estimation of Input Seismic Energy for MDOF Building Frames 45
2.9.2 Energy Based Design 46

2.9.3 Energy Attributable to Damage 48

2.9.3.1 Flexural Members 49

2.9.3.2 Total Energy Input in Elastic-Perfectly Plastic Systems 49

2.10 Nonlinear Static Pushover Analysis Procedure: Energy Based Capacity Curve 51

2.11 Distribution of Input Seismic Energy 51

2.12 Normalized Hysteretic Energy 53

2.12.1 Number of Yield Excursion Cycles (NYEC) 53

2.13 Nonlinear Modeling for Basic Elements of Moment Resistant Frame 54

2.13.1 Mass Matrix 54

2.13.2 Damping Matrix 54

2.14 Nonlinear Modeling 55

2.15 Ductility 55

CHPATER 3. PROBLEM FORMULATIONS AND SOLUTION STRATEGIES

3.1 Introduction 57

3.2 Formulations of Performance Objectives for the Present Study 59

3.3 Problem Formulation 59

3.3.1 Objective Functions 59

3.3.2 Steel Building Frameworks used in the Present Study 60

3.3.3 Modeling for Linear and Nonlinear Analysis 60

3.4 Input Seismic Energy Evaluation 61

3.4.1 Energy Evaluation using Pseudo Velocity Spectra 61

3.4.2 Absolute Input Seismic Energy 62

3.4.3 Relative Input Seismic Energy 63

3.4.4 Input Seismic Energy for the Inelastic Structure using Energy Balance Equation 63

3.4.5 Input Seismic Energy for the Inelastic Structure using Energy Balance Equation for MDOF Systems 65

3.5 Energy Based Capacity Curve 66

3.6 Floor Spectra and Inter Story Drift Relation 67

3.6.1 Interpretation of Floor Spectra and Inter Story Drift Relation with Velocity and Absolute Acceleration 68

3.7 Distribution of Input Seismic Energy 69

3.7.1 Normalized Strain Energy 69

3.7.2 Normalized Kinetic Energy 69

3.7.3 Normalized Damping Energy 69

3.7.4 Normalized Hysteretic Energy 70

3.8 Energy Input in Elastic-Perfectly Plastic Systems 70

3.9 Normalized Hysteretic Energy 73

3.10 Relation between Hysteretic Energy (E_D) and Strain Energy (E_s) 75

3.11 Simplification of Park and Ang Damage Model 76

3.11.1 Elasto-Plastic Hysteretic Loop for Evaluation of Damage during Monotonic Inelastic Deformation 78

3.12 Number of Yield Excursion Cycles and PBSD 79

3.13 Analysis of Critical Sections 83

3.13.1 Characterization of the Flexural Behavior of Beam 83

3.14 PBSD vs. Limit States, Usage Ratios 85

CHAPTER 4. MODELING AND ANALYSIS

4.1 Introduction 91

4.2 Development of Performance Objectives 91

4.2.1 Design Spectra Parameters 92

4.2.1.1 Site parameters for 2%/50-year and 10%/50-year earthquakes 92

4. 2.1.2 Site parameters for 20%/50-year and 50%/50-year earthquakes 92

4.3 Evaluation of Seismic Response of Building Frames in the Present Study 95

4.3.1 Example Problem 1: Three Story Four Bay 2D Frame Building 95

4.3.2 Example Problem 2: Nine Story Five Bays 2D Frame Building 97

4.3.3 Example Problem 4.3: Fifteen Story 2D Three Bay Steel Frame Building 100

4.3.4 Example Problem 4.4: Twenty Story 2D Three Bay Steel Frame Building 103

4.3.5 Example Problem 4.5: Three Story Five Bays Three Story 3D Frame Building 106

4.4 Modeling of Steel Frame Building in Ram Perform 3D for the Present Study 107

4.5 Aim of Modeling 108

4.5.1 Beam Element 109

4.5.1.1 Plastic Hinges 109

4.5.1.2 FEMA Steel Beam 111

4.5.2 Columns 112

4.5.2.1 Components and Model Types of Columns 112

4.5.2.2 Hinges with P-M-M Interaction 113

4.5.2.3 Extension to P-M Interaction 113

4.6 Panel Zone Element 113

CHPATER 5. RESULT AND DISCUSSIONS

5.1 Result and Discussions 121

5.1.1 Input Seismic Energy Evaluation 122

5.1.2 Result Discussions for Input Seismic Energy Evaluation 122

5.2 Energy Capacity Curve 133

5.2.1 Result Discussions for Energy Capacity Curve 133

5.3 Floor Spectra vs.Inter story Drift 141

5.3.1 Result Discussions for Floor Spectra vs. Inter Story Drift 141

5.27	Energy distributions for table 5.17, 3 story 3D frame (El Centro: 0.2148g)	155
5.28	Energy distributions for table 5.17, 3 story 3D frame (El Centro: 2x0.2148g)	156
5.29	Energy distributions for table 5.18, 3 story 2D frame (Centro: 0.2052g)	156
5.30	Energy distributions for table 5.18, 3 story 2D frame (El Centro: 2x0.2052g)	157
5.31	Energy distributions for table 5.18, 3 story 2D frame (El Centro: 0.2148g)	157
5.32	Energy distributions for table 5.18, 3 story 2D frame (El Centro: 2x0.2148g	158
5.33	Energy distributions for table 5.19, 9 story 2D frame (Northridge: 0.5165g)	158
5.34	Energy distributions for table 5.19, 9 story 2D frame (Northridge:2x 0.5165g)	159
5.35	Energy distributions for table 5.19, 9 story 2D frame (Northridge: 0.4158g)	159
5.36	Energy distributions for table 5.19, 9 story 2D frame (Northridge:2x0.4158g)	160
5.37	Energy distributions for table 5.19, 9 story 2D frame (El Centro 0.2148g)	160
5.38	Energy distributions for table 5.19, 9 story 2D frame (El Centro: 2x 0.2148g)	161
5.39	Energy distributions for table 5.19, 9 story 2D frame (El Centro: 0.2052g)	161
5.40	Energy distributions for table 5.19, 9 story 2D frame (El Centro: 2x0.2052g)	162
5.41	Energy distributions for table 5.20, 15 story 2D frame (Northridge: 0.5165g)	162
5.42	Energy distributions for table 5.20, 15 story 2D frame (Northridge: 0.4158g)	163
5.43	Energy distributions for table 5.20, 15 story 2D frame (El Centro: 2x0.2148g)	163

4.3.1 Example Problem 1: Three Story Four Bay 2D Frame Building 95

4.3.2 Example Problem 2: Nine Story Five Bays 2D Frame Building 97

4.3.3 Example Problem 4.3: Fifteen Story 2D Three Bay Steel Frame Building 100

4.3.4 Example Problem 4.4: Twenty Story 2D Three Bay Steel Frame Building 103

4.3.5 Example Problem 4.5: Three Story Five Bays Three Story 3D Frame Building 106

4.4 Modeling of Steel Frame Building in Ram Perform 3D for the Present Study 107

4.5 Aim of Modeling 108

4.5.1 Beam Element 109

4.5.1.1 Plastic Hinges 109

4.5.1.2 FEMA Steel Beam 111

4.5.2 Columns 112

4.5.2.1 Components and Model Types of Columns 112

4.5.2.2 Hinges with P-M-M Interaction 113

4.5.2.3 Extension to P-M Interaction 113

4.6 Panel Zone Element 113

CHPATER 5. RESULT AND DISCUSSIONS

5.1 Result and Discussions 121

5.1.1 Input Seismic Energy Evaluation 122

5.1.2 Result Discussions for Input Seismic Energy Evaluation 122

5.2 Energy Capacity Curve 133

5.2.1 Result Discussions for Energy Capacity Curve 133

5.3 Floor Spectra vs.Inter story Drift 141

5.3.1 Result Discussions for Floor Spectra vs. Inter Story Drift 141

5.4 Distribution of Input Seismic Energy 146

5.4.1 Result Discussions 147

5.5 Normalized Hysteretic Energy 168

5.5.1 Result Discussions 168

5.6 Hysteretic Energy (E_D) and Strain Energy (E_s) 169

5.6.1 Result Discussions for Hysteretic Energy 174

5.7 Simplified Park and Ang Damage Model 174

5.7.1 Simplification for Damage Index for Monotonic Displacement 175

5.7.2 Result and Discussions 175

5.8 Number of Yield Excursion Cycles (NYEC) and PBSD 176

5.8.1 Result Discussions 176

5.9 Nonlinear Analysis of Critical Sections 189

5.9.1 Result Discussions 189

5.10 Usage Ratio 194

5.10.1 Usage Ration at Component Levels 194

5.10.2 Usage Ration at Global Level 194

5.10.3 Result Discussion for the Usage Ratio 195

CHAPTER 6. CONCLUSIONS AND RECOMMENDATIONS

6.1 Summary and Conclusions 201

6.2 Recommendations for Future Work 205

Bibliography 207-208

References 209-213

Publications

LIST OF FIGURES

Figure No.	Title	Page No.
2.01	Typical moment resistant frames under lateral loading	30
2.02	Force deformation relations for elasto-plasto components	41
2.03	Plot of energy vs. time for under monotonic loading	42
2.04	Response analysis of rigid and flexible body behavior under earthquake loadings	44
3.01	Absolute and relative displacement relationship	63
3.02	Lee and Goel's energy balance concept (2001)	64
3.03	Energy input in elasto-plastic behavior of a steel frame	71
3.04	Hysteretic loop with strain hardening	74
3.05	Hysteretic loop for elasto-plastic system	75
3.06	Force deformation relations for monotonic and dynamic loading	77
3.07	Hysteretic loops for damage evaluation under monotonic deformation	78
3.08	Accelerogram of Northridge E-S (0.5165g) with SF =5	8 1
3.09	Time history plot of external columns on ground floor of example problem 4.2	81
3.10	Hysteretic loops for external columns on ground floor of example problem 4.2	82
3.11	Cross section behavior of a steel member	83
3.12	Inelastic behavior of cross section behavior of steel member	84
4.01	Earthquake acceleration response spectrum	94
4.02	Diagram of three story four bay steel building 2D frame (Example problem 4.1)	97
4.03	Diagram of nine story three bay 2D steel building frame (Example problem 4.2)	99
4.04	Diagram of fifteen story four bay steel building frame (Example problem 4.3)	102

4.05	Diagram of twenty story four bay steel building frame (Example problem 4.4)	105
4.06	Lump plastic modeling of beam element	109
4.07	Action deformation relationships of beam plastic hinge	110
4.08	Perform chord rotation model of beam element	110
4.09	Implementation of chord rotation model of beam element	111
4.10	Lumped modeling of column	112
4.11	Panel zone elements	113
4.12	Accelerogram of Northridge, 14145 E-W (0.5165g)	114
4.13	Accelerogram of Northridge, N-S (0.4158g)	115
4.14	Accelerogram of El Centro 1940, E-W (0.3265g)	115
4.15	Accelerogram of El Centro 1940, E-W (0.2148g)	116
4.16	Accelerogram of El Centro 1940, N-S (0.3129g)	116
4.17	Accelerogram of El Centro 1940, U-D (0.2052g)	117
4.18	Response spectra of Northridge 14145 E-W (0.5165g))	117
4.19	Response spectra of Northridge N-S (0.4158g)	118
4.20	Response spectra of Northridge U-D (0.3265g)	118
4.21	Response spectra of El Centro E-W (0.2148g)	119
4.22	Response spectra of Northridge El Centro N-S (0.3129g)	119
4.23	Response spectra of Northridge El Centro U-D (0.2052g)	120
4.24	Spectral acceleration components to OP, IO, LS and CP	120
5.01	Pseudo velocity spectra of Northridge, 14145 Mulholland, E-W (0.5165g)	127
5.02	Pseudo velocity spectra of Northridge, 14145 Mulholland, N-S (0.4158g)	127
5.03	Pseudo velocity spectra of Northridge, 14145 Mulholland; Up-Down (0.3265g)	128
5.04	Pseudo velocity spectra for El Centro 1940, E-W (Peak acceleration: 0.2148g)	128
5.05	Pseudo velocity spectra of El Centro 1940, Up-D (PGA: 0.2052g)	129
5.06	Base shear/Energy vs. Displacement of three story 2D frame	134
5.07	Base shear/Energy vs. Displacement of three story 3D frame	136

5.08	Base shear/Energy vs. Displacement of nine story 2D frame	136
5.09	Base shear/Energy vs. Displacement of fifteen story 2D frame	138
5.10	Base shear vs. Displacement of twenty story 2D frame	138
5.11	Base Energy vs. Displacement of twenty story 2D frame	140
5.12	Floor spectra at 3rd floor of three story 3D frame for Northridge E-W (3x0.5165g)	140
5.13	Floor spectra at 2nd floor of 3D, three story frame for Northridge E-W (3x0.5165g)	143
5.14	Floor spectra at 3rd floor of 3D, three story frame for Northridge E-W (3x0.5165g)	143
5.15	Floor spectra vs. along building height of three story 2D frame	144
5.16	Relative velocities vs. along building height of three story 3D frame	144
5.17	Floor spectra/drift vs. along building height of three story 3D frame	145
5.18	Hysteretic energy per unit input seismic energy Input seismic energy.	145
5.19	% Strain, kinetic and hysteretic energy vs. Input seismic energy	148
5.20	Energy dissipated in beams along the building height of nine story2D frame	152
5.21	Energy dissipation in columns of nine story frame for input seismic energy =135800kNm	152
5.22	Distribution of energy among external and internal beams of nine story frame for input seismic energy =14580 kNm	153
5.23	Distribution of energy among external and internal beams a of nine story frame for input seismic energy =14580 kNm	153
5.24	Energy distributions for table 5.17, 3 story 3D frame (Northridge: 0.5165g)	154
5.25	Energy distributions for table 5.17, 3 story 3D frame (Northridge: 0.4158g)	154
5.26	Energy distributions for table 5.17, 3 story 3D frame (Northridge: 2x 0.4158g)	155

5.27	Energy distributions for table 5.17, 3 story 3D frame (El Centro: 0.2148g)	155
5.28	Energy distributions for table 5.17, 3 story 3D frame (El Centro: 2x0.2148g)	156
5.29	Energy distributions for table 5.18, 3 story 2D frame (Centro: 0.2052g)	156
5.30	Energy distributions for table 5.18, 3 story 2D frame (El Centro: 2x0.2052g)	157
5.31	Energy distributions for table 5.18, 3 story 2D frame (El Centro: 0.2148g)	157
5.32	Energy distributions for table 5.18, 3 story 2D frame (El Centro: 2x0.2148g	158
5.33	Energy distributions for table 5.19, 9 story 2D frame (Northridge: 0.5165g)	158
5.34	Energy distributions for table 5.19, 9 story 2D frame (Northridge:2x 0.5165g)	159
5.35	Energy distributions for table 5.19, 9 story 2D frame (Northridge: 0.4158g)	159
5.36	Energy distributions for table 5.19, 9 story 2D frame (Northridge:2x0.4158g)	160
5.37	Energy distributions for table 5.19, 9 story 2D frame (El Centro 0.2148g)	160
5.38	Energy distributions for table 5.19, 9 story 2D frame (El Centro: 2x 0.2148g)	161
5.39	Energy distributions for table 5.19, 9 story 2D frame (El Centro: 0.2052g)	161
5.40	Energy distributions for table 5.19, 9 story 2D frame (El Centro: 2x0.2052g)	162
5.41	Energy distributions for table 5.20, 15 story 2D frame (Northridge: 0.5165g)	162
5.42	Energy distributions for table 5.20, 15 story 2D frame (Northridge: 0.4158g)	163
5.43	Energy distributions for table 5.20, 15 story 2D frame (El Centro: 2x0.2148g)	163

5.44	Energy distributions for table 5.20, 15 story 2D frame (El Centro: 0.2148g)	164
5.45	Energy distributions for table 5.20, 15 story 2D frame (El Centro: 0.2052g)	164
5.46	Energy distributions for table 5.20, 15 story 2D frame (El Centro:2x 0.2052g)	165
5.47	Energy distributions for table 5.21, 20 story 2D frame.(Northridge 0.5165g	165
5.48	Energy distributions for table 5.21, 20 story 2D frame (Northridge:2x0.5165g	166
5.49	Energy distributions for table 5.21, 20 story 2D frame (Northridge 0.4158g)	166
5.50	Energy distributions for table 5.21, 20 story 2D frame (ElCentro0.2148g)	167
5.51	Energy distributions for table 5.21, 20 story 2D frame(El Centro 0.2052g)	167
5.52	Theoretical and experimental damage ratio vs. cumulative ductility	173
5.53	Theoretical and experimental damage ratio vs. cumulative ductility	173
5.54	Accelerogram of Northridge E-W (0.5165g) with scale factor 5	178
5.55	Time history of beam one on nine story 2D frame	178
5.56	Time history of beam two on ground floor of nine story 2D frame	179
5.57	Hysteretic loop of beam two on ground floor of nine story 2D	179
5.58	Time history of beam three on ground floor of nine story 2D frame	180
5.59	Hysteretic loop of third beam on ground floor of nine story 2D frame	180
5.60	Time history of beam fourth on ground floor of nine story 2D frame	181
5.61	Hysteretic loop of beam fourth on ground floor of nine story 2D frame	181

5.62	Time history of fifth beam on ground floor of nine story 2D frame	182
5.63	Hysteretic loop of fifth beam on ground floor of nine story 2D frame	182
5.64	Time history of 1st column on ground floor of nine story 2D frame	183
5.65	Hysteretic loop of 1st column on ground floor of nine story 2D frame	183
5.66	Time history of 2nd column on ground floor of nine story 2D frame	184
5.67	Hysteretic loop of 2nd column on ground floor of nine story 2D frame	184
5.68	Time history of 3rd column on ground floor of nine story 2D frame	185
5.69	Hysteretic loop of 3rd column on ground floor of nine story 2D frame	185
5.70	Time history of 4th column on ground floor of nine story 2D frame.	186
5.71	Hysteretic loop of 4th column on ground floor of nine story 2D frame	186
5.72	Time history of 5th column on ground floor of nine story 2D frame	187
5.73	Hysteretic loop of 5th column on ground floor of nine story 2D frame	187
5.74	Time history of 6th column on ground floor of nine story 2D	188
5.75	Hysteretic loop of 6th column on ground floor of nine story 2D frame	188
5.76	Normal stresses for beam on first floor of nine story frame.	190
5.77	Crack section stress axial stress for beam on first floor of nine story frame	190
5.78	Axial stress for external column on first floor of nine story frame$W_{360x551}$, Maximum moment =4795 kNm, Minimum M =106.5 kNm Axial force = 8528 kN	191
5.79	Normal stress for external column on first floor of nine story frame $W_{360x551}$, Maximum moment =4795 kNm, Minimum Moment =106.5 kNm Axial force = 8528 kN	191

5.80	Normal stress for external column on first floor of nine story frame $W_{360x551}$, Maximum moment =4795 kNm, Minimum Moment =106.5 kNm Axial force = 8528 kN	192
5.81	Cracked section - stress for internal column on first floor of nine story frame, W360x744, Maximum moment =4795, Minimum M =106.5 kNm, Axial force = 3500 kN	192
5.82	Normal stress distributions along depth of the column section $W_{360x551}$ of three story 3D frame	193
5.83	Normal stress distributions along depth of the beam section $W_{590x140}$ of three story 3D frame	193
5.84	Usage ratios for 3story 3D frame under Northridge E-W (0.5165g)	196
5.85	Usage ratios for 3story 3D frame under Northridge E-W	196
5.86	Usage ratios for 3story 3D frame under Northridge N-S (0.4158g)	197
5.87	Usage ratios for 3story 3D frame under Northridge N-S (2x0.4158g)	197
5.88	Usage ratios for 3story 3D frame under El Centro E-W (0.2148g)	198
5.89	Usage ratios for 3story 3D frame under El Centro Up-Down (0.2052g)	198
5.90	Usage ratios for 3story 3D frame under El Centro Up-Down (2x0.2052g)	199

LIST OF TABLES

Table No.	Title	Page No.
1.01	Single performance level design	15
1.02	SEAOC VISION 2000, Recommended performance objectives (After OES, 1995)	15
1 .03	FEMA 273 Performance objectives (After ATC, 19997	16
1.04	Building performance levels (FEMA-273,1997)	16
1.05	SEAOC VISION 2000 general damage descriptions for new building designs (After OES, 1995)	17
4.01	Performance level site parameters	94
4.02	Base shear for 3 story 2D frame for performance levels	96
4.03	Base shear distribution for 3 story 2D frame	96
4.04	Details of beams and columns used in the frame	97
4.05	Base shear for nine story 2D frame for performance levels	98
4.06	Base shear distribution for nine story 2D frame.	98
4.07	Details of beam and columns of nine story 2D frame	98
4.08	Base shear distribution for pushover loading for fifteen story 2D frame	100
4.09	Pushover loading of fifteen story steel frames for performance levels	101
4.10	Beam and column details for fifteen story 2D frame	101
4.11	Pushover loading of twenty story frame for performance levels	103
4.12	Pushover load distribution for twenty story frames	104
4.13	Beam and Column details for twenty story frames	106
4.14	Base shear for three story 3D frame for performance levels	107
4.15	Base shear distribution for pushover loading for three story 3D	107
4.16	Accelerograms used in the analyses	114

5.01	Details of input seismic energy under varying ground motions for three story 2D steel building frame (Example problem 4.3.1)	124
5.02	Details of input seismic energy under varying ground motions for 2D, nine story steel building frame (Example problem 4.3.2).	125
5.03	Details of input seismic energy under varying ground motions for 2D, fifteen story steel building frame (Example problem 4.3.3).	125
5.04	Details of input seismic energy under varying ground motions for 2D, twenty story steel building frame (Example problem 4.3.4)	126
5.05	Details of input seismic energy under varying ground motions for 3D, three story steel building frame (Example problem 4.3.5).	126
5.06	Energy ductility and energy factor for three story 2D and three story 3D steel building frames.	130
5.07	Energy ductility, and energy factor for nine story 2D and fifteen story 2D steel building frames	131
5.08	Energy ductility and energy factor for twenty story 2D steel building frames	132
5.09	Base shear/Energy curve of three story 2D steel building framework.	134
5.10	Base shear/Energy curve of three story 3D steel building framework	135
5.11	Base shear/Energy curve of nine story 2D steel building framework	137
5.12	Base shear/Energy curve of fifteen story 2D steel building framework.	137
5.13	Base shear/Energy curve of twenty story 2D steel building framework.	139
5.14	Input seismic energy, floor spectra and drift for three story 3D framework	142
5.15	Floor spectra. vs. inter story drift for three story 2D frameworks	142
5.16	Energy distribution for three story 2D steel framework	148
5.17	Distribution of input seismic energy for 3D three story framework	149

5.18	Distribution of input seismic energy for three story 2D framework	149
5.19	Distribution of input seismic energy for nine story framework	149
5.20	Distribution of input seismic energy for fifteen story framework.	150
5.21	Distribution of input seismic energy for twenty story framework	150
5.22	Energy dissipated among beams/ columns of nine story 2D framework	151
5.23	Energy dissipated among beams /columns of nine story 2D framework.	151
5.24	Energy distribution (%) for three story 3D building framework	169
5.25	Normalized hysteretic energy for three story 2D framework	169
5.26	Normalized hysteretic energy for three story 3D framework	169
5.27	Hysteretic energy of the successive hysteretic loop	170
5.28	Damage index	170
5.29	Hysteretic energy for elasto-plasto loop for successive displacement ductility	171
5.30	Theoretical and experimental damage ratio for three story 3D framework under Northridge E-W (0.6g)	172
5.31	Theoretical and experimental damage ratio for three story 3D framework under El Centro E-W (0.6g).	172
5.32	Hysteretic energy, number of loops, NYEC, and cumulative ductility for critical member of three story 3D framework	177
5.33	Hysteretic energy, number of loops, NYEC, and cumulative ductility for nine story framework	189

LIST OF FLOW CHARTS

Flow Chart No	Title	Page No
3.01	SEAOC Vision 2000 methodologies for performance based seismic design (After OES, 1995)	86
3.02	Proposed methodologies for performance-based seismic design	87
3.03	Nonlinear static pushover analysis procedures	88
3.04	Proposed energy balanced criterion for input seismic energy distribution	89

NOTATIONS

W	Seismic weight of the building
μ	Displacement ductility
Γ	*Modal participation*
γ	Energy correction factor
g	Acceleration due to gravity
I	Importance factor
R	Response Reduction Factor for over strength and ductility
S_d	Spectral Displacement
S_{dp}	Spectral displacement corresponding to performance point
Spv	Spectral velocity
S_{du}	Spectral displacement corresponding to ultimate roof displacement
S_{dy}	Spectral displacement corresponding to yield point
T_e	Effective fundamental period of the building
T_0	Time period corresponding to performance levels
T_s	Characteristic period of the response spectrum
V_y	Lateral yield strength of the building
α	Strength coefficient
η	Damage coefficient
k	Stiffness
k_{eq}	Equivalent stiffness
δ_y	Yield displacement
σ_y	Yield stress
N	Number of yield excursion cycles

ABBREVIATIONS

FEMA	Federal Emergency Management Agency
NEHRP	National Earthquake Hazard Reduction Program
EQRD	Earthquake Resistant Design
SBWC	Strong Beam and Weak Column
SCWB	Strong Column and Weak Beam
SAC	SEAOC, ATC and CUREE
SEAOC	Structural Engineers Association of California
ATC	Applied Technology Council
CUREE	California Universities for Research in Earthquake Engineering
PBE	Performance Based Engineering
PBEE	Performance Based Earthquake Engineering
PBSE	Performance Based Seismic Engineering
PBSD	Performance Based Seismic Design
PL	Performance Levels
PO	Performance Objectives
BSO	Basic Safety Objectives
OP	Operational
IO	Immediate Occupancy
LS	Life Safety
CP	Collapse Prevention
NSPA	Nonlinear Static Pushover Analysis
NDA	Nonlinear Dynamic Analysis
CSI's	Computer Structures Inc.
ETABS	Extended Thee Dimensional Building Systems
THA	Time History Analysis
UBC	Uniform Building Code
HAZUS	Hazard Analysis Zonal United States
IDRS	Inelastic Design Response Spectra
OES	California Office of Emergency Service
AISC	American Institute of Steel Construction

FNA	Fast Nonlinear Analysis
SRSS	Square Root of Sum of Squares
MPA	Modal Pushover Analysis
PGA	Peak Ground Acceleration.
OMRF	Ordinary Moment Resisting Frames
SMRF	Special moment resistant frame
SMRF	Special Moment Resisting Frames
NYEC	Number of Yield Excursions Cycles
WSMF	Welded Steel Moment Frame
SDOF	Single Degree of Freedom
MDOF	Multi Degree of Freedom
E_I	Input seismic energy
E_S	Elastic strain energy
E_K	Kinetic energy
E_D	Energy due to viscous damping
$E_{H\xi}$	Hysteretic energy
%SE	% Strain energy
%KE	% kinetic energy
%HE	% Hysteretic energy
SF	Scale factor

Chapter 1

INTRODUCTION

1.1 General

The principle of performance based seismic design (PBSD) is to meet the assigned performance objectives to a structure during its design life under earthquake loadings. Performance objectives are the design attributes of PBSD, which comprise performance levels to the corresponding levels of seismic hazard. The task of PBSD is an iterative re-analysis/re-design, in which an initial design is modified repeatedly to meet the performance objectives of the structure. Any development towards demand evaluation and the analysis procedures in order to reduce the number of iterations for achieving performance objectives of a structure is the issue of further research. Three major documents [1, 2, and 3] are credited with laying the foundation for performance-based design concepts. These documents attempted to develop procedures that can be used as seismic provisions in building codes. The controlling parameters of PBSD are dynamic response of the structure with permissible limits of damages. On the other hand, nonlinear static analysis is required to trace out the seismic response of structures during severe earthquake ground motions. Development of nonlinear static pushover as PBSD tool has been widely recognized [4] over the existing methodologies in the literature.

Building construction materials have greater role for accomplishing the desired goals of PBSD. In this context, building structures with steel moment resisting frames as the primary load resisting system are considered to be the safest type of construction for earthquake resistance because of its capacity to sustain large plastic deformations [5]. However, structural damage and brittle failure of beam-column joints during Northridge and Kobe earthquakes highlighted the deficiencies of the code compliant SMRF building structure.

Multi-disciplinary characteristics of earthquake resistant design in terms of PBSD through exciting development as has been the issue of innovative seismic design [6]. The design approach of PBSD in its basic characteristics is an iterative procedure, in which the initial design is modified through the results of structural analysis to meet the performance objectives. Pushover analysis [3] is widely adopted as the primary tool for nonlinear analysis because of its simplicity compared with the dynamic procedures. The pushover analysis accounts for both geometric and material nonlinearity at multiple loading levels,

involve tremendous computational effort. Therefore, building components for best possible design using pushover analysis to consider the effect of seismic loading is extremely computationally intensive [7]. An efficient algorithm is yet to be found to incorporate pushover analysis together for better performance based seismic design using its analysis results. The N2 method towards simplification and visualization of the building frame behavior through nonlinear static pushover analysis using the relation of assumed displacement shape and lateral force has been appreciable for performance based seismic evaluation [4]. Identification and quantification of damages under varying earthquakes still remain the area of promising research for development of design algorithm using nonlinear response control assessment. A wealth of literature [8, 9, 10, 11, 12, 13, 14, and 15] is available on formulation of energy based concepts, which are further capable for developing damage indices and their relations with performance based seismic design in due course under varying seismic loading. Input seismic energy (demand) and corresponding demand evaluation for EQRD has been in use for long [12]. The energy concept of seismic design is based on the premise that the energy demand during an earthquake (or an ensemble of earthquakes) can be predicted and that the energy supply of a structural element (or a structural system) can be established. A satisfactory design implies that the energy supply should be larger than the energy demand. Use of energy based seismic design for PBSD is recently recognized [13]. Seismic designs in the energy format are useful for decision making for the use of the external devices to take care of the excess energy to the capacity of the structure in terms of energy. The external devices are active or passive dampers, or the control of input seismic energy through base isolation [13]. Controlling behavior with the structural system relies much more on the energy dissipating through yielding mechanism of the selected structural components [16]. However, the motivation for its application for design improvement has been recently recognized. Probably, the reason behind this is the development of computational tools along with tremendous growth of high-rise building structures in the recent past. [7, and 13].

The aim of the present research study is to focus on performance based seismic design using energy balance criterion. The initial phase of this study introduces the conventional procedures of PBSD with emphasis on the nonlinear static pushover analysis. Formulation of energy based capacity curve using the nonlinear static pushover analysis data (base shear vs. displacement) in order to quantify capacity in terms of energy is the preliminary task of the study. In order to apply base shear corresponding to performance levels and seismic hazards for various performance objectives, a design spectrum (chapter

4) using the clauses of FEMA 273, 1997 [3] has been prepared. Base shear corresponding to performance levels have been estimated in order to apply these loads to the steel building frames as lateral loads in sequence. Capacity curve in energy format has been developed to quantify damage due to increasing sequential hinges. Second phase of the present study were to focus on the energy based seismic evaluation. Nonlinear static pushover and nonlinear dynamic analyses requires modeling of structural components for the desired behavior. RAM Perform 3D [17] is mainly used for nonlinear modeling and the corresponding analysis under a set of varying accelerograms. This particular software automates the nonlinear analysis results for performance based design validation. Various developed elements available in the software are capable to trace out the behavior as desired for performance evaluation and check for the assigned boundary conditions of the modeled building structures [17].

1.2 Performance-Based Seismic Design

The aim of the performance-based seismic design is to design a structure so that it will perform in the specified manner to meet the performance objectives [Table1.2]. Performance is the acceptable levels of damages; seismic hazard is the earthquake for which the damage is likely. The performance objective is the combination of performance levels and seismic hazards. A building performance is a combination of structural and nonstructural components, and is expressed in terms of building performance levels [Table 1.4]. The building performance levels are discrete damage states [Tables 1.2, 1.3] selected from among the infinite spectrum of possible damage states that buildings could experience as a result for the earthquake response. Literature available prescribes a number of building performance levels, such as Operational (OP), Immediate Occupancy (IO), Life Safety (LS), and Collapse Prevention (CP) [1, 3]. A building at operational level suffers no structural and non-structural damages, resulting into the normal occupancy. At immediate occupancy, structural damage is nil with minor no-structural damage, so that the building may be occupied immediately just after the earthquake, for life safety, there is significant damages to structural and non-structural components with low risk of life. The intensive repair is required and may be economically not viable. At collapse prevention, non-structural damage is complete with the possibility of life threat due to non-structural damages. Structural damage is significant and suffered significant loss of lateral strength and stiffness with some permanent lateral deformation. However, gravity load carrying capacity still remains to carry the gravity load demands.

The major task during performance based seismic design is identification and quantification of damages since a structure is intentionally designed to be in the inelastic region during large earthquake. Nonlinear analysis is essential for assessment of possible damages during earthquake loading. During the nonlinear pushover analysis and nonlinear time history analysis, various performance levels are assigned by the drift and inter story drift indices which are indicative of damages in quantitative terms. Damage is directly expressed in energy parameters, therefore, assessment of performance objectives in terms of damage indices are the content of many literatures [9]. Energy based design criteria are close to PBSD as perceived in the recent past with the application of capacity design [13]. Normalization of energy components in order to develop damage indices for design aid is addressed [14]. Number of loops and their corresponding yield excursion cycles are important characteristics while a structural components undergo large plastic deformation under the reversal of stresses, such parameters are attractive response parameters as may be used for performance based design attributes [18]. Since the existing performance levels are the discrete damages on the possible continuous damage spectrum under varying earthquake ground motions, use of relation among energy parameters (e.g., elastic strain energy & hysteretic energy) is subjected to provide some close relations of performance levels.

1.2.1 Nonlinear Static Pushover Analysis for Performance Based Seismic Design

Since the inception of performance based seismic design, efforts are continued to provide better analytical tool in order to make out the design solution simple to simpler through innovative approach using nonlinear pushover analysis [3, 7, and 19]. Four analytical analysis procedures are in literature: linear static, linear dynamic, nonlinear static and nonlinear dynamic [3]. However, PBSD requires nonlinear analysis, due to the reason that some components are expected to deform beyond linear elastic behavior, when subjected to strong ground motions. Nonlinear dynamic analysis needs expertise, more time for analysis and skill for interpretation of results. Therefore, nonlinear static pushover analysis (NSPA) has been recognized as workable analysis procedure in order to make a sense of understanding of nonlinear behavior. However, NSPA results are not suitable for those structures, which have higher modes are significant [19].

1.2.1.1 Conventional Pushover Analysis

Conventional pushover analysis works on the principle of monotonically increasing lateral loads along with constant gravity loading to a framework until a control node sways to a predefined target lateral displacement, or to a target base shear, which corresponds to a performance level. The target displacement is the maximum roof displacement likely to be experienced during the design earthquake. Different performance levels have different target displacements, which represent different seismic intensities [20]. Structural deformation and internal forces are monitored continuously as the model is displaced laterally. The method allows tracing the sequence of yielding and failure at the member and system levels, and can determine the inelastic drift distribution along the height of the building and collapse mechanism of the structure. The strength and ductility demands at the target displacement (or target base shear) are used to check the acceptance of the structural design. The base shear versus roof displacement relationship, referred to as a capacity curve, is the fundamental product of a pushover analysis.

The agreed lateral inertia load pattern for pushover analysis is based on the concept that the response of the structure is controlled by a single mode, and that the shape of this mode remains constant throughout the time response. This is a kind of limitation of SDOF assumption consideration of MDOF's system. Therefore, the low-rise to mid-rise buildings are being analyzed using the conventional pushover analysis.

The static pushover was presented first by Saiidi and Sozen [21] and further the methodology was used for seismic structural analysis by various researchers Gupta and Krawinkler [19], and others. The method is also described and recommended as a tool of design assessment assigned by National Hazard Reduction Program "NEHRP" guideline for the seismic rehabilitation of existing buildings. Further, the technique is accepted by the Structural Engineers Association of California "SEAOC". Now, the method is a popular tool for the performance check for the various assignments.

1.2.1.2 Load and Displacement Control Pushover Analysis

Most literature defines performance levels by displacement standards. For example FEMA-273 [3] prescribes the roof drift having values of 0.7%, 2.5%, and 5% of the building height is at IO, LS, and CP respectively. A displacement control pushover procedure is thus required to evaluate the seismic demands at the corresponding displacement levels. To evaluate the seismic demand at a specified earthquake loading level, a load control pushover analysis procedure is necessary. For a displacement-control procedure, pushover analysis is

terminated when the maximum specified target displacement is reached at the target node (e.g., the roof), while for a load-control procedure, pushover analysis is terminated when the maximum specified design base shear is reached. In fact, a feasible design that is found using a load-control pushover analysis procedure is also feasible if it is verified by a displacement-control procedure.

In this study, both pushover analysis procedures are adopted for evaluating earthquake demands and displacement-control pushover analysis is conducted to evaluate the structural plastic states and ductility demands for the final design solution corresponding to the specified displacement standards. Energy based pushover analysis procedure is more compatible for performance based seismic design, since energy distribution directly reflect the damage to the corresponding displacement.

1.2.1.3 Nonlinear for Two Dimension (N2) Method of Pushover Analysis

It combines pushover analysis of a multi degree of freedom (MDOF) model with the response spectrum analysis of an equivalent single degree of freedom (SDOF) system [4].

1.2.1.4 Energy Based Pushover Analysis

Energy based pushover analysis procedure recently developed [11] addresses energy as lateral loading and displacement as response. The capacity curve is obtained from the base shear and displacement form the conventional pushover analysis. Further taking the product of base shear with the corresponding lateral displacements at various levels of the building height, energy is obtained. Plot of the energy with the displacement is capacity curve in between energy and displacement.

On the same axes, demand curve in terms of energy and displacement is plotted. Intersection of the demand curve and capacity curve provides performance point. This performance point has been found very near to the displacement from the time history plot [11]. A critical review for the energy based pushover analysis has been presented in the current study by the author.

1.3 Energy Based Seismic Design vs. Performance Based Seismic Design

The most fundamental problem in carrying out performance based seismic design is to grasp the nature of seismic input on building structures. Energy input has been considered as the principal loading effect for seismic loading on building. Despite high irregularity of ground motions, the energy input into a building is a stable quantity [8]. On the other hand, the

energy absorbed by a structure can be predicted by tracing its restoring force-deformation characteristics. Consequently by equating the energy input induced by an earthquake and the energy absorption of a structure, a quantitative prediction of deformation and damage to a structure is obtained. Identification of the deformation-damage relationship is the major task of PBSD. The total amount of input energy by an earthquake is balanced by the elastic strain energy, kinetic energy, energy dissipated due to damping and energy dissipated through yielding. The law of dynamic equilibrium also exists in between the input seismic energy and the capacity of structure in energy parameters under earthquake loadings. This relation is popularly expressed through energy balance equation. With the concept that earthquake effect is through imposing demand on a structure in terms of energy, Huosner [12] used effectively the energy spectra in terms of pseudo velocity for estimating the input seismic energy to a structure, with the expectation that the structure response is linear. Further, Housner [12] emphasizes the use of limit state for the effective application of energy concept for the earthquake resistant design. Blume [22] used the concept of reserved energy for seismic resistant design and evaluation with the perception that capacity of structures in terms of reserve energy as an economical method of seismic resistant analysis and design. Later on, reserve energy concept [22] for analysis of structures at various levels has been used in the literature. For the period 1960-1970, the concept of energy method is addressed from time to time for design evaluation. A landmark in the history of seismic resistant design is recognized from the date of emergence of capacity design and its further application with the limit state design became the real start of PBSD [23]. Since the perception of the performance-based seismic design, the method of energy concept always has been in discussion for its effective use for resolving critical issues of PBSD. Akiyama [8] addressed the method of energy as an effective tool with the assurance that energy concept is stable and reliable methods, during which assessment of capacity and demand in terms of energy parameters is made. Concept of equivalent velocity for estimating the input seismic energy was used by Akiyama [8]. A book on Limit state earthquake resistant design of buildings was published by Akiyama Hiroshi in 1985[8]. A great deal of the energy based derivation of input and capacity evaluation in terms of energy remained the major task of the book. Priestley [23] clearly emphasized the performance-based seismic design is the extension of limit state design and severe earthquake demands may be reliably met through the fail safe design using the capacity design. Capacity design for the steel buildings design for some components to yield (beam yielding) if required is satisfactory in comparison to the other materials design. Using the limit state design approach and energy

balance equation, its popularity has increased many times. The advantage of the energy concept remained with its simplicity and applicability to various structures in effective manner. Demand and capacity, both are uncoupled events, since, these two can be evaluated and be equilibrated to a successful design aids without much more affective to each other. Mechanical characteristic: stiffness, strength and ductility have the relation with the capacity in terms of various energy parameters. Allowing structures through yielding some of its important components in desirable manner if damage is unavoidable under severe earthquake ground motions, is the marvelous achievement in the history of design development. This can be true start to performance based seismic design, where the overall performance of the building is controlled as a function of the design process [23].

Uang and Bertero [24] expressed the input seismic energy in two forms. Absolute and relative input seismic energy. The concept of absolute input seismic energy is under the fact that earthquake imposes its effect to the structure through the inertia. Therefore, work is done by the inertia force through the absolute displacement. The work done imposes input seismic energy, which is known as absolute input energy. Absolute input energy is the physical loading in the energy form. The next concept for the input seismic energy was estimated through the product of inertia force and the relative displacement, which is recognized as relative input seismic energy. Such input seismic energy has been supported by Chopra [25] and other with the concept that it is the relative displacement of the structural components which is responsible for the input seismic energy.

Drift and inter-story drift is the performance indicator for structural and nonstructural damages respectively. A nonstructural damage due to floor varying acceleration is sub judice for further investigation [13], since the lateral drift and floor acceleration are inversely related. i.e., the value of floor acceleration is least for the SMRF and maximum for the rigid structures [13]. Since earthquake imposes effect due to inertia force and the inertia force when multiplied with the ground displacement provides input seismic energy. When the structure is rigid, the relative displacement is least; thereby the energy absorbed is least during lateral deformation. The energy distribution along building height becomes significant due to larger value of absolute kinetic energy, which causes the larger floor acceleration. Energy balance equation is equally economically for linear and nonlinear behavior of structures during the earthquake ground motions. For linear behavior estimating demand and capacity in terms of strain and kinetic energy are stable. During nonlinear behavior estimating the seismic effects in terms of hysteretic energy is also popular due to its reliability.

Damage criteria for earthquake-resistant design can't be based on limiting the displacement ductility ratio alone. Further, the damage criteria based on the simultaneous consideration of ductility ratio, hysteretic energy (including cumulative ductility ratio and NYEC) are promising for defining rational earthquake-resistant design procedures and further extension for solving ongoing issues of PBSD.

Input seismic energy in excess represents damage and damage is physically used for performance levels quantification; however, representing energy in terms of mechanical characteristics of the construction materials (stiffness, ductility, young's modulus of elasticity, damping coefficient etc) is under the practice of design. Quantification of damages during severe earthquake using the hysteretic energy has been popular in the recent past [9, 26]. Use of normalized hysteretic energy as performance indicators by researchers [27] in order to use as design tool for PBSD is also suggested.

Formulation of energy based indicator using roof drift and intermediate story drift, multiplying by the inertia force arises due to the earthquake ground motions. Recent literature favors the use of such energy capacity curve and energy demand curve formulations through data generated form the conventional static pushover analysis procedures. The point of intersections of the energy capacity curve and the energy demand curve will be better estimation for performance points [11]. A scope remains with capacity curve for further investigation through sensitivity analysis under earthquakes of different intensities.

Number of yield excursions due to the reversals of stresses under earthquake loadings has been the content of literatures [27] with the conception that yield excursions may be effectively used as indicator of PBSD on a suitable scale. Yield excursions during severe earthquake ground motions through yielding of limited structural components as capable to trace out the sever ness of performance evaluation. However, such findings needs much more investigation for developing analytical tool for design aids

How can the Energy Concepts are used in Performance Based Seismic Design? [13]. The review part of the energy concept reveals the conceptual use of this method provides fast convergence of the perspective seismic design in order to meet the performance objective goals. In order to simplify the PBSD issues and challenges, search of reliable and stable response parameters are the contents of the present research in the new direction and energy concept, has been recognized where demand and capacity are estimated in terms of energy with high sensitivity. Looking at the energy concept design, it is very much clear where and how the input action, i.e., the input seismic energy will be balanced through the

energy capacity of the structure as elastic, in elastic strain and kinetic energy. Though, elastic strain and kinetic energy are dissipated through the viscous damping at the end of earthquakes, but the damages due to their vibrations remains unacceptable from serviceability conditions at the end of earthquake. Inelastic energy due to yielding on the other hand is effective for damage assessment which may be used for corrective measurement for existing as well as for new structures.

1.3.1 Damage Indices

The main objective of performance based seismic design is to identify and quantify the variation of stiffness, strength and ductility during severe ground motions into a single entity, which may further represent post earthquake response, are commonly expressed in damage indices. The damage indices have close relation with various energy components. The literature on damage indices listed for normalization of energy components have been recently addressed for their refinement and their further use as PBSD design attributes. The input energy as per the guideline [12, 28] with a modification that energy input multiplied by a factor and that factor is the ratio of energy input from direct integration of the second order differential equation of dynamic equilibrium of SDOF system to the energy input as the product of half of the mass and square of spectral velocity. As the input seismic energy is consumed as various types of energy-strain energy, kinetic energy (if the mode contribution from the other modes is significant), viscous damping energy due to mass contribution and the stiffness contribution, damping energy due to active and passive systems, and the plastic energy (hysteretic energy). Keeping the strain energy as basic design entity, damage indices have been formulated and their significance has been assessed. The one which gives a better index will be considered as performance evaluation as a tool of performance based seismic design. A separate damage index with hysteretic energy normalized with yield energy ($q_y d_y$) for bilinear elasto-plastic system has been found up to the mark for moment resistant building frames [5].

1.4 Motivation for the Present Work

A wealth of literature on energy concept of seismic evaluation and design [4, 9, 10, 11, 12, 13, 14, 15, 24, 27, and 29] and further advancements in the computational tools (nonlinear static and dynamic analyses procedures) [30] are the major source of inspiration for me to consider the energy balance criterion for the present study. Characteristics of demand and capacity, approach are analysis and design procedures, are the major issues of performance

based seismic design. Energy concept of seismic resistant design is recognized as stable approach [8, 10], where demand and capacity evaluation can be dealt separately. Identification and quantification of demand and capacity for their distribution in space and time is relatively stable through energy based evaluation [8]. Due to advancement in computational facilities it has become possible to express the seismic energy in terms of mechanical characteristics. The main task for performance based seismic design is to incorporate degradation of stiffness, strength and ductility. Corresponding relations of these mechanical characteristics during energy based formulations exist. Redistribution of input seismic energy among the energy components (strain, kinetic, damping and hysteretic) as well as at the structural components through the use of capacity design in the recent past has been attractive for further development of damage assessment under the varying earthquake ground motions. Besides these the seismic action as energy is based on the physical interaction of building with earthquake ground motions. Under ground motion, the base of a structure gets displaced and at the same time other parts have the tendency to remain in its initial position (inertia effect). There are two actions of the building: rigid body translation and relative motions. During rigid body translation the amount of work done gets accumulated in the building (which change the internal states of building structure) and the amount of work done due to relative displacement of the various components gets accumulated in the building components. Whenever a structure is inputted seismic energy during earthquake loading, the structure tends to resist them through the capacity of the structure in terms of elastic strain, damping, kinetic, and hysteretic energy. When the input energy exceeds its elastic limit, a part of energy is dissipated through inelastic energy through monotonic inelastic deformation and a significant amount of energy dissipation through hysteretic energy. There are sufficient structures which strongly rely on the dissipation of inelastic energy for robust performance during any uncalled/unseen large seismic hazards. Damage to a structure is possible only because of losing certain energy (strain and inelastic energy). Energy beyond elastic limit is additive since energy in this domain gets dissipated and by this amount the energy capacity of the structure is reduced. For the design life of a structure, there may be so many small earthquakes for which intended life of the structure may be settled through calculating residual energy capacity one after another earthquakes.

Automation in software's for nonlinear analysis and significant post analysis storage back up for response facilitates towards the use of energy based seismic evaluation are to be used for further development of understanding in the seismic

earthquake resistant design under varying ground motions. Nonlinear modeling through softwares in order to trace out the physical damages (normalized energy components) is of extreme important for automation of performance based application..

1.5 Gap Identified for the Present Study

Performance based seismic design includes identification of seismic hazards, selection of performance levels and their corresponding performance objectives, determination of site suitability, conceptual design, acceptability check during design, and finally design review. Identification and quantification of damages for taking the decision for acceptability during varying earthquakes is the important phase of PBSD. Present state of art provides the discretized format of performance levels. Currently available information to quantify the requirements for all performance levels is not reliable [13]. PBSD requires reliable methods to predict earthquake demands on structures, and particularly inelastic deformations, to insure that specific damage based criteria are met. Practically all structural and non structural damages sustained in buildings as a result of earthquake are unique in their nature. Furthermore, most structures experience inelastic deformation during severe earthquake ground motions are yet to be quantified into simpler damage indices so that they can be used in seismic design codes.

Conventionally, PBSD is the extension of limit states design [23]. Limit states of serviceability and ultimate limit states are popular for two performance levels of seismic design; however, PBSD is multi performance levels design. Response control design using the reliable parameters has been recently popular for development of multi-performance levels design criteria.

Estimating seismic demands at performance levels, such as operational, immediate occupancy, life safety and collapse prevention, requires explicitly consideration of inelastic behavior of the structure, therefore, damages are likely. The seismic demands are computed by nonlinear static pushover analysis of structure subjected to monotonically increasing lateral forces with height-wise distribution until a predicted target displacement is reached. Both the force distribution and target displacement is controlled by fundamental mode and that mode shape remains unchanged after the structure yields. Such issues require attention for MDOF systems through higher mode contribution in terms of more stable response parameters. Demand and capacity evaluation during the changeable earthquake ground motions have to play significant roles for further investigation in the present state of art. Energy based seismic design and response analysis have been addressed by researchers for

resolving the implication of various damage indices for their use for identification and quantification of damages as required for PBSD.

1.6 Objectives of the Present Study

Keeping in view of the background and the present state of the art in this area, the main objectives of the present study may be summarized as follows

1. To review the exiting literature on the performance based seismic design and identify the research gaps for the present study.
2. To asses the seismic hazards as the basic attributes of performance objectives required for the base of the problem formulations.
3. To conduct nonlinear static pushover analysis and nonlinear time history analyses for the required response parameters in order to data acquisition as required for energy based capacity curve and detailed seismic evaluation under varying ground motions.
4. Formulation for input seismic energy evaluation, energy distribution and development of relation in between elastic strain energy and hysteretic energy for identication and quantification of damages under varying earthquake ground motions.
5. To derive relations of the number of yield excursion cycles under reversal of stresses.
6. To analyze the critical cross section for linear and nonlinear behavior.
7. To relate the energy based relation with performance based seismic design (usage ratio).

1.7 Scope and Organization of Thesis/Thesis Outline

Chapter 1 Presents the overview and background of the present study.

Chapter 2 Discuss the literature review of performance based seismic design and energy based seismic design and their relations in the present state of art.

Chapter 3 Proposed problem formulation for the present study: energy based nonlinear pushover analysis, energy capacity curve, floor spectra and inter story drift relations, evaluation of input seismic energy, distribution of input seismic energy, development of relations in between elastic strain and hysteretic energy, normalization of hysteretic energy, simplification of Park and Ang Damage indices for overall performance in terms of local damages, interpretation of number of yield excursion cycles (NYEC) for performance based seismic design. Critical sections analysis using Section Builders for the study of section for linear and non linear behavior.

Chapter 4 Discusses the procedures for development of modeling and analysis of the building frames used in study.

Chapter 5 Presents result and discussions.

Chapter 6 Outlines conclusions and recommendations for future work

Assumptions and Idealizations

Following are the assumptions and idealizations during this research program

1. The layout of the building frame is predefined and fixed throughout the design process. Performance criteria are achieved through the process of proportioning structural steel member sizes.
2. All members are straight and prismatic and cross-section is chosen as design variables.
3. All member sections are compact sections such that concern instability can be neglected.
4. Connections between members are assumed to be fully rigid. Member lengths are measured using centre to centre dimension such that the width of beam-column joints is not considered.
5. Material characteristics of building frameworks are elasto-plastic during nonlinear response.

Table 1.1 Single performance level design

Seismic Hazard level	Structural Performance Level	
		Life Safety
	Hazard Level: 10% Exceeding in 50 Years	

Table 1.2 SEAOC VISION 2000 Recommended performance objectives (After OES, 1995)

Earthquake ground motions	Structural Performance Levels				
		Fully Operational	Operational	Life Safety	Near Collapse
	Frequent (43 years)	Basic	Unacceptable	Unacceptable	Unacceptable
	Occasional (72 years)	Essential	Basic	Unacceptable	Unacceptable
	Rare (475 years)	Critical	Essential	Basic	Unacceptable
	Very Rare (970 years)			Essential	Basic

Table 1.03 FEMA 273 Performance objectives (After ATC, 1997)

		Building Performance Levels			
		Operational	Immediate Occupancy	Life Safety	Collapse Prevention
Hazard levels	50% / 50 years	a	b	c	d
	20% / 50 years	e	f	g	h
	BSE-110% / 50 years	i	j	k	l
	BSE-2 2% / 50 years	m	n	o	p

o = Enhanced Objective, k alone or p alone = Limited Objective

k+p = Basic Safety Objective

k+p+ any of a, e, l, m or b, f, g, n = Enhanced Objective

c, g, d,h =Limited Objectives.

Table 1.04 Building performance levels (FEMA-273, 1997)

Nonstructural Performance Levels	Building Performance Levels/Ranges					
	S-1 Immediate Occupancy	S-2 Damage Control Range	S-3 Life Safety	S-4 Limited Safety Range	S-5 Collapse Prevention	S-6 Not Considered
N-A Operational	Operational 1-A	2-A	NR	NR	NR	NR
N-B Immediate Occupancy	Immediate Occupancy 1-B	2-B	3-B	NR	NR	NR
N-C Life Safety	1-C	2-C	Life Safety 3-C	4-C	5-C	6-C
N-D Hazards Reduced	NR	2-D	3-D	4-D	5-D	6-D
N-E Not Considered	NR	NR	NR	4-E	5-E Collapse Prevention	NO Rehabilitation

NR: Not Recommend

Table 1.05 SEAOC VISION 2000 general damage descriptions for new building designs (After OES, 1995)

Performance levels ⟶ / Damages ↓	Building performance levels				
	Fully operational	Operational	Life safety	Near collapse	Collapse
Overall building damage	Negligible	Light	Moderate	Severe	Complete
Permissible Transient Drift	<0.2%	<0.5%	<1.5%	<2.5%	>2.5%
Permissible Permanent Drift	Negligible	Negligible	<0.5%	<2.5%	>2.5%
Vertical load carrying element damage	Negligible	Negligible	Moderate to heavy but elements continue to support gravity loads	Light to moderate, but substantial capacity remains to carry gravity loads	Partial to total loss of gravity load support
Lateral load carrying element damage	Negligible generally elastic response; no significant loss of strength or stiffness	Light. Nearly elastic response; Original strength and stiffness substantially retained; Minor cracking/yielding of structural elements; repair implemented at convenience.	Moderate. Reduced residual strength and stiffness, but lateral system remains functional.	Negligible residual strength and stiffness; no story collapse mechanisms, but large permanent drifts; secondary structural elements may completely fail.	Partial or total collapse; primary elements may require demolition.
Damage to architectural systems	Negligible Damage to cladding, glazing, partition, ceiling, finishes, etc. isolated elements may require repair at users convenient	Light to moderate damage to architectural systems; essential and selective protected items undamaged; hazardous materials contained	but large falling hazards not created; major spills of hazardous materials continued	Sever damage to architectural systems; some elements dislodge and may fall.	Highly dangerous falling hazards; destructions of components.

Chapter 2

LITERATURE REVIEW

2.1 Introduction

Prior to the emergence of Performance Based Engineering (PBE) for seismic design, the goals of earthquake resistant design of buildings were understood to be (i) The building should remain undamaged under the frequent minor earthquakes, however, nonstructural members may sustain repairable damages, (ii) Under an occasional moderate earthquake that may occur once or twice in the life-time of structure, the structural members may suffer repairable damages, however, non structural members might suffer severe damages and the cost of repairs of nonstructural members may be substantial, (iii) Under a rare severe earthquake that has remote possibility of occurrence during the service period of a structure, the structural members may suffer irreparable damage but the structure should not collapse. Thus, these levels of earthquakes and their corresponding levels of acceptable damages (performance levels) were desired to be identified and quantified so that the remedial/corrective steps may be taken in order to achieve the desired performance objectives as the major content of seismic design under varying earthquake ground motions. However, building codes specified only one level of earthquake load and its verification criteria. Therefore, the seismic design of building codes for life safety (single performance objective) were needed for changes mainly after Northridge (1994) and Kobe (1995) earthquakes in spite of high life safety but with unacceptable damage during these two earthquakes.

Performance based earthquake engineering (PBEE) implies design, evaluation, and construction of engineered facilities whose performance under common and extreme loads with quantifiable confidence in order to satisfy client requirements based on life cycle considerations rather than construction costs alone [31]. A global framework for PBEE emphasizes the research agenda focuses on structural and inter face issues through the interfacing of process, concepts and issues [32]. PBSD is subset of PBEE. The major task for PBSD development is through the performance objectives. Performance objectives correspond to performance levels for specified seismic hazards. Different expressions may be used for desired performance levels. Engineering input is much needed to identify performance levels that can be described in engineering terms and to establish an emphasis on performance levels that can become the focus of engineering design decisions. In this

context, translation of performance description into engineering limit states is desirable. For practical reasons, engineering design needs to be based on physical parameters that can associate with engineering limit states. Examples of such parameters are strength, stiffness, global and interstory drift, deformation capacity, and energy dissipation capacity [31]. PBSD is the extension of limit states to take care of the damages during varying seismic hazards [23]. Thus performance based seismic design (PBSD) emerged to take care of damages during varying earthquake ground motions in predictable manner.

Conventionally, limit states design is a powerful method for two level design approach in terms of limit state of serviceability and ultimate limit strength [16]. However, performance based seismic design can be viewed as a multi-level design approach. The limit state of serviceability provides fully operational and ultimate limit provides life safety as two performance levels. Estimating seismic demands at performance levels, such as life safety and collapse prevention, requires explicit consideration of inelastic behavior of the structures. The seismic demands are computed by nonlinear static analysis of structure subjected to monotonically increasing lateral forces with an invariant height-wise distribution until a predictable target displacement is reached. Both the force distribution and target displacement are based on the assumption that the response is controlled by fundamental mode and mode shape remains unchanged after the structure yields [32]

The goal of SEAOC Vision 2000 [1] is to develop the framework for procedures that lead to design of structures of predictable seismic performance and is able to accommodate multiple performance objectives. The document presents the concepts and addresses the performance levels for structural and nonstructural systems. Performance levels [Table 1.5] are described with specified limits of transient and permanent drift. It is suggested that capacity design principles should be applied to guide the inelastic response analysis of the structure and to designate the ductile links or forces in the lateral-force-resisting system. Since most of the time, PBSD is design up gradation. Possible design approaches include various elastic and inelastic analysis procedures such as: (1) Conventional force and strength methods; (2) Displacement-based design; (3) Energy approaches; and (4) Capacity design etc.

The future of earthquake resistant design is the function of the past performance. In spite of significant development, we have challenges to develop new techniques and to improve the existing practices in order to make the performance of the structure predictable so that the acceptability criteria may be developed. Seismic risk is the product of seismic hazards vulnerability and the value of its damages and also depends upon the exposure. The

aim of PBSD is to employ the seismic design criteria based on performance objectives. A performance objective is the specification of an acceptable level of damages to a building if it experiences an earthquake of a given intensity. A single performance objective (Table 1.1) that requires buildings remain operational even under largest earthquake will result high initial cost. However, such large earthquake is rare during the life of a structure. PBSD differs from current codified design approaches in that it focuses on a building's individual performance. Major documents addressing performance based seismic design are SEAOC Vision, 2000 [1, 2, and 3]. Procedure for performance evaluation of FEMA 273/FEMA 356 do not directly address the control of economic losses. Secondly, the procedure focuses on the assessment of performance of individual building components, rather than building as a whole [33]. The Structural Engineers Association of California (SEAOC) in their Vision 2000 document defines performance objectives for buildings as the buildings expected performance level, corresponding to a certain level of expected earthquake ground motions [1].

Performance objectives as the design goals are combinations of acceptable damages (performance levels) corresponding to the seismic hazards. Seismic hazards are the key elements for the establishing risk in the design formats [34]. Post earthquake seismic risk evaluation to take care of the socio economic balance is an attribute of performance based seismic design. Loss of functionality during seismic risk evaluation requires linear and nonlinear analysis. PBSD requires nonlinear analysis response since a structure is understood to take advantages of ductility under severe earthquake ground motions. Steel buildings have been found satisfactory in the past earthquake due to the high ductility of the structure at local and global levels. The rigidity and the flexibility of the joint plays significant role for achieving the design goal of built up structures [35].

Energy based seismic design criteria through energy balance equation has been focus of the recent past literatures [8, 10, 12, 13, 15, 24] for its extension towards PBSD. The advantages of energy based seismic design are that energy being a stable quantity and can be dealt separately for evaluation of demand and capacity, provided that the presence of structure may not influence soil structure interaction. For the sake of simplicity such an issue is not of importance at this moment [8, 10]. Input seismic energy depends upon the structure type and on the intensity of earthquakes at the site concerned. To a certain extent, energy based seismic design with performance based seismic design has been recently recognized due to advancement in computational facility and through the application of capacity design [13]. Various software's are in the international state of art which provides

significant information of the energy distribution along the height and among various components [17]. With the development of response control seismic design, energy based evaluation is found to be effective [10]; subsequently; damage identification through normalization of energy components with the known pattern of energy distribution has been recently focused for further researches. A performance-based seismic design procedure requires quantification of performance based on one or multiple structural response indices. Traditionally, ductility, energy dissipation, or a combination of both, has been identified as the parameters that best evaluate the performance level of structural elements. A number of well known damage indices [9, 26, and 36] propose methods to carry through such an evaluation by one of these parameters, or weighted sums of both. Number of yield excursion cycles (NYEC) under severe ground motions also has been addressed for its application to PBSD [27] as a design aid. Pushover analysis for data generation for further development of capacity curve in terms of energy and displacement and plotting this capacity curve against the energy demand for performance evaluation is identified as perspective area for energy based capacity curve. For performance levels under varying ground motions [11] energy based evaluation in order to formulate effective methodology has been identified as promising analysis procedures.

Energy based seismic design is categorized into two parts. The first part is based on equilibrating the input seismic energy through treating energy the principal loading in terms of energy and balancing through the energy absorbing capacity of the building components. Such a kind of energy balancing has been found more reliable in literature. The 2nd part is concerned with the application of base isolation, active and passive devices for energy dissipation in addition to the energy capacity discussed in first phase. Balancing the energy capacity through elastic strain energy during severe earthquake ground motion is highly uneconomical for initial cost. After all a severe earthquake is rare to occur during the design life of structure. Depending upon the type of construction materials a significant amount of energy is dissipated through damping in the elastic region. Keeping pros and cons of the life cycle cost a structure is allowed to take advantages of ductility and dissipates energy through yielding. Structural components undergoing inelastic deformation results into damages due to inability to carry the functional requirement in due course after ground motions. Loosing functionality of the structure in terms of available energy is directly related with the damage, downtime payment and death, as is the major task of PBSD for next generation [37].

The concept of using damage indices as design aid in seismic resistant design is popular, since the damage indices are normalized having numerical values in between 0 and 1. However, such damage indices for the distribution of various parameters of the indices have been subject of interest from time to time towards their simplicity in order to make them practical. Commonly the damage indices have two parts; the first part is the deformation control response. This ration must have some power say x, and the value of x must be identified [37]. The next part is the normalized value of the energy dissipated through yielding and the energy due to the monotonic lading. This ratio should also have power, say y, which must be evaluated for identification of actual contribution of individual components [37]. Most such damage indices have been developed on an element or component basis, but a few have been calculated on a global structural level. Most common and generalized format of damage indices are [37]:

$$DI = \left(\frac{\Delta_i}{\Delta_u}\right)^x + \left(\frac{E_i}{E_u}\right)^y \leq 1.0$$

Where the quantity in the second term having the power y is a measure of cumulative damage resulting from the repeated cycles of inelastic response and has most commonly been expressed in the past as a ratio of inelastic energy dissipation demand and capacity. These damage indices have been widely used for several reasons, including:

- The use of nonlinear response history analysis.
- The energy component is typically a small part of the computed index.
- There is little research available to suggest appropriate values of E_u term.
- Little spontaneous feeling for damage indices and have difficulty relating them to an understanding of a structure's actual performance.

A second method for assigning damage parameters used in the past was to assign a series of discrete damage states or ranges, representing progressively more severe damage. This is the approach taken both by present generation performance based design methodologies such as FEMA 356 [38], and also by loss estimation methodologies such as HAZUS. In FEMA 356, these damages are termed the Operational, Immediate Occupancy, Life Safety, and Collapse Prevention performance levels, with Operational representing a state of negligible damage and Collapses Prevention, a state of near- complete damage. The HAZUS methodology uses damage state termed as Slight, Moderate, Severe, and Complete, assigned based on the analyst's understanding of the extent of damage to the structures as predicted by analysis. It should be possible for particular structural system to develop

relationship between either the FEMA 356 performance levels or HAZUS damage states and computed damage. However, it is not clear that both guidelines and either will be capable to solve the next generation PBSD requirements [37].

A third potential method of paramterizing damage consists of a direct tracking of the condition of individual structural elements and components, on a piece by piece basis, coupled with measures of building –wide damage. e.g., for moment resisting steel frames, damage measures that could be used on a connection by connection basis include: panel zone yielding, beam plastic hinging, beam flange buckling, and welded joint fracturing Similarly non-structural fragilities may be developed taking consideration of factors governing non-structural damages. e.g., floor acceleration, inter story drift. As the development towards better tools for intercepting the real behavior under varying ground motions will remain open due to the fast growth in the computational skill on the other hand the risk management will also be able to capture the seismic hazards at the micro levels [34].

Modeling for nonlinear analysis as required for performance based seismic design is possible in the recent past. Many software's are available in the present state of art, which are capable to provide significant energy based seismic demand and capacity evaluation [10, 17] is one of the most advanced software, used for modeling and simulation for performance based evaluation and the corresponding analysis results to be used for making design decisions in the present study. Accuracy of the analysis results depends upon the nonlinear modeling parameters, which have become possible through software's revolutions. Nonlinear static pushover analysis results through proper modeling are being used for further advancement through data base under the earthquake loadings. Advancement in the nonlinear static pushover analysis for performance base seismic design can be seen from the abundance of recent literature. e.g., use of data generated during conventional pushover analysis has been used for energy based capacity spectrum [11].

Interpretations of damage indices using energy based evaluation results into development of design algorithm in the present state of art. e.g., time history analysis results for the critical members under reversal of stresses provide significant data for yielding of members. The number of yielding may have to be correlated with performance evaluation as required for PBSD. Deformation based design inability to address performance during severe ground motions are because of the lack of information for cumulative ductility. However, energy based evaluation has been used for finding the cumulative ductility using the existing damage indices [10].

2.2 Performance Based Seismic Design

The seismic resistant design emerged with the perception to take care of the acceptability of seismic risk (damages) due to earthquake ground motions is called performance based seismic design (PBSD). PBSD is multi-performance levels design, however, the seismic codes define single performance level, and that is for life safety. The design issue is highly iterative in order to achieve the performance objectives assigned. During earthquake ground motions, demand and capacity, both are coupled. In fact earthquake imposes demand through inertia and the inertial property during reversal of stresses induces additional implications on the seismic demand. Dynamic characteristics of structure and the intensity of earthquake greatly affect the inertial property. The basic attributes which controls the overall performance of structure are identification and quantification of performance levels corresponding to the seismic hazards. Performance levels (acceptable damages) and seismic hazards constitute PO's. All documents available in the literature correlates performance levels with seismic hazards, accept the discrete concept of damages.

Thus, performance based seismic design involves a set of procedures by which a building structure is designed in a controlled manner such that its behavior is ensured at predicted performance levels under varying earthquake loadings. The design process is an iterative re-analysis/re-design task, in which an initial design is modified repeatedly to meet the desired behavior of the structure. Purpose of Performance-Based Seismic Design (PBSD) is to give a realistic assessment of how a structure will perform when subjected to either particular or generalized earthquake ground motions.

Tasks of PBSD may be categorized as: (i) Selection of performance objectives, (ii) Selection of structural systems, (iii) Definition of performance levels, (iv) Seismic hazards at site, (v) Preliminary design, (vi) Modeling, (vii) Analyses (viii) Performance checks, (ix) Final design, (x) Quality control of construction and (xi) Maintenance etc.

2.2.1 Performance Objectives

Performance objective is defined as coupling of expected performance level with expected levels of seismic ground motions. According to the SEAOC Vision of 2000 document, [1] prepared by the Structural Engineers Association of California, four performance objectives paired with four seismic hazards are defined:

- Fully Operational. Facilities continue with negligible damage.

- Operational. Facility continues in operation with minor damage and minor disruption in nonessential services.
- Life Safety. Life safety is substantial protected, damage is moderated to extensive.
- Near Collapse. Life safety is at risk, damage is severe, structural collapse is prevented. The relationship between these performance levels and earthquake design level is summarized as following (OES, 1995):

Hence, therefore the critical decision of the performance-based design is augmented though the performance levels corresponding to the seismic hazard. The procedures of the PBSD thus are directly controlled by the performance objectives assigned to the structures. A general view of the selection of performance objectives has been discussed below in terms of the cost of construction corresponding to the performance levels. Very important perspective of performance objectives are performance levels and seismic hazards. Performance levels are discrete deterministic points; on the other hand seismic hazards are probabilistic discrete points on the continuous seismic hazards. Therefore, these two attributes of performance objectives are extremely idealization. In authenticity, infinite number of performance levels and seismic hazards are possible. However, identification of large number of performance levels is difficult to achieve. Yes, use of limit states holds back such large issue of performance objectives to limited condition so that design decisions could be made, accordingly. Acceptable damage under specific ground motions are known as performance objectives. Performance objectives are statements of acceptable performance of the structure. The performance target can also be specified through limits on any response parameter such as stresses, strains, displacements, accelerations, etc. It is appealing to express the performance objective in terms of a specific damage state or the probability of failure against a prescribed probability demand level [1, 18]. Various documents [1, 2, and 3] promote the same concepts but differ in detail and specify different performance levels.

It is recognized that drift levels associated with specific damage categories may vary considerably with the structural system and construction material. Attempts have been made to define drift levels for different structural systems and materials [1]. However, more research is needed, particularly in the development of realistic and quantitative estimates of drift–damage relationships. In addition, design criteria that apply to various parameters may be required by different performance objectives. To implement performance-based design, there is a need for consensus on the number and definition of performance levels, associated

damage states, and design criteria. Performance objectives controls the various design procedures to be adopted for PBSD.

2.2.1.1 Selection of Performance Objectives

A building can be subjected to low, moderate or severe earthquakes. During these earthquakes, the building may undergo slight, moderate or heavy damage, may be partially damaged or can collapse. The levels of damage depend on the earthquake intensities. The low intensity earthquake occurs frequently, the moderate earthquake more rarely, while the strong earthquakes may occur once or maximum two times [5] during the structure life. It is also possible that a devasting earthquake will not occur during the life of the structure. The performance of the structure depends during these mentioned levels of earthquakes occurrence. The performance is optimum corresponding to optimum performance level of design.

2.2.1.2 Performance Levels

As recommended by the various agencies and researchers, performance levels are defined in terms of functionality of structure considering acceptable limit for damages. e.g., fully operational for frequent earthquakes, operational for moderate earthquakes, life safety for rare earthquake and near collapse for very rare earthquake. Each performance level associated with minor to significant amount of damages depending upon the levels of earthquake motions. Formulation of performance levels thus needs the interrupted use of permissible damages. Higher performance levels may cost more because formulation of higher performance levels directly affects the initial cost of the structural system. Risk assessment of the damage evaluation so that the performance can be related with the death, damage and downtime payment for the effective PBSD [34, 37].

2.2.1.3 Seismic Hazard Levels

Seismic risk evaluation requires the post earthquake response acceptable for damage cost if any in order to cope the socio-economic minimum hazard impact. The most common and significant cause of earthquake damage to buildings is ground shaking; thus, the effects of ground shaking form the basis for most building code requirements for seismic design [3, 39, and 40].Typically, ground shaking is characterized using acceleration spectra, displacement design spectra, site-specific acceleration spectra, site-specific displacement response spectra, and/or site-specific ground motion records. Further discussions of

methods to characterize site-specific ground motion may be found in the FEMA 273 document and seismic hazard maps may be obtained from the United States Geological Survey.

Performance objective is defined in terms of performance levels and a minimum seismic hazard level. For SEAOC Vision-2000 four seismic hazard levels are defined. The other agencies/research scholars have used some different seismic hazard levels for establishing performance objectives. Basic difference for different seismic hazard levels is in terms of the return periods and the return period for the seismic hazard level depends on the seism city of the region and the site, and is defined to match an acceptable level of uniform risk and this value varies from region to region, hence, the seismic hazard varies depending upon the nature of various factors involved [13].

Performance-based seismic design procedure requires quantification of performance based on one or multiple structural response indices. Traditionally, ductility, energy dissipation, or a combination of both, has been identified as the parameters that best evaluate the performance level of structural elements. A number of well known damage indices [9, and 26] propose methods to carry through such an evaluation by one of these parameters, or weighted sums of both. These parameters are usually calibrated against experimental data to result in a value of one corresponding to failure of the structural system. Furthermore, current investigations on the global performance of buildings during earthquakes have revealed that a large portion of the sustained damage is due to non-structural elements and contents, rather than to the main structural system. This is especially true for low to moderate earthquakes. Although a portion of this damage is acceleration dependent, a considerable amount is due to deformations imposed upon non-structural elements by the main structural system's deformations [13].

2. 2.4 Development of Performance Based Seismic Design

Emergence of performance based seismic design after two earthquakes, namely Northridge and Kobe was ignited due to unacceptable damages in spite of high life safety was necessitated. Further this concept of seismic design has under gone critical reappraisal during the recent past decade with the remark that future seismic design needs to be based on achieving multiple performance objectives. However, there are divergent viewpoints on the meaning of performance based design and its methods of implementation. Three documents are recognized with putting down the foundation for performance-based design concepts: SEAOC Vision 2000, 1995 [1], ATC 40, 1996 [2], and FEMA 273, 1997 [3]. The

documents attempted to develop procedures that can be used as seismic provisions in building codes.

The goal of SEAOC Vision 2000 is to develop the framework for procedures that lead to design of structures of predictable seismic performance and is able to accommodate multiple performance objectives. The document presents the concepts and addresses the performance levels for structural and nonstructural systems. Five performance levels are described with specified limits of transient and permanent drift. It is suggested that capacity design principles should be applied to guide the inelastic response analysis of the structure and to designate the ductile links or forces in the lateral-force-resisting system. Possible design approaches include various elastic and inelastic analysis procedures such as: (1) Limit state of serviceability and Ultimate limit state design; (2) Displacement-based design; (3) Energy approaches; (4) Capacity design and (4) Prescriptive design approaches.

Design criteria for two performance levels and three performance levels using the clear formats of mechanical characteristics-stiffness, strength and ductility have also been presented with the focus on their corresponding analysis procedure under varying earthquake loadings [5].

2.2.5 Comprehensive Approach of Performance Based Seismic Design

The present state of art reveals the conceptual comprehensive approach to simplify the multi-performance level seismic design using some damage control indices because the PBSD is trade off stiffness, strength and ductility and commonly obtained through iterative analysis and design procedures through design improvement. The advantages of using design spectra, local damage spectra, drift spectra, floor spectra and energy spectra at the initial stages during design (preliminary design) are innovative in the approach because the final design is guaranteed to converge with minimum cycle of convergence [13]. In this direction two performance levels seismic design has already been introduced in Euro-code 8 and Japanese code of seismic design. In addition to various design spectra, energy concept, which is based on the energy input and energy output has been recognized as effective methodology for performance-based seismic design with the use of capacity design. The greatest advantages of energy concept of multi-performance seismic design are that energy demand and energy capacity both are separately estimated and using the energy balance equations various performance levels are economically identified and characterized.

2.3 Moment Resistant Steel Building Framework (Literature Review)

Strength, stiffness, ductility and toughness are the basic attributes of steel structures, making them suitable for seismic resistance [5]. Due to higher ductility steel structure deform considerably before failure by fracture allows an indeterminate structure to undergo stress distribution. Ductility also enhances the energy absorbing characteristic of the structure, which is extremely important in seismic design. Thus, high strength with better ductility is the basic characteristic of steel to be used a seismic resistant construction material. Steel is a reusable and is environment-friendly having considerable life cycle cost. Compared with the competing construction, steel frame buildings are significantly better resistance to earthquakes and take less that half the time to build [42].

Buildings that use a system of steel beams, columns, and connections capable of transferring bending moments for primary lateral force resisting system are called steel moment resistant frame (SMRF) buildings. These frames develop their seismic resistance through bending of beams, columns and shearing of the panel zones [5]. A moment resistant steel building frame is a rectangular combination of structural components: beams, columns, panel zones, connection etc. depending upon the behavior of the connection a moment resistant frame is categorized as rigid, semi-rigid or flexible. A rigid steel frame derives its lateral stiffness mainly from the bending rigidity of frame members interconnected by rigid joints..

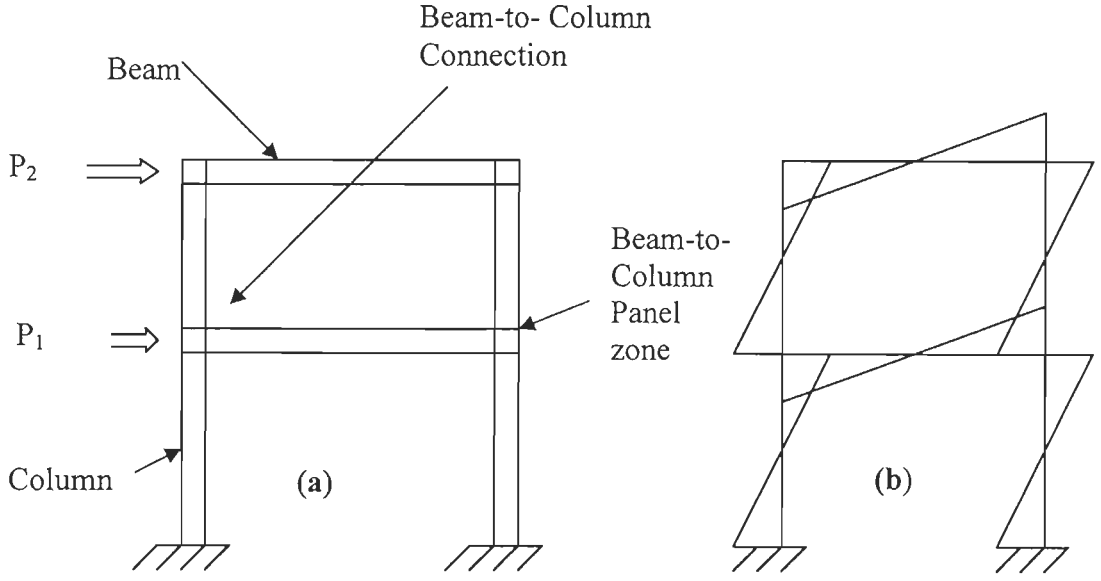

Figure- (a) Geometry considering finite dimensions of members,
(b) Typical moment diagram under lateral loading

Figure 2.01. Typical moment resistant frame under lateral loading

Three types of models are commonly used for seismic resistant design of moment resistant steel building frames: Strong column weak beam, Strong beam and weak column (Shear frame) and Hybrid (mixed of shear and flexural) [8].

Strong Column Weak Beam (SCWB) has been appraised for their use from the better performance criteria during severe earthquake ground motions, while damage becomes desirable. It is moment resistant building frames which can dissipate significant amount of energy through some specific structural components in definite manner [23].

2.3.1 Seismic Performance of Steel Buildings during Past Earthquakes

It is because of the high strength and significant ductility, steel has been the better choice for buildings construction materials. A moment resistant building frame resist the lateral loading through flexural strength of structural components. With the emergence of plastic design and bracing elements, steel structures have been constantly used in seismic regions [20]. Performance of these building structures during the past earthquakes has been the source of motivation for betterment in order to minimize damages with present state of art. Moment resistant building frameworks due to its ability to withstand severe ground motions with the provision of high energy dissipation through yielding of desirable components are popular through the SCWB concept. With the emergence of capacity design in 1970 [23], use of plastic design became simpler as the structural components are certain to be in the inelastic region during severe earthquake motions. Following literature on seismic performance of steel building may be quoted for the performance of steel structures during past earthquakes.

2.3.1.1 Michoacan Earthquake

On 19th September 1985, a major earthquake of magnitude 8.1 occurred, with an epicenter located in Zacatula city, about 350 km from Mexico City, in the south of Micoacan State, Mexico [5, 16]. More than 100 steel buildings were subjected to this earthquake. Among them, 59 buildings were built after 1957 having 7 to 22 stories. This was the first type of verification of the behavior of the steel structures during a strong earthquake showing generally a bad performance. The main cause of this unexpected behavior was due to the double resonance phenomena, seismic wave soil and soil-structure, which gave rise to a required ductility exceeding the normal demand. The influence of the higher modes, which were more active than the first one, caused more damage on the upper stories and also collision between the adjacent buildings. In Mexico, the moment resisting frames behaved

generally well. The second type of buildings used in Mexico City area was the steel dual system with some bays of moment resistant frames braced. Out of twenty five buildings, two totally collapsed, one partially collapsed, four sustained various degrees of damages and the rest remained undamaged [5, 16].

2.3.1.2 Northridge Earthquake

The Northridge earthquake of January 17, 1994 at 4.31 a.m. in California, USA, Pacific Standard Time of magnitude 6.7 challenged the well accepted concept of steel as earthquake resisting structure. Following this earthquake, a number of steel moment frame buildings were found to have experienced brittle fractures of beam-to-column connections. The damaged buildings were of heights varying from one story to 26 stories and ages of some buildings were of 30 years [5, 16].

2.3.1.3 Kobe Earthquake

The Kobe earthquake, Japan, of January 17, 1995, resulted into collapse of 100000 buildings, caused heavy damage in 90000 buildings and light damage in 150000 buildings. Out of these buildings, many were steel buildings and most of these suffered fractures of beam-to-column connections [5, 16].

2.4 Nonlinear Static Pushover Analysis for Performance Based Seismic Design

Static pushover method has been widely accepted as a useful tool for performance based seismic design and evaluation of structures [3, 4, 13, and 37]. In pushover analysis, the structure is idealized as an assembly of components, each with its own nonlinear load-deformation characteristic. The structure is then subjected to a set of increasing lateral loads which pushes the structure monotonically until a target displacement is reached [42]. The drift, component force, and deformation demands at the target displacement levels are then used to evaluate the structure.

Recent developments in the conventional pushover analysis include adoptive load patterns and multiple modal analysis procedures. In most cases, the behavior of the structure is characterized by the capacity curve which is presented by a plot of the base shear versus roof displacement. The capacity curve is used to establish an equivalent SDOF system. The target displacement can then be predicted using one of the methods such as capacity spectrum approach, or the direct use of inelastic constant ductility spectra. Once determined,

the target displacement can then be projected back to the roof displacement from which the story and member demands can be extracted. For MDOF system, use of roof displacement as an index is misleading. The absorbed energy (or work done by external forces) has been suggested as a better index to establish the capacity curve [43].

The underlying theory and the framework for carrying out the analysis are first presented. The analysis procedure is then applied to SDOF and MDOF structures to estimate the displacement demands. The results obtained from the proposed procedure are then evaluated and compared with results from nonlinear dynamic analysis as well as those from other well established nonlinear static procedures with the emergence of performance based seismic design, the need of nonlinear analysis became a necessary tool. Under monotonic increasing loads, study of structural behavior, allowing the structure into nonlinear range has become a popular analysis tools in the research as well as in the design offices. Recent past development towards the nonlinear static pushover analysis is appreciable, since it has revolutionized the understanding of dynamics of earthquake loadings even without much more the knowledge of dynamics. Its emergence as a design tool for identification and quantification of damages during in elastic response of building structures became a necessary tool of seismic resistant design building. NSPA with the present development have tremendous advantages for data base formulation for further design development.

2.4.1 Nonlinear Analysis of Building Frameworks

Performance based seismic design is mainly to diagnose the damages, therefore, needs nonlinear analysis. The method of modeling is the major task for controlling the nonlinear analysis. Fast nonlinear analysis (FNA) using the localized plasticization is the background of development of softwares [44]. The lumped plastic method is popularly known as plastic hinge method, assumes that plasticity is concentrated at a zero-length plastic hinge section at the ends of the elements. The regions in the frame elements other than at the plastic hinges are assumed to behave elastically. This analysis typically involves the use of beam-column element for each frame member, and thus makes the modeling of the large building frameworks easy. After applying loads on the structure, the internal forces for the elements are first evaluated by elastic analysis (ETABS). If any section is found to reach its plastic strength, the element stiffness matrix is adjusted to account for the presence of a plastic hinge. In the analysis of the nonlinear behavior of a structure, the element stiffness matrices are updated constantly to capture the state of equilibrium due to inelastic yielding.

Therefore, it is necessary to it carry out the analysis in incremental-load form. Numerical methods used are simple incremental method and the other is called the Newton-Raphson method [45]. The simple incremental method is the simplest and most direct nonlinear global solution technique. No iteration is required within one load step, and thus the numerical algorithm is generally well behaved and provides efficiency. This is especially true when the structure is loaded into the inelastic region, for which a trace of hinge-by hinge formation is required in the element stiffness formulations. The Newton-Raphson method involves iteration which each load step to eliminate out of balance loads that exists at the end of each load increment. Although, the Newton-Raphson method is more accurate, the simplicity and computational efficiency of the simple incremental method are especially important for the proposed structural synthesis, and therefore is adopted for this research work.

2.4.1.1 Load-Displacement Control Pushover Analysis

Switching over from force controlled performance evaluation to displacement control; since a structure is sure to go into the inelastic region during severe earthquake ground motion to take advantages of inherent ductility are the content of recent past literature. Displacement control performance levels due to better information in terms of damage communication are the fact behind such consideration. For example, a framework that undergoes a roof drift of 0.7%, 2.5% and 5% of the building height is at the IO, LS and CP performance levels respectively [3]. A displacement control pushover analysis procedure is thus required to evaluate the seismic demand at the corresponding displacement levels. However, displacement control pushover analysis procedure is not suitable for the performance based seismic design, since the structural designs are based on the codes specified by governing codes [7]. For example, the magnitude of an earthquake loading is determined from the corresponding acceleration spectrum provided by a specific deign code or standard. To evaluate the seismic demand at a specified earthquake loading, a load control pushover is necessary. Thus for a displacement control procedure, pushover analysis is terminated when the maximum target displacement is reached at the target node (e.g., roof), while for a load control procedure, pushover analysis is terminated when the maximum specified design base shear is reached.

Generally speaking, a feasible design that is found to a load control pushover analysis procedure is also feasible if it is verified by a displacement control procedure. A load control pushover analysis procedure becomes more desirable for the design of a new

structure, since it is able to evaluate the sensitivities of design base shear. On the contrary, a displacement control procedure is more suitable for the performance based analysis of an existing structure [7].

2.4.1.2 Modal Pushover Analysis

The shortcomings of the pushover analysis lies to the fact the structure is of one degree of freedom, is true, otherwise, the participation of the higher modes will develop more errors. Many researchers have given the guidelines for considering the multi-modes response controlled. In this response, modal pushover analysis was conceived by and was demonstrated. Among all, the modal pushover analysis (MPA) procedure by Chopra and Goel [30] is understood the best method.

The MPA procedure uses structural dynamics theory besides maintaining the beauty of the static pushover analysis. The method evaluates the seismic demand in two phases: i) multiple single-mode pushover analyses are carried for different vibration modes of the structure (i.e., multi modes) to determine the corresponding modal responses of the MDOF system at the target displacement; ii) the total structural response is determined by combining the multiple mode responses according to an appropriate modal combination rule, such as the square-root-of sum-of squares (SRSS) rule. The MPA method is equivalent to standard response spectrum analysis of an elastic structural system. For an inelastic system, it is assumed that the modal response can be uncoupled such that conventional pushover analysis is still applicable for each mode. According to its developer the error is small that are acceptable for practical applications. There are two difficulties of MPA application; i) the lack of target displacement data for higher modes; ii) the appropriate determination of higher nodes.

2.4.1.3 N2 Method of Pushover Analysis

The pushover analysis is based on the nonlinear 2 Dimensional building frames. PBSD using the background of this method is based on the premise that strength and ductility relationship can be developed and the corresponding value of demand can be estimated. The advantage of this method over FEMA 273 procedure is that number of iterations has been reduced [4].

2.5 Seismic Loads for Pushover Analysis

Choice of the load distribution is one of the most difficult issues for push-over analysis during an actual earthquake, the effective loads on a structure change continuously in magnitude, distribution and direction. The distribution of story shears over the height of a building can thus change substantially with time, especially for taller buildings, where higher modes of vibration can have significant effects. In a static push over analysis the distribution and direction of the loads are fixed, and only magnitude varies. Hence, the distribution of story shear stays constant. To account for different story shear distributions it is necessary to consider a number of different pushover load distributions. One option in FEMA-356 [38] is to use uniform and triangular distributions over the building height. It is important to know that a uniform distribution usually corresponds to a uniform acceleration over the building height, so that the load at any floor level is proportional to the mass at that floor. Similarly, a triangular distribution usually corresponds to a linearly increasing acceleration over the building height. The best way to prescribe the push over load is proportional to the floor acceleration/spectra.

Corresponding to the compatible response spectra of a particular time history, and for the fundamental natural period of the structure, seismic coefficient is obtained. Form the respective codes, design horizontal coefficients are achieved. Seismic weights of the structure are evaluated and the values of base shear are found by taking the product of design horizontal seismic coefficient and the seismic weight. The value of the base shear achieved is further used for distribution along the height of the building.

The best pattern is controlled through the variation of floor spectra along the building height. The horizontal ground motion intensity of an earthquake defines the spectral response acceleration Sa of a building in the lateral direction, which may be transformed into total horizontal base shear force as following:

$$V_b = \frac{Sa}{g} W \tag{2.1}$$

Where g is the gravitational acceleration constant and W is the total weight of the building. The shear force V is in equilibrium with a distribution of lateral inertia forces F applied over the vertical height of the building, which, for example, FEMA 273 defined as,

$$Fx = Cvx\ V \tag{2.2}$$

$$Cvx = \frac{w_x h_x^k}{\sum_{i=1}^{n} w_i h_i^k} \tag{2.3}$$

Where F_X is the lateral load applied at story level x, and Cvx is the corresponding vertical distribution factor defined by: gravity loads w_x and w_i = the portions of the total building weight at story levels x and i, respectively; the total number n of stories; and an exponent k whose value depends on the fundamental period of the building.

2.6 Push-over Analysis

Conventional push-over analysis performed in the context of performance-based seismic design is a computational procedure where, for static-equivalent loading consisting of constant gravity loads and monotonically increasing lateral loads, the progressive stiffness/strength degradation of a building is monitored at specified performance levels. The analysis procedure is approximate in that it represents a multi-degree-of-freedom (MDOF) building system by an equivalent single-degree-of-freedom (SDOF) system. The fundamental mode of vibration of the MDOF system is often selected as the response mode of the equivalent SDOF system. The selected vibration mode is the basis for estimating the distribution of static-equivalent lateral inertia loads applied over the height of the building. Specified deformation states are often taken as a measure of building performance at corresponding load performance. FEMA identifies operational, immediate-occupancy, life-safety and collapse-prevention performance levels, and adopts roof-level drift at the corresponding load levels as a measure of the associated behavior of the building. The increasing degree of damage that building experiences at the various performance levels are associated with earthquakes having increasing intensities of horizontal ground motion. Performance evaluation at the increasing intensities at various performance levels using response parameters in terms of damage indices are remarkably addressed [37] for further investigations in the present state of art.

2.7 Damage-Based Seismic Design of Structures

Seismic design code mainly allows reducing the earthquake forces in inelastic design if the structure has sufficient ductility and energy dissipation capacity through response reduction factor [46]. Although the intent of the code is to limit the structural damage associated with strength, stiffness, ductility, and energy demands, there is no unique procedure for evaluating for the damage potential for structures. Quantifying damage is complicated since

there are many uncertainties in damage assessment. Damage from the individual members to the entire structure is the main issue for damage assessment [47]. Dissipation of hysteretic energy in base isolated structures is economical way for controlling damages [48] and such method though are becoming the key issue of innovative seismic resistant design in the recent practice

Powell and Allahabadi [47], presented state-of-art reviews for the existing damage indices that have been used on the ground motion and structural parameters. The peak ground acceleration PGA, the peak ground velocity PGV, and spectrum intensity I_s have been used as damage indices; however, they do not correlate well with the observed damage. The ductility ratio μ, or simply ductility (the ratio of maximum deformation to the yield deformation) has been widely used as a damage index. Recent studies [49], however, have shown that ductility alone is not a reliable damage index because it does not account for the influence of the duration of strong shaking and the cumulative inelastic deformation. Lybas and Sozen [50] measured damage in structures as the ratio of the pre-yield stiffness to the secant stiffness corresponding to the maximum deformation. Zahrahh and Hall [27] recommended using the number of yield excursions in assessing damage in structures and proposed an equivalent number of yield excursions as

$$N_{eq}= \frac{E_{hm}}{Q_y u_y (\mu - 1)} \tag{2.4}$$

Where E_{hm} is the maximum hysteretic energy demand and Q_y is the yield strength of the structure.

Park and Ang [9] proposed the following damage index:

$$D_{PA} = \frac{u_m}{u_u} + \beta \frac{E_{hm}}{Q_y u_u} = \frac{\mu}{\mu_u} + \beta \frac{E_{hm}}{Q_y u_y \mu_u} \tag{2.5}$$

Where $u_u = \mu_u u_y$ is the ultimate deformation under monotonic static load, μ_u is the ultimate ductility, and β is a constant that accounts for the effect of cyclic earthquake load and structural properties. The index id based on the idea that earthquake damage is caused by the maximum deformation and hysteretic energy. Later, Park et al. [26] recommended an index $D_{PA} < 0.4$ for repairable damage (Immediate occupancy), $0.4 \leq D_{PA} < 0.7$ for slight damage (Delayed occupancy), $0.7 \leq D_{PA} < 1.0$ for severe damage (Life Safety), and $D_{PA} \geq 1.0$ for collapse (i.e., collapse). Using the dynamic test results for 261 reinforced concrete specimens, Park [26] found that the median of the constant β is approximately 0.15.

2.8 Energy Concept for Seismic Resistant Design

Principle of seismic resistant design

Seismic Capacity	≥	Seismic Demands
of		of
Stiffness		Stiffness
Strength		Strength
Maximum and minimum		Maximum and minimum
deformation capacity		deformation capacity
seismic energy		seismic energy

Estimation of capacity and demand in energy are the main concern of the design development in the recent past [8]. Damage due to excess of demand exceeding the elastic limit is the focus of performance based seismic design. Of all the design attributes, energy parameters are more close to damage and the damage in the design formats represent functionality as required for the downtime payment etc.

2.8.1 Design Principle Using Seismic Input Energy

The most fundamental problem in carrying out earthquake resistant design is to grasp the nature of seismic loading on the buildings. In this regard, energy should be considered as the principal loading effect on the building. In spite of high irregularity of ground motions, the energy input into a building is a stable quantity [8]. Energy absorbed by a structure can be predicted by tracing its restoring force characteristics. As a result the input energy by an earthquake and the energy absorbed by the structure, a quantitative prediction of deformation and damage of the structure can be obtained.

The total energy input exerted by an earthquake, E_I is absorbed by a structure as

$$E_I = E_S + E_p + E_h \tag{2.6}$$

where E_e denotes the elastic vibration energy. E_h is energy absorbed by miscellaneous damping other than inelastic deformations. E_p is the energy absorption due to inelastic absorption. The strain energy which occurs in a structure is expressed by $E_I - E_h$. Expressing elastic vibration energy as E_y, the condition under which a structure can remain almost elastic is

$$E_y \geq E_e = E_I - E_h \tag{2.7}$$

On the other hand for the severest earthquake, the input seismic energy is E_u; the energy absorbed by the inelastic deformation is E_u-E_h-E_e. Therefore denoting the entire inelastic strain energy absorbed by entire frame while the weakest story is brought to collapse state as Wu, the condition under which the structure can survive without collapse is

$$E_u \geq E_p = E_u - E_h - E_e \tag{2.8}$$

E_p is the sum of energy absorbed by each story, E_{pi}

The energy that can be absorbed by each story until it reaches a collapse state is denoted as E_{ui}, so that the equation (2.8) can be known by

$$E_{ui}, \geq E_{pi} \tag{2.9}$$

From the above discussion it is apparent that various performance levels can by identified through the energy content of the structure. Further separation of energy at the story level (sub-assembly) succeeded by energy at component levels can be conveniently be identified. Once the seismic input is known for the intended earthquake and the output seismic energy through the energy of various components. Using the capacity design, major energy dissipation may be confined in the desirable components and the other components are left in the elastic region. This will help the formulation of the energy of the structural components during the probable earthquakes. Such is requirement of PBSD.

How energy concept of seismic design can be applied to performance based seismic design? [13]. The possible answer comes through the comprehensive approach of PBSD. Conceptual design is the most important phase and has been enumerated [13]. Developing energy based capacity and demand expressions directly address the damage, as required for PBSD. Distribution of energy using the capacity design is the marvelous achievement in the past, where the performance can be embedded in the design formats. Identification and quantification of damages using the energy distribution at component levels and its redistribution into various energy parameters using the softwares have become possible in the recent past [10].

2.8.2 Energy Concept of Seismic Design

A wealth of literature [8, 12, 13, 14, 22, 24, 27, 29, 36, 43, 51, 52, and 53] on energy concept of seismic design reveals the scope and advantages of demand vs. capacity evaluation in terms of energy. Input seismic energy and the capacity of the structure in terms of energy are stable quantity [8]. The basic design attributes: stiffness, strength and ductility have close relationship with energy. Degradation of these mechanical

characteristics in terms of energy due to seismic hazards is related with damages of structural components, since seismic design of a structure is characterized considering the energy absorbing capacity at component levels. Input seismic energy has the relation with the stiffness and mass of the system since time period of the structure depends upon these two parameters. For input seismic energy when is consumed, purely by elastic strain energy regulates the performance criteria under frequent earthquakes. When the input seismic energy exceeds the elastic energy capacity, some members' yield depending upon their relative mechanical characteristics and dissipates seismic energy. Input seismic energy to a structure depends mainly the mechanical characteristics of the building structure, the peak ground acceleration , duration of earthquake and the soil-structure interaction etc. the concept of input seismic energy in terms of spectral velocity of the ground motions [12]. Blume [22] introduced the reserve energy concept of seismic evaluation of building structures. Uang C.M. and Bertero [24] emphasized absolute input seismic and relative input seismic energy. Both types of input seismic energy has their importance depending upon the type of structures e.g., strain energy, energy due to damping and kinetic energy is solely controlled by the relative energy. However, absolute input seismic energy is associated problems with rigid structures. Absolute or relative input seismic energy has their relevancy with the interaction of floor spectra and inter story drift [13].

2.8.3 Estimation of Strain Energy and Inelastic Energy

Strain energy is the energy capacity due to the configuration of the elements. This energy absorption depends upon the stiffness, and deformation capacity. Numerically, strain energy

$E_S = \frac{1}{2}kx^2$ (Average of the force- (kx+0)/2 multiplied by the deformation)

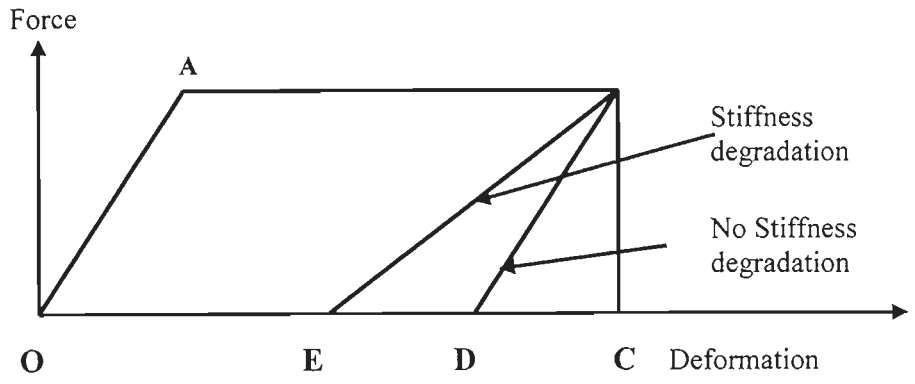

Figure 2.02 Force deformation relations for elasto-plasto components

$E_S = \frac{1}{2}\frac{F^2}{K}$, this implies that strength and stiffness influence the strain energy capacity. The equation in this format is important because these two material characteristics control the seismic behavior for performance levels: Occupancy (OP), and Immediate Occupancy (IO).

2.8.4 Energy Paths

Energy path is the tracing of the energy flow. Distribution of input seismic energy among energy components depends upon the energy path. Smooth distribution of the seismic energy is the major task of designer to insecure the mode of energy distribution

A plot of energy vs. load path has been carried in order to conceive the energy paths. The energy for elastic region OA is of quadratic nature followed by the straight line behavior for inelastic energy AB. When the structure is released at B, the path of recovery is also of quadratic having the magnitude for non degraded stiffness. For the degraded stiffness, the recovery of the strain energy is more resulting into less inelastic energy than the previous case.

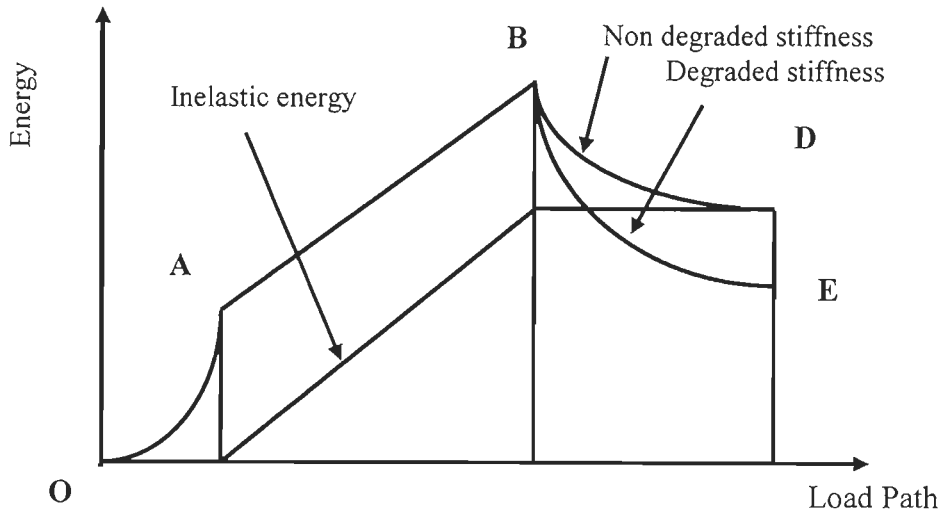

Figure 2.03 Plot of energy vs. load paths

Energy path is controlled through the distribution of mechanical characteristics of the structural system. Load path required for the transmission of inertia force developed at various positions of a structural system to the foundation and ultimately to the soil underlying the foundation. Load path should be minimum in order to avoid the distress in various components through which the load travels. Therefore, mechanical characteristics

are provided as the matching demand of input seismic demand and the corresponding energy capacity. The major task is the development of procedures which can incorporate these parameters into the seismic energy. Allowing the structure into the nonlinear inelastic regions requires the nonlinear analysis procedures. PBSD requires nonlinear analysis for the estimation of response; therefore, the inelastic energy analysis is conceived as performance evaluator.

2.9 Estimation of Input Seismic Energy

Housner used [12] the concept of spectral velocity for estimation of input seismic energy to a structure. Spectral velocity spectrum, being stable for a range of time period (medium rise building structure) [28], therefore, this value may be used fairly input energy through the square of the velocity with mass and divided by 2. i.e. the input energy to a structure is kinetic energy. While the capacity of the structure is one of its component is kinetic energy of mass. Here, the velocity is the spectral velocity of the structural components and comes into action only when the structures starts moving in MDOF's system. This expression of kinetic energy and the expression for energy during estimating input seismic energy is not the same. The spectral velocity for estimation of input seismic energy depends upon the soil structure interaction and the dynamic characteristics of the structure.

Earthquake imposes inertia force on a structure and the inertia force due to its inherent characteristic depends upon the initial condition of a structure. i.e., a body at rest will try to be at rest or in motion will try to be in motion, so long far an external agency (cause-generalized force) does not change it. The base of the structure moves during the seismic action, while the base tries to remain at rest. At the next moment, the base moves in the opposite direction, while the rest of the bodies have the tendency to move in the initial direction of the earthquake ground motion. Earthquake ground motion is to and fro or back and forth type of motion. Due to the inertial effect a demand is imposed on the structure and the demand as the product of the inertia force which is the product of rest mass and the absolute acceleration. Further, mass and absolute acceleration is multiplied with the absolute displacement gives the energy input on the structure. Here, the input seismic energy is as the inertial effect, therefore, more rational as a physical loading [55]. On the other side many of the researchers are of the opinion that the energy input during seismic action is the product of the inertia force multiplied by the relative displacement [25].

However, these two opinions lead the same fact differing only the energy value in terms of the kinetic energy in the absolute and relative motion.

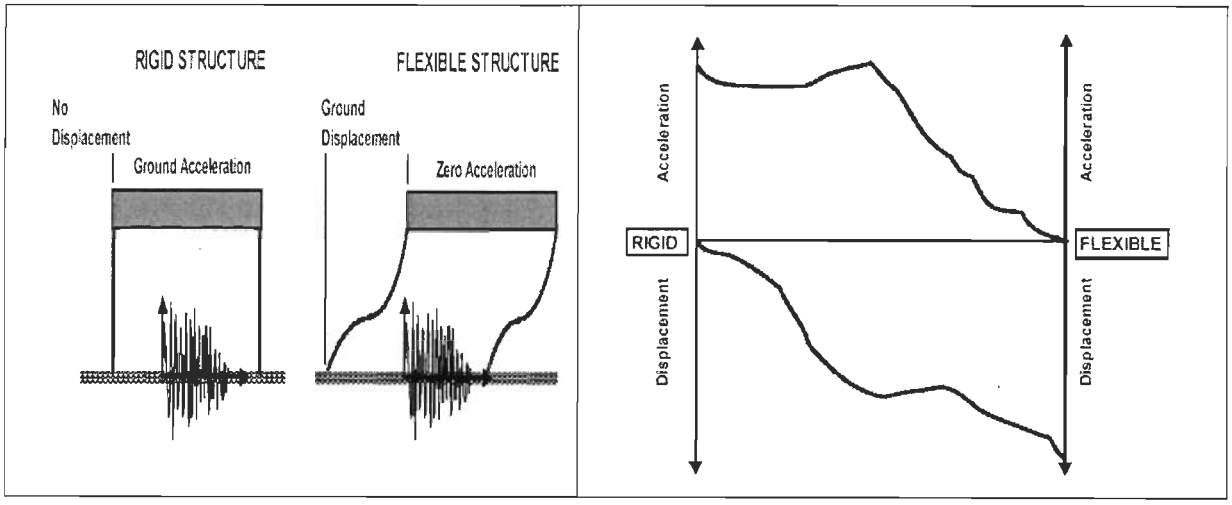

Figure 2.04 Response analysis of rigid and flexible body behavior under earthquake loadings.

A rigid body structure as shown adjacent has minimum displacement and the maximum acceleration including larger ground displacement shown in fig.2.04. The input seismic energy as absolute energy will be larger, while the relative energy will be smaller due to the minimum relative displacement. On the other hand for the highly flexible structure, the relative displacement is maximum and the absolute acceleration is minimum therefore, the relative energy will over rule the input energy as discussed.

Earthquake has been recognized as energy parameter more than a force because quantitatively energy is more rational [8]. The main task for design is the estimation of demand vs. capacity ratio and this ratio must be less than unity. Uncertainty during estimation of earthquake as force has been addressed by so many researchers with less uncertainty towards capacity. Interaction of demand and capacity during their estimation causes so many complex situations resulting into undesirable and furious results.

The dynamic response of a structure is defined by its displacement history, i.e., by the time variation of the coordinates which represent its degree of freedom. Only one equation is written for each degree of freedom system. Earthquake effect is due to the inertia forces, which depends upon the mass as well stiffness property of the structural systems. The distribution of inertia force controls the seismic behavior; however, damage identification is more in terms of energy. Physically absolute energy plays same role as inertia force due to earthquake loadings. In fact absolute energy is inertial effect in terms of input seismic energy. However, relative energy application for seismic resistant design has been popular because of its simplicity. In fact the complete solution of inertia forces acting

in a structure can be determined by evaluating the acceleration (and therefore the displacement) of every mass particle. In every real structure, this means that the displacements must be calculated for every point in the structure, which is a large computational task even in static analysis. This analysis can be simplified greatly if the deflection of the structure can be specified adequately by a limited number of displacement components or coordinates. Two assumptions are frequently used in this regard are lumped mass approach and the generalized coordinate approach.

Mechanical characteristic of the structural system needs to be expressed in terms of seismic energy for effective control of seismic response [8]. Estimation of mechanical characteristics, which is the prime aim of any seismic design based on the seismic demand in terms of absolute seismic energy, is highly potential to address the significant behavior under varying earthquake loadings.

Common approach for input seismic energy are Housner [12]; using pseudo velocity, Akiyama, 1985 using equivalent velocity, Uang and Bertero [24] using the absolute and relative energy approach. SC Goel et.al. [11]; energy factor has been used to incorporate the inelastic effect.

2.9.1 Estimation of Input Seismic Energy for MDOF Building Frames

Input seismic energy as in the SDOF system has been evaluated through the integral of inertia force developed at the roof level with the lateral displacement. The inertia force is the product of lumped mass and the absolute acceleration. For multistory frame the input seismic energy may be recognized as the sum of the input energy at various floors due to the corresponding inertia force and the lateral displacement [13].

Thus energy inputs at the various levels of building structure are added together algebraically to obtain the total input energy.

$$\text{Total input energy } (E_i) = \sum_{i=1}^{n=N} m_i a^t du_i$$

The MDOF's system may be further visualized as a SDOF system and the input seismic energy $(E_i) = Ma^t du$, where M is the equivalent mass, a^t is the absolute acceleration and du is the total displacement.

The input energy to the MDOF systems has been strongly supported in the literature [8, 13].

2.9.2 Energy Based Design

Force controlled design has the limitation due to its inability to trace the inelastic behavior with certain degree of accuracy. Deformation controlled design, though provides better information than force controlled design. However, use of this approach during earthquake loading due to rate and reversal of stresses, becomes difficult to trace out the actual deformation effect. Evaluating the cumulative ductility is computationally cumbersome in terms of time and space.

Energy is though the area of the enclosed curve in between the force and deformation, therefore it is being a more stable/robust design attributes. Plotting the energy ~displacement curve is linear for the inelastic response and varies in the quadratic form in the linear range. Strength and stiffness with ductility in terms of energy format may be expressed in terms of energy ductility, displacement ductility and strength reduction relation. As derived $\mu_e = \frac{2\mu - 1}{R_y^{\ 2}}$ where μ_e is energy ductility, μ is the displacement ductility, R_y is normalized strength factor, the normalized strength reduction factor involves the stiffness and strength characteristics, and both ductility in the above equation is related with the normalized strength. Using the capacity design, the energy based criteria is gaining strength in terms of localizing energy concentration and thus behavioral study in logical design formats in terms of normalized energy parameters. A brief historical overview of the energy concept based evaluation and design if described below:

Housner [12] emphasized the use of spectral velocity for the estimation of input seismic energy to a structure. Limit states application with the energy taking as design constraints was suggested for the effective use of energy based seismic design. Akiyama Hiroshi [8] used the equivalent velocity for the evaluation of input seismic energy with its variation to the time period. Demand and capacity estimation are independent without much more interactions, with a fair degree of accuracy. Mechanical characteristics are the design parameters, so the relation development in between energy and mechanical characteristics are desirable. Stiffness, strength and ductility are the base mechanical characteristics and these are the basic attributes of PBSD [4] also. For IO, stiffness is essential with strength as optional, for life safety strength is essential and stiffness is desirable and ductility is essential for collapse prevention with other parameters as desirable. With the emergence of capacity design, energy distribution in desirable manner became possible. The flow of input seismic energy to the structural components in definite manner is the core problem for energy based design criteria. Using capacity design, identification of region where the

energy concentration may be developed and the corresponding elements may be damaged in the prescribed manner was possible after 1970, the year for capacity design emergence.

Uang and Bertero [24] emphasized two types of input seismic energy, depending upon the situation. Absolute energy as the product of inertia force and the total displacement and the relative energy as the product of inertia force with the relative displacement were presented with the comment that absolute energy is the physical loading and justified for certain types of structural systems (rigid frames). Relative energy for flexible structures is useful energy estimation. The difference in between absolute and relative energy is of the kinetic energy and other energy components are same. For the absolute input energy the corresponding kinetic energy is absolute kinetic energy. For the absolute kinetic energy, the velocity tem is the sum of two components: ground motion velocity and the relative energy. For the rigid body the absolute energy is equal to the half mass and ground velocity square. The absolute energy for highly flexible system is nearly vanishes; however, the relative velocity is maximum. These two extreme values of energy have been used for the solution of floor spectra and lateral inter story drift as one of the task of the present study.

Evaluation of input seismic energy to a structure and the corresponding capacity in terms of energy have been the subject matter of the recent past literature with the assessment that mechanical characteristics of the structural system may have to be fully expressed in terms of energy, then this methodology of design will be fully used as design approach [8]. With the use of limit state extension to the energy based design, damage controlled issues are likely to be resolved since energy parameters are more close to damage [12]. Use of the energy based seismic evaluation and further its use for performance based seismic design with capacity design, has been recently subject of interest of researchers [13]. PBSD needs simplicity for further identification and quantification of damages under varying ground motions. Use of damage indices using normalized hysteretic energy were studied in the recent papers [14, 50, 51, 52, 53, 54]. Distribution of energy among its components and structural components are considered in the present study so that the uniformity may be maintained as required for performance based seismic design. Of all the energy components, strain energy and kinetic energy constitutes vibration energy. A close relation in between strain energy and hysteretic energy provides direct relations among various performance levels. Such related energy parameters have been developed in the next chapter as the major contents of the present study. Severe damages are found during rare earthquake ground motions. For such a condition, significant amount of energy gets

dissipated through yielding and the number of yielding has been identified as a powerful design aid for PBSD [27].

The content of the topic is to enumerate seismic design using energy concept and to use the concept as performance based seismic design [13]. Energy based design has the relation with the performance based seismic design once the overall design is controlled through capacity design accompanied with damage indices in terms of normalized energy.

2.9.3 Energy Attributable to Damage

The energy attributable to damage absorbed by translation is derived from the internal work for elastic-perfectly plastic models [8]

$$(E_D)_i = F_Y \delta_Y (0.5 + \eta)$$

Where the left part of the above equation is the energy attributable to damage absorbed by the i th member, δ_Y is the member yield displacement and η is the cumulative ductility as a damage measure. Further cumulative ductility η is defined as

$$\eta = \sum_{j=1}^{n} \mu_j$$

Where μ_j is the maximum plastic ductility at the j th yield excursion as obtained by the elastic-perfectly behavior, where n is the number of yield excursions. When the energy attributable to damage is expressed in terms of the equivalent velocity V_D, the member strength can be defined as

$$F_Y = V_D \sqrt{\frac{fkM}{1+2\eta}}$$

Where f is the fraction of energy attributable to damage absorbed by the member, M is the total reactive mass of the building, and k is the member stiffness. Distribution of energy is important for structural members.

Above relations define the relationship between strength and damage of a given member under a given earthquake showing that more flexible or stronger members suffer less damage. Due to cumulative formulations, the strength and damage relationship can also be applied several consecutive or a single earthquake with a long duration. Thus the equation (i) is not only valid for a single earthquake but also valid for a sequence of earthquakes during the design life of the structure [10].

2.9.3.1 Flexural Members

For flexural members the forces are measured in terms of moments, and deformations in terns of rotations. Hence the energy absorbed by the member becomes $M_Y\theta_Y$ $(0.5+\eta)$ replacing the right hand side of equation (i) where M_Y and θ_Y are the yield moment and rotations, respectively. For higher the value of strength reserve factor, the more will be energy absorbing capacity. In a structure where all members yield at the same time, its energy absorbing capacity is determined by the member with the smallest capacity, whereas in a structure where the member yields sequentially it is usually determined by the member which yields first..

2.9.3.2 Total Energy Input in Elastic-Perfectly Plastic Systems

The elastic vibrational energy has a range of

$0 \le W_e \le \frac{Q_y \delta_y}{2}$; Where Q_y is the horizontal force at the elastic limit, and δ_y is the displacement at the elastic limit. Total energy input for an elastic-perfectly plastic system as a steel moment frame is closely recognized as an elasto-plasto system [16].

For an elasto-pasto behavior, the amount of input plastic which is due to severe earthquake ground motion is $W_P = \eta \delta_y Q_y$; for an undamped inelastic system, the total input energy (E) is given by

$$E = W_E + W_P = \frac{1}{2} Q_y \delta_y + \eta Q_y \delta_y \qquad (2.10)$$

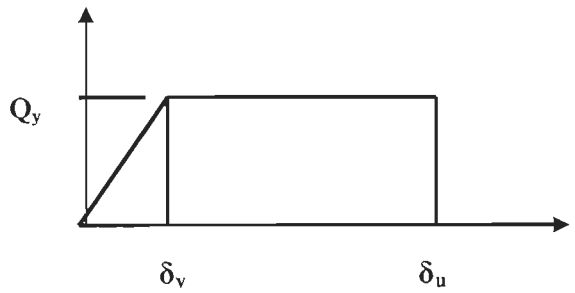

The above equation may be further extended in the simpler for as given below

$E = W_E + W_P = Q_y \delta_y (\eta + 0.5)$

Using coefficient of yielding α, the above equation may be further reduced as

$E = \frac{Mg^2 T^2 \alpha^2}{4\pi^2}(\eta + 0.5)$; Expressing the energy in terms of equivalent velocity

$$\frac{1}{2}MV_E^2 = \frac{Mg^2T^2\alpha^2}{4\pi^2}(\eta + 0.5)$$

$$\Rightarrow \frac{2\pi^2 V_E^2}{g^2T^2} = \alpha^2(\eta + 0.5) \tag{2.11}$$

The above equation indicates the fundamental relationship between strength (α) and damage (η) to a structure, in which α indicates the strength and η corresponds to the damage.

As the collapse of a structure usually occurs due to the accumulation of plastic deformation, η, thus directly indicate the approach of collapse. Non-structural claddings of buildings, such as exterior or interior walls which are laid on the structural body, can't follow an excessive deformation of the structure and may fail. This implies that η can also be used as indicator for non-structural damage since η can be considered to be proportional to the apparent deformation.

For constant value of equivalent velocity, since it is independent of the strength form the seismic design consideration, and neglecting the contribution of elastic vibration energy, damage η can be expressed as proportional to $(\alpha T)^{-2}$.

With α and T determined, η is calculated by numerical analysis of an earthquake and neglecting the elastic energy portion, we obtain in non-dimensional forms given below

$$E \Big/ \frac{Mg^2T^2}{4\pi^2} = \alpha^2\eta \tag{2.12}$$

The equation (2.12) provides a relation for the same energy input and the exchange of strength ~damage through their relation as below

$$\alpha^2\eta = \alpha^{*2}\eta^* \tag{2.13}$$

Using the equation (2.13), the damage may be evaluated for the varying strength of a structural system and the data generated may be used for further design algorithm.

Thus, we find the total energy input is denoted in terms of α and A, which is made dimensionless as follows:

$$A_E = E \Big/ \frac{Mg^2T^2}{4\pi 2} = \frac{2\pi^2 V_E^2}{g^2T^2} \tag{2.14}$$

It follows from equation (2.12) that if we neglect the terms 0.5, which represents the elastic vibration energy A_E is proportional to η.

2.10 Nonlinear Static Pushover Analysis Procedure: Energy Based Capacity Curve

Emergence of energy based nonlinear pushover analysis procedure is a recent advancement over the conventional pushover analysis procedures. The content of the present study is confined to the capacity curve formulation using the conventional pushover analysis procedures on steel building frameworks and the analysis results.

Capacity curve in terms of energy as ordinate and displacement as abscissa is developed, as the content of the present stud. Such a plot is a more rational for its use for performance evaluation as required for PBSD. Here, the capacity curve implies the capacity (energy) along the height of a building under lateral displacement due to the earthquake loadings

2.11 Distribution of Input Seismic Energy

McKevitte et al. [51] computed the input energy, hysteretic energy, and the ratio of the cumulative hysteretic energy to input energy for SDOF and MDOF structures (three- and ten-story) with different structural properties subjected to four earthquake records (El Centro 1940, Taft 1952, Parkville 1956, and Pacoima Dam 1971). They concluded that the energy dissipated through inelastic deformation depends on the force-deformation characteristics, yield strength, and damping. They observed that the percentage of input energy dissipated by the hysteretic action was approximately the same for different records. McKevitte et al. concluded that the ratio of the maximum hysteretic energy to the maximum input energy for an MDOF structure can be estimated from an SDOF structure with the same fundamental period, yield strength, and damping.

Zahrah and Hall [27] computed the input energy for eight earthquake records and proposed an equivalent number of yield excursions to quantify the earthquake damage potential. They observed that ductility, damping, and the post- to pre-yield stiffness ratios have small effects on the input and hysteretic energies for a structure with bilinear behavior. They stated that the equivalent number of yield excursions may be different for different accelerograms.

Akiyama [8] compared the input energy from the Fourier Spectra of ground acceleration for a five-story building with different structural properties, and for an equivalent one-story building having the same fundamental period, total mass, and yield strength using 1940 El Centro record. He showed that the total input energy transmitted to a

five-story building can be computed from the input energy transmitted to the equivalent one-story building with the same fundamental period, damping, and yield strength.

In a seismic design procedure based on energy, one should limit the structural damage by providing sufficient ductility and energy dissipation capacity by hysteretic action and/or damping in the structure. The damage potential is associated with the maximum hysteretic energy demand during the excitation and during the largest yield excursion. The hysteretic energy demand can be computed from the input energy spectra if the ratio of the maximum hysteretic energy to the maximum input energy E_{hm}/E_{irm} is known. To examine the relationship between hysteretic energy and damage potential three energy ratios are considered: 1) the maximum ratio of hysteretic to input energy $(E_h/E_{ir})_m$ generally occurring during the largest yield excursion, 2) the ratio of the maximum hysteretic energy to the maximum input energy E_{hm}/E_{irm} occurring at the end of the excitation, and 3) the equivalent number of yield excursions N_{eq}.

In developing an energy-based design approach and assessing the damage potential of structures, one must know the distribution of earthquake input energy among energy components: kinetic, elastic strain, hysteretic, and damping. This study examines the influences of the ground motion characteristics, and the structural properties: ductility, damping, and hysteretic behavior on the distribution of input energy for some steel building framework using various sets of ground motions.

The current seismic design practice which is based on strength principles (using the acceleration spectra) does not directly account for the influence of the hysteretic behavior of the structure. The hysteretic behavior is addressed indirectly by using the response modification factor R which is based primarily on the structural system selected. A design approach based on energy [1], on the other hand, has the potential to address the effects of hysteretic behavior directly.

The earthquake input energy transmitted to a structure consists of the kinetic energy, elastic strain energy, damping energy, and hysteretic energy. Kinetic energy reflects the work done due to inertia force. Elastic strain energy is the portion of the input energy stored in the structure in the form of elastic strain. Damping energy is the work done due to damping force. Hysteretic energy is the energy dissipated through the hysteretic action and is associated with the damage potential of the structure [Kuwamura and Galambos, 1989].

In an energy-based design approach, once the energy demand for a structure is estimated from the earthquake ground motion, the damage potential can be quantified by a combination of response and energy parameters [9]. Sufficient strength and energy

dissipation capacity should be provided in the structure for an acceptable damage threshold, i.e. a desired performance objective.

In seismic design of structures, the strength demand is defined by the story shear and the energy demand should be defined by the hysteretic energy for each story. While the strength and energy dissipation capacities can be increased by using members with larger area and section modulus or by using materials with greater yield strength, the energy dissipation capacity can be increased by using ductile structural systems such as the eccentrically braced frames (EBF) instead of concentrically braced frames (CBF), see Newmark and Rosenbluth 1971. The energy dissipation capacity for moment resisting frames can be increased by providing special detailing in steel and reinforced concrete

Ductility alone is a poor damage indicator [23]; however, deformation control design needs limited ductility with sufficient energy dissipation capacity. Global ductility composes various ductility Normalization of damage indices using ductility is a wealth of literature for using these as damage indices [5].

2.12 Normalized Hysteretic Energy

Hysteretic energy reflects the energy absorbing capacity during reversal of stresses. A wealth of literature [8, 14]. Once the hysteretic energy is normalized with respect to its counterpart during elastic region, i.e., through elastic strain energy, it becomes dimensionless and is useful as design aid. One of the main objectives is to incorporate normalized strength with or without stiffness or strength degradation for performance based seismic design [14]. Normalized hysteretic may be further used for evaluation of damage assessment under varying earthquake loading. Effect of PGA, time of earthquake and the frequency of earthquake are apparently observed through the normalized hysteretic energy. Performance based seismic design requires such type of the normalized energy parameters, since these have close relation with damages.

2.12.1 Number of Yield Excursion Cycles (NYEC)

The major task for quantification of damage range during successive increasing hysteretic loops through number of yield excursions has been recently recognized [27]. Such number of yield excursions has a close relation with amount of total energy dissipated during the reversal of stresses. Identification of threshold damage in terms of NYEC has been assessed as an effective tool for PBSD. Critical loading or capacity evaluation using NYEC also has been the part of literature for its strong relationship with PBSD [27].

2.13 Nonlinear Modeling for Basic Elements of Moment Resistant Frame

A model mimics a real structure. The accuracy of analysis results is the mirror image of the quality of model. A moment resistant frame comprises beam, column and panel zones as basic components. A wealth of literature is available for the nonlinear modeling of the basic components of moment resistant frame [17, 42]. All these documents have significant number of nonlinear elements required for modeling of steel building frameworks. Lumped plastic, distributed plastic models with finite element, fiber section have been successfully used in the recent past for evaluating damages.

2.13.1 Mass Matrix

Earthquake imposes loads through inertia force. Inertia force is proportional to the mass. For the sake of simplicity, the mass of a structure are commonly modeled in an equivalent lumped in place of consistently distributed matrix. It is found in frame analysis the use of distributed mass system is not much affected by the type of idealization through equivalent lumped mass [25].

Since the mass is lumped at the floor level, [M] is a sparse diagonal matrix with nonzero terms associated only with the horizontal degrees of freedom. The coefficient values of the mass matrix are assumed to remain constant during the dynamic response of the frame [25].

2.13.2 Damping Matrix

Energy dissipation in the form of damping is commonly idealized in linear elastic dynamic analysis as viscous or velocity proportional for convenience of solution. In reality, damping forces may be proportional to the velocity or to some power of velocity. Alternatively these forces may be of frictional nature, and in some cases they may even be proportional to displacements or relative displacements [25]. Once significant yielding takes place, hysteretic damping becomes a major source of energy dissipation. Hysteretic energy is comparable and so effective that a seismic design may be done for reliable seismic performance.

The most effective means of deriving a suitable damping matrix is to assume appropriate values of modal damping ratio for all significant modes of vibration of the structure and then compute a damping matrix based on this damping ratio Clough and Penzien, 1975 [54]. For simplicity the Raleigh type mass and stiffness proportional damping of the following is used

$$[C] = \alpha [M] + \beta [K] \tag{2.15}$$

Where α and β are constants derived by assuming suitable damping ratios for two modes of vibration. Using a normal coordinate transformation of the equations of motion the n-the mode damping ratio is

$$\lambda_n = \frac{\alpha}{2w_n} + \beta\frac{w_n}{2} \tag{2.16}$$

Where ω_n is the circular frequency of the n-th mode. For mass dependent damping λ_n is inversely proportional to the frequency such that the higher modes have little damping. [46].

2.14 Nonlinear Modeling

A wealth of literature is available for nonlinear modeling as required for inelastic behavior interpretation. Lumped plastic and distributed plastic models are commonly used for research activities, since all situations the chances of concentration of actions is likely. Fast non linear analysis requires the concentration of seismic actions [42]. Damage assessment is the mirror image of the accuracy of the nonlinear model.

2.15 Ductility

A wealth of literature is available [5] on ductility. Overall, ductility of a structure depends upon the ductility at component levels, cross section, curvature etc. Story ductility is related with ductility at component levels through the ductility of connection has been subject of researches [5].

Chapter 3

PROBLEM FORMULATION

3.1 Introduction

A crucial part of the PBSD is selection of basic performance objectives corresponding to different levels of seismic hazard and a suitable method for preliminary design in order to minimize the number of iterations for achieving the performance objectives (Flow charts 3.1 3.2, and 3.3). An important aspect of PBSD is the design verification at all stages of design process. The verification process involves linear and nonlinear analyses to obtain structural response quantities based on the selected performance objectives.

A performance level is a statement of the desired building behavior when it experiences earthquake demands of specified severity. Four building performance levels are defined in the literature [3], namely, Operational (OP), Immediate Occupancy (IO), Life Safety (LS) and Collapse Prevention (CP). Different levels of seismic hazard are prescribed corresponding to each of these performance levels.

Four levels of seismic hazards-corresponding to 50%, 20%, 5%, and 2% probability of exceedence in 50 years-have been prescribed in FEMA-273 [3] for different performance levels.

The design base shear for different levels of seismic hazard is given by

$$V_B = (S_a^i/g)\, Wb \qquad i = OP, IO, LS, CP \tag{3.01}$$

where, the superscript i refers to building performance; Sa^i is the spectral response acceleration; and W_b is the seismic weight of the particular moment frame of the building under consideration.

The spectral response acceleration Sa^i for a performance level is calculated by the following equations:

$$Sa^i = \begin{cases} Fa^i Sa^i \left(0.4 + \dfrac{3T_e}{Ta^i}\right) & 0 < T_e \le 0.2T_0^i \\ Fa^i Sa^i & 0.2T_0^i < T_e \le T_0^i \\ \dfrac{F_v^i S_1^i}{T_e} & T_e > T^i{}_0 \end{cases} \qquad i = OP, IO, LS, CP \tag{3.02}$$

where T_0 is the time period corresponding to the performance levels, and T_e is the time period of the concerned structure. S_s, S_1 F_a and F_v are design spectra parameters.

A complete design objective specification is composed of a quantified structural performance description corresponding to specified earthquake intensity. A commonly defined objective called the Basic Safety Objective requires the building to be designed to achieve both the LS performance level for a 10/50-year earthquake and the CP performance level for a 2%/50 year earthquake. Other desired design objectives are: achieving the IO performance level for a 20%/-50 year earthquake, and the OP performance level for a 50%/-50 year earthquake. An illustrative example of determination of design spectra parameters is presented in chapter 4.

Performance based seismic design is commonly conceived through design improvement or it is optimum structural design where desirable performance are achieved during varying seismic demands with assigned performance objectives as the design goal through iteration procedures. The number of iterations depends upon the adequacy of the preliminary design. Existing design philosophy and design formats are the base where from foundation of PBSD is laid. In this context, limit states design extension in order to accomplish performance objectives of PBSD having the design philosophy of working stress, ultimate limit states, capacity design are the contents of recent past literatures [23]. Force based design is under the criticism for performance based evaluation under varying earthquake ground motions due to its inability to capture the damage assessment, since PBSD is a nonlinear analysis based design. Deformation controlled design though have been closely related to PBSD due to its ability to assess damages under earthquake loadings. However, the cumulative deformation due to successive earthquake ground motions is always judicious. The manner how the seismic action is applied with its further distribution has been recently addressed using the energy concept. Formulations of damage indices in terms of energy components make its suitability for PBSD [13]. Park and Ang damage model [9] specifies damage distribution based on the idea that earthquake damage is caused by the maximum deformation and hysteretic energy. Park et al [26] recommended an index for repairable damage (Immediate occupancy), slight damage (Delayed occupancy) for severe damage (Life safety) and collapse based on the quantitative assessment of the normalized damage index. Steps of the problem formulations with the reference of present state of art have been identified for the present study and listed below:

Assumptions made during the study are:

- Building structures are 2D frames.
- Deterministic approach has been used.

- Force deformation relation during nonlinear modeling has been considered as elasto-plastic.
- Centre line dimensions have been used for dimensioning.

3.2 Formulation of Performance Objectives for the Present Study

Using the guidelines of FEMA-273 [3], performance levels have been formulated and presented as the content of the present study in the chapter 4, for development of design algorithm in this study. The base shear for each performance level has been evaluated from the guidelines of FEMA-273, 1997 for the performance objectives assigned to the present study. Using scale factors, a set of earthquake ground motions in-built in RAM perform 3D have been applied to the building framework modeled in this study.

3.3 Problem Formulation

PBSD is structural design for acceptable damages (performance levels) corresponding to the specified earthquake ground motions (seismic hazard). For achieving the assigned performance objectives under earthquake ground motions, objectives functions have to be developed.

3.3.1 Objective Functions

Keeping in view of the present state of the art, objective functions considered for the present study are: formulation of performance objectives, estimation of input seismic energy, evaluation of structural response (identification of energy components and their distribution) and building damages (using hysteretic energy, relation in between energy parameters etc, minimization of damages) under varying earthquake ground motions. Minimizing the damage to the building under earthquake loading is most favorable design objective. In fact, it is the post earthquake damage cost that addresses the downtime payment including its own cost for recovery of structures. Death and direct damage cost also comes under this purview. Damage cost during Northridge and Kobe earthquakes were so high that even the developed economy of these two countries disallowed such high damages during earthquakes. It is high time to formulate structural damage in terms of structural response (energy as considered in this study).

One way to quantify the amount of damage to a structure is by damage index [9]. A damage index is expressed as a combination of the damage caused by excessive deformation and that caused by repeated cyclic loading. Several damage index expressions

are available, but none of them are widely applicable. Since the damage index concept is still as issue under development [7, 37] further its evaluation involves the calculation of hysteretic energy, which is beyond the capability of static pushover analysis, however, this study use damage indices to quantify building damage.

Another way to quantify the level of damage to a building is to establish relation ship between damage and inter story drift. Inter story drift is the primary parameter in evaluating structural performance [3] and is widely regarded as a major parameter characterizing the extent of plastic deformation of a building [56]. Energy demand and the energy supply (capacity) constitute a balanced design under earthquake loadings. Identification and quantification of energy components under earthquake ground motions have close relations with damages. For example, strain energy has two components: Elastic and inelastic energy. Yielding of structural components results into the inelastic energy. The inelastic strain energy is due to monotonic deformation or due to reversal of stresses (hysteretic energy). These two energy components are responsible for damages. Steps for problem formulations are listed below:

3.3 2 Steel Building Frameworks used in the Present Study

Five sets of steel frame buildings have been taken from the literature where these frames have been used for performance evaluation using various methodologies and are well conceived for using these frames for data generations to be required for further development of design algorithm. These building frames have been used for performance evaluation under the varying ground motions by researchers [7, 56, and 57] in the past so, the advantage of these building frames is that their mechanical characteristics are well defined and many of their response parameters have been documented. The present study uses these building frameworks with some modifications for the evaluation to get the response parameters. Details of the building frames have been given in the chapter 4 for modeling and analysis and use of response parameters for further investigation [Example problems: 4.3.1, 4.3.2, 4.3.3, 4.3.4, and 4.3.5].

3.3.3 Modeling for Linear and Nonlinear Analysis

Performance based seismic design is mainly to diagnose the damages, therefore, needs nonlinear analysis. The method of modeling is the major task for controlling the nonlinear analysis. A model replicates real problem. Therefore, frame steel building must be modeled for nonlinear behavior. It is the components, which are modeled for yielding when the

demand exceeds the yield strength. A steel building frame composes beam, columns, and panel zones and combined together by connections. Beams are allowed to yield in stable manner. For this a beam is modeled as two components: elastic and plastic. Yields are allowed at both ends of beam columns at the ground floor [17].

3.4 Input Seismic Energy Evaluation

The manner how seismic demand is estimated on a structure has a great impact on the design methodologies due to randomness of earthquake ground motions. Input seismic demand in term of energy has been found more stable since earthquake ground motions are random. Effect of period of ground motions, frequency of earthquake and the peak ground acceleration all three important parameters may be observed through apparent changes of energy demand. Cumulative and residual seismic effect, while a structure is in the inelastic region, energy based evaluation gives reasonable initial boundary condition. While demand is in terms of energy, it is easy to develop corresponding structural capacity in terms of energy. Identification and quantification of damages in terms of energy have been found reasonably more attractive. Since PBSD is the extension of limit states, any design development using the limit states in energy parameters are becoming popular. Inelastic energy is directly related to the damage. As damage indices have not been popular and needs further simplification, since these damage indices require nonlinear dynamic analysis. Due to the advancement in computational technique, and know how technique for nonlinear modeling in softwares, the possibility for damage assessment through nonlinear dynamic analysis under earthquake loading is feasible in the present state of at. In order to estimate the input seismic energy, the following methodologies have been reassessed.

3.4.1 Energy Evaluation using Pseudo Velocity Spectra

$$\text{Input seismic energy} = \frac{1}{2} M S_{pv}^{\ 2} \qquad [12] \tag{3.03}$$

Where M is the mass and S_{pv} is the spectral velocity, which has be derived for each ground motions used in the present study (Figures 5.01 to 5.05). Energy input per unit mass is complete functions of spectral velocity of the site for the specified accelerogram. Such kind of input seismic energy evaluation supports for the use of the energy expression of SDOF system for evaluating the energy input for MDOF system [8]. The input seismic energy using expression (3.3) remains as elastic strain energy, use of energy correction factors with the input energy evaluated above provides inelastic energy, which is desirable, since a

structure is allowed to inelastic region to take advantages of ductility. The energy based design is based on the energy spectra expressed in terms of velocity spectra. Relations of acceleration and velocity spectra shows that the higher input energy does not always corresponds to the higher acceleration. [10]. Pseudo velocity is related with the pseudo acceleration and pseudo displacement through time period. Pseudo Velocity spectra is independent of period of vibration, therefore has been recognized more table for input seismic action evaluation.

A comparative statement has been prepared for input seismic energy using the velocity spectra, energy ductility and energy correction factor for inelastic response and energy evaluated directly from software have been compared in order to develop simplicity for the evaluation of input seismic energy.

3.4.2 Absolute Input Seismic Energy

Energy based design has been proposed by Housner [12] as alternative to criterion of inelastic design response spectra (IDRS) for the earthquake resistant design of buildings. Two types of energy equations: absolute and kinetic under the earthquake loadings have been content of literature review. Absolute energy equation is physically more meaningful [24], since such input energy is the consequence of inertia effect on the structure. Absolute kinetic energy corresponding to the absolute input seismic energy is of great importance for interpretation for floor spectra and interstory drift relation.

Using the dynamic equilibrium equation in terms of absolute acceleration as the basic equation, absolute input seismic energy is estimated through integration of motion of an inelastic system shown as follows:

$$\int_0^U M\ddot{U}_t\left(du_t - du_g\right) + \int_0^U C\dot{U}\,du + \int_0^U F_S\,du = 0 \tag{3.04}$$

$$\int_0^U M\ddot{U}_t\left(du_t\right) + \int_0^U C\dot{U}\,du + \int_0^U KU\,du = \int_0^U M\ddot{U}_t\,du_g \tag{3.05}$$

$$E_{abs} = \frac{1}{2}M\dot{U}_t^{\,2} + \frac{1}{2}C\dot{U}^{\,2} + \frac{1}{2}KU^2 + \text{Hysteretic energy} \tag{3.06}$$

The left side of the equation (3.06), i.e., E_{abs} is the absolute input energy to the structure since the earthquake excitation began.

3.4.3 Relative Input Seismic Energy

Relative displacement is the subject concerned of relative input energy evaluation. For highly flexible structures, relative input seismic energy of great important. Integrating the equation of motion of an inelastic system as follows input relative seismic energy is known:

$$\int_0^U M\ddot{U}_t\,du + \int_0^U C\dot{U}\,du + \int_0^U F_S\,du = 0 \tag{3.07}$$

$$\int_0^U M(\ddot{U}+\ddot{U}_g)du + \int_0^U C\dot{U}\,du + \int_0^U F_S\,du = 0 \tag{3.08}$$

$$\int_0^U M\ddot{U}\,du + \int_0^U C\dot{U}\,du + \int_0^U KU\,du = -\int_0^U M\ddot{U}_g\,du \tag{3.09}$$

$$E_{rel} = \frac{1}{2}M\dot{U}^2 + \frac{1}{2}C\dot{U}^2 + \frac{1}{2}KU^2 + \text{Hysteretic energy} \tag{3.10}$$

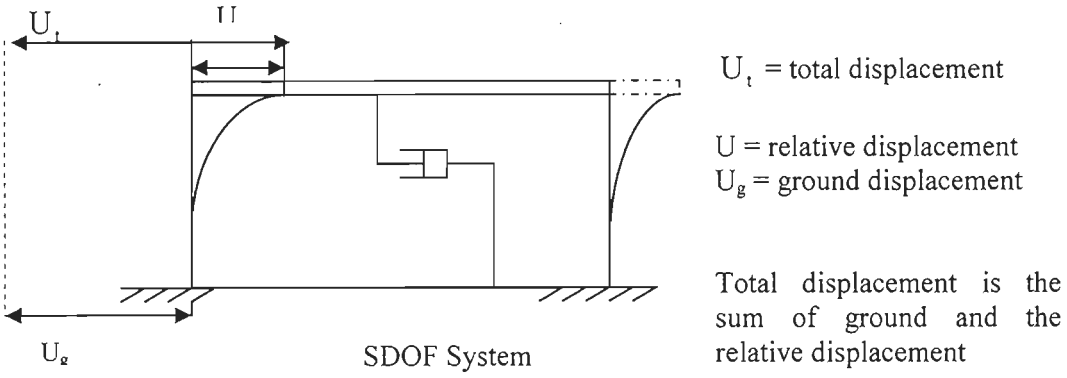

Figure 3.01 Absolute and relative displacement relationship

Equations (3.06) and (3.10) represent the relative input seismic energy. They differ only because of the kinetic energy in terms of absolute and relative velocity.

3.4.4 Input Seismic Energy for the Inelastic Structure using Energy Balance Equation

The energy balance equation concept has been used by early researchers to determine constant ductility inelastic design spectra [58, 59]. New mark showed that the response of the elastic-plastic systems in a certain range of periods can be determined by assuming that the energy computed from the monotonic load-deformation response of the inelastic system and its corresponding elastic system is the same.

$$\frac{1}{2}MS_v^2 = E_e + E_P \tag{3.11}$$

Where M is the mass of the system, S_v is the pseudo velocity; E_e and E_P are the elastic and the plastic yield energy under monotonic load-deformation response, respectively.

As recognized by New mark, the above equation (3.11), using the inelastic design spectra developed by New Mark and Hall showed that the energy balance equation can be modified so that it can be used for all period. Lee and Goel introduced the energy factor, γ and modified the energy balance equation as follows

$$\gamma\frac{1}{2}MS_v^2 = E_e + E_P \tag{3.12}$$

In which γ is defined as the ratio of the energy absorbed by the inelastic system to that of the equivalent elastic system. For a system with load-deformation characteristic as shown in the figure 3.02, the energy factor is defined as γ, can determined

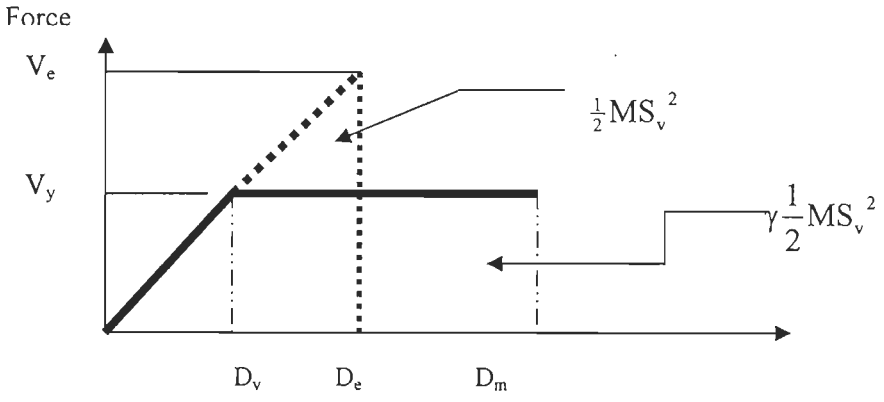

Figure 3.02 Lee and Goel's energy balance concept (2001)

$$\gamma = \frac{E_e + E_P}{\frac{1}{2}MS_v^2} = \frac{\frac{1}{2}V_yD_y + V_y(D_m - D_y)}{\frac{1}{2}V_eD_e} = \frac{2\mu - 1}{R_y^2} \tag{3.13}$$

Where V_y is the yield strength, D_y is the yield displacement, D_m is the maximum inelastic displacement, V_e is the maximum force in the corresponding elastic system, and D_e is the maximum displacement in the elastic system, μ is the displacement ductility factor and R_y is the yield strength reduction factor. The yield strength reduction factor, R_y is generally a function of the displacement ductility μ and the period of the system.

In order to determine the energy factor from equation (3.13), a relationship between R_y- μ-T is needed. This relationship has been a subject of much research in the past and various researchers have proposed several methods that relate the yield strength reduction

factor to the ductility level for different period ranges of the system. Using R_y- μ-T equations such as the one developed by New mark and Hall, the energy factor γ can be computed, for given ductility level and the period of the system. Using the energy factor, the energy balance equation can be applied for all period ranges.

3.4.5 Input Seismic Energy for the Inelastic Structure using Energy Balance Equation for MDOF Systems

The energy balance equation for MDOF systems is based on the concept of equivalent single degree of freedom system.

The final equation of energy balance for MDOF systems is

$$\gamma \frac{1}{2} M_n^* S_v^{\,2} = E_e + E_P \tag{3.14}$$

The left side of the equation (3.14) is the energy demand and the right hand side of the equation is the absorbed energy or the work done by the lateral forces to push the system monotonically up to the maximum displacement. The above equation also shows the concept of equivalent simple oscillator by Housner which can be extended into the inelastic range. The energy balance concept as discussed earlier has been successfully applied in the design framework called Performance Based Plastic Design [11].

The conventional pushover analysis results are used for energy capacity and using the demand in terms of energy, the required displacement is obtained through the intersection of energy demand and energy capacity. Further the displacement corresponding to the performance point for estimation of other parameters.

In dealing with MDOF systems, the concept of displacement ductility may be some what difficult to define. Energy ductility (μ_E) is the ratio of the energy corresponding to the total energy to the energy corresponding to the yield is used.

$$\mu_E = \frac{V_y D_m - \frac{1}{2} V_y D_y}{\frac{1}{2} V_y D_y} = 2\mu - 1 \tag{3.15}$$

From equations (3.14) and (3.16), we can write this energy factor in terms of energy ductility as following

$$\gamma_E = \frac{\mu_E}{R_y^{\,2}} \tag{3.16}$$

Expressing normalized strength (R_y) in terms of energy ductility, the above equation can be expressed into the equation (3.17)

$$\gamma_E = \frac{\mu_E}{\left(\frac{\mu_E + 1}{2}\right)^2} = \frac{4\mu_E}{(\mu_E + 1)^2} \tag{3.17}$$

For the given displacement ductility, the energy correction factor can be estimated. In order to get energy correction factor, equation (3.17), displacement ductility is required. Using nonlinear static pushover analysis procedures, the value of the displacement for performance levels may be suitably used for estimating, energy ductility.

3.5 Energy Based Capacity Curve

Energy based derivation using the various approaches in the literature, provides a clear in site for further development of the concept for performance evaluation under varying earthquake ground motions. One of the aims of the present study is formulation of capacity curve using data base form the conventional pushover analysis procedures on steel building frameworks. Capacity curve in terms of energy as ordinate and displacement as abscissa is developed, as the content of the present study. Such a plot is a more rational for its use for performance evaluation as required for PBSD. Here, the capacity curve implies the capacity (energy) along the height of a building under lateral displacement due to the earthquake loadings. The conventional nonlinear static push over curve for a given earthquake have been used for data base using the excel program. Further, using the distributed base shear for a particular ground motion and the corresponding lateral displacement at the various floor levels.

From energy balance equation (3.12) the right side of the equation

i.e., Capacity (Energy) = lateral load at the floor level x corresponding lateral deformation

$E_I = E_e + E_p$ = Sum of elastic energy and plastic energy (3.18)

Data generated from well conceived building frameworks under pushover analysis in terms of base shear and lateral displacement will be used for evaluation of capacity of the structure in terms of energy. (i) Energy versus lateral displacement plot

The conventional pushover analysis data have been used in this research program for the energy capacity curve formulation. Perspective response of pushover curve may provide significant information for the possible degradation or formulation of hinges in sequence

under varying ground motions. A building structure under pushover loading deflects and the relation up to elastic behavior is elastic strain energy, which is of quadratic in displacement. When either of the component yields, energy is being controlled through plastic energy and depends upon how many elements are yielded first and in sequence. Using the slope properties of energy vs. displacement curve the trend of the sequence of hinge formation can be predicted. If all limited components are yielded at a time, the slope of energy vs. displacement becomes constant increasing. During this region the structure counter balance the demand through only energy dissipation

3.6 Floor Spectra and Inter Story Drift Relation

Identification and quantification of structural and non-structural damages during the earthquake ground motions are the main aim of performance based seismic design. Non structural damage is the function of the lateral drift or floor spectra or both. It has been perceived that a ductile structure is more sensitive to the lateral drift and less sensitive to the floor spectra while a rigid structure behaves just in the opposite manner. As per the literature, the physics of the inverse relation is the least understood [13]. Such a problem has been recognized during the energy based development and the reason behind such relation has been resolved as a content of the present study.

Rewriting equation (3.06) as equation (3.19) and equation (3.10) as (3.20)

$$E_{abs}\ (\text{Absolute input seismic energy}) = \frac{1}{2}M\ddot{U}_t^{\,2} + \frac{1}{2}C\dot{U}^{\,2} + \frac{1}{2}KU^2 + E_{H\mu} \qquad (3.19)$$

E_i (Absolute input seismic energy) = Absolute kinetic energy + Structural damping energy dissipation + Strain energy + Hysteretic Energy

$$E_{rel} = \frac{1}{2}M\ddot{U}^{\,2} + \frac{1}{2}C\dot{U}^{\,2} + \frac{1}{2}KU^2 + \text{Hysteretic energy} \qquad (3.20)$$

E_{rel} = Relative kinetic energy + Structural damping energy + Strain energy + hysteretic energy

E_{abs}-E_{rel} = Absolute kinetic energy-Relative kinetic energy (3.21)

Sum of vibration energy in equation (3.19) is controlled by absolute kinetic energy. The absolute kinetic energy is due to the ground velocity, while the relative kinetic energy depends upon the relative velocity (sum of kinetic energy and the elastic strain energy at floor constitutes vibration energy). For the same value of elastic strain energy, the floor spectra is higher for greater value of the absolute kinetic energy and the inter story drift is

smaller due to the smaller value of the relative velocity. Such situation arises for rigid body under the ground motions. For flexible structure the condition of absolute and relative energy is reverse, i.e., the relative velocity is more than the ground motion. Energy based such approach for interpretation of larger floor spectra with smaller inters story drift and vice-versa has been verified in the chapter 4.

The derived equation (3.24) for relation in between the absolute acceleration and the velocity at any floor supports the floor spectra and inter story drift on the basis of tow types of energy contents.

3.6.1 Interpretation of Floor Spectra and Inter Story Drift Relation with Velocity and Absolute Acceleration

If V_D is the velocity of mass on the building frames (mass is lumped on the floor levels), then the input energy is given as

$$W_e = \frac{1}{2} M V_D^{\,2} \tag{3.22}$$

Further, the energy stored in the system may be estimated as

$$W_e = \frac{Q_y \delta_y}{2} = \frac{Q_y^{\,2}}{2k} = \frac{\alpha^2 (Mg)^2}{2M\omega^2} = \frac{T^2 Mg^2}{4\pi^2} \times \frac{\alpha^2}{2} \tag{3.23}$$

$$Q_y = k\delta_y \Rightarrow \delta_y = \frac{Q_y}{k};\ \alpha(\text{Coefficient} - \text{of} - \text{yielding}) = \frac{Q_y}{Mg}$$

Equating energy from equations (3.22) and (3.23)

We get a relation in between velocity and absolute acceleration as

$$\omega V_D = \alpha g \tag{3.24}$$

For higher the value of the velocity, the more will be the absolute accelerations. On the ground, such acceleration is known as spectral acceleration and these values on all floors except ground are known as floor spectra. Thus, the floor spectra are directly related with the absolute kinetic energy.

3.7 Distribution of Input Seismic Energy

Performance of a structure under the seismic load depends upon the distribution of input seismic energy among energy components as well as members (Flow chart 3.4). Left side of the energy balance equation (3.25) is input seismic energy and right side represent the energy distributed among energy components. A component is capable to absorb a significant amount of energy as elastic strain energy and dissipates energy through damping in the elastic region. Rest of the energy is dissipated through yielding in the inelastic region. Therefore, distribution of energy among its components is the first task for further proceeding to design

$$E_i = E_S + E_K + E_D + E_{h\xi} \tag{3.25}$$

The energy balance equation (3.25) is derived through integration of SDOF system for the period of earthquake ground motion.

Dividing equation (3.25) by the input seismic energy to both sides of the equation

$$1 = E_S/E_i + E_K/E_i + E_D/E_i + E_{h\xi}/E_i \tag{3.26}$$

Equation (3.26) is in the normalized form, where the normalizing parameter is input seismic energy itself. Expanding the various energy parameters on the right side of the equation (3.26), the following simple normalized values, we get.

3.7.1 Normalized Strain Energy $= \dfrac{\frac{ku^2}{2}}{\frac{1}{2}ms_{pv}^2} = \omega^2\left(\dfrac{u}{s_{pv}}\right)^2 = \left(\dfrac{u}{s_d}\right)^2$ (3.27)

Where u is the relative displacement and S_d is the spectral displacement. In the absence of other energy, the normalized strain energy will be one.

3.7.2 Normalized Kinetic Energy $= \left(\dfrac{\dot{u}}{s_{pv}}\right)^2$ (3.28)

Where the numerator is relative velocity and the denominator is the pseudo velocity.

3.7.3 Normalized Damping Energy $= 2\xi\omega_n\left(\dfrac{\dot{u}}{s_{pv}}\right)^2$ (3.29)

Equations (3.28) and (3.29) reveal that normalized damping and kinetic energy ratio is $2\xi\omega_n$

e.g., T=0.1 sec, damping coefficient =3%, the normalized ratio is 3.77

3.7.4 Normalized Hysteretic Energy $= (\mu_i - 1) \times \left(\frac{u}{s_d}\right)^2$ (3.30)

This implies that normalized strain energy is related with the normalized hysteretic energy by a factor equal to cumulative ductility minus 1.

As discussed above distribution of input seismic energy among its components is required for making the design decision.

Validation of normalized energy components from equations (3.27) to (3.30) requires time history analyses analysis and spectral velocity of the ground motions.
Response parameters in terms of energy after nonlinear analysis of representative steel building frames under varying earthquake ground motions will be the contents of the next chapter: modeling and analysis.

Some more investigations based on the structure and ground motion interaction in terms of energy input and mechanical characteristics will be formulated as following.

3.8 Energy Input in Elastic-Perfectly Plastic Systems

Input seismic energy in terms of mechanical characteristics is required for the proper flow of energy to a structural system [8] and algorithm development for better seismic response in terms of design format.

The elastic vibrational energy has a range of

$0 \le W_e \le \frac{Q_y \delta_y}{2}$; Where Q_y is the horizontal force at the elastic limit, and δ_y is the displacement at the elastic limit.

Total energy input for an elastic-perfectly plastic system as a steel moment frame is closely recognized as an elasto-plasto system [16].

For an elasto-pasto behavior, the amount of input plastic which is due to severe earthquake ground motion is $W_P = \eta \delta_y Q_y$

For an undamped inelastic system, the total input energy (E) is given by

$E = W_E + W_P = \frac{1}{2} Q_y \delta_y + \eta Q_y \delta_y$: Where η is cumulative ductility

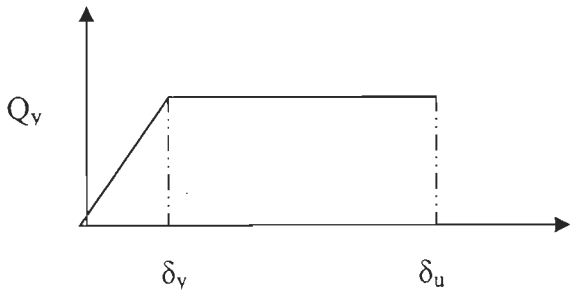

Figure 3.03 Energy input in elasto-plastic behavior of a steel frame

The above equation may be further extended in the simpler for as given below

$$E = W_E + W_p = Q_y \delta_y (\eta + 0.5)$$

Using coefficient of yielding α, the above equation may be further reduced as

$E = \frac{Mg^2T^2\alpha^2}{4\pi^2}(\eta + 0.5)$; Expressing the energy in terms of equivalent velocity

$$\frac{1}{2}MV_E^{\ 2} = \frac{Mg^2T^2\alpha^2}{4\pi^2}(\eta + 0.5)$$

$$\Rightarrow \frac{2\pi^2 V_E^{\ 2}}{g^2T^2} = \alpha^2(\eta + 0.5) \qquad (3.31)$$

The above equation indicates the fundamental relationship between strength (α) and damage (η) to a structure, in which α indicates the strength and η corresponds to the damage and depends upon ductility.

As the collapse of a structure usually occurs due to the accumulation of plastic deformation, η, thus directly indicate the approach of collapse. Non-structural claddings of buildings, such as exterior or interior walls which are laid on the structural body, can't follow an excessive deformation of the structure and may fail. This implies that η can also be used as indicator for non-structural damage since η can be considered to be proportional to the apparent deformation.

For constant value of equivalent velocity, since it is independent of the strength form the seismic design consideration, and neglecting the contribution of elastic vibration energy, damage η can be expressed as proportional to $(\alpha T)^{-2}$.

With α and T determined, η is calculated by numerical analysis of an earthquake and neglecting the elastic energy portion, we obtain in non-dimensional forms given below

$$\frac{E}{\frac{Mg^2T^2}{4\pi^2}} = \alpha^2\eta \tag{3.32}$$

The equation (3.33) provides a relation for the same energy input and the exchange of strength vs. damage through their relation as below

$$\alpha^2\eta = \alpha^{*2}\eta^* \tag{3.33}$$

Using the equation (3.33), the damage may be evaluated for the varying strength of a structural system and the data generated may be used for further design algorithm.

SDOF system in terms of ductility as the content of standard form for the dynamic equilibrium, reveal that for the higher earthquake intensity, through reducing the strength the demand can be accommodated by the larger value of the ductility. i.e., lower the yield strength, higher will be ductility implies more damage for lower strength. Such a relation fits for strength damage evaluation under varying ground motions.

Thus, we find the total energy input is denoted in terms of α and A_E, which is made dimensionless as follows:

$$A_E = \frac{E}{\frac{Mg^2T^2}{4\pi 2}} = \frac{2\pi^2 V_E^{\ 2}}{g^2T^2} \tag{3.34}$$

It follows from equation (3.31) that if we neglect the terms 0.5, which represents the elastic vibration energy A_E is proportional to η. i.e., higher input seismic energy causes more damage in terms of cumulative ductility.

Equation (3.31) is expanded and the energy absorption (E_{Di}) of a single component is known through the distribution of input seismic energy, an effective expression is obtained

$$F_Y = V_D\sqrt{\frac{fkM}{1+2\eta}} \tag{3.35}$$

Where V_D, is the velocity attributable to damage, f is the fraction of energy absorbed by a particular member, K is the stiffness, M is the mass, and η is the damage coefficient.

Expanding the equation (3.35), damage coefficient (η) can be expressed as

$$\eta = \frac{E_{Di}k}{F_Y^{\ 2}} - \frac{1}{2} \tag{3.36}$$

Ignoring half term on the right side of the above equation, damage is directly proportional to the stiffness, inversely proportional to the yield strength and directly proportional to the

displacement, since the absorbed energy (E_{Di}) depends upon the ductility of the member. A single degree of freedom system expressed in terms of ductility reveals that increase of ground acceleration, if the yield strength is reduced in the same proportion as the ground motion intensity has increased, then the structure will resist the ground motion but with larger damage.

3.9 Normalized Hysteretic Energy

Hysteretic energy model that incorporates all important phenomena contributing to demand prediction as the structure enters into the inelastic region and finally approaches collapse. For the sake of simplicity, the proposed normalized hysteretic energy models is based on the assumption that strength and stiffness both are non degradable. Since hysteretic energy is directly related with the damage. Further, this energy (E_h) is normalized with its counterpart elastic strain energy (E_S), a stable damage index is obtained, which is a useful tool for making design decision. Elasto plastic with strain hardening behavior is considered for derivation of the normalized hysteretic energy. Stiffness, normalized strength reduction factor and ductility have been incorporated for the proposed normalized hysteretic model.

$k = \frac{F_y}{d_y}$, Normalized strength reduction factor $= \beta = \frac{F_{max}}{F_y}$,

$$k_f = \frac{F_{max} - F_y}{d - d_y} = \frac{(\beta - 1)}{(\mu - 1)}k$$

$$k_{eff} = \frac{F_{max}}{d} = \frac{F_y + F_{max} - F_y}{d} = \frac{F_y}{d} x \frac{d_y}{d_y} + \frac{F_{max} - F_y}{d} x \frac{(d - d_y)}{(d - d_y)} = \frac{k}{\mu} + k_f\left(1 - \frac{1}{\mu}\right)$$

$$k_{eff} = \frac{\beta k}{\mu}, E_{eff} = \text{Effective strain energy} = \frac{\mu\beta k}{2} dy^2$$

(E_N) = Ratio of the hysteretic energy and the effective strain energy = $\frac{E_h}{\frac{\mu\beta k}{2} dy^2}$

(E_h) = $2F_y d_y[(\mu - 1)(\beta + 1)]$ = area of the hysteretic loop

$$E_N = \text{Normalized Hysteretic Energy} = \frac{4[(\mu - 1)(\beta + 1)]}{\mu\beta} \quad (3.37)$$

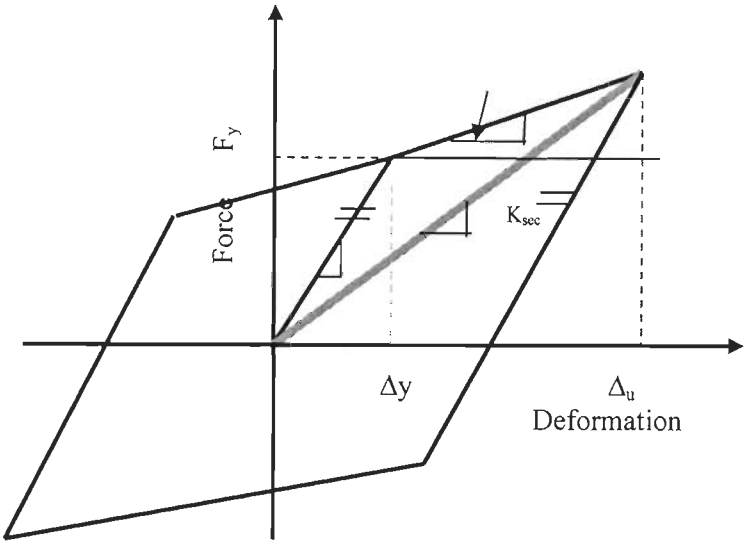

Figure 3.04 Hysteretic loop with strain hardening

Normalized hysteretic energy with the strain energy grows with the increase of seismic demands as increased since the strain energy almost remains same. However, during formulations of the problems, the major contents are concerned with the evaluation of total hysteretic energy for the elastic-plastic structures. Therefore, the normalized hysteretic energy as a single loop has been formulated in terms of strength reduction factor. Analytical derivation for the hysteretic energy for the above loop condition has been formulated and has been validated during the research study.

3.10 Relation between Hysteretic Energy (E_D) and Strain Energy (E_s).

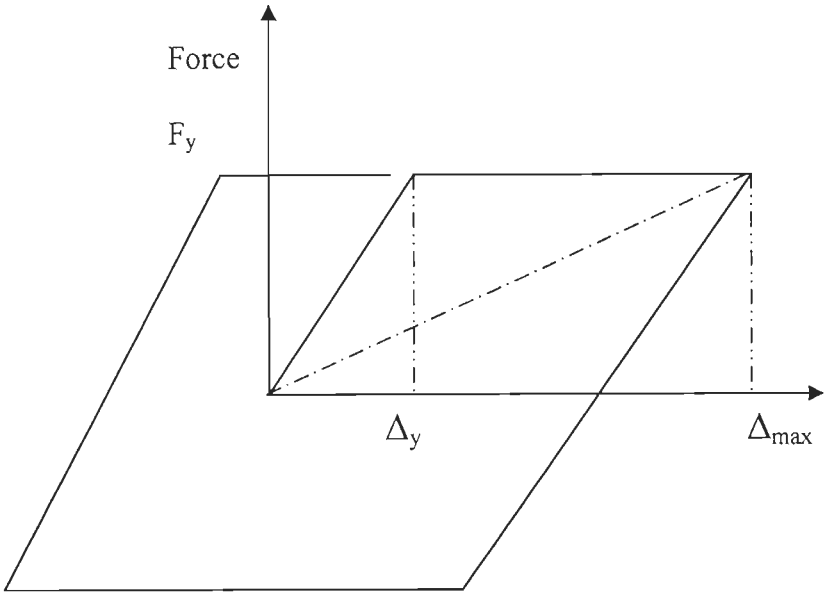

Figure 3.05 Hysteretic loop for elasto-plastic system

Hysteretic energy through yielding is the outcome of the severe ground motion, when a structure yield and takes the advantage of ductility. Elasto-plastic behavior of steel frames has been considered since such a behavior is closely related with the steel frame actual behavior.

$$E_{hi} = 4k\delta_y^{\,2}(\mu_i - 1) = 8E_s(\mu_i - 1) \tag{3.38}$$

During successive loop under varying earthquake ground motions, the total energy dissipated for displacement ductility = 2, 3, 4, 5, 6, 7 etc is following

$$E_D = \sum_{i=1}^{n} E_{hi} = 8E_s + 16E_s + 24E_s + 32E_s + 40E_s \tag{3.39}$$

The above equation (3.39) forms the arithmetic progression with the resultant values.

$$\text{i.e., } E_D = 8n \times \frac{(n+1)}{2} E_s \tag{3.40}$$

Where E_D is the total energy dissipated, n is the total number of loops and E_s is the strain energy. For performance based criteria the equation (vii) is an important equation since, elastic strain energy (E_s) presents IO/OP performance levels and the successive values of total hysteretic energy reveals the other performance levels(LS, CP etc)

The values of the successive hysteretic energy are normalized by the total hysteretic energy will be an effective damage index.

A damage index through normalizing the successive hysteretic energy with the sum of hysteretic energy is the proposed damage index as the content of present study. The normalized values provide a trend of continuous damage spectrum. In spite of small portion of the energy during the hysteretic energy in comparison the first part of the damage (Park and Ang damage model), however, this part of energy is crucial/critical since it is the energy beyond LS and controls CP. Cumulative ductility is the concern of the literature due to its complex characteristics. Hysteretic energy approach provides simplicity for the evaluation of cumulative energy as can be seen from the following tables estimated from the successive loop formation during the varying earthquake ground motion

3.11 Simplification of Park and Ang Damage Model

Park and Ang damage model is simplified for overall damage index in order to correlate the local damage index to the global performance.

Damage models accounting for the combination of maximum deformation and dissipated energy have been introduced [9]. The model proposed by Park and Ang model uses damage index D_e defines by

$$D_e = \frac{U_{max}}{U_u} + \frac{\beta \int dE_H}{R_y U_y} \tag{3.41}$$

Where U_{max}= maximum deformation under earthquake

U_u = ultimate deformation under monotonic loading

U_y = yield deformation

$\int dE_H$ =cumulative hysteretic energy

β = non-negative parameter =0.025 for steel structures

$$\frac{U_{dyn}}{U_{mon}} = \frac{\text{maximum} - \text{deformation} - \text{in} - \text{dynamic} - \text{loading}}{\text{maximum} - \text{deformation} - \text{in} - \text{monotonic} - \text{loading}}$$

A structure under equivalent loading will yield more than the actual dynamic loading

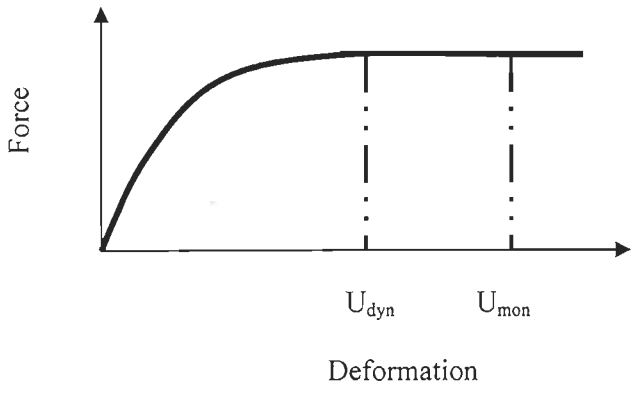

Figure 3.06 Force vs. deformation relation for monotonic and dynamic loading [8]

A structure under equivalent loading will yield more than the actual dynamic loading Extension of equation (3.41) for a generalized form, where the damage at component levels may directly be incorporated for the overall damage index. Rearranging the eqn (3.41), we get the following expression

$$\frac{(D_e U_{mon} - U_{dyn})}{U_{mon}} \times \frac{R_y U_{mon}}{\beta} = \int dE_H$$

Using $\alpha = \frac{R_y}{Mg}$ and $\mu = \frac{U_{mon}}{U_y}$

$$\alpha Mg(D_e U_{mon} - U_{dyn}) = \mu\beta \int dE_H \qquad (3.42)$$

Putting $\frac{U_{dyn}}{U_{mon}}$=0.6 as suggested by some researchers Park and Ang (26) the maximum damage under unidirectional dynamic loading normalized with the max deformation under monotonic loading. $\int dE_H = E_H^{\,i} = \frac{\alpha U_y Mg(5D_e - 3)}{5\beta}$ (3.43)

$$D_e^{\,i} E^i_H = \frac{\alpha U_y Mg D_e^{\,i}(5D^i_e - 3)}{5\beta} \qquad (3.44)$$

$$\frac{D_{1e}E_{1H} + D_{2e}E_{2H}}{E_{1H} + E_{2H}} = \text{Overall} - \text{Damage} - \text{Index} = \frac{D_{e1}^{\,2} + D_{e2}^{\,2} - 0.6(D_{1e} + D_{2e})}{D_{e1} + D_{e2} - 1.2}$$

The generalized expression for overall damage index (D_{Tn})

$$D_{Tn} = \frac{D_{1e}^{\,2} + D_{2e}^{\,2} + D_{3e}^{\,2} + D_{4e}^{\,2} + \ldots\ldots - 0.6(D_{1e} + D_{2e} + D_{3e} + \ldots.)}{D_{1e} + D_{2e} + D_{3e} + \ldots\ldots - (0.6 + 0.6 + 0.6 + \ldots..)} \qquad (3.45)$$

The above expression of damage index is the extension of Park and Ang damage index for overall damage which includes the damage index at the element level to the global level. D_{ie} is the damage index at the element level.

3.11.1 Elasto-plastic Hysteretic Loop for Evaluation of Damage during Monotonic Inelastic Deformation.

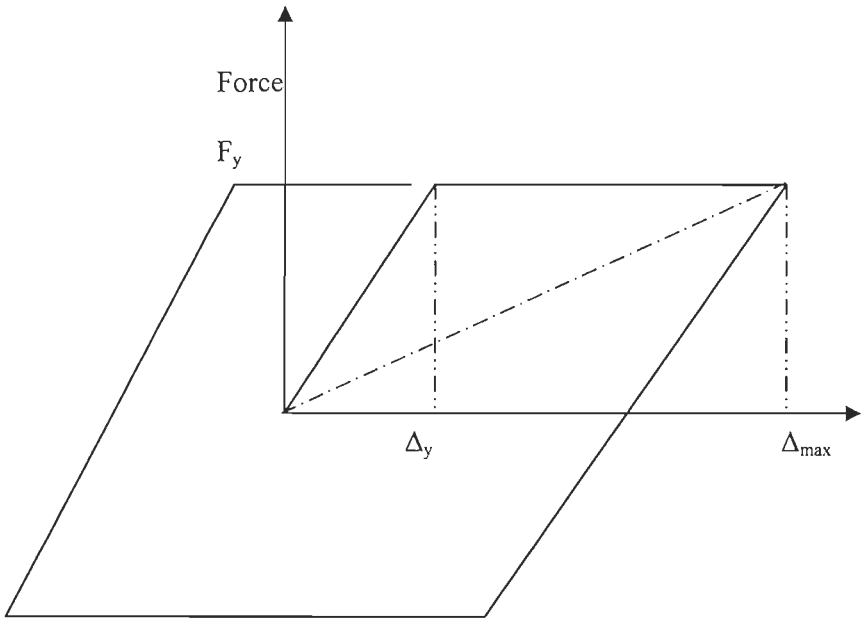

Figure 3.07 Hysteretic loop for damage evaluation under monotonic deformation

The size of the loop gives information of the amount of effective strain energy during the varying demand. Let E_{s1} is the strain energy up to yielding $=\frac{1}{2}k\delta_y^{\,2}$; Let E_{s2} is the strain energy up to maximum deformation $= \frac{1}{2}k_{eq}\delta_{max}^{\,2}$

$$\frac{E_{s2}}{E_{s1}} = \frac{\frac{1}{2}k_{eq}\delta_{max}^{\,2}}{\frac{1}{2}k\delta^{\,2}} = \left(\frac{k_{eq}}{k}\right)\left(\frac{\delta_{max}^{\,2}}{\delta_y^{\,2}}\right);$$ From the relation, $F = k\delta_y = k_{eq}\delta_{max}$; $k_{eq}/k = \frac{\delta_y}{\delta max}$

Using the above equations, $\frac{E_{s2}}{E_{s1}} = \frac{\frac{1}{2}k_{eq}\delta_{max}^{\,2}}{\frac{1}{2}k\delta^{\,2}} = \left(\frac{\delta y}{\delta_{max}}\right)\left(\frac{\delta_{max}^{\,2}}{\delta_y^{\,2}}\right)$.

$$\frac{E_{s2}}{E_{s1}} = \frac{\frac{1}{2}k_{eq}\delta_{\max}{}^{2}}{\frac{1}{2}k\delta^{2}} = \left(\frac{1}{\mu}\right)\left(\mu^{2}\right) = \mu \tag{3.46}$$

From the equation (3.46), it is concluded that the amount of strain energy increases the ductility times the initial strain energy.

Normalizing the inelastic strain energy with the elastic strain energy is the damage index for the first part of the damage index of the Park and Ang damage model.

$$\text{Damage} - \text{index} - \text{for} - \text{uniaxial} - \text{deformation} = \frac{E_{s2} - E_{s1}}{E_{s2}} \times 0.6 \tag{3.47}$$

0.6 implies for the total part of the damage, which is contributed by the direct deformation. The damage index will tend to 0.6 for maximum value of direct inelastic energy. The above equation (3.47) in terms of ductility $= \frac{\mu - 1}{\mu} \times 0.6$ (3.48)

3.12 Number of Yield Excursion Cycles and PBSD

Equivalent number of yield cycles (NEYC) is a useful comparative index of the severity of ground shaking. For each cycle under reversal of stresses, a structural component yields in tension and compression. There is significant amount of residual energy for the successive yielding. This index is numerically equal to the ratio of the hysteretic energy and the inelastic energy during monotonic loading.

While a component undergoes reversal of stresses without yielding, the input energy is stored as strain energy and during reversal it is dissipated as damping energy. However, reversal of stresses beyond yielding directly dissipates energy and as a result the capacity decreases tending towards collapse if the components are directly taking the loads e.g., a column undergoes reversal of loads in the yielded portion, the chances of collapse increases. If a horizontal components like beam yields and undergoes reversal of stresses, and the input seismic energy is dissipated in safe mode. The number of yields while a structure or the structural components passes from tensile to compression and from compression to tension are important for quantifying the damages, because the functionally of the structure is adversely affected by the number of yield excursions.

The most important parameters for number of yield excursions are the well defined yield point, and steel components have such a characteristics. Demand on components through capacity design can be met through the limited number of members. In this regards

weak beam and strong column is fully established. During severe earthquake ground motions allowing some components into the inelastic region in desirable manner are well documented and needs simplicity for code based applications. Significant inelastic deformation before a components releases from tension and comes into compression and vice-versa which is important for documentation for control of energy dissipation in the definite manner. Such kinds of the above possibility of the formation of yielding and changing from tension to compression and vice-versa are the key points of identification and quantification

Number of yield and yield excursions are not required to be same because some of the yield may not participate for yield excursion. Such a possibility may be very close to the collapse zone. Number of loops has the relation with the number of yielding. In one complete loop the number of yield excursions are $2N+1$ or $2N$ (3.49)

Where N is the number of loops. If the loop is complete and tends to the next loop, the number of yield is 2+1=3, otherwise the loop is tending to complete the loop, and the yield excursions are 2. Performance of a component depend upon the number of loops which can be possible without detrimental any consequences which results into collapse procedures. The size of the loop also important because the larger the area of the more will be damage.

Figures 3.08 to 3.10 represent the ground motion, number of yield excursion cycles and hysteretic loop respectively. NYEC directly relates the severity of the damage. The corresponding energy through the area of the hysteretic loop reflects the same effect. Equation (3.40) provides number of loops (Figure 3.10) and NYEC from equation (3.49). Since the building frames used has been found to satisfy performance levels under the prescribed loading, therefore, number of loops and the corresponding NYEC may be used as performance indicator. The cross section of the external columns is

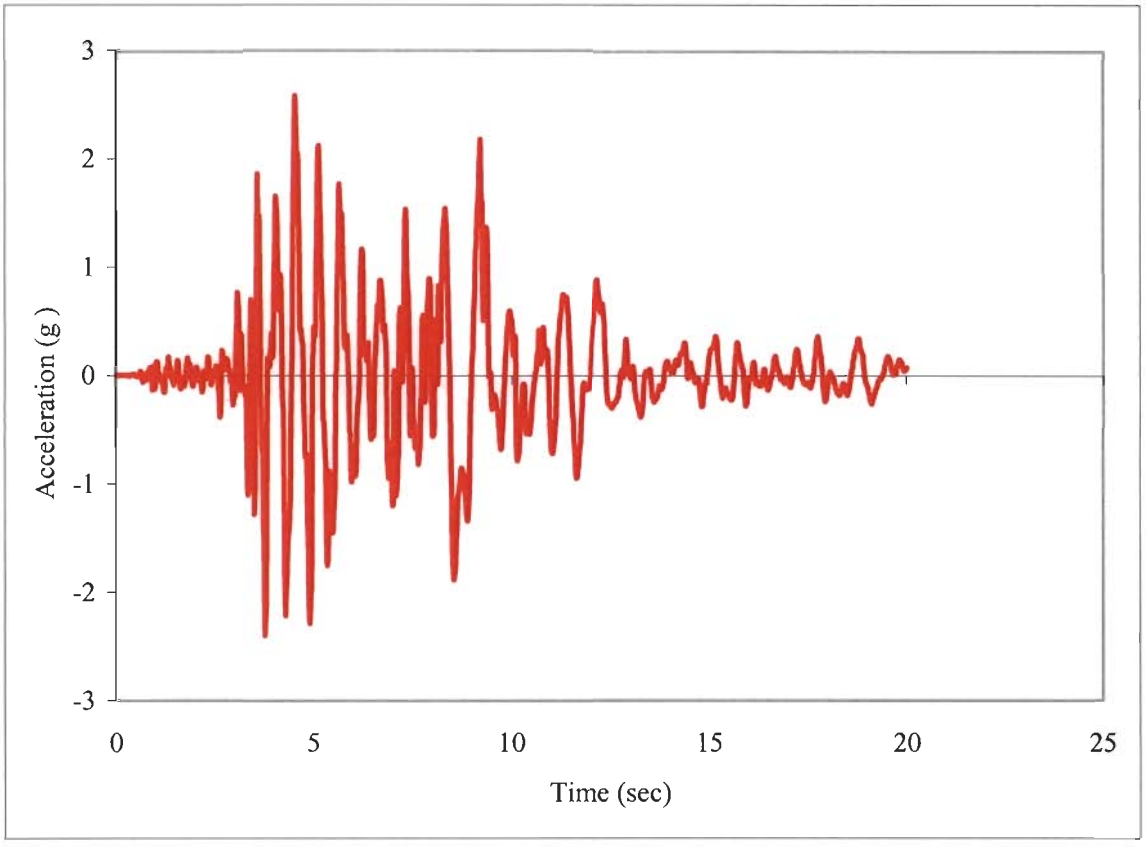

Figure 3.08 Accelerogram of Northridge E-W (0.5165g) with SF = 5

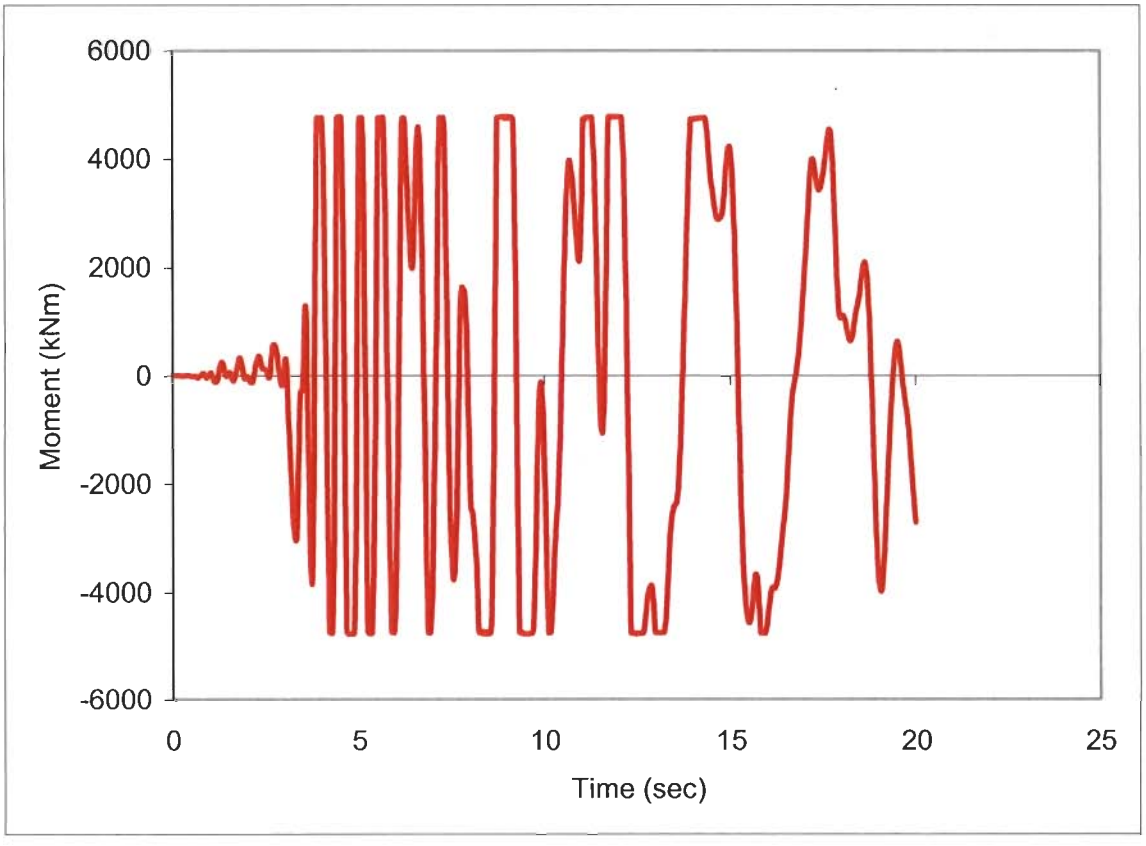

Figure 3.09 Time history plot of external columns on ground floor of example problem 4.2

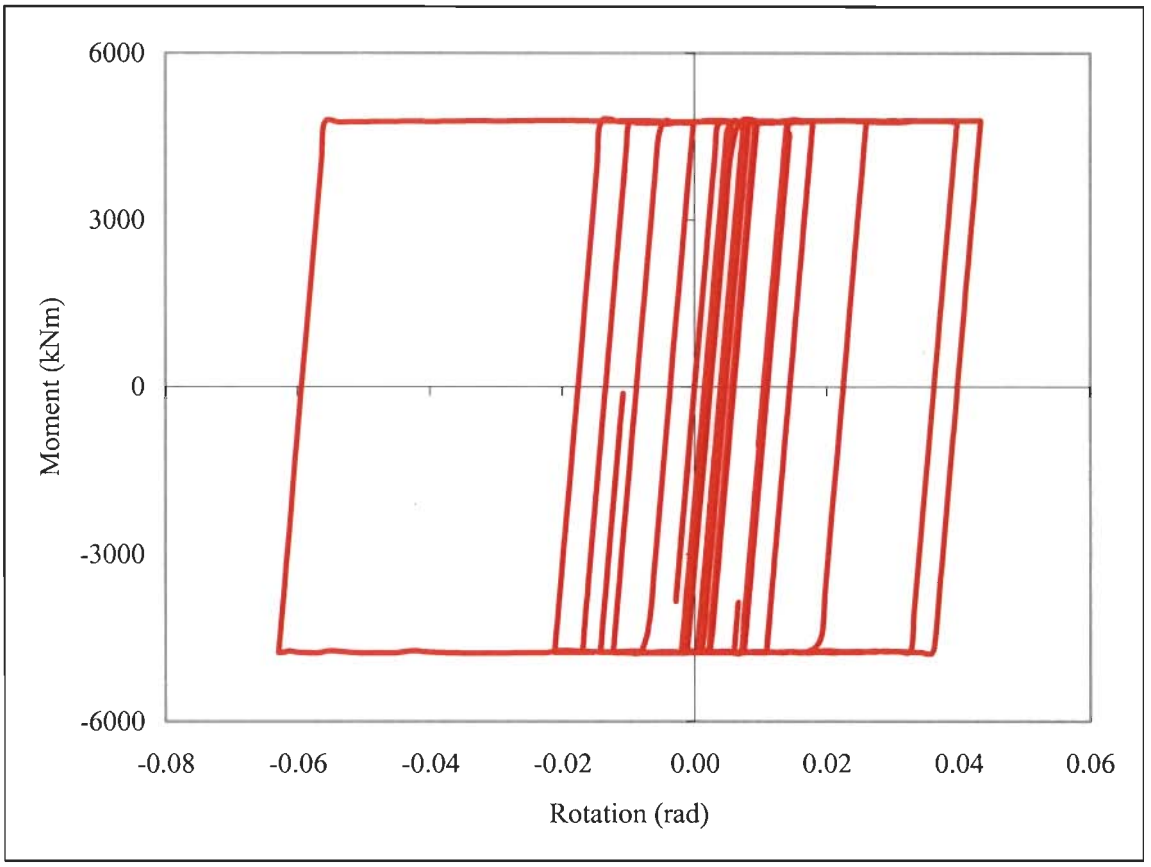

Figure 3.10 Hysteretic loops for external columns on ground floor of example problem 4.3.2

3.13 Analysis of Critical Sections

Wide flange cross sections have been used during the present study. Cross sections of critical components need to be investigated for the nonlinear behavior, since the chances of progressive failure is high when a cross section is heavily stressed under reversal of stresses. A cross section may be under combine loading, in this case the interaction of actions reduces the capacity. e.g., a heavily loaded column, its bending moment carrying capacity decreases with the increase of axial loads etc. Sections used in the study are tabulated and presented. Some of the critical sections were studied through modeling these sections in Section Builders (CSI's softwares). The members used for critical assessment for performance evaluation are used for their section analyses.

For beams the maximum value of bending moments and for columns maximum bending moment, axial force in columns are known using time history analysis of these elements in Perform 3D.

A critical beam and a column are analyzed through modeling in Section Builders. Response parameters of the cross sections are used for the nonlinear analysis. Analytical derivations for the stress condition of cross sections are also presented.

Section analysis is required since a cross-section is highly sensitive for damage concentration accompanied by progressive failures. This happens when the plastic moment exceeds the limit, the failure of the extreme fiber results into the progressive failures.

3.13.1 Characterization of the Flexural Behavior of Beams

The linear relationship between stress and strain, to examine member behavior in the elastic, inelastic and post-yield strain state is presented from first principle.

Elastic behavior

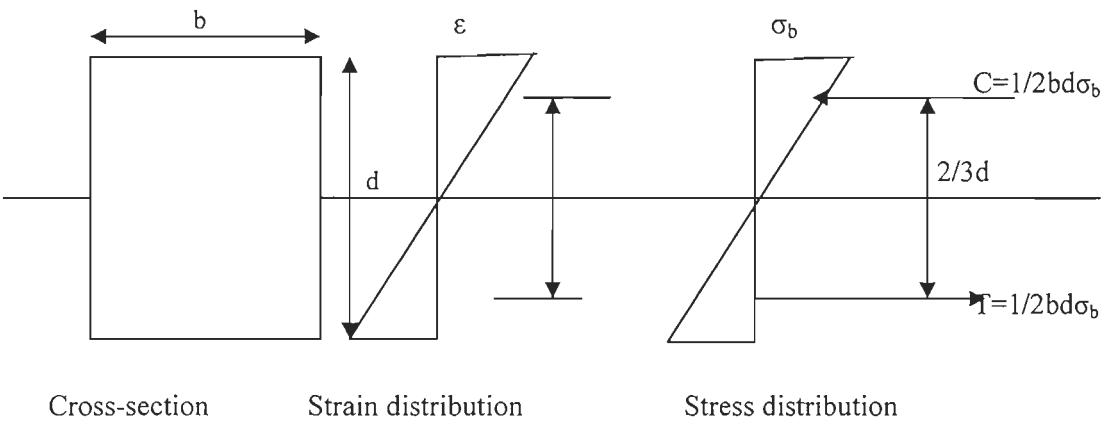

Figure 3.11 Cross section behavior of steel member

$$M = \sigma_b Z \qquad (3.50)$$

Where σ_b is the bending stress and is important for seismic design criteria. Z is the section modulus.

$\varphi = \frac{M}{EI}$; Where φ is the curvature of beam.

According to the strength limit, $\varphi_y = \frac{M}{EI}$ or $\varphi = \frac{\sigma_y Z}{EI}$, where σ_y is the yield stress

This idealized behavior corresponds to behavior, one would expect in the absence of residual stresses.

The moment curvature relationship in the inelastic behavior range is not linear. If the moment changes to M+dM, the plasticization is d/6 from extreme fiber. $dM=\frac{5}{18}\sigma_y Z$, thus the increase of the moment is 28% Corresponding change in the curvature is as following, $\varphi_1 = 1.5\varphi_y$, then the increase in curvature is 50%, K is the ratio of the effective depth of elastic region to the over all depth of the section. As k tends to 0, the section is pure plastic and if k tends to 1, the moment is pure elastic.

Inelastic behavior of beam/column cross section

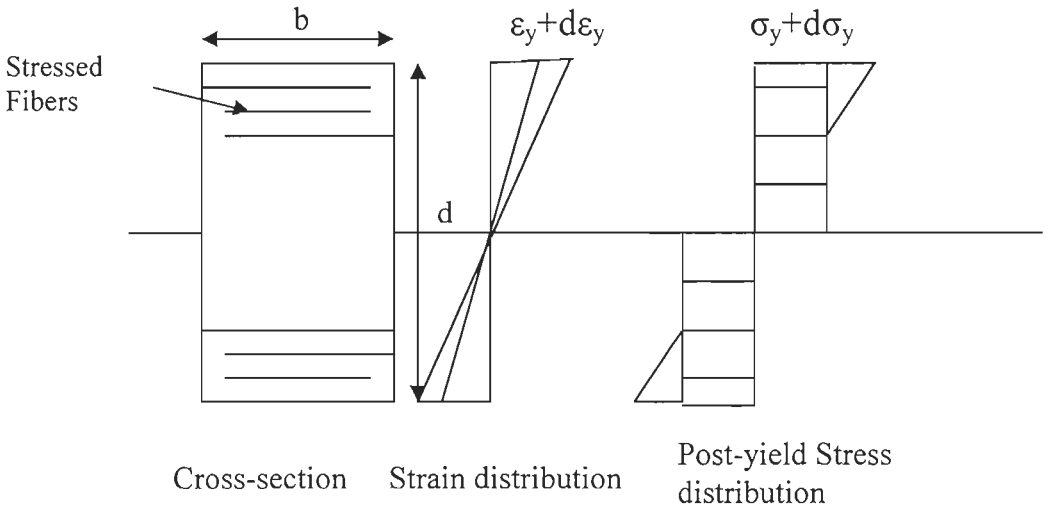

Figure 3.12 Inelastic behavior of cross section behavior of steel member

The sections are capable to deform inelastic ally in order to take advantages of basic mechanical characteristics-ductility to maximum level of satisfaction under earthquake loading. Under reversal of stresses due to severe earthquake loading dissipation of energy

(hysteretic energy) takes with or without degradation of loop. Robustness of third hysteretic loop [38] has been used in the estimation of the total energy dissipation.

The aim of section analysis for nonlinear response using modeling of the section in Section Builders has been presented as the content of the present study in order to address the response of the structural components in order to trace the progressive failure at the cross section levels.

3.14 PBSD vs. Limit States, and Usage Ratios

A nonlinear analysis produces a huge amount of analysis results. Effective use of limit states may be used for refinement of analysis results to a few usage ratios (Demand /Capacity) for identification and quantification of performance objectives. For hysteretic energy, energy ratio may also be distilled for their use as performance criteria. The major objectives of performance based seismic design are to incorporate stiffness, strength and ductility into the expression of hysteretic energy.

Since extension of limit states results into close relation with the performance based seismic design, therefore, further understanding or development using energy ratio may have to be looked upon for development of design algorithm under varying earthquake ground motions. Usage ratio is the ratio of demand and capacity, while energy ratio is the ratio of energy of degraded loop and the non degraded loop. Usage ratio and energy ratio imply the similar effects as required by PBSD, once a structure is dissipating hysteretic energy under severe ground motions. Limit states extension using the energy parameters have been addressed for damage assessment by Housner, 1956 [12]. Concept, process and issues of PBSD [19] through energy dissipation as engineering limit states, which further require researches since such parameter is closely related with physical damages under earthquake loadings. Understanding of recent development in the computational facilities has been incorporated in the present study with the access of damage assessment at component and global performance levels. Usage ratio (demand/capacity) are to be calculated during the structural analysis, therefore, limit states are defined in modeling phases. Energy ratio depends upon the amount of degradation of hysteretic loop during reversal of stresses. Energy ratio (area of degraded hysteretic loop/area of non degraded hysteretic loop) participation for degradation of stiffness, strength and ductility is controlled modeling process in the present study. Finally usage ratios have to be plotted for the validation of assigned performance objectives to the building frames.

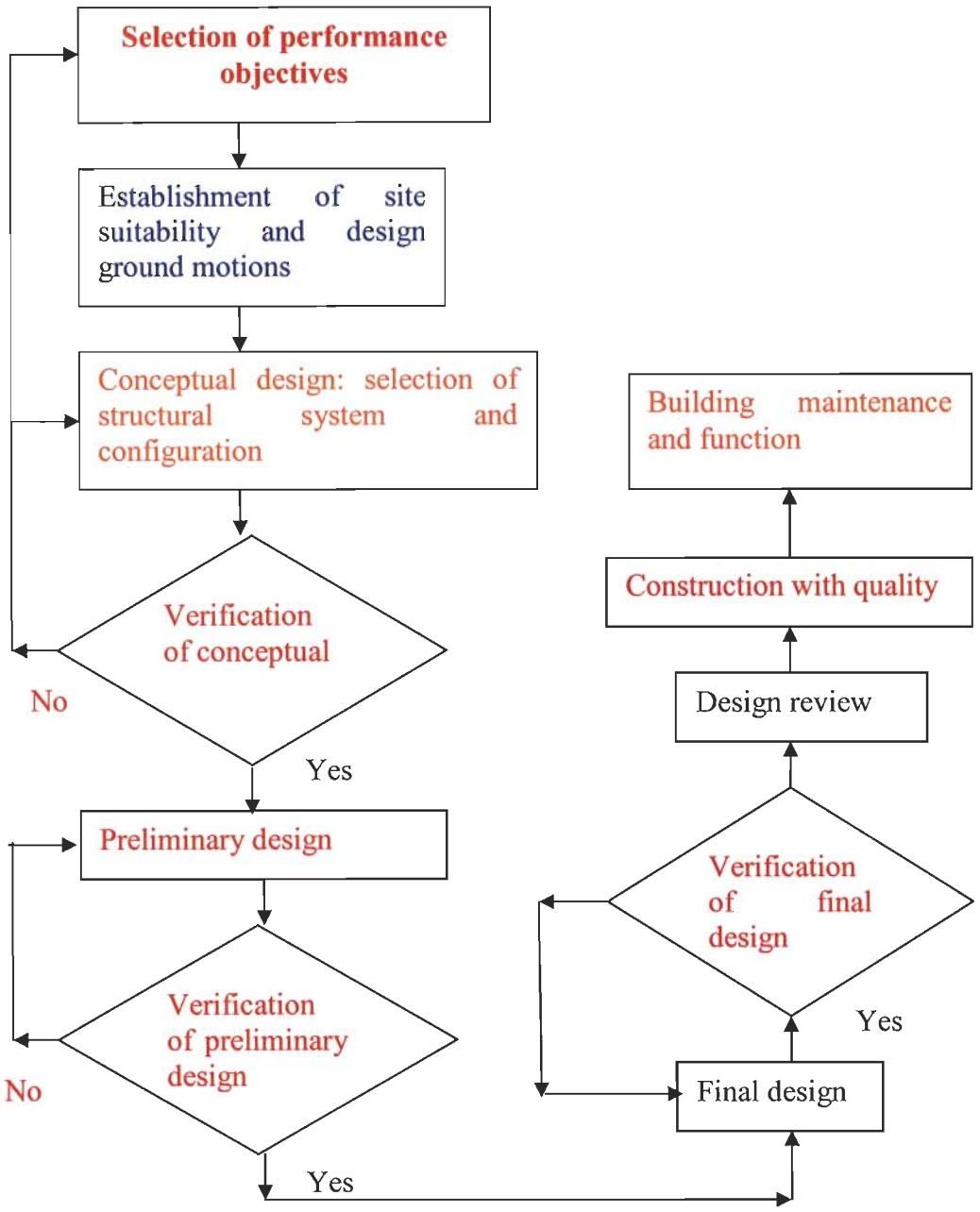

Flow Chart 3.01 SEAOC Vision 2000 methodologies for performance-based seismic design

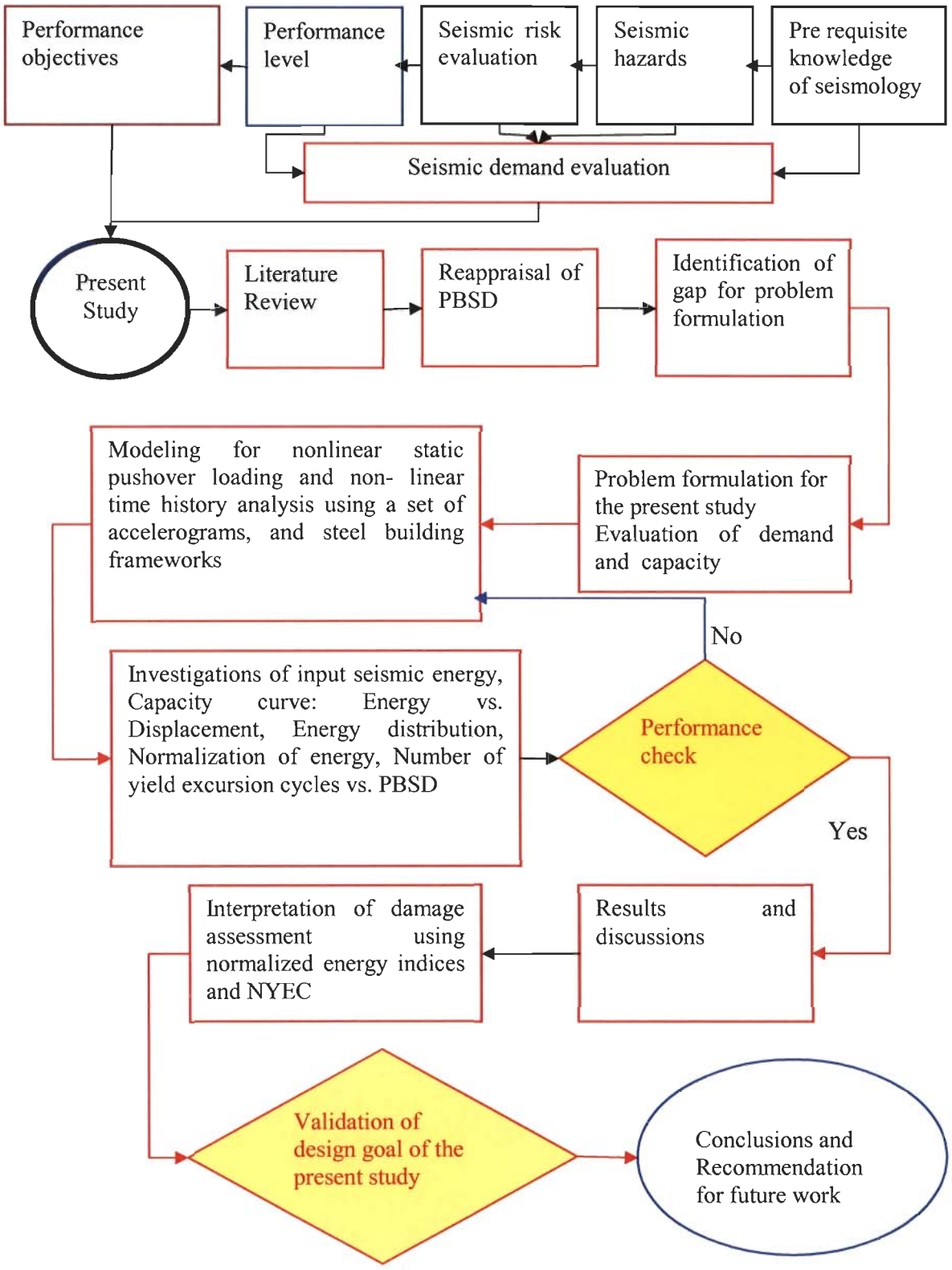

Flow Chart 3.02 Proposed methodologies for performance-based seismic design

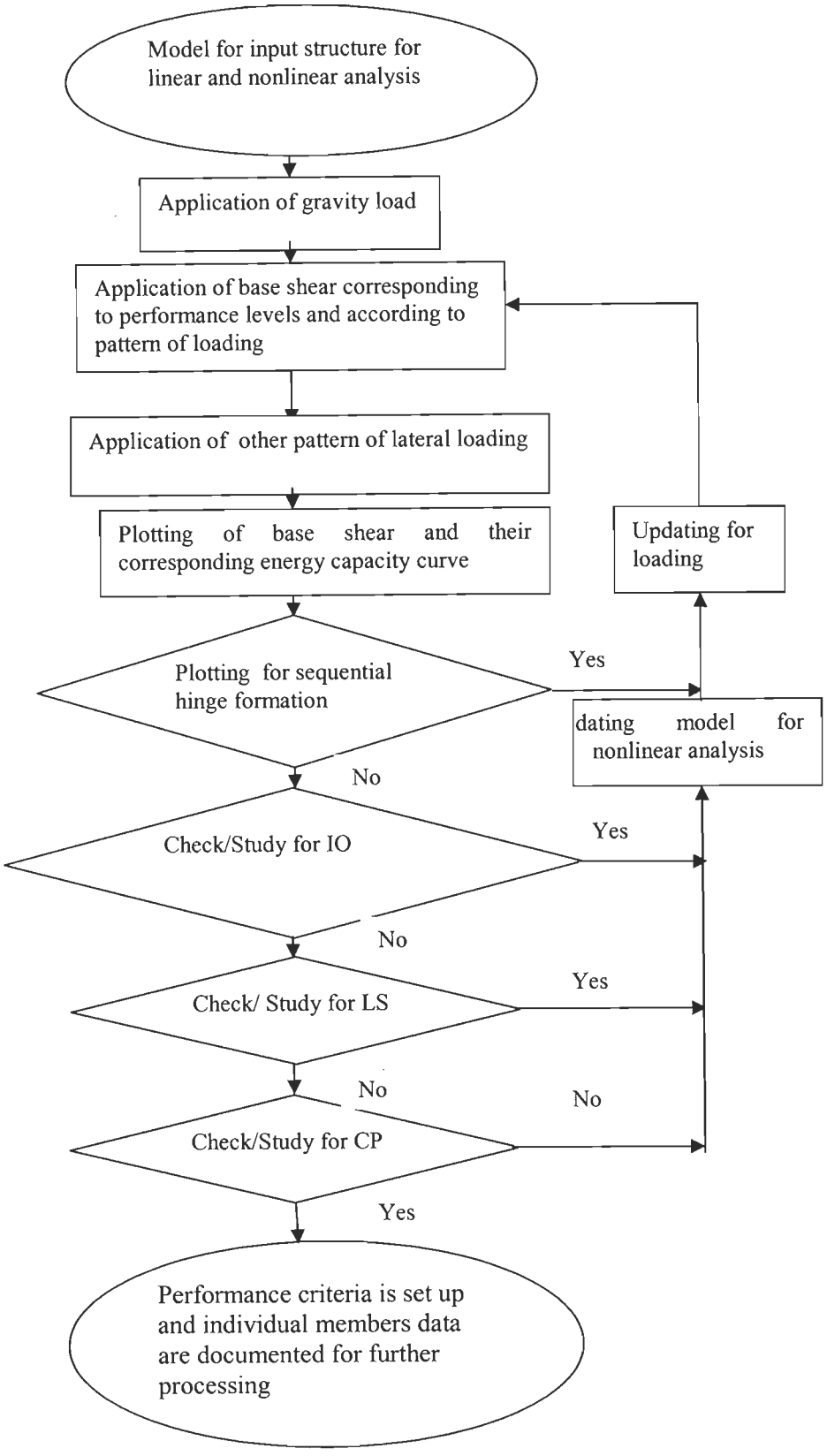

Flow Chart 3.03 Nonlinear static pushover analysis procedures

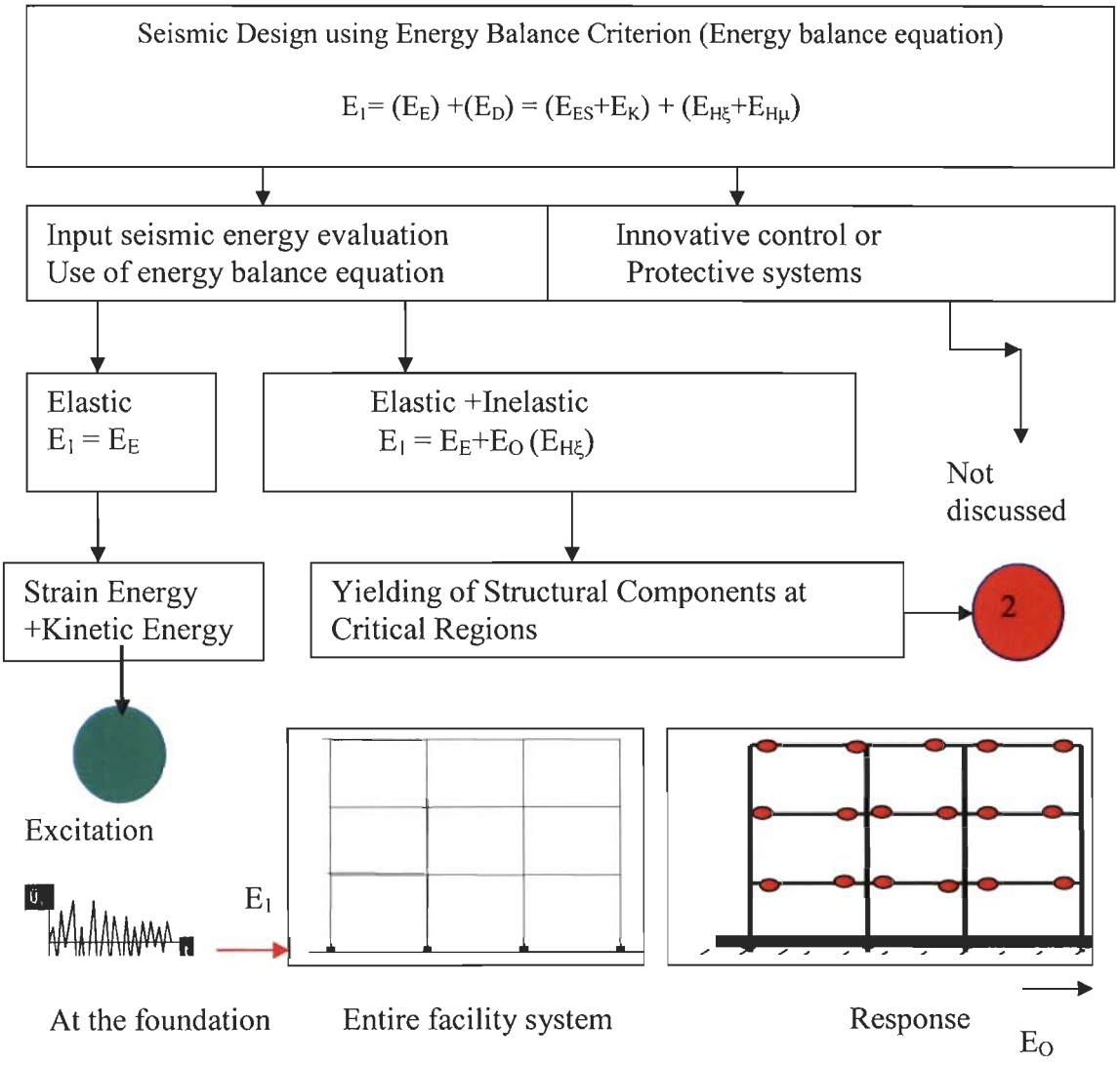

E_I stands for input seismic energy

Sum of elastic and kinetic energy is important for controlling the floor vibration in order to check non structural damage.

The amount of energy released through yielding of structural components is important for damage assessment. Energy released during inelastic deformation is closely related with the elastic strain energy.

Flow Chart 3.04 Proposed energy balanced criterion for input seismic energy distribution

Chapter 4

MODELING AND ANALYSIS

4.1 Introduction

For performance based seismic design development, it is the first task to assess the performance capability of the structural systems for the performance objectives assigned. Scaling down damage at global and local locals is the key element for an effective analysis procedure under seismic loading. Analysis of response for the determination of damages at various performance levels depends upon the modeling and their corresponding analysis procedures. Analysis procedures require the requisite nonlinear model of the building frames along with the loading on the structures. In order to accomplish the desired objectives of this study, nonlinear static pushover analysis and time history analysis have been conducted on the building frames modeled in Perform 3D, 2006 [17] under seismic loading. Five steel frames building have been taken from the literature, where these frames have been used for performance evaluations and their mechanical properties are established. These frames have been modeled using RAM Perform 3D [17]. Using FEMA 273, [3] guidelines, base shear corresponding to performance objectives have been estimated and were applied to the respective building frames. Accelerograms in-built to this software have been used for time history analysis. Nonlinear static pushover analysis and time history analysis for the modeled building frames have been conducted. Subsequently analysis results were recorded for performance assessment. Various steps for modeling and analysis in this study are listed below:

4.2 Development of Performance Objectives

The main objective of performance based seismic design is to evaluate the performance of a system at different seismic hazards. Selection of performance objectives is the first task of performance based seismic design. A comprehensive performance assessment needs to be taken care from the conceptual phase of design procedure in order to reduce the number of iterations for achieving the assigned performance.

Using FEMA-273 [3], a generalized format of performance objectives corresponding to various performance levels have been developed for the present study. A set of earthquake ground motions in-built in RAM Perform 3D have been used further for evaluation and data base, as required for damage assessment in this study. Scale factors

have been used to meet the PGA corresponding to the desired seismic hazards. The aim of performance criteria using energy criterion from the response analysis and further PBSD development remains the major part of the problem formulations and their investigation.

4.2.1 Design Spectra Parameters

4. 2.1.1 Site parameters for 2%/50-year and 10%/50-year earthquakes

For the purpose of present study demonstration, we adopt design spectra parameters from FEMA 273 (1997) maps for a site located at Latitude 36.9^0 N and Longitude 120^0W. It is assumed that the site is class D or stiff soil. The following maps provide the site parameters for 20%/50-year and 50%/50-year Earthquakes:

(i) Map 29: Probabilistic Earthquake Ground Motion for California/Nevada of 0.2 sec spectral Response Acceleration (5% of critical damping), 10% of probability of Exceedance in 50 years.

(ii) Map 30: Probabilistic Earthquake Ground Motion for California/Nevada of 1.0 sec spectral Response Acceleration (5% of critical damping), 10% of probability of Exceedance in 50 years

(iii) Map 31: Probabilistic Earthquake Ground Motion for California/Nevada of 0.2 sec spectral Response Acceleration (5% of critical damping), 2% of probability of Exceedance in 50 years.

(iv) Map 32: Probabilistic Earthquake Ground Motion for California/Nevada of 1.0 sec spectral Response Acceleration (5% of critical damping), 2% of probability of Exceedance in 50 years.

The above maps give accelerations for site Class B only. They need to be adjusted for the other site classes. The adjustment coefficients are found in tables 2-13 and 2-14 of FEMA-273 [3]. The design spectra parameters S_s, S_1 F_a and F_v obtained from the above noted maps and tables are listed in table 4.01 The period T_0 is available from the site parameters as

$$T_0 = \frac{F_v S_1}{F_a S_s} \qquad (4.A.1)$$

4. 2.1.2 Site parameters for 20%/50-year and 50%/50-year earthquakes

FEMA-273 does not provide maps for 20%/50-year and 50%/50-year earthquakes, but does provide equations for calculating corresponding site parameters from the two earthquake

hazards considered in 4.A.1. Parameters S_s and, S_1 20%/50-year and 50%/50-year Earthquakes are calculated through the equation (2-3) of FEMA-273 as below,

$$S_i = S_{i10/50}\left(\frac{P_R}{474}\right)^n \qquad (4.A.2)$$

Where subscript I (=s, 1) represents an acceleration response of short period (0.2 sec.) or long period (1.0 sec); n is a zone factor (n=0.44) at the site of Latitude 36.9_0 N and Longitude 120^0 W); $S_{i10/50}$ are parameters of the 10%/50 year earthquake; and P_R is the mean return period given by, (4.A.3)

Where P_{E50} is the probability of exceedance in 50 years of the earthquake under consideration. For example, for the 20%/50-year earthquake located at the site having Latitude 36.9^0 N and 120^0 W,

$$P_R = \frac{1}{1-e^{0.02\ln(1-0.2)}} = 225 \qquad (4.A.3)$$

From eqn. (4.A.2), the parameters for the 20%/50year earthquake are then calculated as,

$$S_{i20/50} = S_{i10/50}\left(\frac{225}{474}\right)^{0.44} = 0.72047S_{i10/50}$$

That is: $S_{s,\,20/50}$ = (0.72047) (0.29) = 0.209 (g), an $S_{1,\,20/50}$ = (0.72047) (0.14) = 0.10 (g)

Where $S_{s,\,10/50}$=0.29 and $S_{1,\,10/50}$= 0.14 are taken from table 4.1 for the given site.

The parameters for the 50%/50-year earthquake located at the site are similarly found as

$$P_R = \frac{1}{1-e^{0.02\ln(1-0..5)}} = 72$$

$$S_{i50/50} = S_{i10/50}\left(\frac{72}{474}\right)^{0.44} = 0.4364S_{i10/50}$$

That is: $S_{s,\,50/50}$ = (0.4364)(0.29) = 0.12(g), and $S_{1,\,520/50}$ = (0.72047) (0.14) = 0.061 (g)

Where $S_{s,\,10/50}$=0.29 and $S_{1,\,10/50}$= 0.14 are taken from table 4.A for the given site.

The same procedure was applied to find the parameters for another site at Latitude 41^0N and 115.2^0W, and the results are tabulated in table 4.01

Table 4.01 Performance level site parameters

Site Location	Site Class	Performance Level	Earthquake Level	S_s (g)	S_1 (g)	F_a	F_v
Latitude 36.9^0N Longitude 120^0W	D	OP	50%/50	0.126	0.061	1.60	2.40
		IO	20%/50	0.209	0.100	1.60	2.40
		LS	10%/50	0.290	0.140	1.57	2.24
		CP	2%/50	0.500	0.230	1.40	1.94
Latitude 41^0N Longitude 115.2^0W	D	OP	50%/50	0.109	0.035	1.60	2.40
		IO	20%/50	0.180	0.0580	1.60	2.40
		LS	10%/50	0.250	0.080	1.60	2.40
		CP	2%/50	1.100	0.410	1.06	1.59

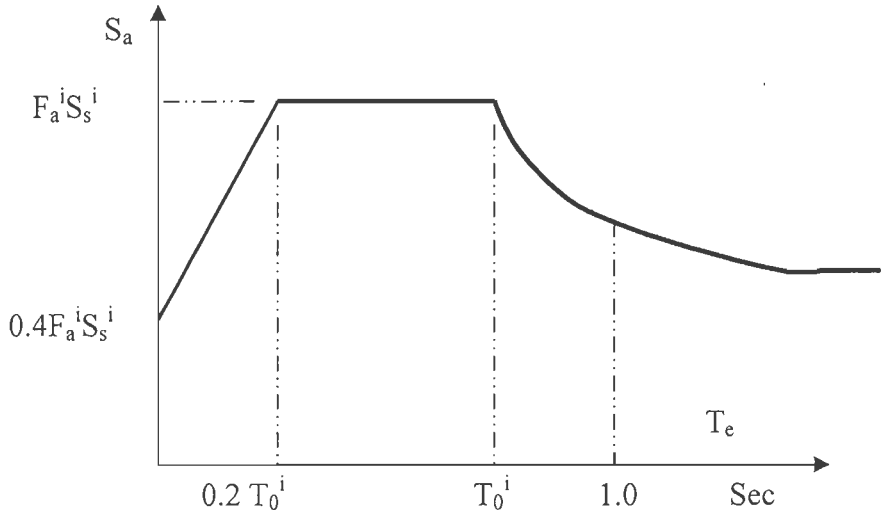

Figure 4.01 Earthquake acceleration response spectrums

$$\text{Estimation of } T_O = \frac{F_v S_1}{F_a S_s} \qquad (4.A.4)$$

$$T_0^i = \frac{F_v S_1}{F_a S_s} \qquad (4.A.5)$$

i = OP, IO, LS, CP

$$Sa^i = \begin{cases} Fa\ {}^iSa\ {}^i\left(0.4 + \dfrac{3T_e}{Ta^i}\right) & 0 < T_e \le 0.2T_0{}^i \\ Fa\ {}^iSa\ {}^i & 0.2T_0{}^i < T_e \le T_0{}^i \\ \dfrac{F_v{}^iS_1{}^i}{T_e} & T_e > T^i{}_0 \end{cases}$$

Using equation and the values of parameters from the table 4.1 and the equation 4.A.4, the value of T_O be calculated and tabulated corresponding to performance levels. T_0 is the period corresponding to specific performance level and T_e is the time period of the structure. S_s, S_1 F_a and F_v are site parameters required for the evaluation of T_0.

4.3 Evaluation of Seismic Response of Building Frames in the Present Study

Recent advances in computational skill and the softwares that may analyze 2D as well as 3D structures to a larger number of earthquake records with different characteristics can now be carried out to enable building response. Using the environment of the softwares [17], enable to automate nonlinear analysis for performance based seismic evaluation, selected steel building frames have been modeled for linear and nonlinear response analyses in RAM Perform 3D. Frameworks modeled for nonlinear response were run for nonlinear static and nonlinear dynamic analysis using the desirable base shear and earthquake ground motions. Details of the building frameworks are listed below.

(i) Example problem 1:Three story four bay 2D frame building
(ii) Example problem 2:Nine story four bay 2D frame building
(iii) Example problem 3:Fifteen story four bay 2D frame building
(iv) Example problem 4:Twenty story four bay 2D frame building
(v) Example problem 5:Three story four bay 3D frame building

4.3.1 Example Problem 1: Three Story Four Bay 2D Frame Building

The building frame has been used for performance evaluation under earthquake ground motions in the mentioned literature [7, 11, and 56].

This is a perimeter moment frame of a building, which was designed according the UBC 1994. The frame consists of 27 members. All bay width is 9.14 m wide and stories are 3.96 m high, each. The frame has rigid moment connections, with all the column bases fixed at the ground level. All the columns use 345000 kN/m^2 steel (expected yield strength =397000 kN/m^2) wide flange sections, while all the beams use 248000 kN/m^2 steel

(expected yield strength =339000 kN/m^2, wide flange sections. The exterior columns have W_{14x257} sections, while the interior columns, all have the same W_{14x311} section. The first, second, and roof beams have W_{33x114}, W_{30x116}, W_{24x68} sections, respectively. Constant gravity loads of 32 kN/m are applied to the first and second story beams, while gravity loads of 28.7kN/m are applied to the roof beams. The seismic weight is 4688 kN for each of the first and second stories and 5071 kN for the roof.

Using equation and the values of parameters from the Table 4.01 and the equation 4.A.4 the, value of T_O is calculated and tabulated corresponding to corresponding performance levels [Table 4.02]. Spectral acceleration and Base Shear for three story 2D steel framework have been tabulated and recorded [Table 4.02], Time period (T_e) =1.13 sec.

Table 4.02 Base shear for 3 story 2D frame for performance levels

Performance Levels	T_O^1 (sec)	S_a^1 (g)	V_B^1 (kN)
OP	0.744	0.1296	1872
IO	0.7356	0.2124	3069
LS	0.6887	0.2775	4009
CP	0.6374	0.3949	5705

Table 4.03 Base shear distribution for 3 story 2D frame

Story No from top	Height from base of the structure in meters	Uniform pushover (kN)	Triangular pushover(kN)
03	11.88	1901.67	2852.49
02	07.92	1901.67	1901.66
01	03.96	1901.67	950.83
	00.00	00.00	00.00

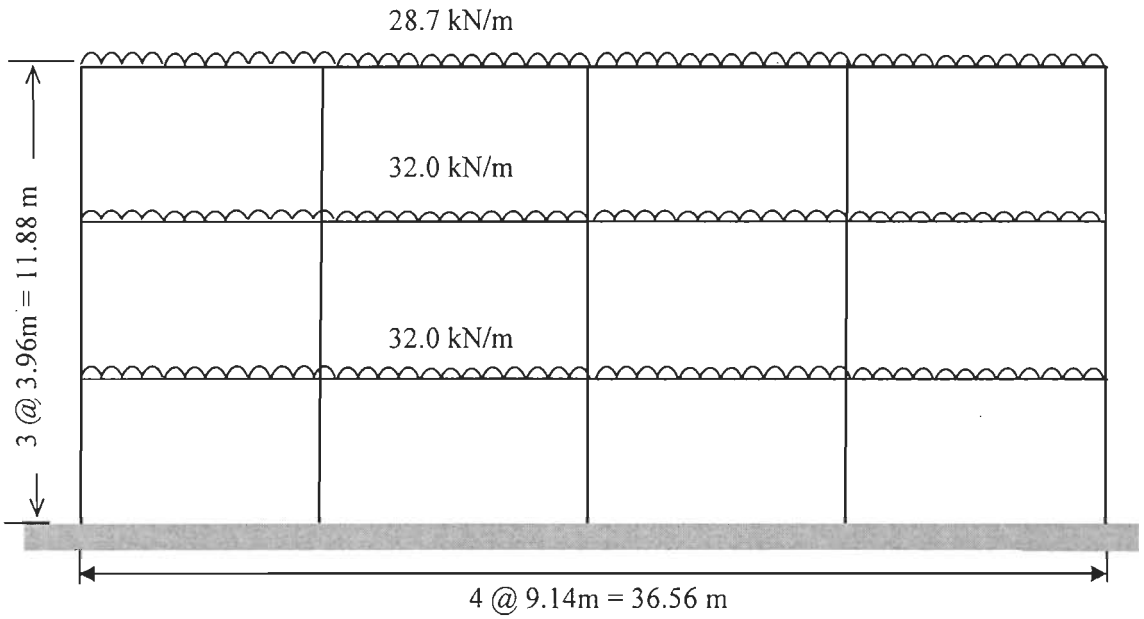

Figure 4.02 Diagram of three story 3 bay 2D steel building frameworks

Table 4.04 Details of beams and columns used in the frame

Floors	Beams	Columns	
		Exterior	Interior
First	W_{33x114}	W_{14x257}	W_{14x311}
Second	W_{30x116}	W_{14x257}	W_{14x311}
Third	W_{24x68}	W_{14x257}	W_{14x311}

4.3.2 Example Problem 2: Nine Story Five Bays 2D Frame Building

The building frame has been used for performance evaluation under earthquake ground motions in the mentioned literature [7, 11, and 56]. This is a perimeter moments frame of a building. The fame consists of 99 members. All five bays span is 9.14m (centerline dimensions) and stories are 3.96 m high. The frame has rigid moment connections, with all the column bases fixed at the ground level. All the columns use 345000 kN/m^2 steel (expected yield strength =397000 kN/m^2) wide flange sections, while all the beams use 248000 kN/m^2 steel (expected yield strength =339000 kN/m^2, wide flange sections. All beams at the same floor levels are same sections. Details of the sections are given separately. Constant gravity loads of 32 kN/m are applied to the beams in the first to eighth story, while gravity loads of 28.7kN/m are applied to the roof beams. The seismic weight is

4942 kN for the first story, 4857 kN for each of the second to the eight stories, and 5231 kN for the roof.

Using equation and the values of parameters from the Table 4.01 and the equation 4.A.3, the value of T_O be calculated and tabulated corresponding to performance levels for nine story steel frame, Since T_O^i is smaller than T_e (T_e=2.076 sec), Seismic weight of nine story frame = 44,172 kN. Tables 4.2 and 4.3 represent base shear and distribution of base shear.

Table 4.05 Base shear for nine story 2D frame for performance levels

Performance Levels	T_O^i (sec)	S_a^i (g)	V_B^i (kN)
OP	0.744	0.07	3092
IO	0.735	0.12	5106
LS	0.688	0.15	6670
CP	0.637	0.21	9493

Table 4.06 Base shear distribution for nine story 2D frame

Story no from top	Height from base of the structure in meters	Uniform pushover (kN)	Triangular pushover(kN)
09	35.64	1054.78	1898.36
08	31.68	1054.78	1687.68
07	27.72	1054.78	1476.72
06	23.76	1054.78	1265.96
05	19.80	1054.78	1054.80
04	15.84	1054.78	843.84
03	11.88	1054.78	632.88
02	07.92	1054.78	421.92
01	3.96	1054.78	210.96
	00.00	00.00	00.00

Table 4.07 Details of beam and columns of nine story 2D frame

Beams details	Columns details
W_{24x68}, W_{27x87}, W_{30x99} W_{36x135}, W_{36x160}	W_{14x233}, W_{14x257}, W_{14x283}, W_{14x370}, W_{14x455}, W_{14x500}

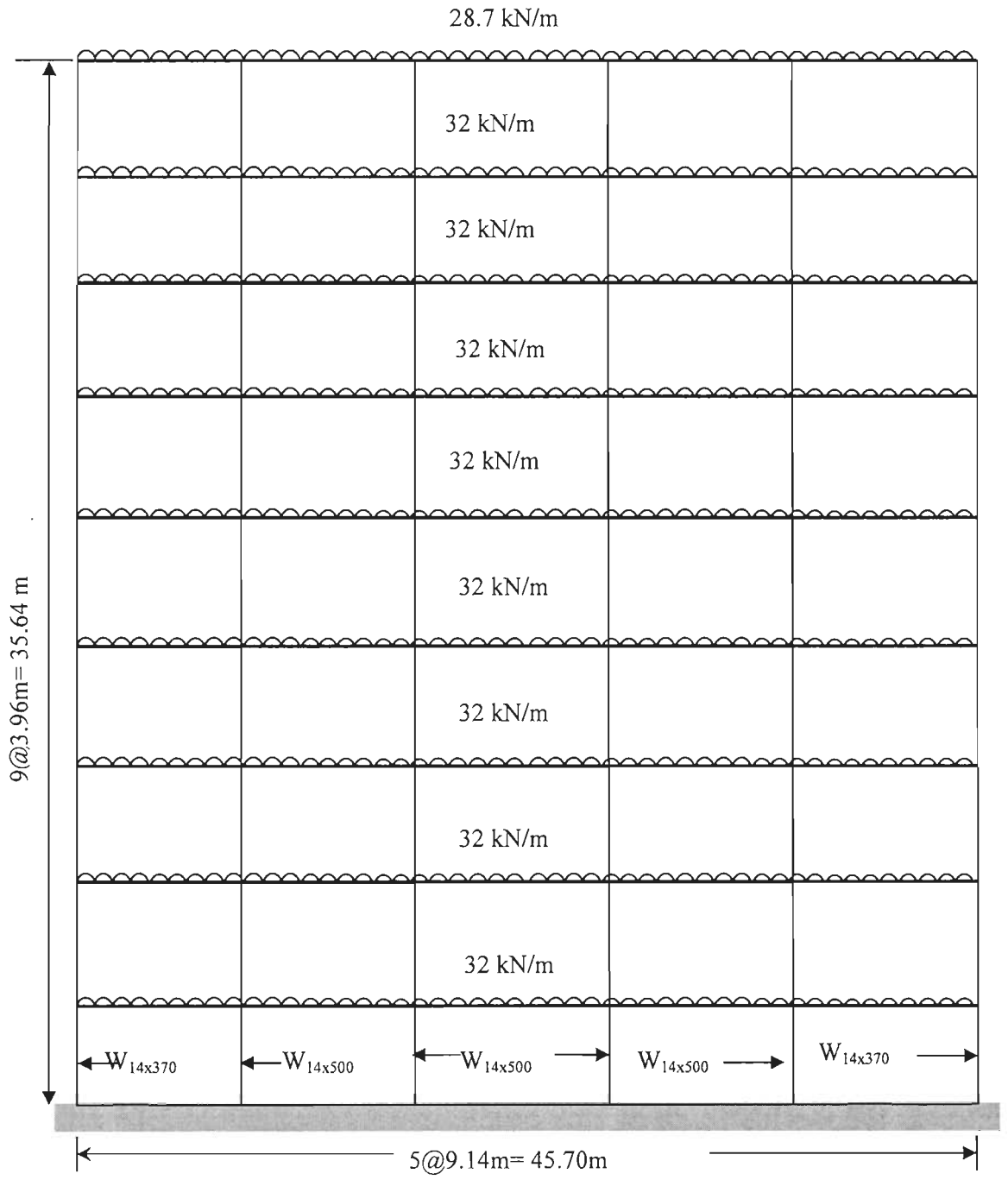

Figure 4.03 Diagram of nine story five bay 2D steel building frameworks

4.3.3 Example Problem 4.3: Fifteen Story 2D Three Bay Steel Frame Building

The building frame has been used for performance evaluation under earthquake ground motions in the mentioned literature [57]

This is a perimeter frame of a building. All three bays are 9.14 m (centerline dimensions) and stories are 4.57 m. the frame has rigid moment connections, with all columns fixed at the ground level. All the columns use 345000 kN/m^2 steel (expected yield strength =397000 kN/m^2) wide flange sections, while all the beams use 248000 kN/m^2 steel (expected yield strength =339000 kN/m^2, wide flange sections. All beams at the same floor levels are same sections. Details of the sections are given separately. Constant gravity loads of 46 kN/m are applied to the beams of all stories. The seismic weight on these frames is 58959 kN (3930 kN/floor for each frame). Using UBC, 1985, the base shear calculated is for each frame for limit states of serviceability is 2135 kN. Uniform and triangular pattern of pushover analyses have been used. The distributed lateral load for each pushover analysis has been estimated (Tables 4.08 and 4.09), Spectral acceleration and Base Shear for fifteen story 2D steel framework, Time period (T_e) =5.63 sec, Seismic weight =58959 kN.

Table 4.08 Base shear distribution for pushover loading for fifteen story 2D frame

Story No from top	Height from base of the structure in meters	Uniform pushover (kN)	Triangular pushover(kN)
15	68.55	142.33	266.94
14	63.98	142.33	249.14
13	59.41	142.33	231.35
12	54.84	142.33	213.55
11	50.27	142.33	195.76
10	45.7	142.33	177.96
09	41.13	142.33	160.16
08	36.56	142.33	142.37
07	31.99	142.33	124.57
06	27.42	142.33	106.78
05	22.85	142.33	88.98
04	18.28	142.33	71.18
03	13.71	142.33	53.39
02	9.14	142.33	35.60
01	4.57	142.33	17.80
00	0.00	0.00	0.00

Table 4.09 Pushover loading of fifteen story steel frames for performance levels

Performance Levels	T_O^i (sec)	S_a^i (g)	V_B^i (kN)
OP	0.744	0.026	1533
IO	0.735	0.043	2535
LS	0.688	0.055	3284
CP	0.637	0.079	4675

Table 4.10 Beam and column details for fifteen story 2D frame

Levels	Beams (F_Y = 248000kN/m^2)	Columns (F_Y = 345000kN/m^2)	
		Exterior	Interior
15	W_{30x108}	W_{14x193}	W_{14x193}
14	W_{30x108}	W_{14x193}	W_{14x193}
13	W_{30x108}	W_{14x193}	W_{14x193}
12	W_{36x135}	W_{14x257}	W_{14x257}
11	W_{36x135}	W_{14x257}	W_{14x257}
10	W_{36x160}	W_{14x342}	W_{14x342}
09	W_{36x160}	W_{14x342}	W_{14x342}
08	W_{36x182}	W_{14x398}	W_{14x398}
07	W_{36x182}	W_{14x398}	W_{14x398}
06	W_{36x194}	W_{14x426}	W_{14x426}
05	W_{36x194}	W_{14x426}	W_{14x426}
04	W_{36x210}	W_{14x455}	W_{14x455}
03	W_{36x210}	W_{14x455}	W_{14x455}
02	W_{36x210}	W_{14x455}	W_{14x455}
01	W_{36x210}	W_{14x455}	W_{14x455}

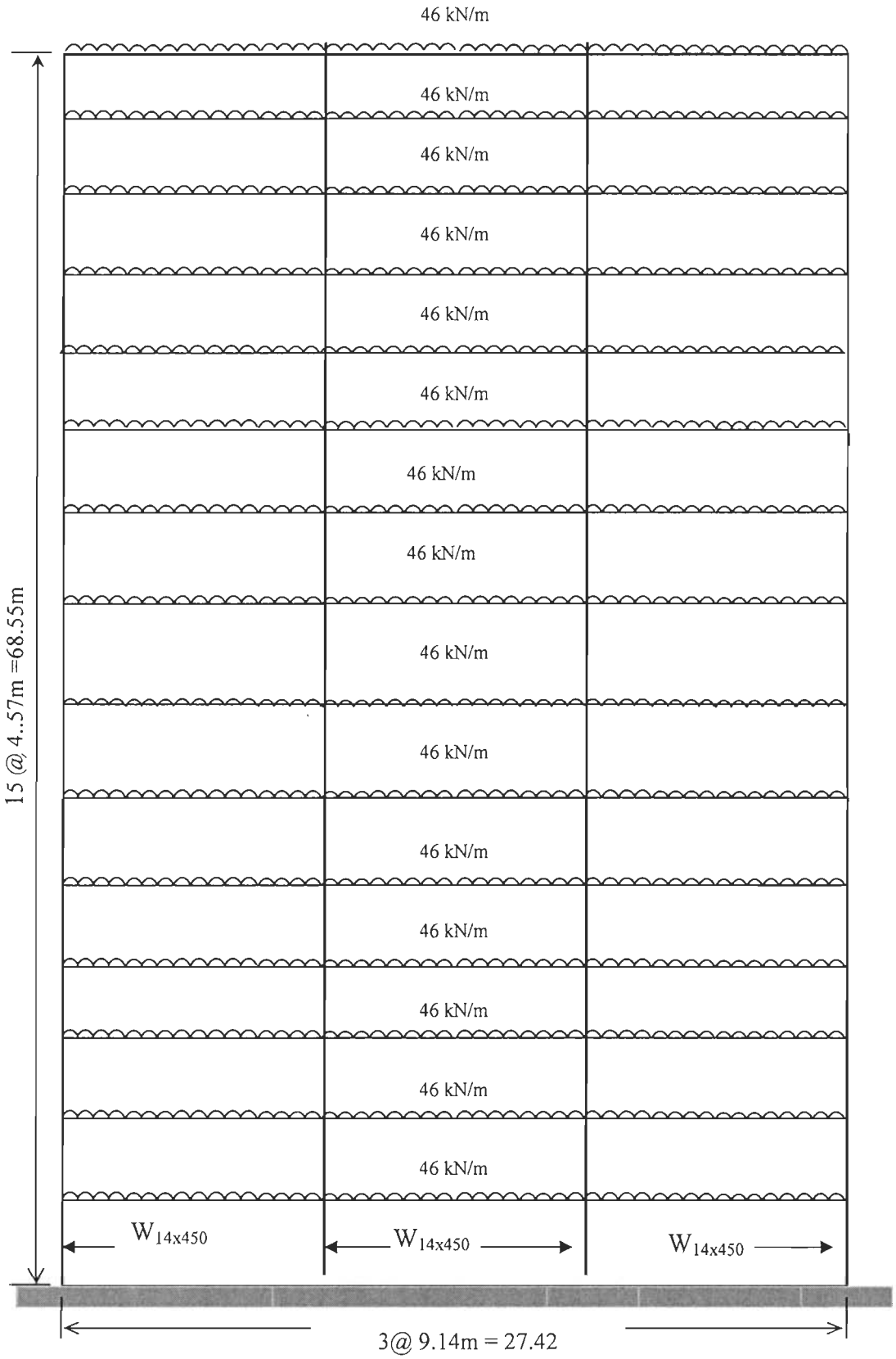

Figure 4.04 Diagram of fifteen story four bay steel 2D building frameworks

4.3.4 Example Problem 4.4: Twenty Story 2D Three Bay Steel Frame Building

The building frame has been used for performance evaluation under earthquake ground motions in the mentioned literature [57]

The frame is ductile to strength and drift criterion. The strength criterion requires that the components of the frame be capable of resisting a triangular distributed lateral load having the base shear of 6230 kN. Factored dead load plus live load to each column at each level is 360 kN. The load is distributed over the span and is 40 kN/m with additional 180 kN point load on the external columns. The base shear estimated for this frame from the basic criteria are 1826 kN, 2993 kN, 3911 kN, and 5564 kN for OP, IO, LS, CP respectively.

This is a perimeter frame of a building. All three bays are 9.14 m (centerline dimensions) and stories are 4.57 m. the frame has rigid moment connections, with all columns fixed at the ground level. All the columns use 345000 kN/m^2 steel (expected yield strength =397000 kN/m^2) wide flange sections, while all the beams use 248000 kN/m^2 steel (expected yield strength =339000 kN/m^2, wide flange sections. All beams at the same floor levels are same sections. Details of the sections are given separately. A constant gravity load of 40 kN/m is applied to the beams of all stories. The seismic weight on these frames is 29,140 kN (1457 kN/floor for each frame). The estimated base shear is given as 6230 kN. Uniform and triangular pattern of pushover analyses have been used. The distributed lateral load for each pushover analysis has been estimated (tables 4.12). Spectral acceleration and Base Shear for twenty story 2D steel framework

Time period (T_e) =2.337 sec, Seismic weight =29,140 KN

Table 4.11 Pushover loading of twenty story frame for performance levels

Performance Levels	T_O^i (sec)	S_a^i (g)	V_B^i(kN)
OP	0.744	0.0626	1826
IO	0.735	0.1027	2993
LS	0.688	0.1342	3911
CP	0.637	0.1909	5564

Tables 4.12 Pushover load distribution for twenty story frames

Story No from top	Height from base of the structure in meters	Uniform pushover (kN)	Triangular pushover (kN)
20	79.2	311.50	593.40
19	75.24	311.50	563.73
18	71.28	311.50	534.06
17	67.32	311.50	504.39
16	63.36	311.50	474.72
15	59.40	311.50	445.05
14	55.44	311.50	415.38
13	51.48	311.50	385.71
12	47.52	311.50	356.04
11	43.56	311.50	326.37
10	39.60	311.50	296.70
09	35.64	311.50	267.03
08	31.68	311.50	237.36
07	27.72	311.50	207.69
06	23.76	311.50	178.02
05	19.80	311.50	148.35
04	15.84	311.50	118.68
03	11.88	311.50	89.01
02	07.92	311.50	59.34
01	03.96	311.50	229.67
00	00.00	00.00	00.00

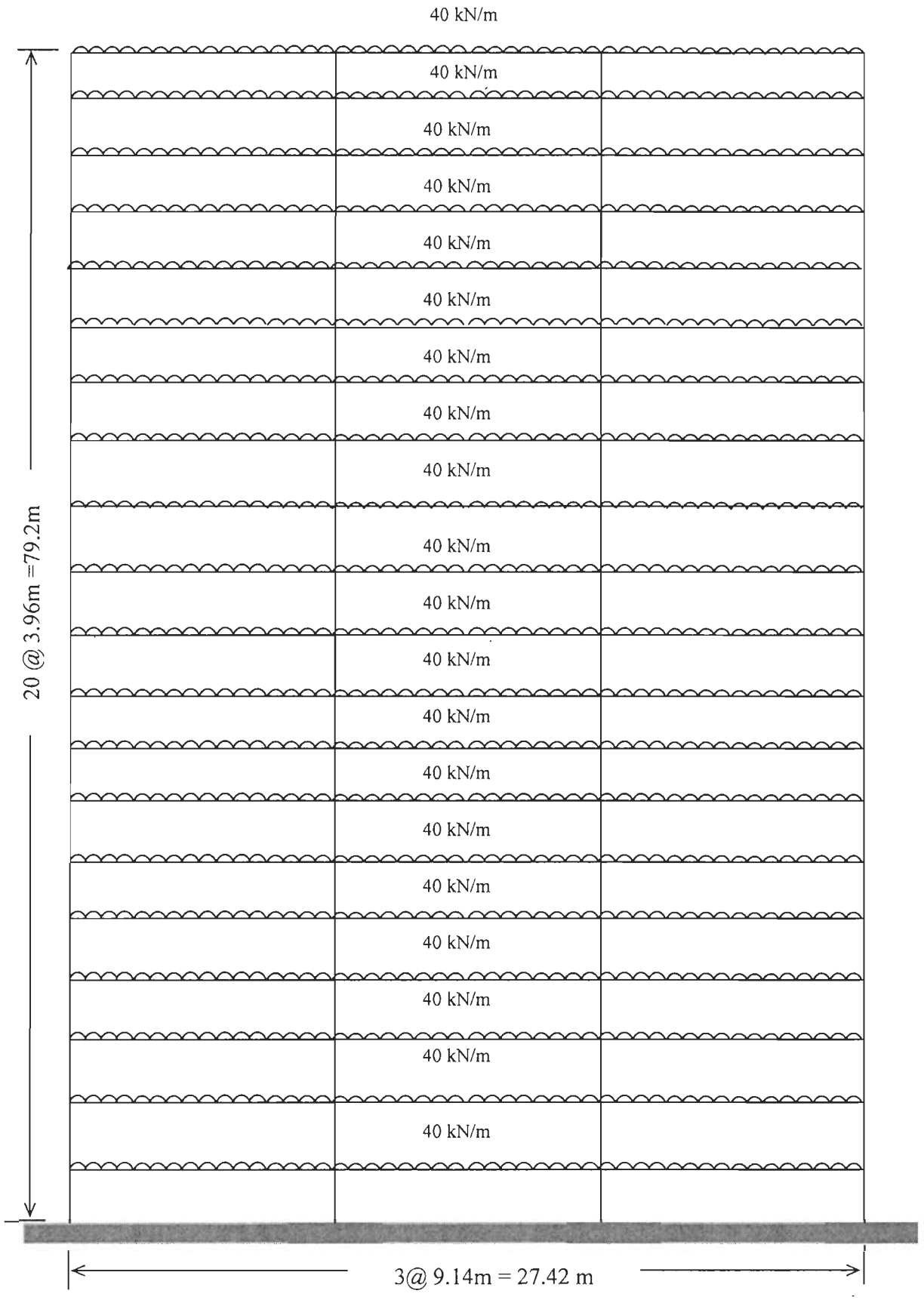

Figure 4.05 Diagram of twenty story three bay steel 2D building frameworks

Table 4.13 Beam and Column details for twenty story frame

Levels	Beams (F_Y = 248000kN/m^2)	Columns (F_Y = 345000kN/m^2)	
		Exterior	Interior
20	W_{30x108}	W_{14x145}	W_{14x145}
19	W_{30x108}	W_{14x145}	W_{14x145}
18	W_{36x135}	W_{14x176}	W_{14x176}
17	W_{36x135}	W_{14x176}	W_{14x176}
16	W_{36x182}	W_{14x211}	W_{14x257}
15	W_{36x182}	W_{14x211}	W_{14x257}
14	W_{36x210}	W_{14x257}	W_{14x342}
13	W_{36x210}	W_{14x257}	W_{14x342}
12	W_{36x245}	W_{14x383}	W_{14x398}
11	W_{36x245}	W_{14x283}	W_{14x398}
10	W_{36x260}	W_{14x342}	W_{14x426}
09	W_{36x260}	W_{14x342}	W_{14x426}
08	W_{36x260}	W_{14x398}	W_{14x455}
07	W_{36x260}	W_{14x398}	W_{14x455}
06	W_{36x280}	W_{14x455}	W_{14x455}
05	W_{36x280}	W_{14x455}	W_{14x455}
04	W_{36x300}	W_{14x500}	W_{14x500}
03	W_{36x300}	W_{14x500}	W_{14x500}
02	W_{36x328}	W_{14x550}	W_{14x500}
01	W_{36x328}	W_{14x550}	W_{14x500}

4.3.5 Example Problem 4.5: Three Story Five Bays Three Story 3D Frame Building

The building frame refer to the example problem of RAM Perform 3D [17]. The frame consists of 140 members.

The building frame has been used for performance assessment by RAM Perform 3D. This is a perimeter moment frame of a building, which was designed according the UBC 1994. All bay width is 7.12 m wide and stories are 3.66 m high, each. The frame has panel zones, with all the column bases fixed at the ground level. All the columns use 3450000 kN/m^2 steel (expected yield strength =3970000 kN/m^2) wide flange sections, while all the beams use 2480000 kN/m^2 steel (expected yield strength =3390000 kN/m^2, wide flange sections. The perimeter columns have W_{14x193} and internal columns are W_{14x82} sections. The perimeter girders are W_{27x94}, E-W interior girders are W_{27x94}, and N-S interior girders are

W24x55 sections, Constant gravity loads of 19 kN/m are applied to all the spans running longitudinal direction and constant gravity loads of 36 kN/m to all the spans in the transverse direction. The seismic weight is 7472.33 kN for each floor including the roof. Base shear is 5918 kN (LS).

Seismic weight = 22,417 kN, Time period =1.187 sec

Table 4.14 Base shear for three story 3D frame for performance levels

Performance Levels	T_O^i (sec)	S_a^i (g)	V_B^i (kN)
OP	0.744	0.123	2757
IO	0.735	0.202	4528
LS	0.688	0.264	5918
CP	0.637	0.376	8429

Table 4.15 Base shear distribution for pushover loading for three story 3D frame

Story no from top	Height from base of the structure (m)	Uniform pushover (kN)	Triangular pushover(kN)
03	10.98	1972.67	2958.99
02	07.32	1972.67	1972.66
01	03.66	1972.67	986.33

4.4 Modeling of Steel Frame Building in Ram Perform 3D for the Present Study

Modeling of steel frames of example problems 4.3.1 to 4.3.5 have been carried using RAM Perform 3D [17]. Only the material nonlinearity is considered here. The frames consist of 27, 99, 105, 140, and 140 members, respectively. All frames are perimeter moment resistant frames. All supports are fixed. All floors are modeled as rigid floor diaphragms. Nodal masses are specified for time period and mode shape analysis and for dynamic time-history analysis.

Following elements are used to model the building frame.

(i) All beams are modeled as FEMA steel beams [17].

(ii) All columns are modeled as FEMA steel columns [17].

(iii) Panel zones are modeled as inelastic panel zone elements to increase the yielding and allowing dissipation of energy [17].

RAM Perform 3D in-built, crosses sections (U.S. steel tables) are used for modeling of beam column. All the elements are capable of undergoing inelastic deformation and are

modeled as elasto-plastic elements without any strength degradation and dissipation factors. The nonlinear modeling parameters and acceptance criteria for steel and column elements are taken from Table 5.06 of FEMA-356 [38]. The nonlinear modeling programs and acceptance criteria for panel zones are taken from Table 5.04 of FEMA-273 [3]. P-Delta effects are considered. Self weight of the columns and beams are applied as nodal loads. All other loads are applied as member loads on beams.

For nonlinear static pushover analysis, two types of lateral load patterns have been considered: Uniform and Triangular pushover. In uniform pushover, the floor loads are proportional to the gravity loads on the floor. In the triangular pushover, the floor loads are proportional to the gravity loads on the floor times the height of t he floor above the fixed base. The base shear has been calculated as per the guidelines of FEMA 273 for different performance levels [Tables 4.02, 4.05, 4.08, 4.11, and 4.14], respectively for the frames used in the study. Accelerograms :Northridge E-W, Northridge N-S, EL Centro 1940 NS, EL Centro 1940 E-W, in-built RAM Perform 3D were used for time history analysis with suitable scale factors. The following analyses were conducted using RAM Perform 3D:

G_1: Gravity load analysis for gravity loads for mode shape and time period analysis.

NSP-H_1: G_1+ Nonlinear static pushover analysis (NSP) for uniform load pattern in H_1 direction.

NDP-NOR-EW -H_1: G_1 + nonlinear dynamic analysis for Northridge EW earthquake

NDP-NOR- N-S-H_1: G_1 + nonlinear dynamic analysis for Northridge NS earthquake

NDP-EL Centro- N-S-H_1: G_1 + nonlinear dynamic analysis for EL Centro EW earthquake

NDP-EL Centro- N-S-H_1: G_1 + nonlinear dynamic analysis for EL Centro U-D earthquake

4.5 Aim of Modeling

There are two main concerns for modeling a beam-column or any other structural members.

(i) Force-deformation relationship. A beam-column member exerts force on the adjacent members and connections including this member have deformations that contribute to the displacements of the complete structure [17].

(ii) Demand-capacity measures. Forces and deformations are important for modeling the behavior of the structure, but demand-capacity ratios are required to access performance. Drifts or deflections at the element level may be used for performance assessment without demand-capacity ratios; however, member performance assessment requires demand-capacity ratios. For sufficient accuracy, both may be used.

4.5.1 Beam Element

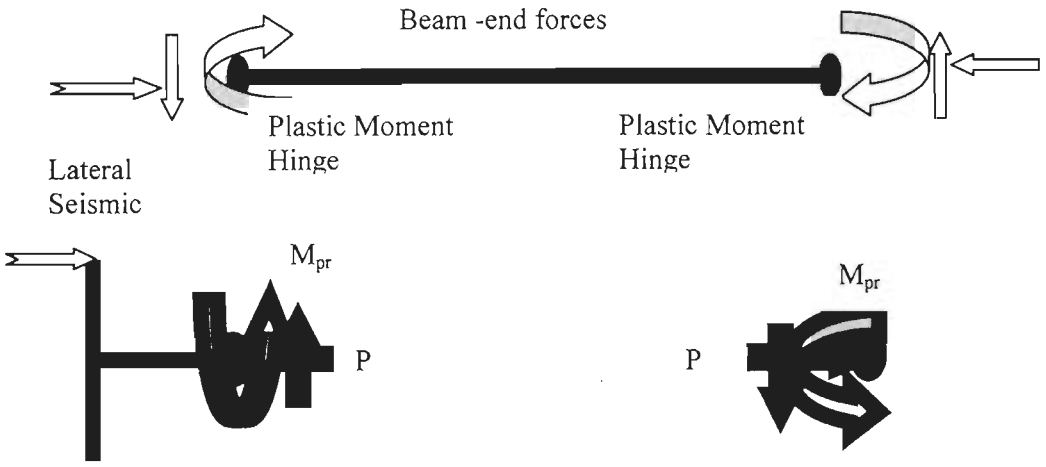

Figure 4.06 Lump plastic modeling of beam element

A beam is one dimensional structural component, takes the vertical loads and transfers to the column through flexural behavior. Since the moment is uniaxial and the uniaxial pull or push is small enough to be neglected, the flexural action is robust. Allowing the beam components for fail safe through yielding of beams near the beam column connections in order to save the whole structure from failure. Failure of beams is not threat for the collapse; therefore beam hinging has been recognized as most favorable during severe ground motions. However, beam models as prescribed in RAM Perform 3D as FEMA-beam has been used in the present study with all the possibility of modeling background of this software.

To develop understanding of the inelastic response of beam, a mathematical modeling of hinge formation has been enumerated. A frame compound component using one or more basic components is defined for beam element. Basic Components: RAM Perfrom-3D includes beam-type basic components. Few of them have been used for modeling in this research program

(i) Stiff end zone, (ii) P/V/M release or linear hinge, (ii) FEMA steel beam, (iv) Moment hinge, rotation model, (v) Moment hinge, curvature model, (vi) Moment connection.

4.5.1.1 Plastic Hinges

There are a number of ways to model inelastic beams in Perform 3D [17]. Among the available models, the plastic hinge model has been used for inelastic modeling of beam. Since some locations of beams, hinges are to be provided in this research program

Rigid-plastic moment hinges have been used to model inelastic bending. A rigid plastic hinge concept provides the in formations regarding this hinge. The hinge is initially rigid, and begins to rotate at the yield moment.

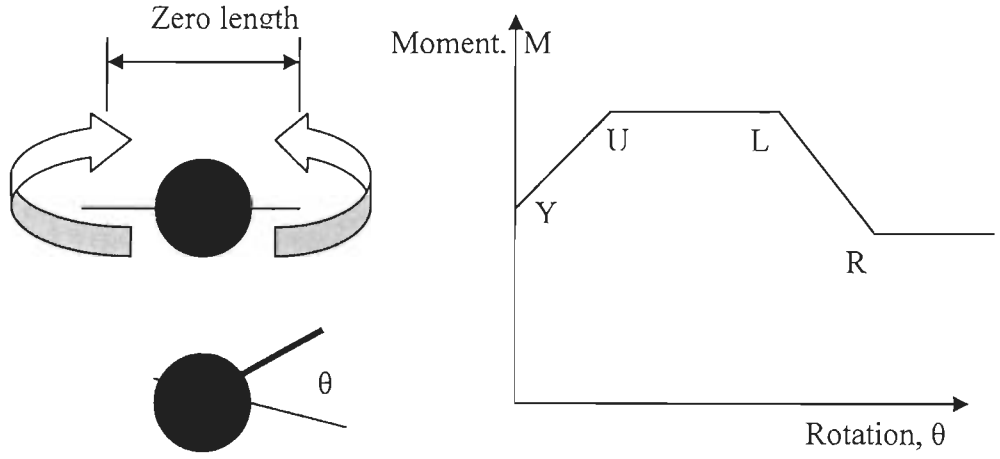

Figure 4.07 Action deformation relationships of beam plastic hinges

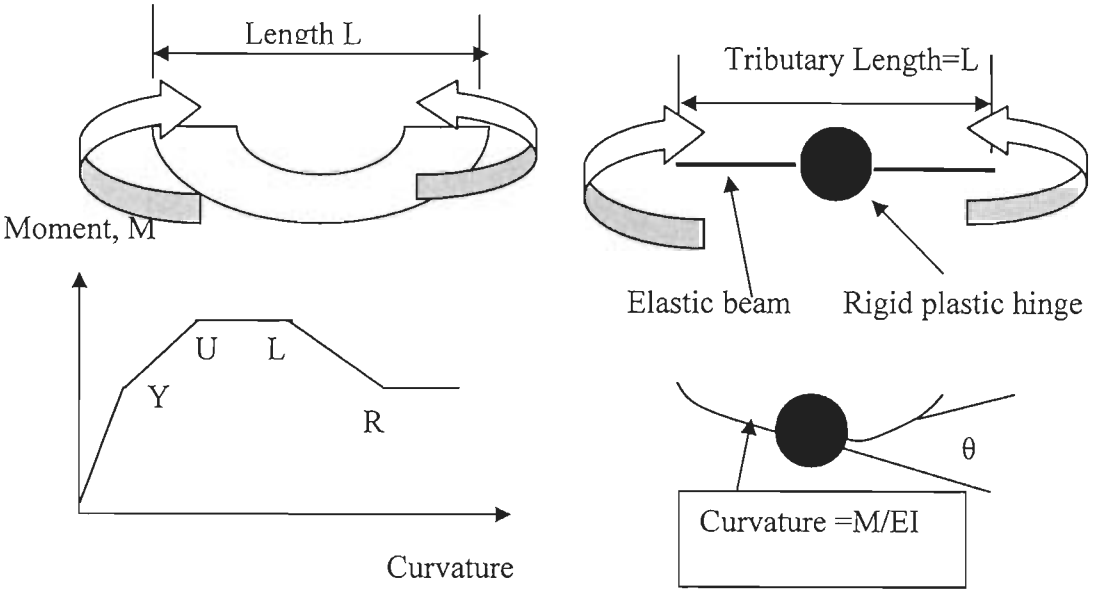

4.2 Figure 2 Rigid plastic hinges

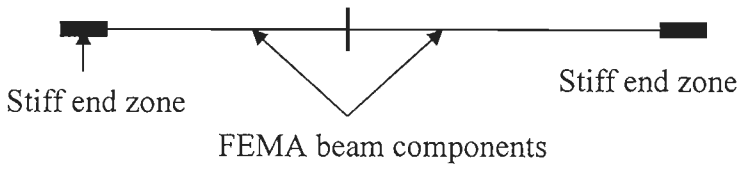

Figure 4.08 Perform chord rotation model of beam element

The key parts in this model are the FEMA beam components. These are finite length components with nonlinear properties. The model has two of these components, to allow for the case where the strengths are different at the two ends of the element.

FEMA beam, steel type: PERFORM 3D uses a chord rotation model as shown above. It then converts this model to the model shown below. Each FEMA beam component is actually two components, namely a plastic hinge and an elastic segment.

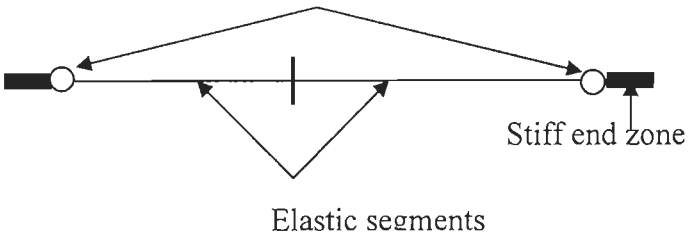

Figure 4.09 Implementation of chord rotation model of beam element

Hinge properties

PERFORM 3D calculates the properties of the plastic hinge components to give the required relationship between member end moment and end rotation.

4.5.1.2 FEMA Steel Beam

Various steps for the implementation of chord rotation model to the FEMA steel beam component.

(i) The EI value for the elastic beam segment is the EI value for the FEMA component.

(ii) The hinges at the element ends are curvature hinges.

(iii) The initial stiffness in the hinge moment-curvature relationship is the EI value of the FEMA component.

(iv) The shape of t he moment-curvature relationship for the hinge is the same as the shape of the relationship between end moment and end rotation for the FEMA component.

(v) The tributary length of each hinge is 1/3 of the FEMA component length (1/6 of the clear length between end zones for a symmetrical element)

4.5.2 Columns

A column is structural element having large axial forces as well as biaxial bending moment. Since columns may have significant bi-axial bending moment, hence it is necessary to consider P-M-M interaction. For shear hinges these can also be biaxial shear, with V-V interaction.

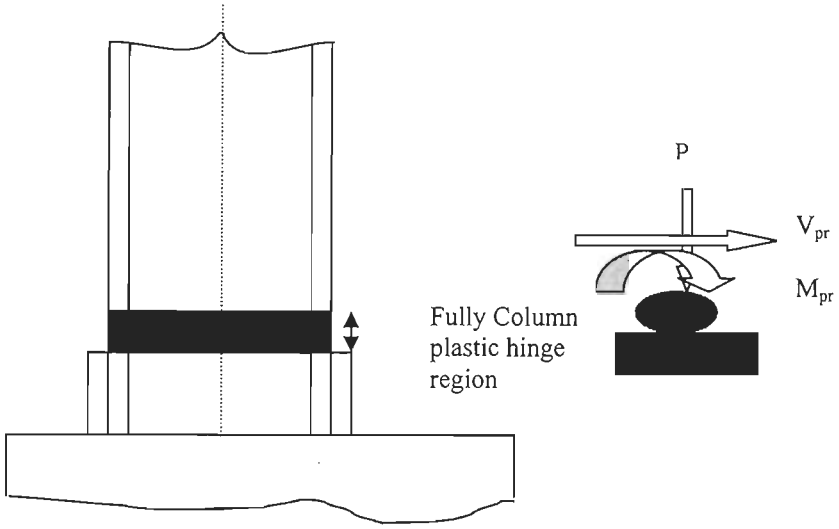

Figure 4.10 Lumped modeling of column

4.5.2.1 Components and Model Types of Columns

Perform 3D includes the following column-type basic components. There are three elastic components and the rest are inelastic.

(i) Stiff end zone.

(ii) P/V/M release or linear hinge

(iii) Uniform elastic X-section segment.

(iv) Uniform inelastic segment with fiber cross section.

(v) FEMA-356 type steel column. For inelastic bending in steel columns, use of this component is preferable.

(v) P-M-M steel hinge, rotation model.

(vii) P-M-M steel hinge, curvature. It is preferable to uses in comparison to the hinge rotation, with the comment that these two have the same for beam hinges.

(viii) Biaxial shear hinge, with V-V interaction. This is a rigid plastic shear hinge that can yield in two directions.

4.5.2.2 Hinges with P-M-M Interaction

Limited points have been discussed as used in this study.

(i) P-M-M Hinge: A rigid-plastic hinge with P-M-M interaction is conceptually similar to a uniaxial moment hinge. Perform used plasticity theory to model P-M-M interaction.

(ii) Steel Type P-M-M interaction Surface. Two types of P-M_M yield surface are P-M interaction at M=0, and M-M interaction at P=0.

4.5.2.3 Extension to P-M Interaction

In a piece of steel under biaxial stress, the major and minor principal stresses interact each other. Plasticity theory models this interaction. By analogy, plasticity theory can be extended to P-M interaction in a column, where the axial force, P and the bending moment interact with each other. For the E-P-P cases the yield surface is now P-M strength interaction surface for the column cross-section. For the steel columns such an analogy works properly as tested [16].

4.6 Panel Zone Element

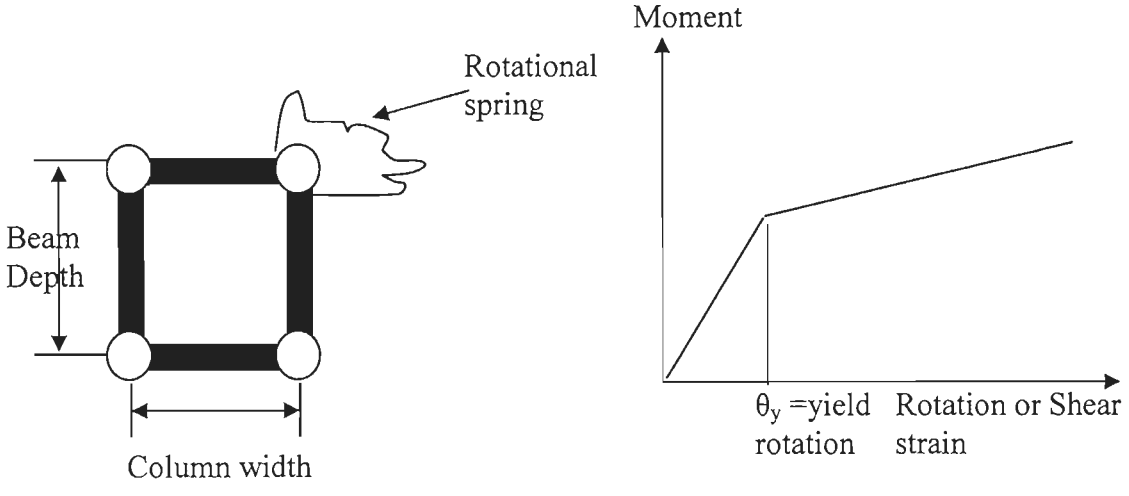

Non-linear response

Steel Panel Zone Deformation Capacities

Guidelines	Measures	IO	LS	CP
ASCE 41	θ_p/θ_y	1	8	11
FEMA 273	θ_p/θ_y (F_y=348 kN)	0.6	10	17

Figure 4.11 Panel zone elements

Table 4.16 Accelerograms used in the analyses

Sl. No	Name of earthquake	Maximum acceleration (g)	Duration (Sec)	Compilers
01	Northridge 14145 Mulholland E-W	0.5165	25	RAM Perform 3D
	Northridge 14145 Mulholland N-S	0.4158	25	Do
	Northridge 14145 Mulholland Up-Down	0.3265	25	Do
02	El Centro (E-W)	0.2148	25	RAM Perform 3D
	El Centro (N-S)	0.3129	25	Do
	El Centro (U-D)	02052	25	Do

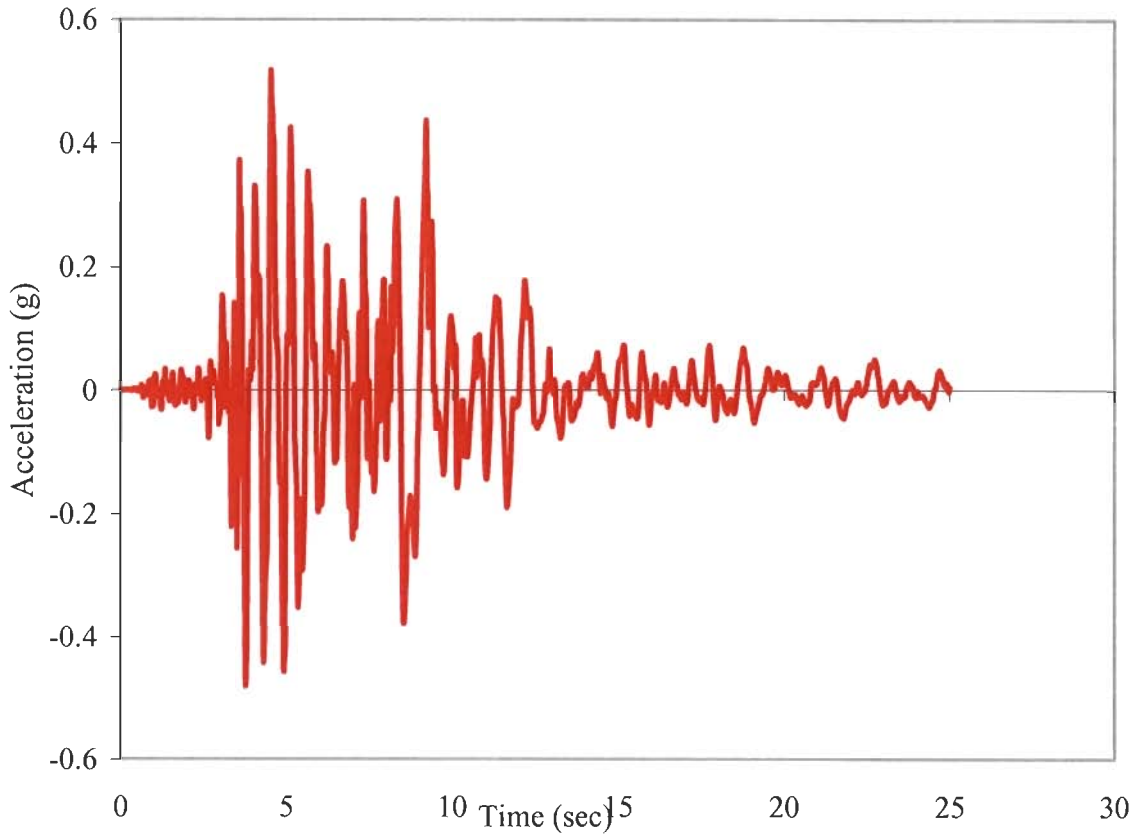

Figure 4.12 Accelerogram of Northridge, 14145 E-W (0.5165g)

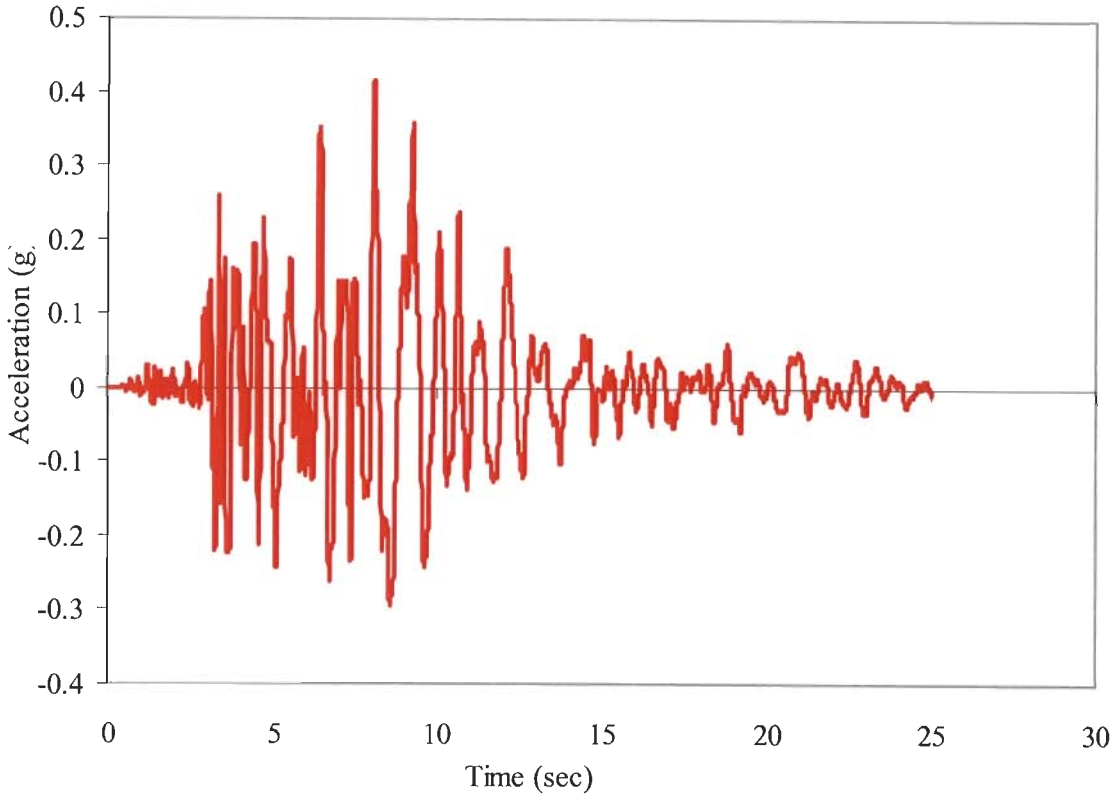

Figure 4.13 Accelerogram of Northridge, N-S (0.4158g)

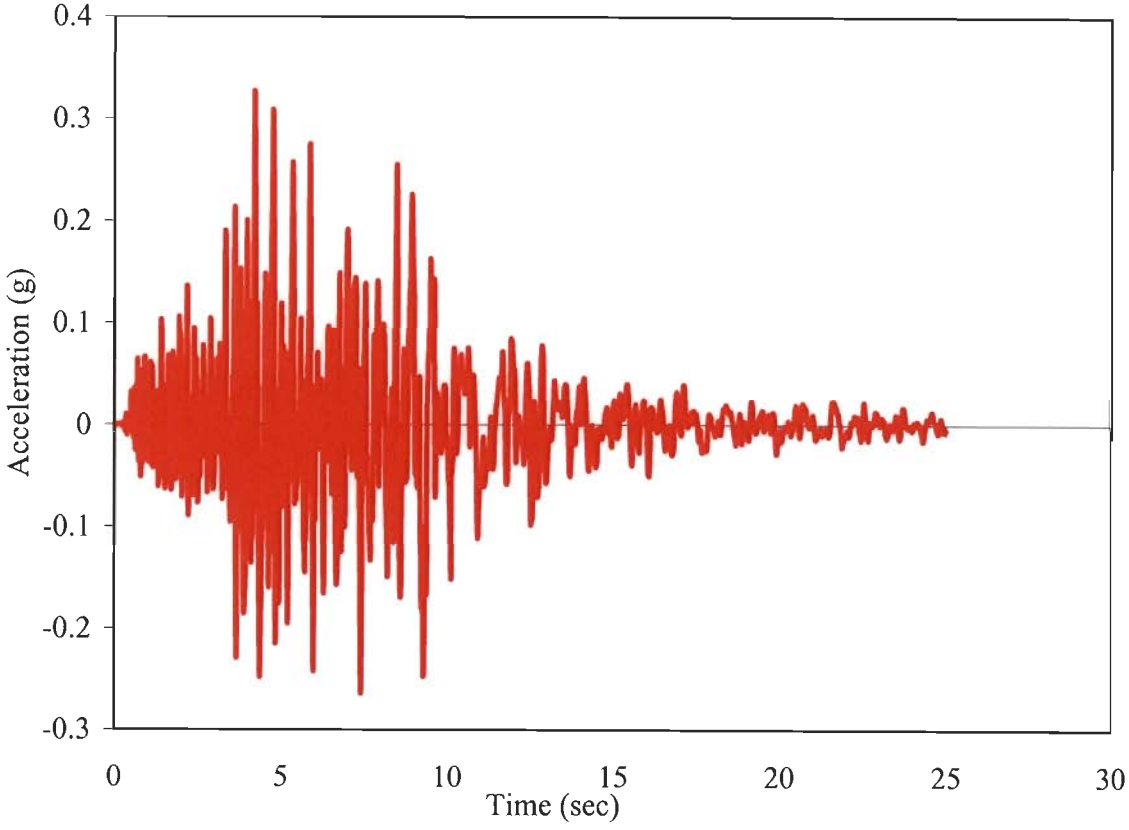

Figure 4.14 Accelerogram of El Centro 1940, E-W (0.3265g)

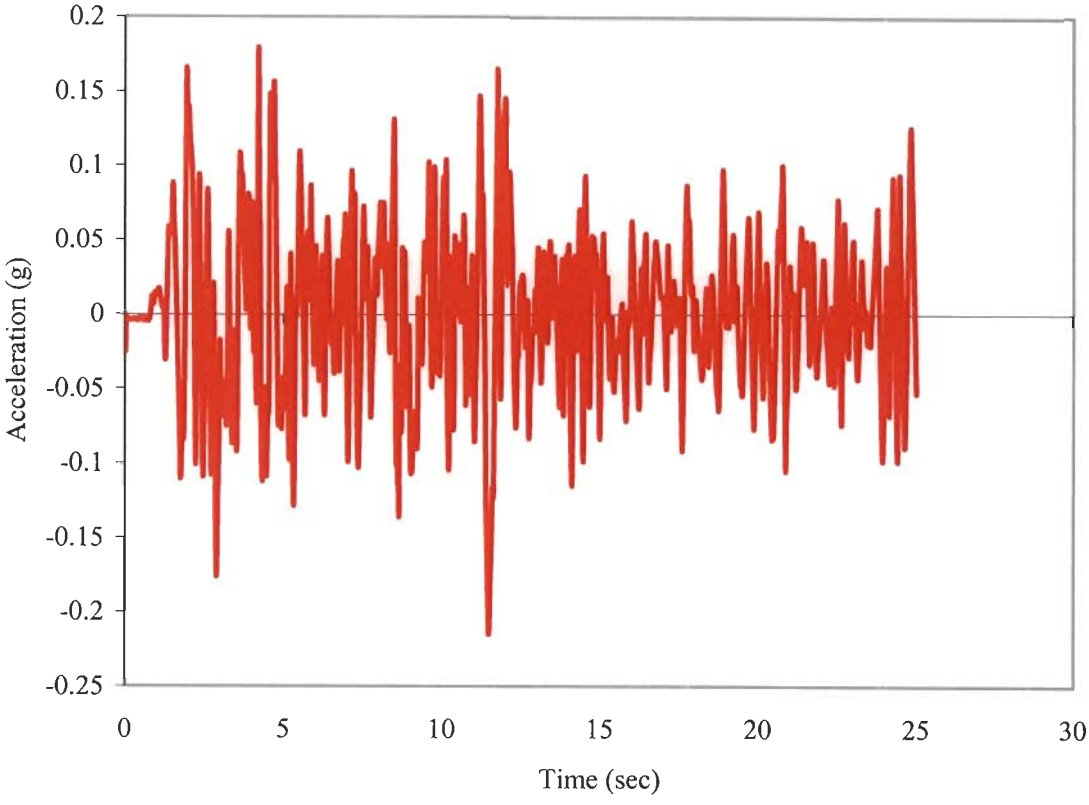

Fi

Figure 4.15 Accelerogram of El Centro 1940, E-W (0.2148g)

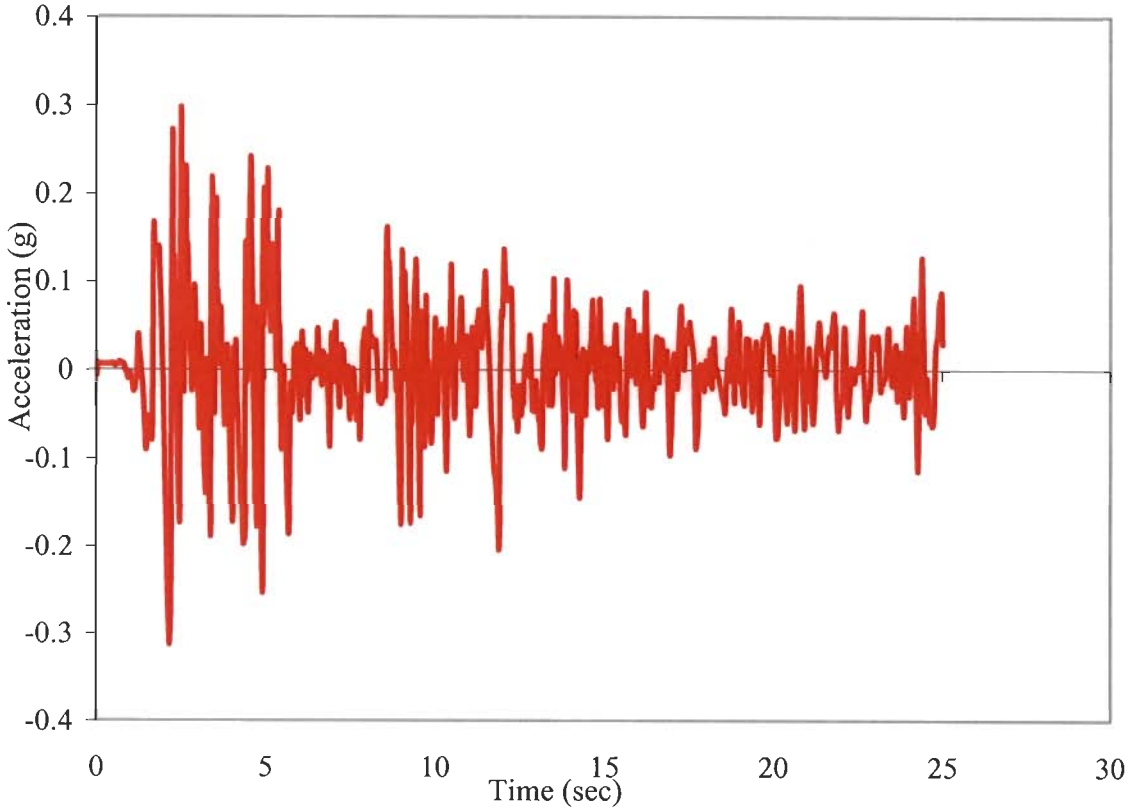

Figure 4.16 Accelerogram of El Centro 1940, N-S (0.3129g)

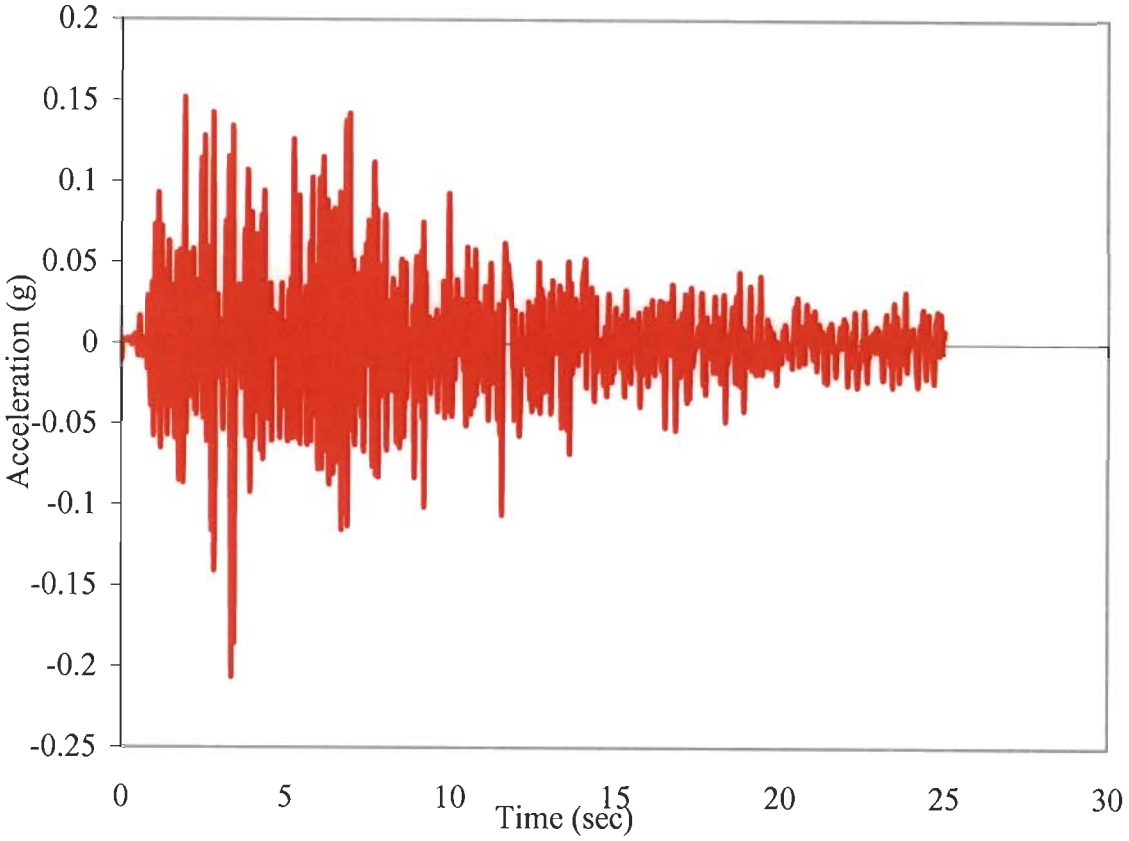

Figure 4.17 Accelerogram of El Centro 1940, U-D (0.2052g)

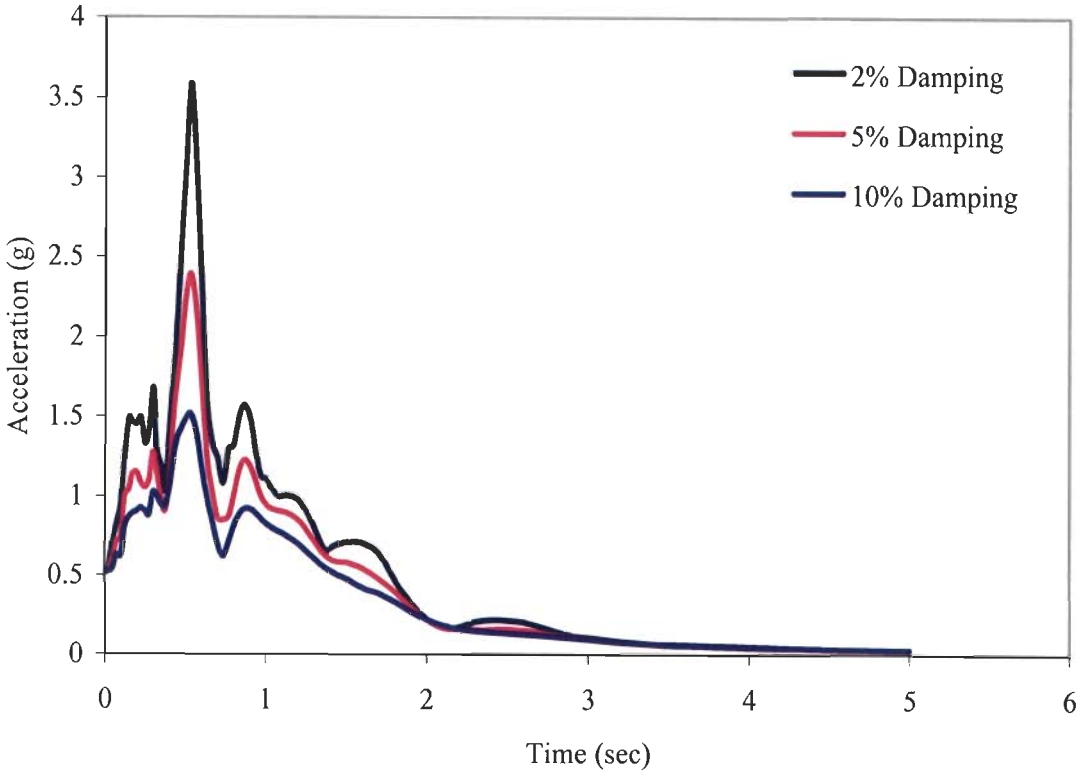

Figure 4.18 Response spectra (acceleration) of Northridge 14145 E-W (0.5165g))

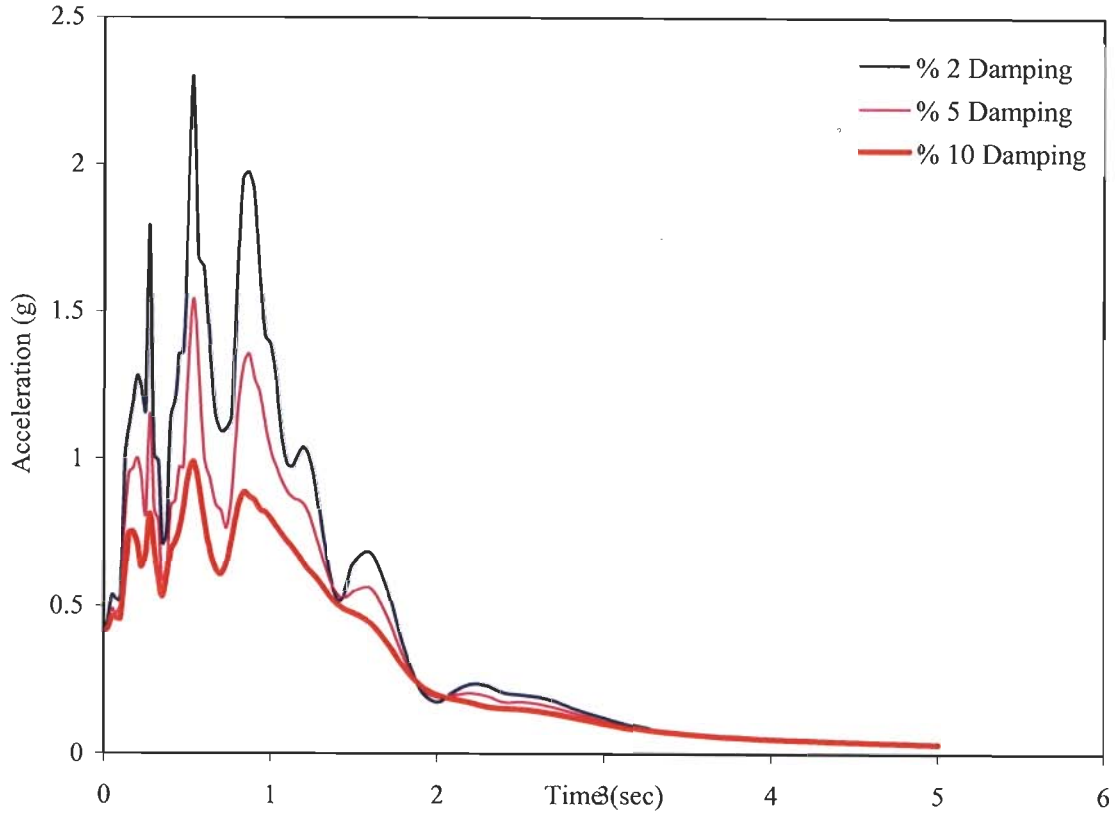

Figure 4.19 Response spectra (acceleration) of Northridge N-S (0.4158g)

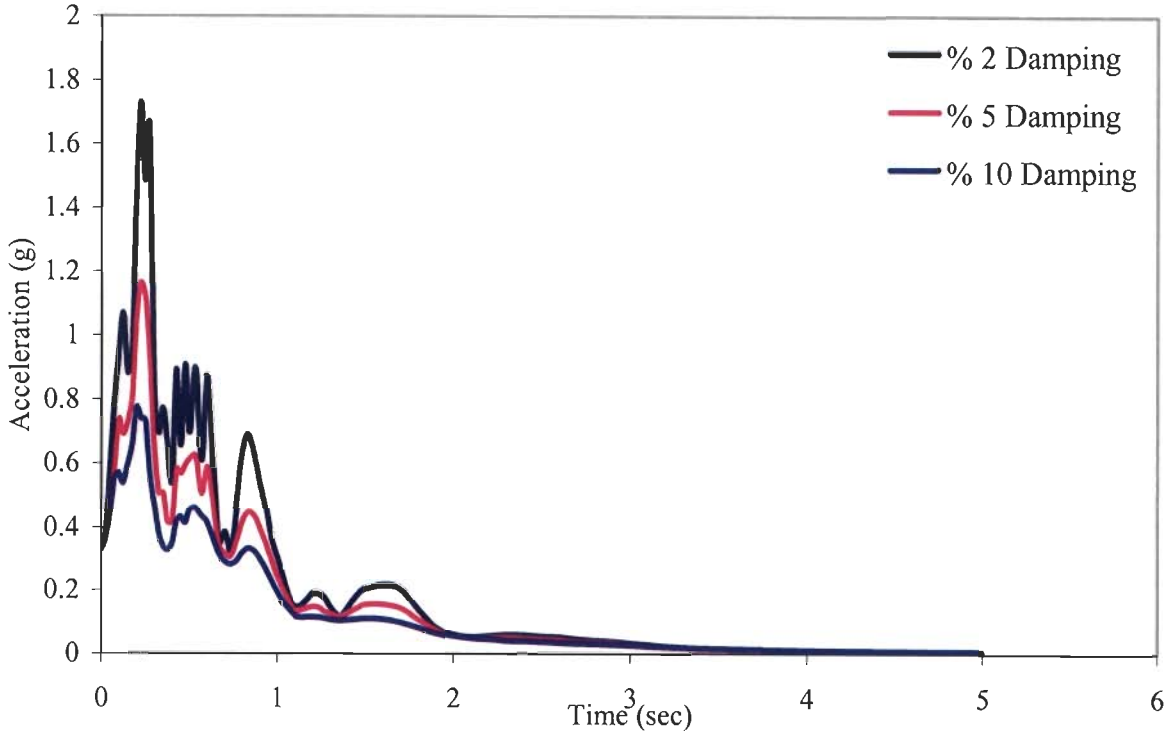

Figure 4.20 Response spectra of Northridge U-D (0.3265g)

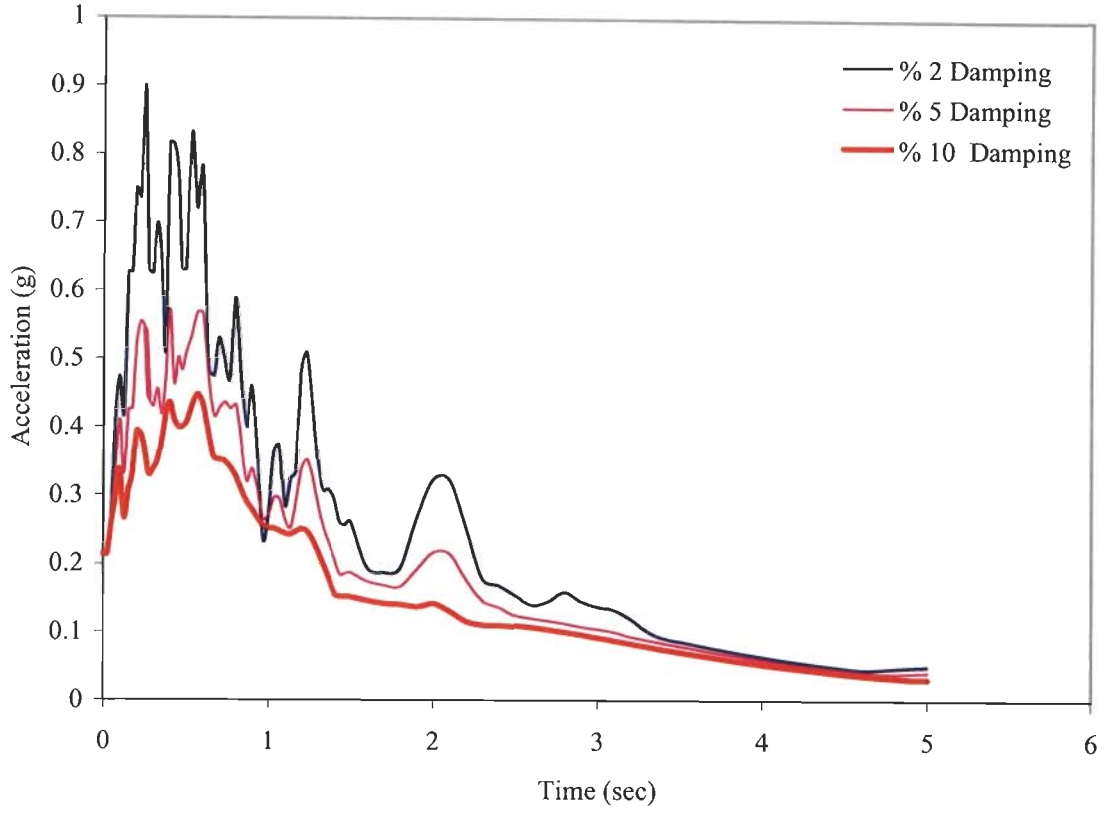

Figure 4.21 Response spectra of El Centro E-W (0.2148g)

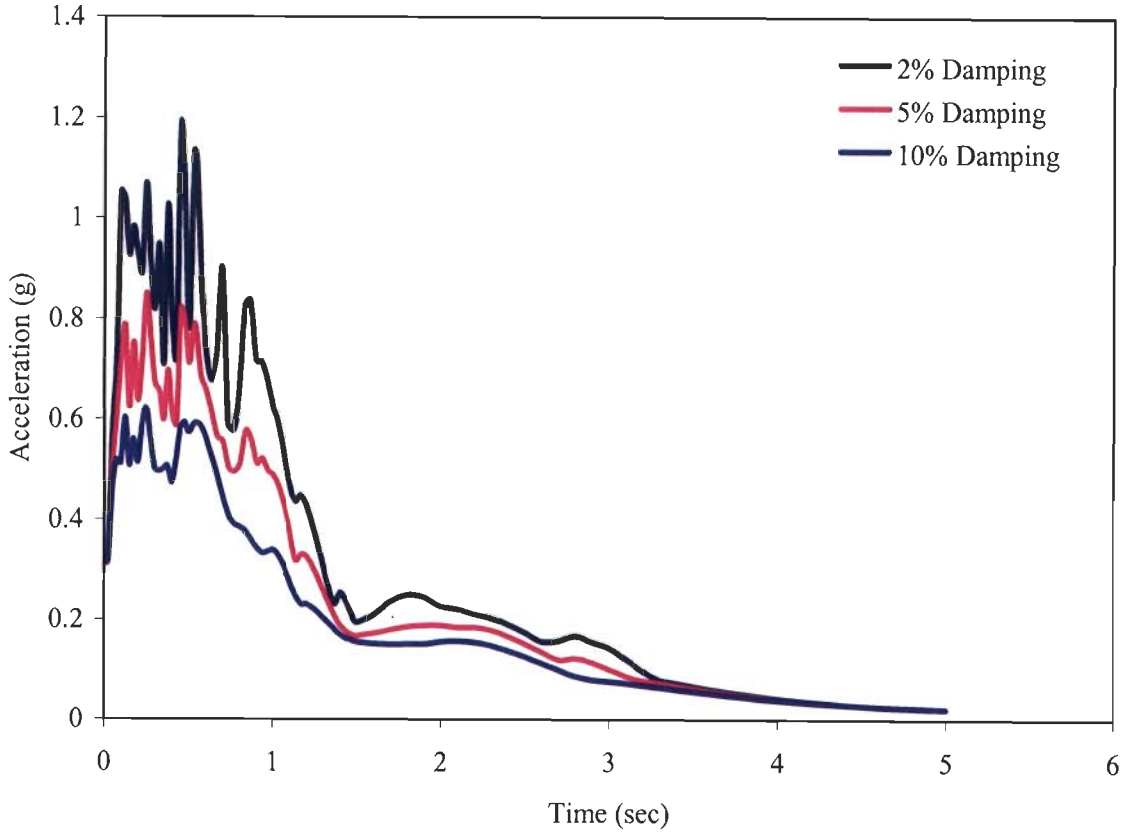

Figure 4.22 Response spectra of Northridge El Centro N-S (0.3129g)

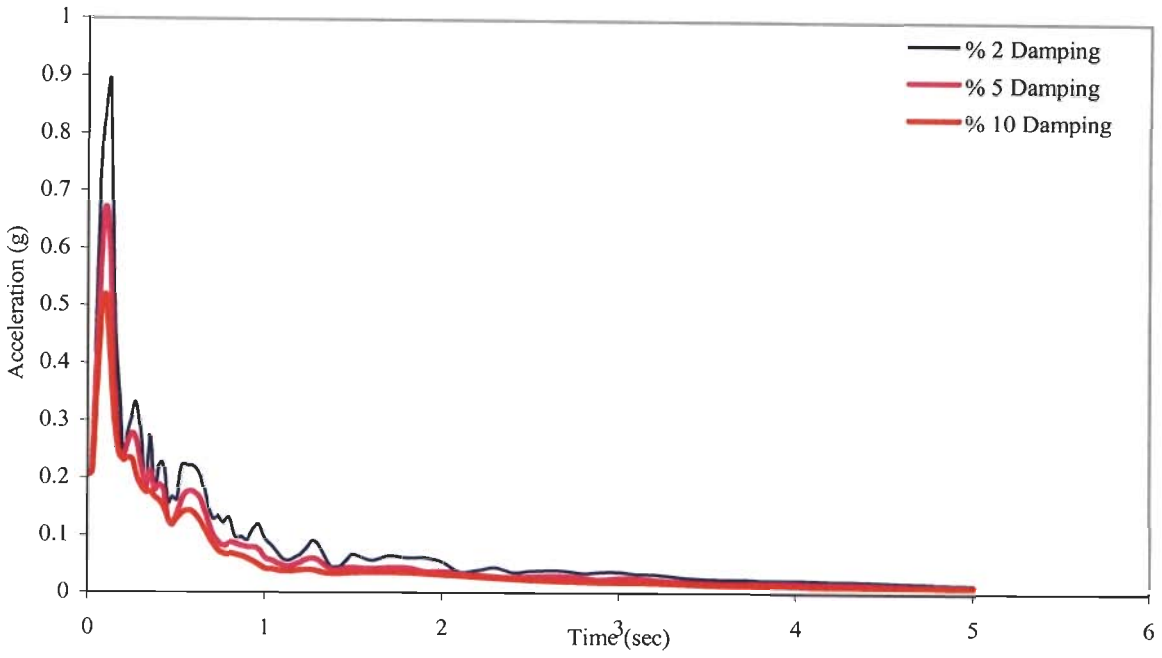

Figure 4.23 Response spectra of Northridge El Centro U-D (0.2052g)

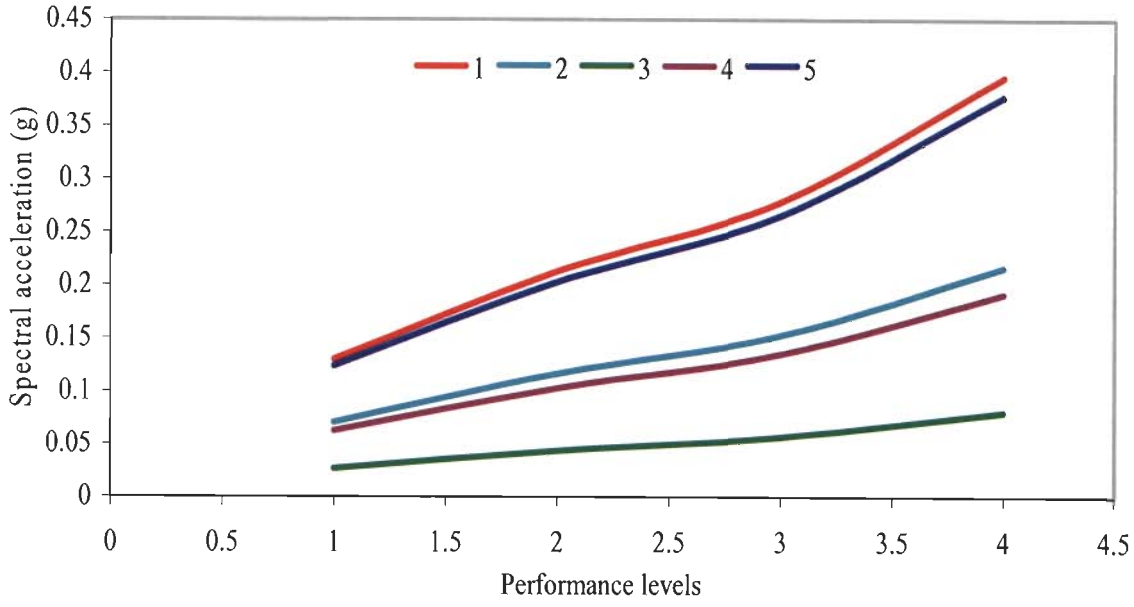

Trends of variation of base shear corrreponding to performance levels

Figure 4.24 Spectral acceleration corresponding to OP, IO, LS, and CP for building frames used in the present study

1 corresponds to spectral acceleration vs. performance levels for three story 2D frame

2 corresponds to spectral acceleration vs. performance levels for three story 3D frame

3 corresponds to spectral acceleration vs. performance levels for nine story 2D frame

4 corresponds to spectral acceleration vs. performance levels for fifteen story 2D frame

5 corresponds to spectral acceleration vs. performance levels for twenty story 2D frame

Chapter 5

RESULT AND DISCUSSIONS

5.1 Result and Discussions

Performance based seismic design is the extension of limit states [23]. Limit states necessitate explicit expressions for the response parameters in order to quantify the performance levels to the corresponding seismic hazards for PBSD development. Energy dissipation is one of the responses having close relationship with damages. Therefore, identification and quantification of damages using energy based relations for physical interpretation are possible. The present study is based on the premises that demand and capacity of structural systems can be developed for assigned performance objectives using energy criterion. For performance objectives, energy based damage indices are effective for performance assessment. For extreme reversal of stresses for which number of yield excursion cycles is very high, the damage behavior is closely associated with low cycle fatigue. Energy based criterion outlined such all behavior during extreme earthquake loadings. During successive increasing earthquake ground motions, the number of hysteretic loops accordingly increases. Using such pre conditions for development of a generalized relation in between hysteretic energy and elastic strain energy in terms of cumulative ductility, during the present study. From this relation, number of loops has been calculated with the predicted hysteretic energy. The number of hysteretic loops has the relations with the number of yield excursions.

Steel building frameworks used for performance evaluations in this present study are taken from literature with modification as described in chapters 3 and 4. Energy based seismic evaluation using normalized hysteretic energy with respect to the input energy or elastic strain energy discloses relations during varying earthquake demands. Analysis results of steel building frames modeled and analyzed in chapter 4 for the assigned performance objectives and accelerograms are subsequently tabulated in the chapter 5. In order to emphasis the damage content at the component levels, structural components are assigned individual name during modeling phase. The advantage of modeling at component level by individual name is that the known fraction of input seismic energy may be used for the design of the particular member, since the energy at component level has the relation with the stiffness and strength of the member (equation 3.36). With the information of the energy

at component level, further strategy for distribution of energy may be carried out in order to achieve uniform damage pattern during severe earthquake ground motions.

The steps of the result discussions are to be maintained in order to assess the objectives of the present study are:

(i) Input seismic energy evaluation.

(ii) Energy based capacity curve formulations.

(iii) Inter story drift and floor spectra relation in terms of energy parameters (absolute and relative input energy derivation and further their interpretation).

(iv) Distribution of input seismic energy.

(v) Normalization of hysteretic energy.

(vi) Elastic strain energy versus hysteretic energy (through yielding) derivation and its validation through the seismic evaluation.

(vii) Interpretation of damage indices using energy parameters as the PBSD tools (cumulative ductility is economically accessible).

(viii) Number of yield excursions, using the relation of the above equation (v) as the PBSD index.

(ix) Sections analysis using Section Builder analysis tools.

(x) Overall overview of the PBSD in terms of the above mentioned parameters.

5.1.1 Input Seismic Energy Evaluation

Result: Input seismic energy evaluated for example steel building frames 4.3.1 to 4.3.5 for the specified velocity spectra corresponding to the accelerograms applied in the study (Figures 5.01 to 5.05) are listed in tables 5.01 to 5.05. Energy ductility has been evaluated from the pushover curve analysis for assigned performance objectives. Energy factors corresponding to the performance levels also have been estimated and are listed in tables 5.06 to 5.08. For the set of earthquake ground motions, as used in the present study, input seismic energy by the software and pseudo velocity spectra, considering the effect of energy correction factor (inelastic effect on input seismic energy) have been tabulated in the 4^{th} and 3^{rd}columns of tables 5.01 to 5.05.

5.1.2 Result Discussion for Input Seismic Energy

The present study emphasis the use of energy based criterion for performance based seismic design development. Principal tasks of performance based seismic design is to perceive the manner how the input seismic action is evaluated. The mode of energy demand evaluation

in energy format is considered as principal loading during earthquake loading. Absolute input seismic energy is treated as physical loading. Relative input seismic energy differs from the absolute input seismic energy for lower and longer period structure, however these two energy are very close for the buildings period range of 0.3 to 5 sec. A seismic design procedure that does not take into account the maximum and cumulative plastic deformation demands that a structure is likely to under go during severe ground motions could lead to unsatisfactory performance. Input seismic energy using the linear elastic spectral pseudo velocity corresponding to the accelerograms used in the study has been modified for inelastic input seismic energy with energy factor. Based on correlation that exists between the displacement ductility/energy ductility, energy correction factor corresponding to performance levels are determined. Building frames (Figures 4.3.1 to 4.3.5) under a set of accelerograms and base shear are used for input seismic energy both by the spectral velocity and by the software modeled in RAM Perform 3D. Velocity spectra for the accelerograms used in the study are developed and have been given in figures 5.01 to 5.05. Input seismic energy evaluated for the accelerograms and the building frames are tabulated in the column 3 of tables 5.01 to 5.05. Results of the pushover analysis were tabulated in the tables 5.6 to 5.8. Energy correction factor was evaluated using the equation (3.17) developed in terms of energy ductility (Tables 5.06-5.08). Values of input seismic from velocity spectra and the energy correction factors were tabulated in 4^{th} column (Tables 5.01-5.05). 5^{th} column of tables (5.01 to 5.05) represented. Ratios of input seismic energy evaluated using velocity spectra along with the energy correction factor for inelastic response and the energy evaluated by the software were tabulated in the sixth columns of tables 5.01 to 5.05 in the ratio form. Both types of input seismic energy are compared. For the building frames used in the study, both input seismic energy have constancy.

Evaluation of seismic action on a structure in terms of energy is one of the content of the present study. Velocity spectra directly give the seismic input in terms of energy. At the same time, velocity spectra is uniform for building structures having period greater than zero and less than 3 (medium rise building structures) [13].

Input seismic evaluation is one of the major tasks for performance based seismic design for performance assessment. Input seismic action in energy format is principal loading during earthquake loadings [8]. Input seismic energy during inelastic response, which a building structure is bound to be during earthquake ground motions, seismic demand in energy format. Looking at the energy balance equation, the first step is to have a good estimate of the input seismic energy for the critical ground motions. The amount of the

input seismic energy is further used towards balancing the input seismic energy by suitable capacity of the structure. For example, only the elastic energy can balance, or a combination of hysteretic energy. Energy dissipation devices and base isolation techniques, which still is the innovative approach for further development to control the energy supply.

The maximum input seismic energy that is absorbed by an elastic SDOF system can be estimated from the linear elastic pseudo velocity spectra [12]. Linear elastic pseudo velocity is an index that Housner [12] used to express the damage potential of an earthquake. Usually it is assumed that input energy is maximized by elastic response and therefore, this energy used as the input seismic energy for an inelastic system also. For an inelastic system, the input seismic energy by using the elastic pseudo velocity has been corrected through the use of energy correction factor [11]. Nonlinear static pushover analysis for base shear corresponding to performance levels response for displacement ductility is used for determination of energy correction factor in the present study.

Table 5.01: Details of input seismic energy under varying ground motions for three story 2D steel building frame (Example problem 4.3.1)

Sl. No	Earthquake ground motions PGA (g)	Mass (kg) Time (sec)	Energy using velocity spectra (kNm)	Input, Seismic Energy Using Perform 3D	Energy ratio: columns (5)/ (4)
01	Northridge E-W (0.5165)	Mass=14447 Period=1.13	987	1118	1.132
02	Northridge E-W(2x0.5165)		2246	2745	1.222
03	Northridge N-S (0.4158)		1289	1582	1.227
04	Northridge N-S(2x0.4158)		2988	3764	1.259
05	El Centro E-W (0.2148)		399	503	1.262
06	El Centro E-W (2x0.2148)		1765	2188	1.239
07	El Centro U-D(0.2052)		29	30.38	1.047
08	El Centro UD(2x0.2052)		98.6	112.7	1.143

Table 5.02: Details of input seismic energy under varying ground motions for 2D, nine story steel building frame (Example problem 4.3.2).

Sl. No	Earthquake ground motions PGA (g)	Mass (kg) Time (sec)	Energy using velocity spectra (kNm)	Input, Seismic Energy Using Perform 3D	Energy ratio: columns (5)/ (4)
01	Northridge E-W (0.5165)	Mass=44172 Period=2.086	3342	3834	1.147
02	Northridge E-W(2x0.5165)		11543	14580	1.263
03	Northridge N-S(0.4158)		2654	3141	1.183
04	Northridge N-S (2x0.4158)		9876	12440	1.259
05	El Centro E-W (0.2148)		2045	2782	1.359
06	El Centro E-W (2x0.2148)		7865	9908	1.259
07	El Centro U-D (0.2052)		87	109.4	1.250
08	El Centro U-D(2x0.2052)		321	386.6	1.202

Table 5.03: Details of input seismic energy under varying ground motions for 2D, fifteen story steel building frame (Example problem 4.3.3)

Sl. No	Earthquake ground motions PGA (g)	Mass (kg) Time (sec)	Energy using velocity spectra (kNm)	Input, Seismic Energy Using Perform 3D	Energy ratio: columns (5)/ (4)
01	Northridge E-W (0.5165)	Mass=58959 Period=5.63	2765.5	3235	1.169
02	Northridge E-W(2x0.5165)		8876	9484	1.068
03	Northridge N-S(0.4158)		2543	2820	1.109
04	Northridge N-S (2x0.4158)		9877	10630	1.076
05	El Centro E-W (0.2148)		1543	1716	1.112
06	El Centro E-W (2x0.2148)		4675	5119	1.094
07	El Centro U-D(0.2052)		102	190	1.863
08	El Centro U-D (2x0.2052)		301	491	1.632

Table 5.04: Details of input seismic energy under varying ground motions for 2D, twenty story steel building frame (Example problem 4.3.4)

Sl. No	Earthquake ground motions PGA (g)	Mass (kg) Time (sec)	Energy using velocity spectra (kNm)	Input, Seismic Energy Using Perform 3D	Energy ratio: columns (5)/ (4)
01	Northridge E-W (0.5165)	Mass=29140 Period=2.337	2766	3275	1.184
02	Northridge E-W(2x0.5165)		11064	13070	1.181
03	Northridge N-S(0.4158)		2600	2836	1.091
04	Northridge N-S (2x0.4158)		9765	11310	1.158
05	El Centro E-W (0.2148)		612	814.8	1.331
06	El Centro E-W (2x0.2148)		2448	3226	1.318
07	El Centro U-D (0.2052)		54	68	1.269
08	El Centro U-D(2x0.2052)		216	240	1.113

Table 5.05: Details of input seismic energy under varying ground motions for 3D, three story steel building frame (Example problem 4.3.5)

Sl. No	Earthquake ground motions PGA (g)	Mass (kg) Time (sec)	Energy using velocity spectra (kNm)	Input, Seismic Energy Using Perform 3D	Energy ratio: columns (5)/ (4)
01	Northridge E-W (0.5165)	Mass=22427 Period=1.187	2665	3513	1.318
02	Northridge-E-W (2x0.5165)		7876	10730	1.362
03	Northridge N-S (0.4158)		2930	4342	1.482
04	Northridge N-S (2x0.4158)		8654	11379	1.310
05	El Centro E-W (0.2148)		1134	1399	1.233
06	El Centro E-W (2x0.2148)		4277	4790	1.119
07	El Centro U-D(0.2052)		57	88.26	1.548
08	El Centro U-D (2x0.2052)		176	218.42	1.241

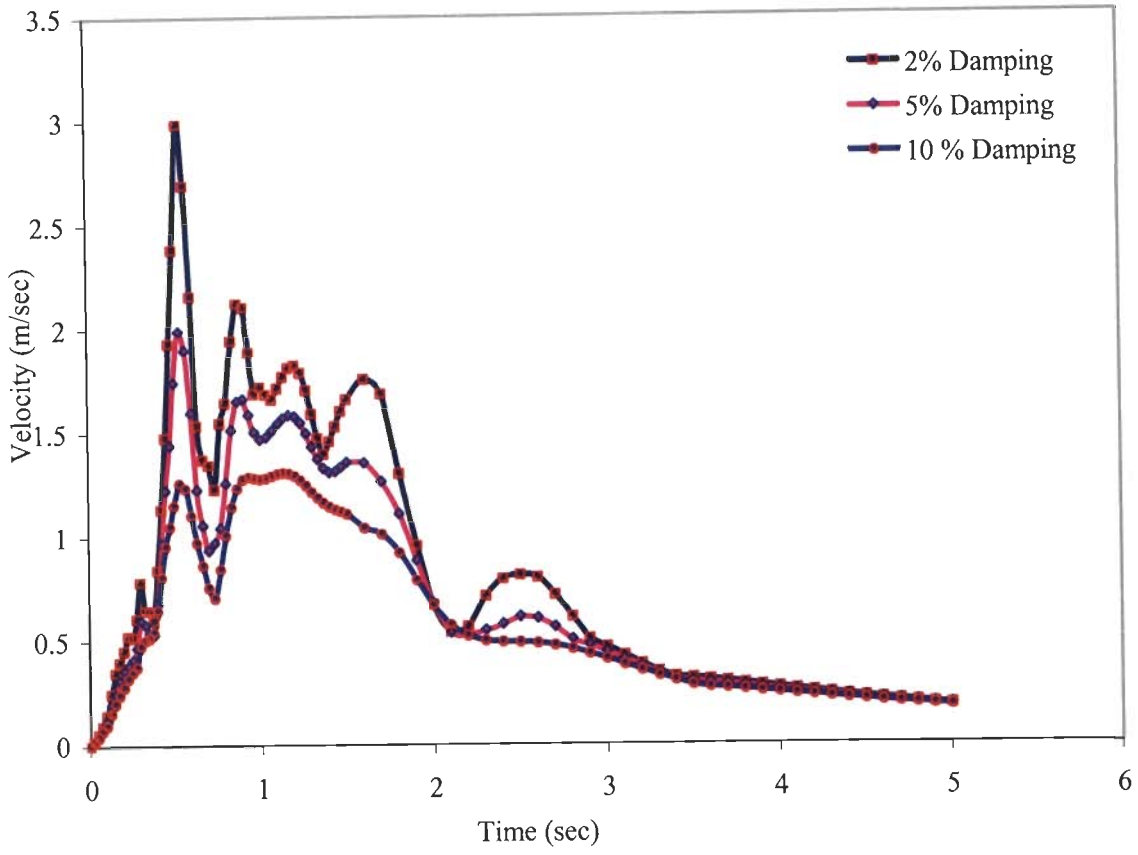

Figure 5.01: Pseudo velocity spectra of Northridge, 14145 Mulholland, E-W (0.5165g)

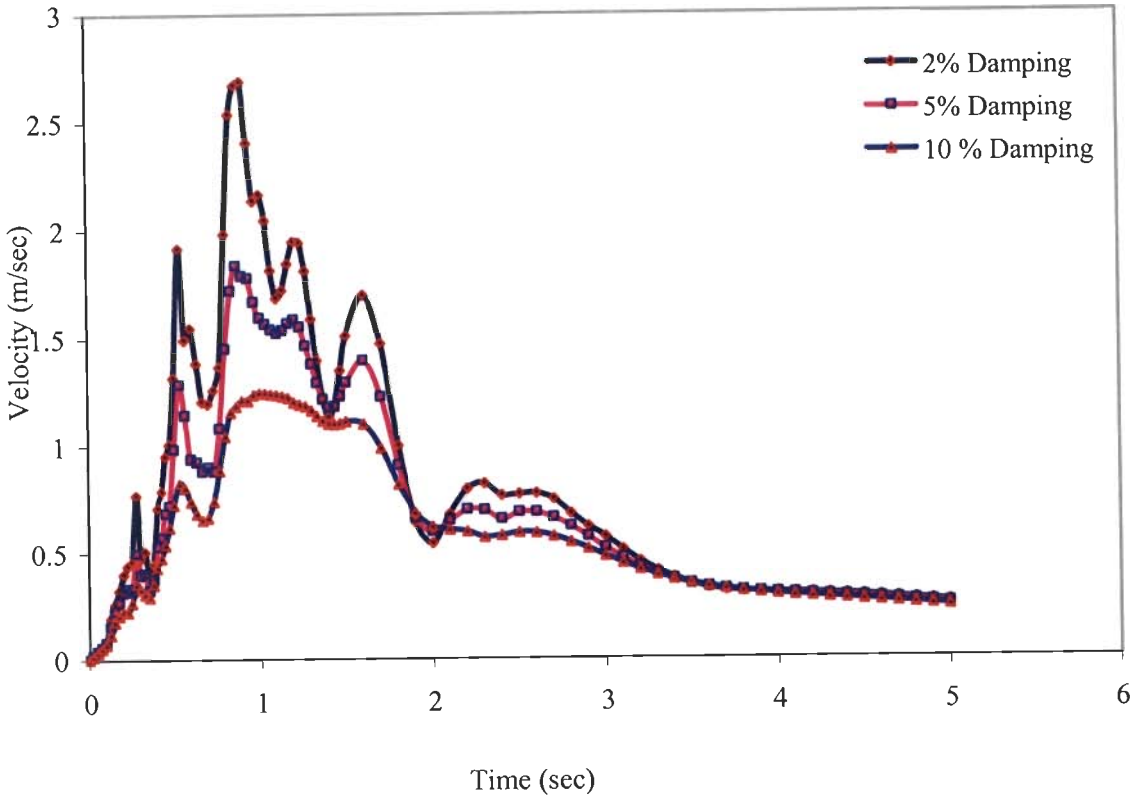

Figure 5.02: Pseudo velocity spectra of Northridge, 14145 Mulholland, N-S (0.4158g)

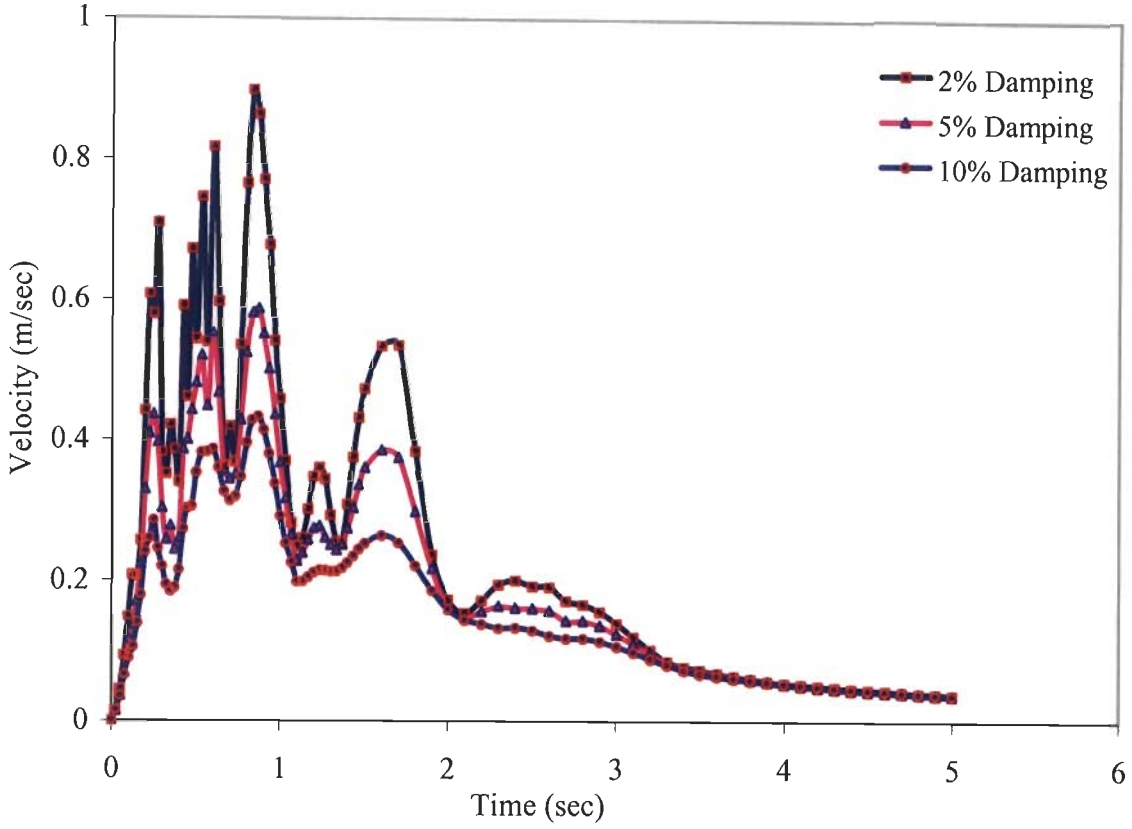

Figure 5.03: Pseudo velocity spectra of Northridge, 14145 Mulholland; Up-Down (0.3265g)

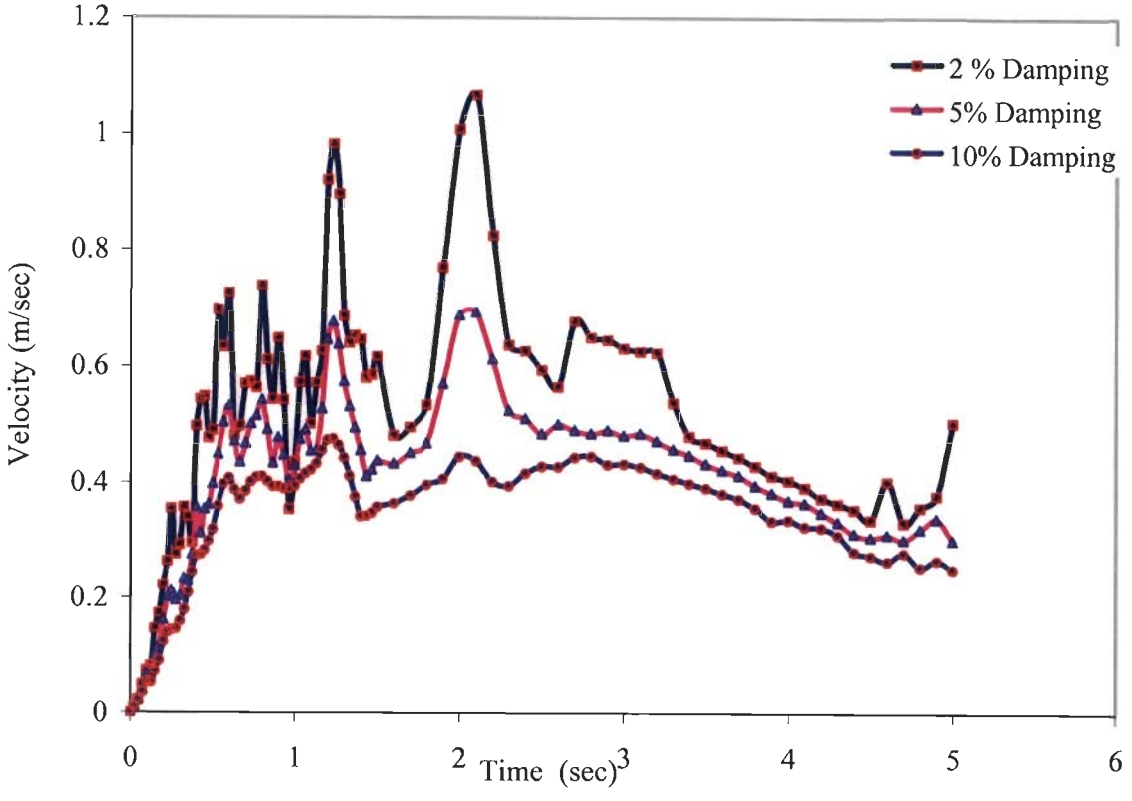

Figure 5.04: Pseudo velocity spectra for El Centro 1940, E-W (0.2148g)

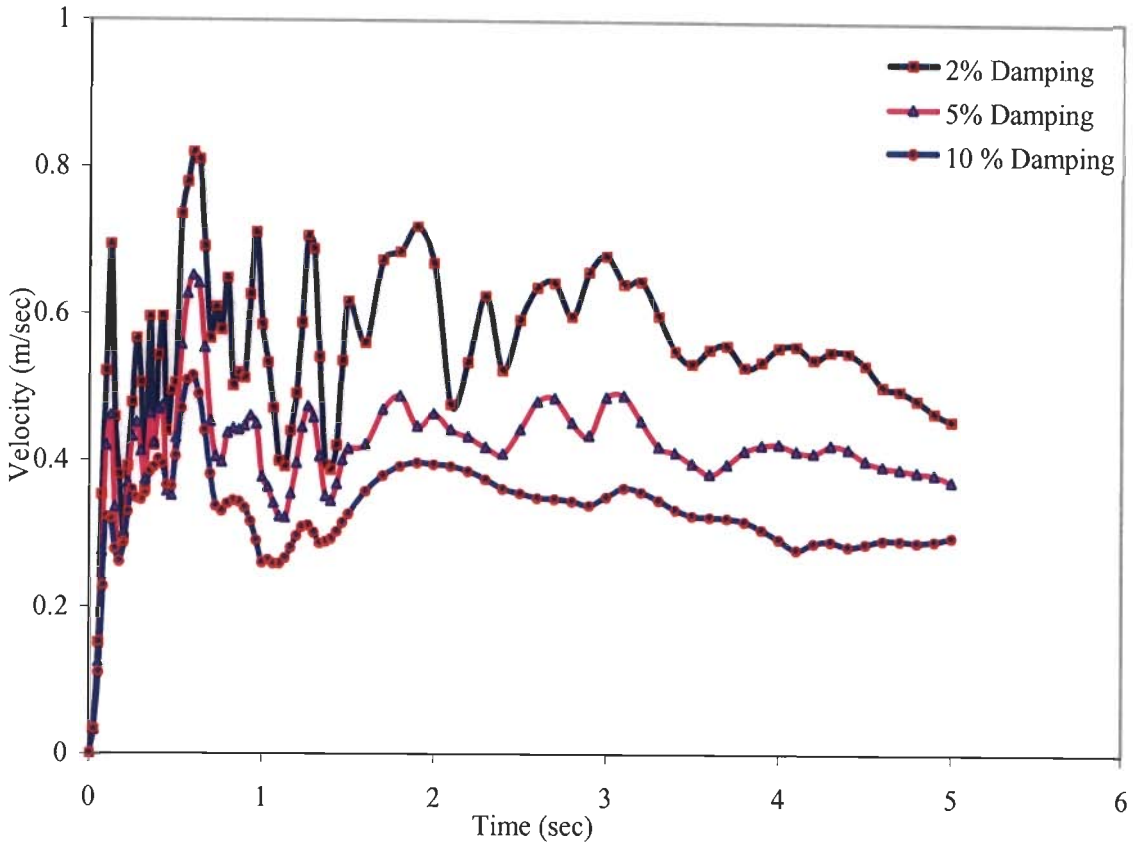

Figure 5.05: Pseudo velocity spectra for El Centro 1940, U-D (0.2052g)

Table 5.06: Energy ductility, and energy factor for three story 2D and three story 3D frames

Building frame	Performance level	Roof displacement (mm)	Displacement Ductility	Spectral Acceleration $=\frac{V_B}{W}(g)$	μ_E	γ_E
Three story 2Dsteel frame	IO	$\delta_Y = 57.99$ $\delta_{IO} = 131.99$	2.28	0.213	3.56	0.685
	LS	$\delta_{LS} = 232.37$	4.00	0.278	7.00	0.571
	CP	$\delta_{CP} = 280.0$	4.83	0.396	7.83	0.402
	μ_E (Energy ductility) = 2μ-1, μ= Displacement ductility γ_E (Energy correction factor) = $\frac{4\mu_E}{(\mu_E+1)^2}$ Seismic weight = 14417kN V_{IO}= 3069 kN, V_{LS} = 4009 kN, V_{CP} = 5705 kN,					
Building frame	Performance level	Roof Displacement. (mm)	Displacement Ductility	Spectral Acceleration $=\frac{V_B}{W}(g)$	μ_E	γ_E
Three story 3D steel frame	IO	$\delta_Y = 115.43$ $\delta_{IO} = 151.75$	1.31	0.205	1.62	0.494
	LS	$\delta_{LS} = 432.43$	3.75	0.268	6.5	0.462
	CP	$\delta_{CP} = 470.15$	4.07	0.381	7.14	0.431
Seismic weight = 22117 kN V_{IO}= 4528 kN, V_{LS} = 5918 kN, V_{CP} = 8429 kN						

Table 5.07: Energy ductility and energy factor for nine story and fifteen story 2D frames

Building frame	Performance level	Roof displacement (mm)	Displacement Ductility	Spectral Acceleration $=\frac{V_B}{W}(g)$	μ_E	γ_E
Nine story 2D steel frame	IO	$\delta_Y = 242$ $\delta_{IO} = 399$	1.65	0.21	2.3	0.844
	LS	$\delta_{LS} = 807$	3.33	0.229	5.66	0.530
	CP	$\delta_{CP} = 1103$	4.56	0.234	8.12	0.350
	μ_E (Energy ductility) = 2μ-1, μ= Displacement ductility γ_E (Energy correction factor) $=\frac{4\mu_E}{(\mu_E + 1)^2}$ Seismic weight = 44172kN V_{IO}= 9318 kN, V_{LS} = 10140 kN, V_{CP} = 10340 kN					

Building frame	Performance level	Roof Displacement. (mm)	Displacement Ductility	Spectral Acceleration $=\frac{V_B}{W}(g)$	μ_E	γ_E
Fifteen story 2D steel frame	IO	$\delta_Y = 214$ $\delta_{IO} = 419.5$	1.96	0.244	2.92	0.760
	LS	$\delta_{LS} = 597$	2.79	0.300	4.58	0.588
	CP	$\delta_{CP} = 729.8$	3.41	0.31	5.82	0.500
Seismic weight = 58959 kN V_{IO}= 1533 kN, V_{LS} = 2535 kN, V_{CP} = 4675 kN						

Table 5.08: Energy ductility and energy factor for nine story and fifteen story 2D frames

Building frame	Performance level	Roof displacement (mm)	Displacement Ductility	Spectral Acceleration $=\frac{V_B}{W}(g)$	μ_E	γ_E
Twenty story 2D steel frame	IO	$\delta_Y = 980.5$ $\delta_{IO} = 3017.5$	3.07	0.103	5.14	0.543
	LS	$\delta_{LS} = 3507.77$	3.577	0.134	6.154	0.481
	CP	$\delta_{CP} = 4232.34$	4.317	0.191	7.634	0.409
	μ_E (Energy ductility) = 2μ-1, μ= Displacement ductility γ_E (Energy correction factor) = $\frac{4\mu_E}{(\mu_E+1)^2}$ Seismic weight = 29140 kN V_{IO}= 2993 kN, V_{LS} = 3911 kN, V_{CP} = 5564 kN,					

5.2 Energy Capacity Curve

Results: Capacity of a structure in terms of energy to resist an earthquake through Nonlinear static pushover analysis results for five sets of steel frame buildings in the present study for base shear vs. roof displacement are the contents of tables 5.09 to 5.13. Using excel program the pushover analysis results for base shear vs. roof displacement have been converted into energy vs. roof displacement and the values have been recorder in the same tables in the adjacent columns.

5.2.1 Result Discussions for Energy Capacity Curve

Capacity curve is the plot of base shear vs. roof displacement, which is mostly used for study of characteristic behavior of a structure under earthquake ground motions. The absorbed energy has been considered as a better index to establish the capacity curve Enrique et al., 2004, [43]. Nonlinear pushover analyses were performed using the example problems 4.3.1 to 4.3.5 under the guidelines of FEMA 273/356; through nonlinear modeling in RAM perform 3D. Tables 5.09 to 5.13 contain the base shear, roof displacement and absorbed energy for the five sets of steel building frameworks used in the study. Figures 5.06 to 5.11 represent the base shear and energy along ordinates and roof displacement along abscissa. Understanding of capacity of structure in energy format has the advantages that capacity may be ensured through various energy parameters. Death, damage and downtime payments are the three major attributes of PBSD. Damage is unavoidable during severe earthquake ground motions and replacement of damage components in order to re occupancy may be settled to minimize downtime payments using energy based devices. Thus, knowing the capacity in energy formats, and input seismic energy as discussed in 5.1, an effective algorithm for PBSD may be developed. For estimating the input seismic energy, the same pushover analysis data has been incorporated for energy correction factor evaluation, therefore demand and capacity in terms of energy may be produced for the practical applications to consider the intrinsic behavior

Table 5.09: Base shear/Energy curve of three story 2D steel building framework

Sl. No	Roof Displacement (m)	Base shear (kN)	Energy (kNm)	Sl No	Roof Displacement (m)	Base shear (kN)	Energy (kNm)
01	0	0	0	09	0.183	4227.607	775.495
02	0.054	031.532	109.976	10	0.203	4412.589	898.887
03	0.071	2480.229	176.146	11	0.226	4542.759	1027.132
04	0.088	2849.775	252.694	12	0.245	4652.476	1142.559
05	0.106	3219.320	342.288	13	0.264	4757.973	1257.577
06	0.124	3570.990	443.652	14	0.283	863.474	1376.546
07	0.143	3838.021	550.632	15	0.301	4968.967	1499.467
08	0.163	4036.421	659.561				

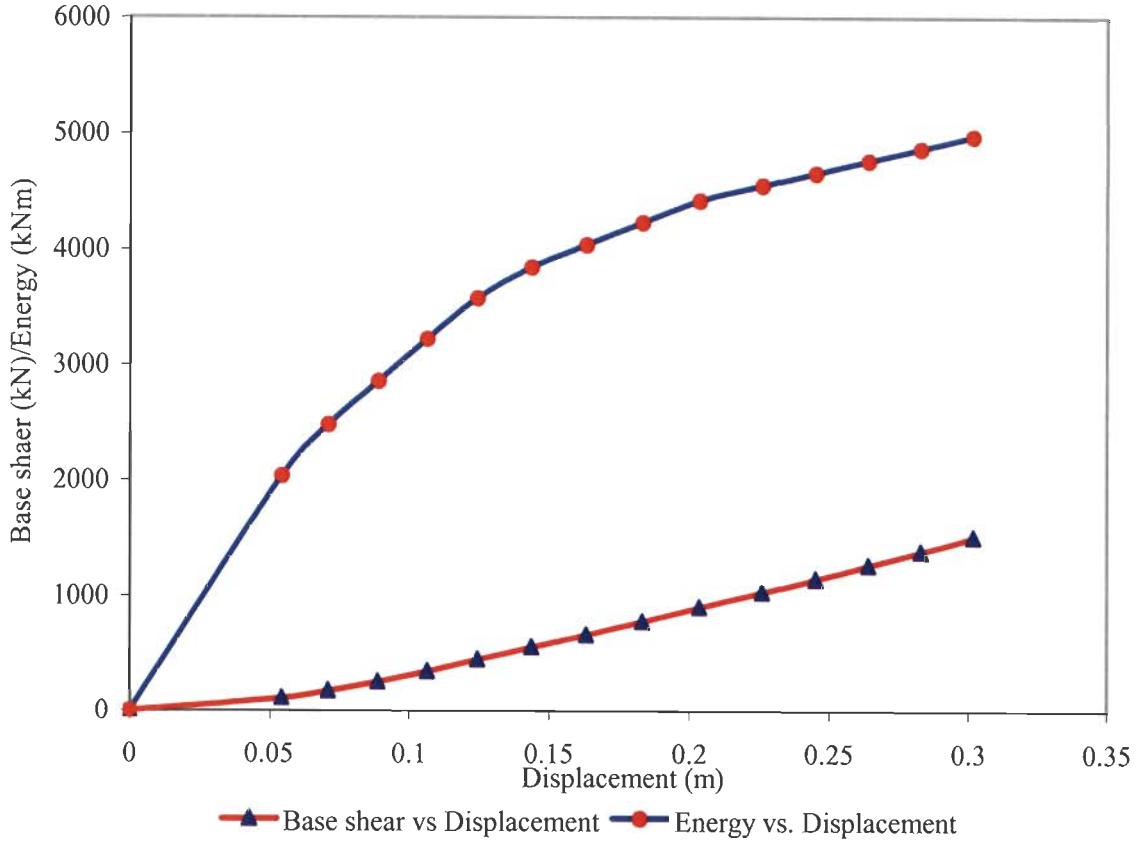

Figure 5.06: Base shear/Energy vs. Roof displacement of three story 2D frame

Table 5.10: Base shear/Energy pushover curve of three story 3D frame

Sl. No	Roof Displacement (m)	Base shear (kN)	Energy (kNm)	Sl No	Roof Displacement (m)	Base shear (kN)	Energy (kNm)
01	0.000	0.000	0.000	26	0.277	9320.318	1294.945
02	0.011	603.509	3.362	27	0.289	9426.695	1366.364
03	0.022	1207.019	13.449	28	0.301	9532.894	1439.052
04	0.033	1810.529	30.260	29	0.313	9636.617	1512.297
05	0.044	2414.038	53.796	30	0.325	9740.713	1586.908
06	0.055	3017.548	84.057	31	0.337	9844.445	1662.638
07	0.066	3621.0580	121.042	32	0.349	9943.020	1737.431
08	0.077	4224.568	164.752	33	0.361	10041.760	1813.455
09	0.089	4828.078	215.187	34	0.372	10133.880	1889.584
10	0.100	5431.587	272.346	35	0.384	10217.060	1965.896
11	0.110	5973.573	330.452	36	0.397	10292.530	2044.607
12	0.121	6365.973	385.543	37	0.410	10362.790	2124.733
13	0.132	6721.205	444.530	38	0.423	10430.920	2206.685
14	0.143	7047.161	505.389	39	0.436	10485.960	2290.353
15	0.154	7372.503	569.837	40	0.451	10535.380	2377.53
16	0.165	7682.449	636.240	41	0.466	10570.500	2465.626
17	0.176	7948.767	699.812	42	0.483	10593.190	2558.408
18	0.186	8192.264	762.632	43	0.501	10590.730	2654.33
19	0.196	8408.904	825.976	44	0.519	10591.840	2749.239
20	0.207	8597.037	891.842	45	0.537	10593.090	2844.491
21	0.218	8760.313	957.121	46	0.554	10594.350	2939.838
22	0.230	8884.789	1022.577	47	0.572	10595.600	3035.118
23	0.241	8999.249	1088.818	48	0.590	10596.860	3130.512
24	0.253	9106.452	1156.200	49	0.608	10598.110	3225.915
25	0.265	9213.71	1224.988				

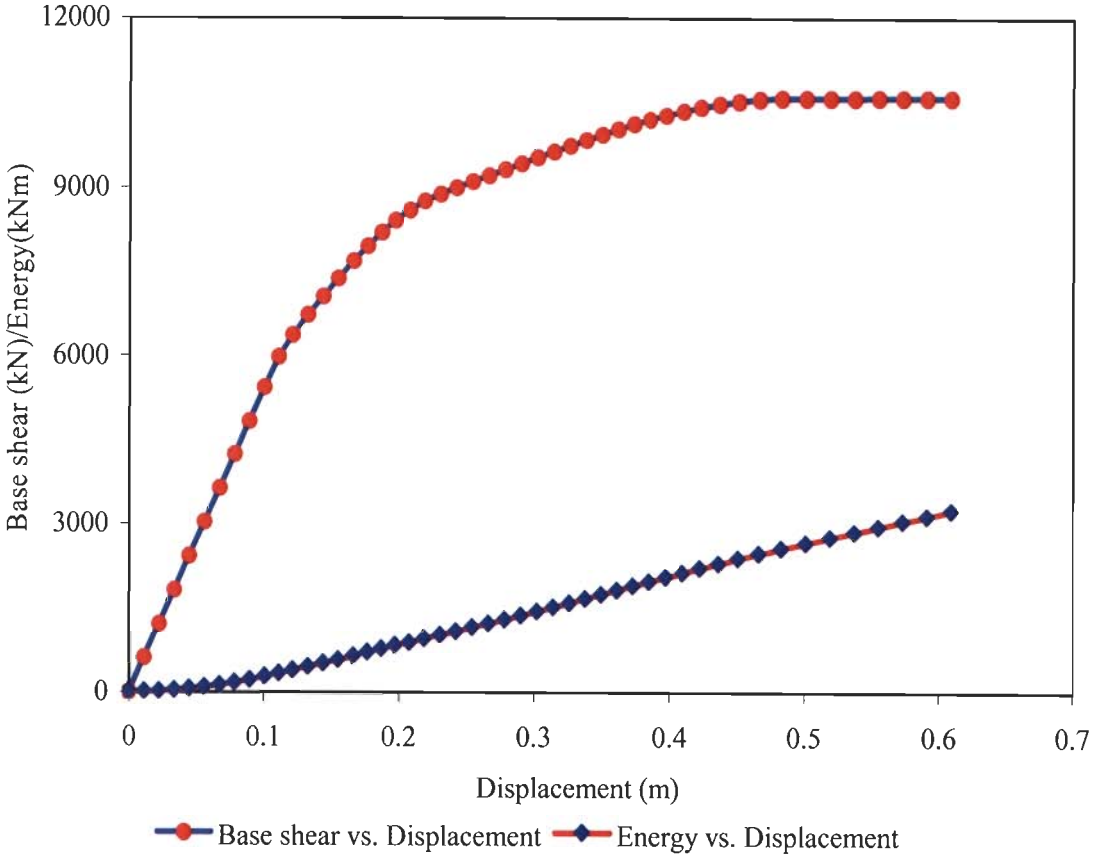

Figure 5.07: Base shear/Energy vs. Roof displacement of three story 3D frame

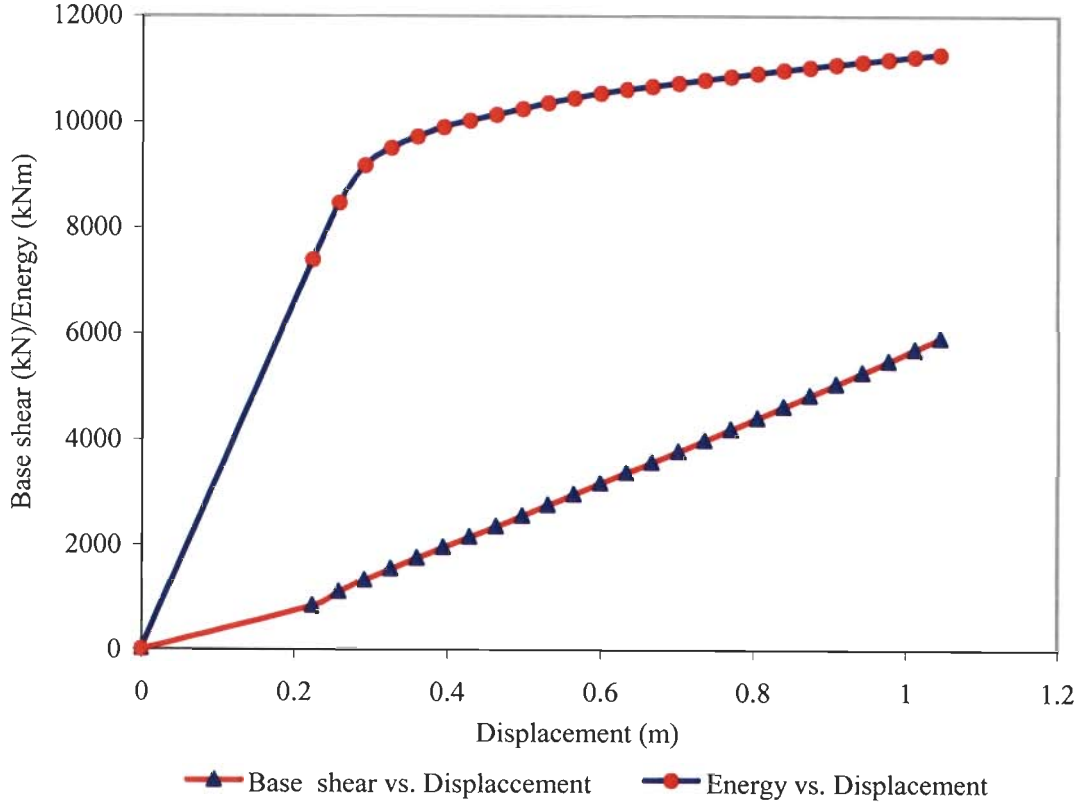

Figure 5.08: Base shear/Energy vs. Roof displacement of nine story 2D frame

Table 5.11: Base shear/Energy pushover curve of nine story 2D frame

Sl. No	Roof Displacement (m)	Base (kN)	Energy (kNm)	Sl No	Roof Displacement (m)	Base (kN)	Energy (kNm).
01	0.000	0.000	0.000	09	0.463	10134.280	2346.127
02	0.222	7382.372	822.253	10	0.497	10245.710	2547.895
03	0.257	8452.154	1086.575	11	0.530	10352.440	2747.470
04	0.291	9174.785	1337.053	12	0.565	10443.700	2951.063
05	0.325	9505.861	1548.566	13	0.599	10536.970	3158.392
06	0.360	9719.500	1750.304	14	0.633	10607.620	3361.759
07	0.394	9900.950	1951.805	15	0.668	10669.860	3564.740
08	0.428	10019.930	2147.559	16	0.702	10732.100	3769.861

Table 5.12: Base shear/Energy curve of fifteen story 2D frame

Sl. No	Roof Displacement (m)	Base Shear (kN)	Energy (kNm)	Sl No	Roof Displacement (m)	Base Shear (kN)	Energy (kNm)
01	0.000	0.000	0.000	09	0.414	2093.284	867.361
02	0.164	1049.457	172.325	10	0.444	2164.448	962.615
03	0.211	1345.042	284.796	11	0.474	2232.705	1059.880
04	0.249	1526.699	380.282	12	0.504	2300.962	1161.299
05	0.282	1663.611	470.787	13	0.532	2355.524	1254.800
06	0.317	1799.200	571.466	14	0.560	2407.851	1349.527
07	0.351	1923.300	676.225	15	0.382	2093.284	867.361
08	0.382	2011.138	770.010	16			

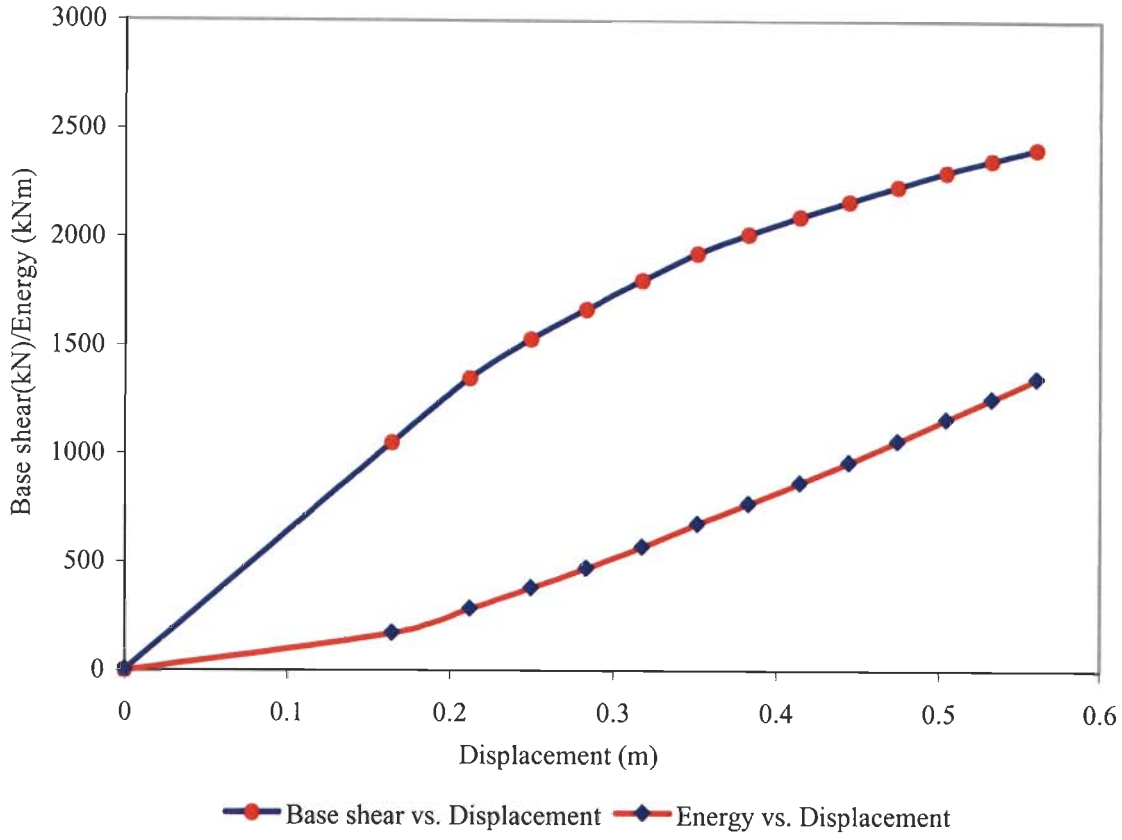

Figure 5.09: Base shear/Energy vs. Roof displacement of fifteen story 2D frame

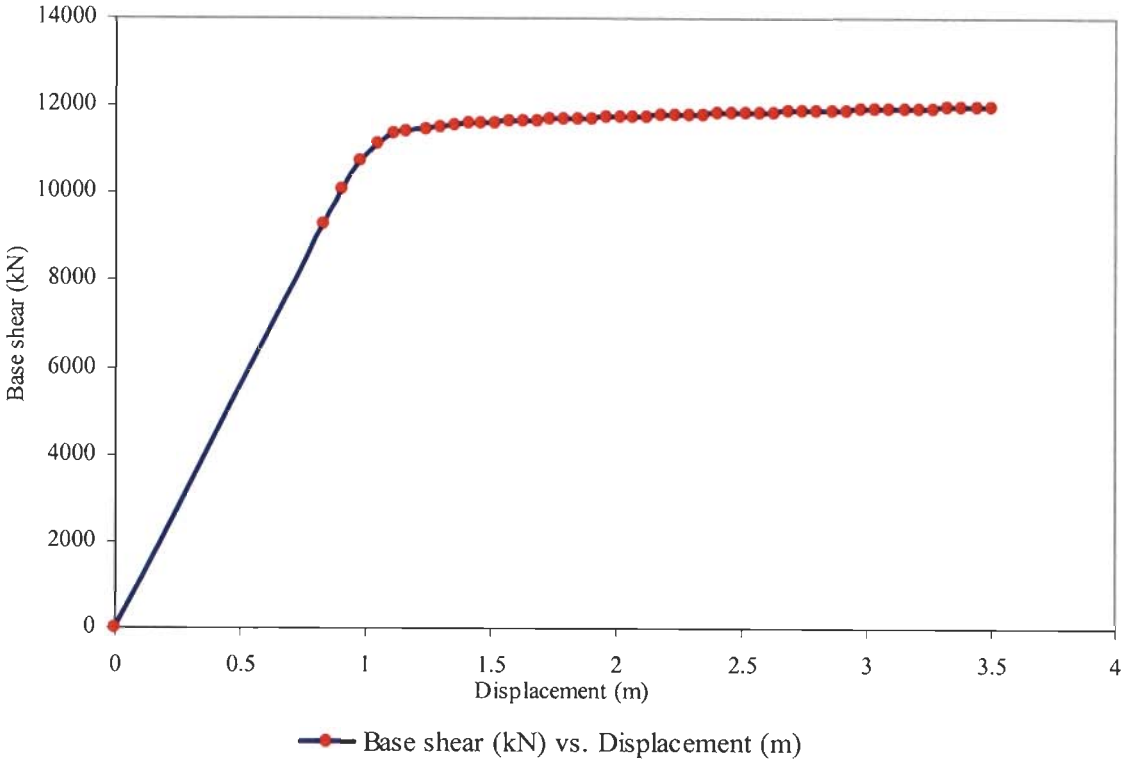

Figure 5.10: Base shear vs. Displacement of twenty story 2D frame

Table 5.13: Base shear/Energy pushover curve of twenty story 2D frame

Sl. No	Roof Displacement (m)	Base shear (kN)	Energy (kNm)	Sl No	Roof Displacement (m)	Base shear (kN)	Energy (kNm)
01	0	0	0	25	2.179	11758.150	12814.700
02	0.829	9261.686	3840.157	26	2.235	11769.640	13155.740
03	0.906	10055.430	4555.765	27	2.291	11781.130	13497.440
04	0.975	10692.800	5218.077	28	2.347	11792.620	13839.770
05	1.045	11116.080	5811.548	29	2.403	11804.110	14182.740
06	1.111	11339.710	6301.954	30	2.458	11815.590	14526.340
07	1.163	11417.710	6641.436	31	2.516	11825.190	14880.880
08	1.244	11472.800	7141.424	32	2.574	11834.720	15236.810
09	1.299	11513.350	7482.765	33	2.633	11844.250	15593.300
10	1.354	11546.970	7820.34	34	2.687	11852.910	15924.550
11	1.409	11574.290	8154.228	35	2.744	11861.460	16278.920
12	1.463	11593.920	8483.288	36	2.802	11869.180	16630.920
13	1.517	11610.570	8810.930	37	2.860	11877.350	16984.930
14	1.572	11626.240	9138.351	38	2.918	11885.390	17341.550
15	1.626	11638.50	9467.367	39	2.976	11893.470	17698.030
16	1.681	11651.190	9797.717	40	3.034	11901.560	18054.980
17	1.736	11663.520	10128.360	41	3.092	11909.640	18412.400
18	1.791	11675.670	10459.360	42	3.1499	11917.720	18770.270
19	1.846	11687.860	10791.080	43	3.207	11925.800	19128.620
20	1.902	11699.570	11126.730	44	3.265	11933.890	19487.450
21	1.957	11711.520	11461.440	45	3.323	11941.970	19846.740
22	2.012	11723.470	11796.810	46	3.382	11949.790	20211.150
23	2.067	11735.420	12132.830	47	3.441	11957.720	20574.040
24	2.123	11746.660	12474.290	48	3.499	11965.650	20937.400

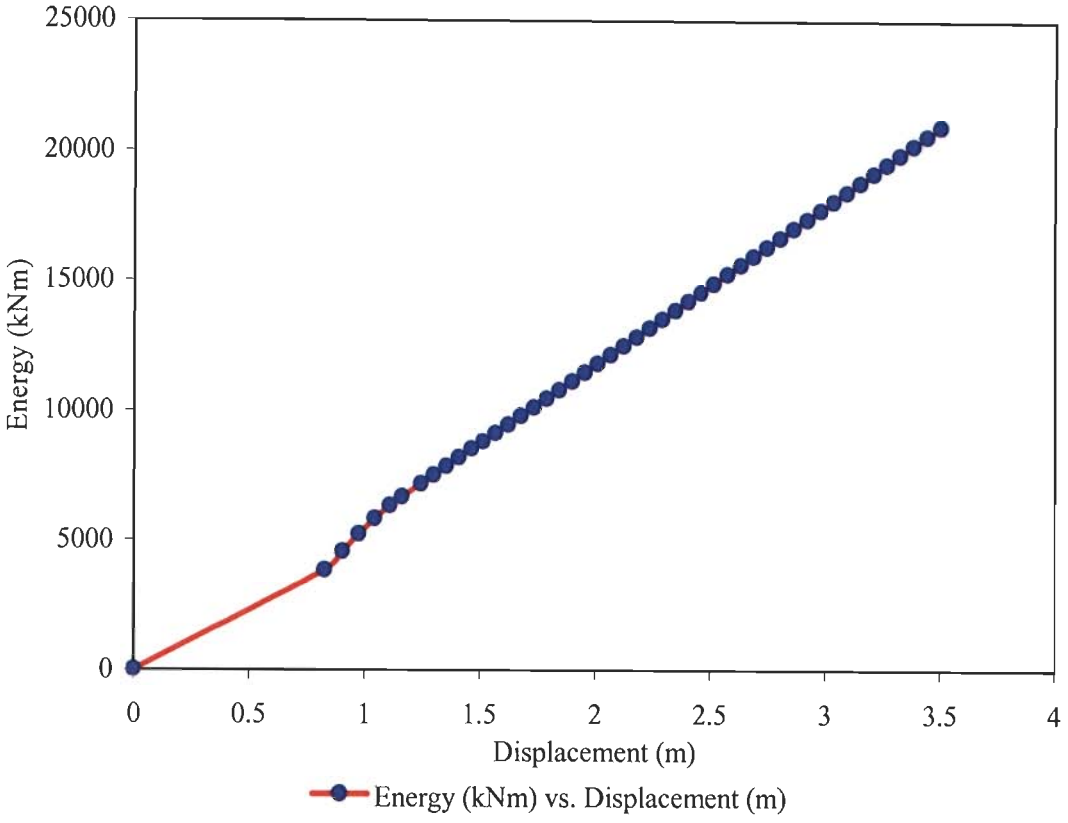

Figure 5.11: Base Energy vs. Displacement of twenty story 2D frame

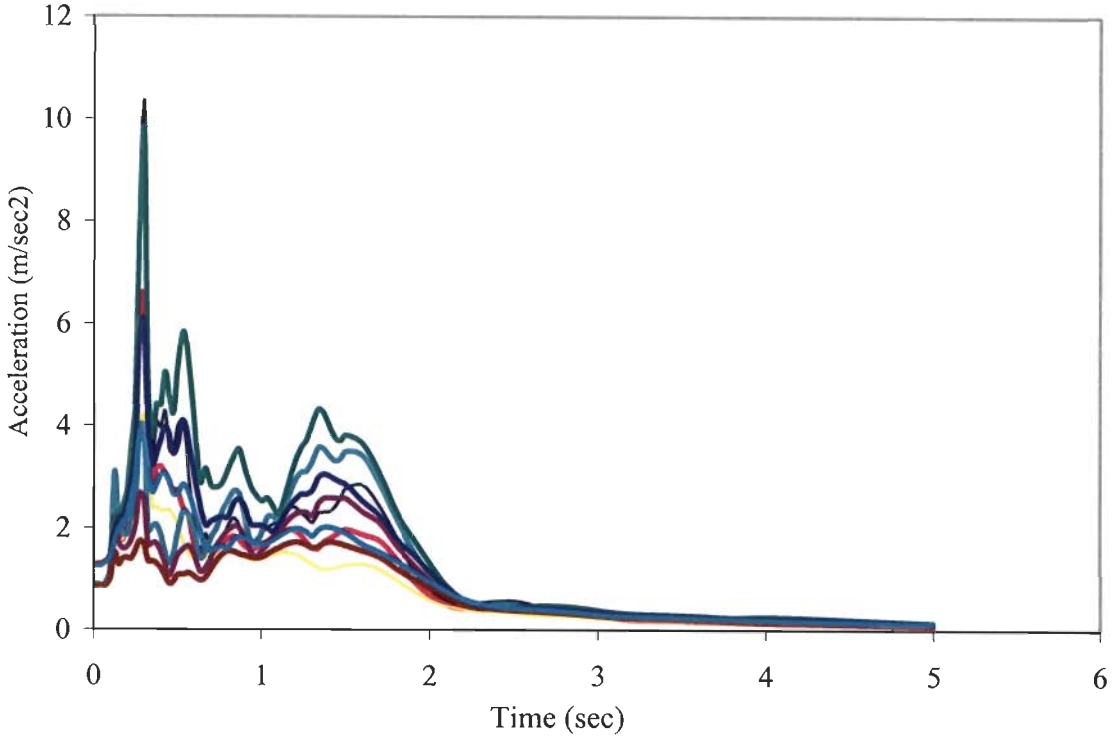

Figure 5.12: Floor spectra of three story 3D frame for Northridge E-W (3x0.5165g)

5.3 Floor Spectra vs. Inter story Drift

Result: Table 5.14 consists of floor spectra and inter story drift of three story 3D frame for the input seismic energy 7418 kNm and 8014 kNm and the table 5.15 consists three story 2 D frame comparative frames response parameters for drift and floor spectra. Figures 5.12 to 5.17 represent the variation of floor spectra and inter story drift for three story 3D building frames. Variation of drift (Figure 5.13), floor spectra (Figure 5.14), relative displacement (Figure 5.15), and relative velocity of three story 3D and the combined effect of drift and floor spectra (Figure 5.17). Floor spectra and drift have incorporated in tables 5.14 for three story frames under varying two ground motions. With the increase of input seismic energy, changes in floor spectra and drifts are found varying in the reverse order, as predicted through the relation developed in the chapter 3. Table 5.15 consists of the floor spectra and drift for three story 2D frame. The variation of floor spectra along with the story height under the varying ground motions also describes the variation of drifts and floor spectra through inverse relation.

5.3.1 Result discussions

Floor spectra correspond to absolute accelerations of floors except ground floor. Inter story drift while is the lateral displacements to adjacent floors per unit story height. These two are related with the non structural damage. Input seismic energy has the relation with these two parameters as perceived in the present study. Absolute and relative input seismic energy may be used for the interpretation of the inverse relations of these two response parameters. For the increase of the floor spectra, the drift values decreases with the increase of the input seismic energy. The content of the individual energy content (strain and kinetic energy) also increase with the floor spectra, however, the drift decrease as can be seen in the table 5.14. The ratio of consecutive floor spectra and drift ratio (Table 5.14) bears such a value, which supports the inverse relation of floor spectra and drift. This happens because of the energy content of the floor increases due to the increase of kinetic and strain energy as shown in the table.

A rigid structure during an earthquake experiences more input energy. The value of the absolute kinetic energy for the rigid structure increases, however, the relative kinetic energy decreases. Such results reveal the floor spectra are greatly influenced due to the absolute kinetic energy associated with the floor levels. For flexible structure the effect is reverse, i.e., the inter story drift increases with the decrease of the floor spectra.

Floor spectra tabulated in the tables (5.15) corresponding different floors of three story 3D frame. Figure 5.17 represent the relationship in between the floor spectra and drift corresponding to different PGA. Floor spectra are seen to increase with the increase of story number, while the drifts for the corresponding story number are found to decrease. Such relations show the inverse relationship of floor spectra and drift for the increase values of PGA, thereby the increase of input seismic energy

Table 5.14: Input seismic energy and variation of floor spectra and drift for three story 3D frame.

Input Energy (kNm)	KE (kNm)	SE (kNm)	E_h (kNm)	Floor Spectra	Drift
7418	52	194.13	4732.7	4.007 3.244 4.172	0.032 0.029 0.056
8096	337.19	221.03	5168.5	4.716 3.358 4.837	0.027 0.023 0.047

Table 5.15: Floor spectra vs. Inter story drift for three story 2D comparative frames

Sl. No (1)	Floor spectra (2)	Drift (3)	1)x(2) =(4)	Floor spectra (5)	Drift (6)	(5)x(6) =(7)	(7)/(4)
01	0.477	0.058	0.027	0.849	0.037	0.032	1.146
02	0.622	0.040	0.024	0.966	0.023	0.022	0.890
03	0.540	0.040	0.021	0.722	0.024	0.017	0.801

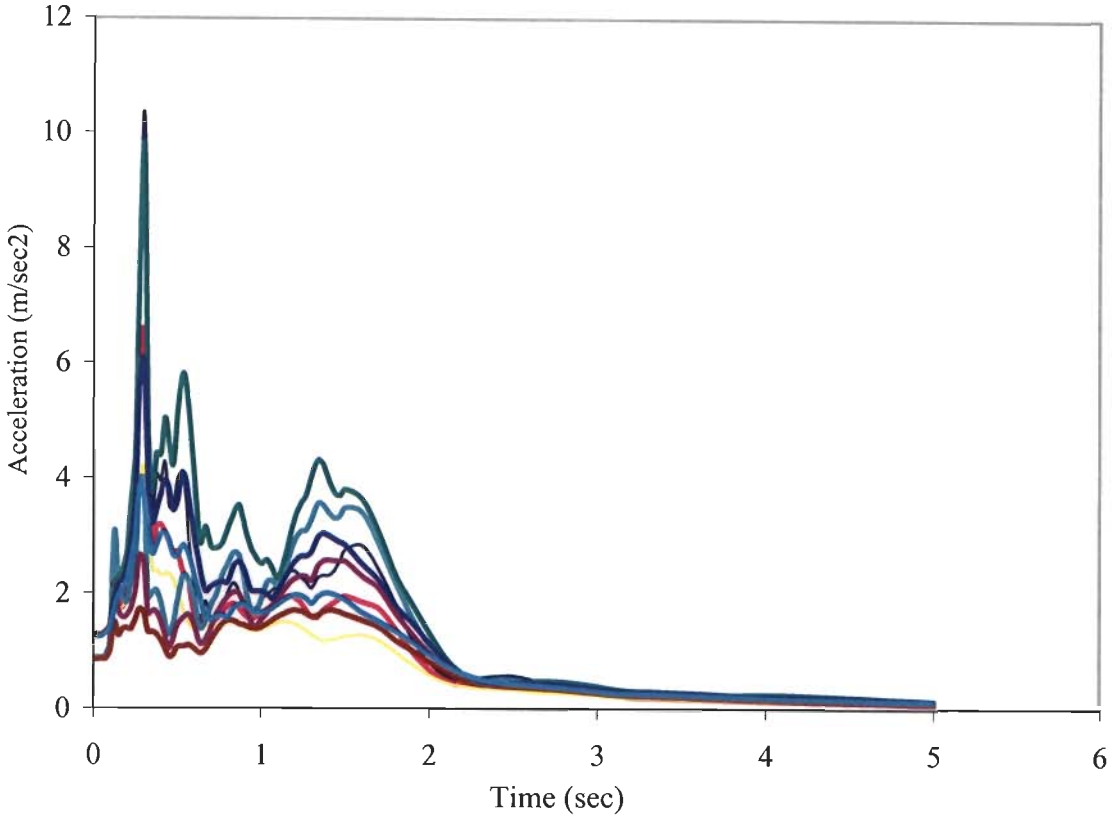

Figure 5.12: Floor spectra of three story 3D frame for Northridge E-W (3x0.5165g)

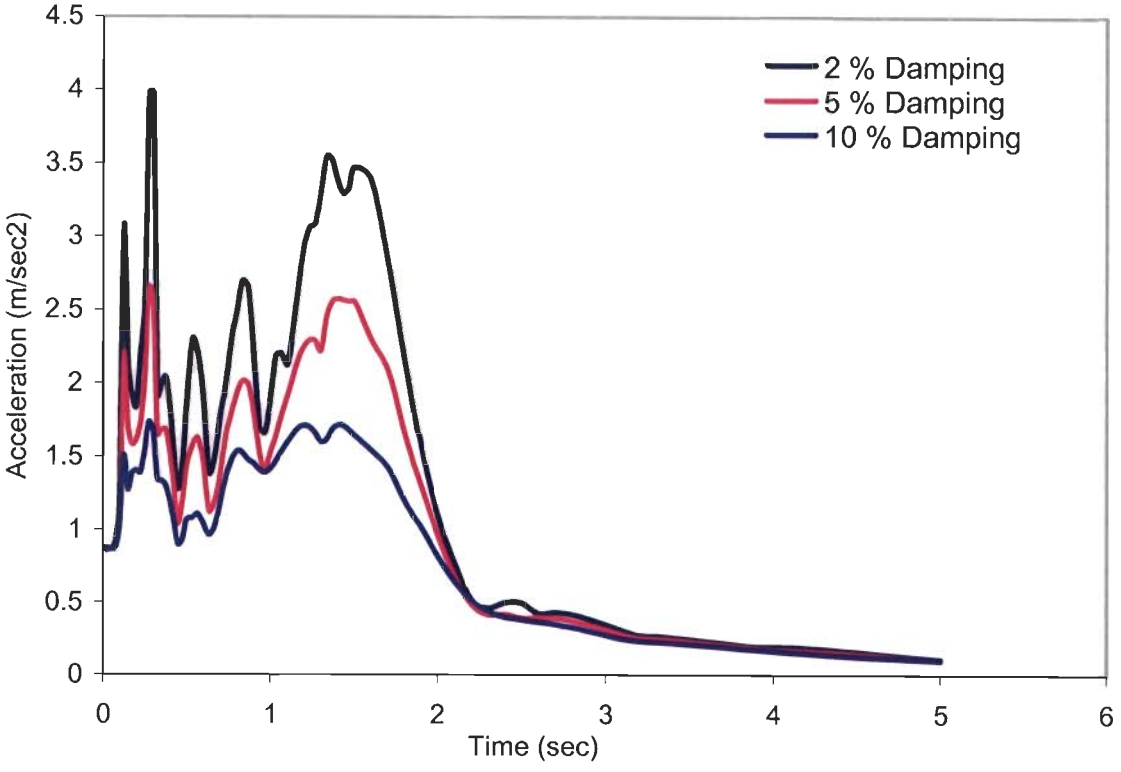

Figure 5.13 Floor spectra at 2nd floor of three story frame 3D for Northridge E-W (3x0.5165g)

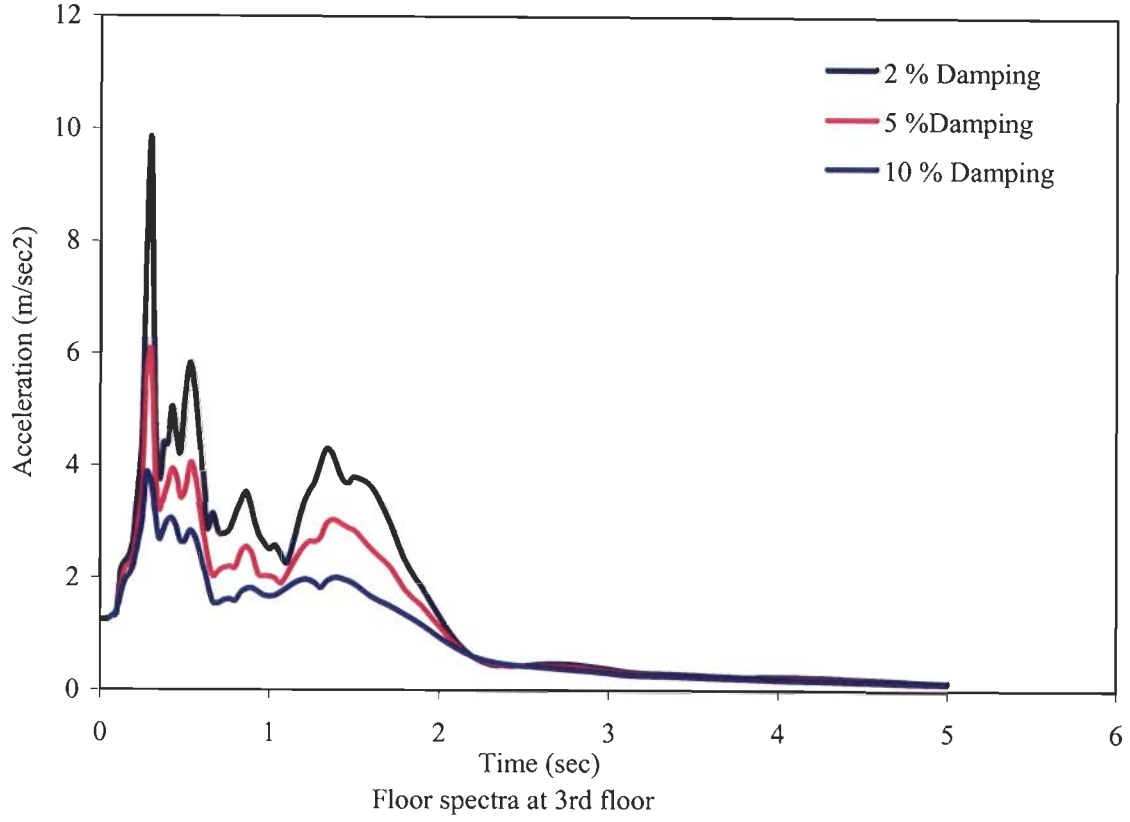

Figure 5.14: Floor spectra at 3rd floor of three story 3D frame for Northridge E-W (3x0.5165g)

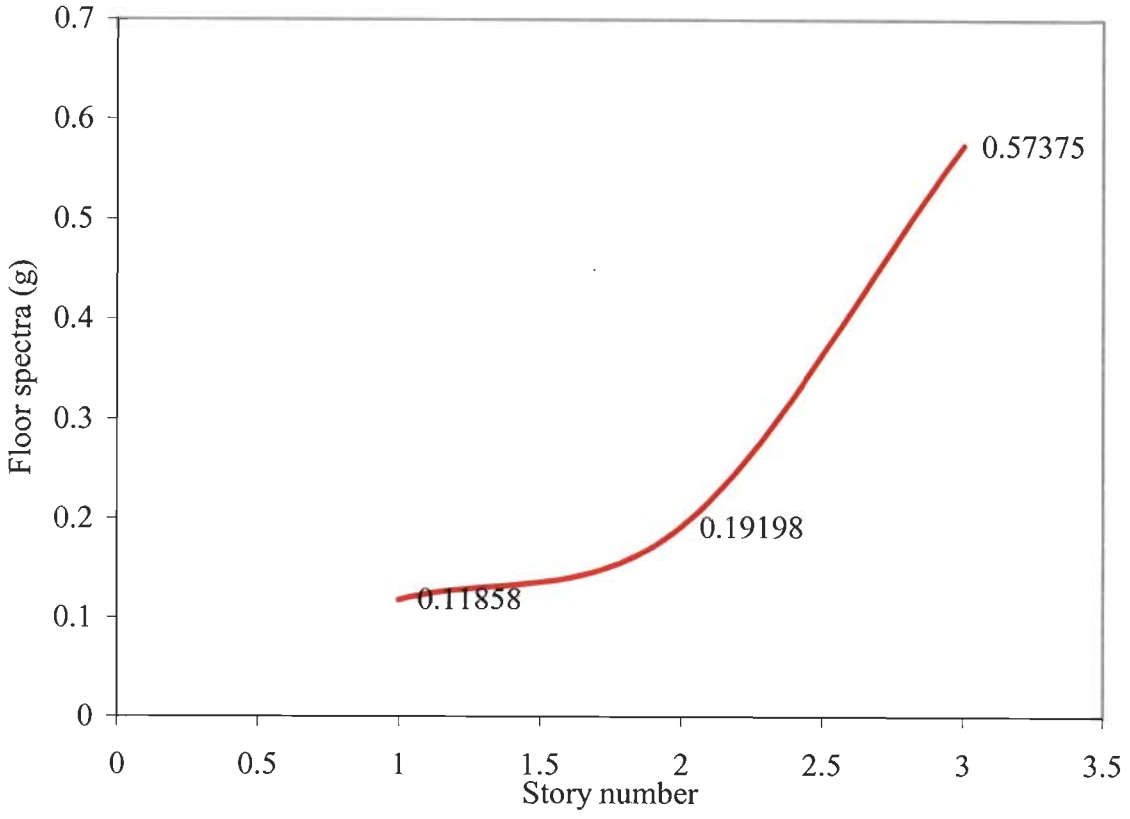

Figure 5.15: Floor spectra vs. Story number of three story 3D frame

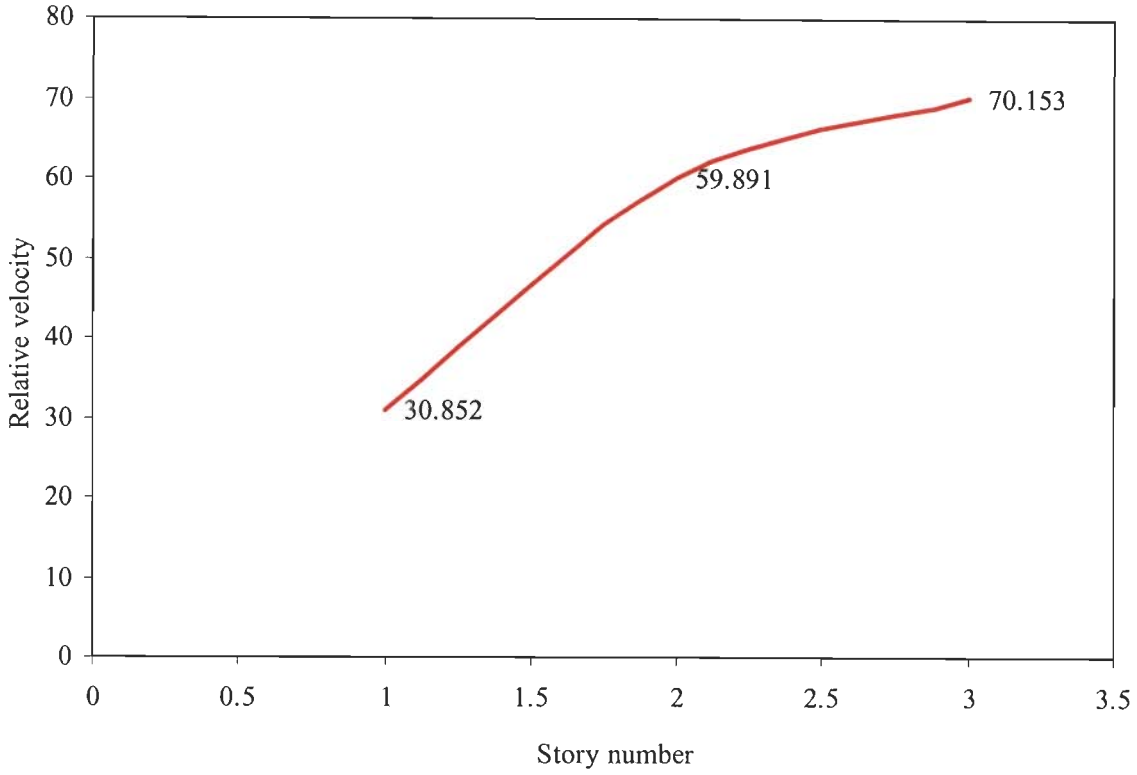

Figure 5.16: Relative velocities vs. Story number of three story 3D frame

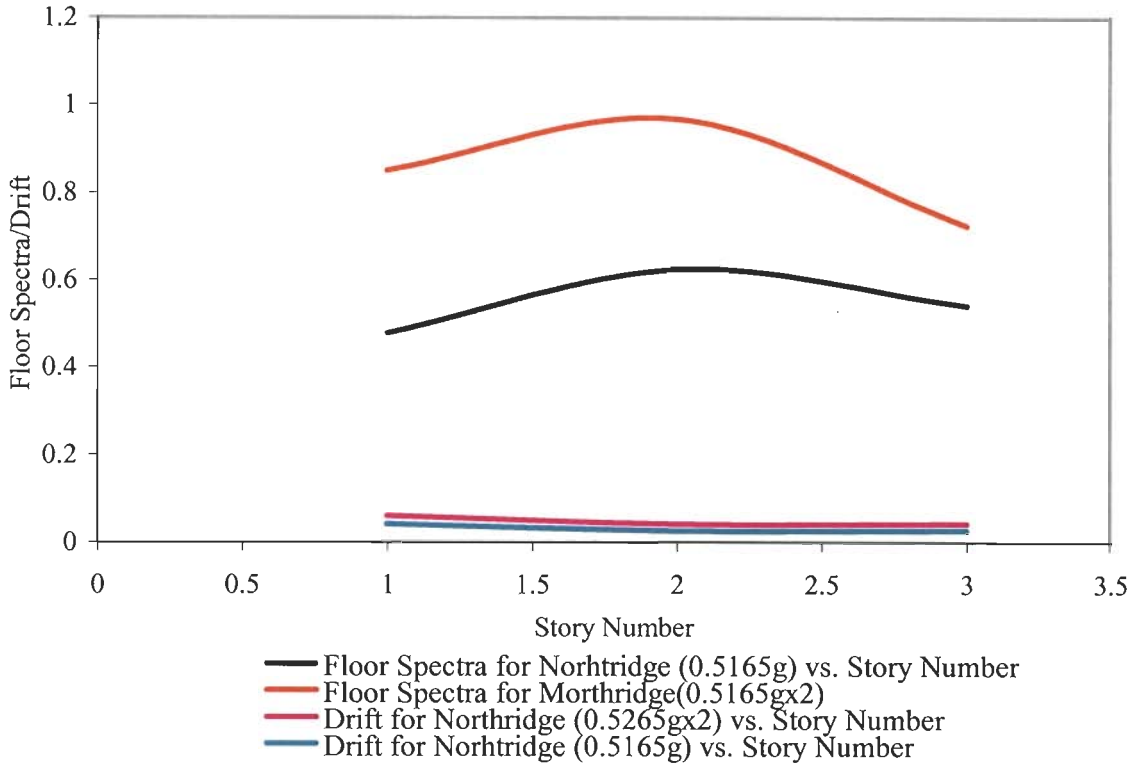

Figure 5.17: Floor spectra/drift vs. Story number of three story 3D frame

5.4 Distribution of Input Seismic Energy

Distribution of earthquake input energy among energy components: kinetic, elastic strain, hysteretic is desirable for the development of an energy-based design approach and assessing the damage potential of structures, This study examines the influences of the ground motion characteristics: intensity, frequency content, and duration of strong motion and the structural properties: ductility, and hysteretic behavior on the distribution of input energy for a three, nine, fifteen, and twenty story steel building frames using a set of accelerograms.

Table 5.16 represents the distribution if input seismic energy among energy components and specifies the hysteretic energy variation with the increase of the input seismic energy. Figure 5.18 is the plot of the % variation of the hysteretic energy/input seismic energy vs. to the input seismic energy. Figure 5.17 display the % of strain energy, kinetic and hysteretic energy variation with respect to the input seismic energy. Tables 5.17 to 5.21 correspond to the distribution of input seismic energy among energy components for the steel frames building under a set of accelerograms in the present study.

Table 5.22 reveals the energy dissipation among critical beams and columns of nine story 2D frame under input seismic energy. Table 5.23 represents the distribution of input seismic energy (1459kN) of nine story frame. Figure 5.20 is the plot of energy dissipated through beams at different floor of nine story frame. Figure 5.21 shows the variation of energy dissipated among columns of nine story under the influence of input seismic energy. In the figure 5.22 dissipation of energy through columns have been shown. Figure 5.23 is the plot of energy dissipated among beams of nine stories at different floors due to the input seismic energy of 14580 kNm. Figure 5.24 to 5.51 corresponds to the energy components vs. time of earthquake occurrence period.

Chapter 3, during the problem formulations for this research program, though distribution of energy among its components has been formulated for SDOF system in normalized format using the energy balance equation, however, the approach has been used for MDOF system too, taking example steel building frames under varying ground motions. As the major task for earthquake resistant design using the energy concept is the distribution of input seismic energy into the various energy components, therefore a set of building frames used for the previous discussion in this research program has been further analyzed for energy response under earthquake loadings. Energy response for the various frames and earthquake ground motions have been incorporated in tables 5.16 to 5.21 and their variations have also been presented through figures.5.19 to 5.52.

5.4.1 Result Discussions

Tables 5.16 to 5.21 depicts the distribution of energy among its energy components (strain, kinetic, damping, hysteretic energy) as well as distribution of input seismic energy among beams and columns for limited number of frames. Figures 5.18 to 5.51 represent the graphical presentation of distribution of input seismic energy among energy components and some figures represent the distribution of input seismic energy among beams and columns along the building height. The pattern of distribution of input seismic energy among its energy components as found from the response analysis of the building frameworks under the varying seismic demands show the strain energy variation with time is more stable than the kinetic energy. Hysteretic energy variation for severe earthquake ground motions with respect to the input seismic energy is stable and the variation of hysteretic and strain energy is similar.

Nonlinear modeling of structural components plays significant roles for the distribution of distribution of energy inputted to the structure. It is relatively easy to know the energy distributed among its components if the components are assigned different identification during the modeling phase. Modeling of various components of three story 3D frame and nine story 2D frames have been given separate name; therefore, energy components at components levels are known (Tables 5.22, 5.23 and Figures 5.21 to 5.24). Thus, it is because of the software's strong background for modeling and nonlinear analysis procedures development, energy distribution has become possible in earthquake loading.

As derived expressions for energy distribution for SDOF system in chapter needs validation using more examples taking into considerations of materials, geometry of the structures. The expression also requires check for MDOF system through taking equivalent structures.

Table 5.16: Energy distribution for three story 2D steel framework

E_i Input energy	E_S (kNm)	E_K (kNm)	E_h (kNm)	% E_S	% E_K	% E_h	Earthquake
3379.83	51.69	157.66	2098.86	1.529	4.67	62.1	Northridge (0.5165g)
10730.48	89.89	57.856	7598.12	0.84	0.54	70.81	Northridge (2x0.5165g)
21684.7	142.75	31.83	15142	0.66	0.15	69.82	Northridge (3x0.5165g)
32860.4	333.16	54.13	24667.9	1.01	0.16	75.07	Northridge (4x0.5165g)

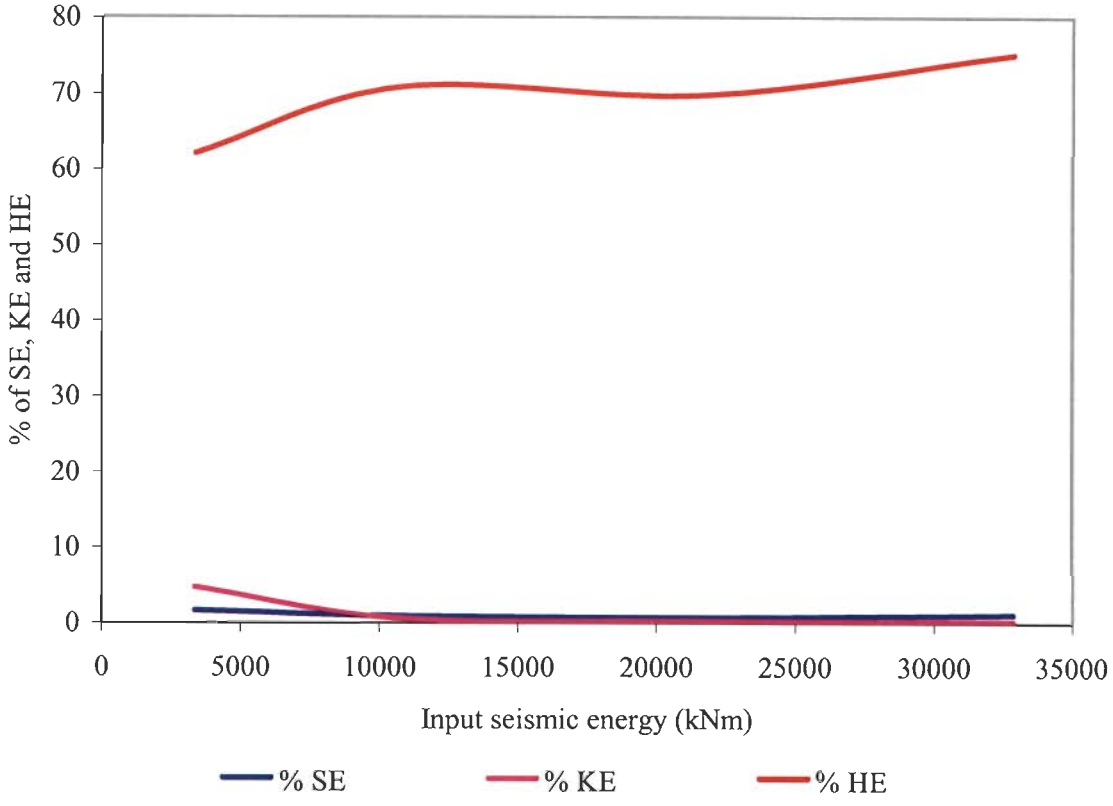

Figure 5.19: % Strain, kinetic and hysteretic energy vs. Input seismic energy

Table 5.17: Distribution of input seismic energy for three story 3D frame

Earthquake ground motions	Input Energy kNm	Strain Energy kNm	Kinetic Energy kNm	Hysteretic Energy kNm
Northridge E-W, 0.5165g	3313.17	107.86	33.13	2120.45
Northridge E-W,2x0.5165g	7273.81	146.97	137.13	3179.37
Northridge N-S, 0.4158g	4342.00	63.85	3.27	2145.42
Northridge N-S,2x 0.4158g	11379.10	89.41	4.56	7727.84
El Centro E-W, 0.2148g	1398.94	46.29	50.19	254.15
El Centro E-W 2x0.2148g	4790.00	58.85	101.37	2571.43
El Centro U-D, 0.2148g	88.26	40.90	0.09	$6.9x10^{-6}$
El Centro U-D, 2x 0.2148g	218.43	44.97	0.36	$2.7x10^{-5}$

Table 5.18: Distribution of input seismic energy for three story 2D frame

Earthquake ground motions	Input Energy kNm	Strain Energy kNm	Kinetic Energy kNm	Hysteretic Energy kNm
Northridge E-W, 0.5165g	1118.00	268.26	10.06	389.7
Northridge E-W, 2x0.5165g	1022.00	158.94	14.75	381.34
Northridge N-S, 0.4158g	1582.00	212.08	143.29	635.92
Northridge N-S, 2x 0.4158g	3764.00	383.66	781.23	1326.8
El Centro E-W, 0.2148g	503.70	20.157	3.48	70.157
El Centro E-W, 2x0.2148g	2188.00	49.42	15.858	943.72
El Centro Up-Down, 0.2148g	30.38	3.09	0.28	00.00
El Centro Up-Down,2x 0.2148g	112.70	3.52	1.13	$9.54x10^{-7}$

Table 5.19: Distribution of input seismic energy for nine story 2D frame

Earthquake ground motions	Input Energy kNm	Strain Energy kNm	Kinetic Energy kNm	Hysteretic Energy kNm
Northridge E-W,0.5165g	3834	19.405	43.3	1245
Northridge E-W, 2x0.5165g	14580	39.696	190.32	1968.6
Northridge N-S, 0.4158g	3141	20.054	16.691	Nil
Northridge N-S, 2x 0.4158g	12440	43.49	76.049	1478.4
El Centro E-W,0.2148g	2782	25.38	66.303	0.741
El Centro E-W, 2x0.2148g	9908	238.29	70.788	2146.4
El Centro U-D, 0.2148g	109.4	17.721	1.498	Nil
El Centro U-D, 2x 0.2148g	386.6	19.94	5.99	Nil

Table 5.20: Distribution of input seismic energy for fifteen story 2D frame

Earthquake ground motions	Input Energy kNm	Strain Energy kNm	Kinetic Energy kNm	Hysteretic Energy kNm
Northridge E-W, 0.5165g	3235	97.745	4.03	116.65
Northridge E-W, 2x0.5165g	9484	310.12	24.5	4121.4
Northridge N-S, 0.4158g	2820	104.7	3.01	122.56
Northridge N-S, 2x 0.4158g	10630	568	89.56	2345.34
El Centro E-W, 0.2148g	1716	117.95	5.64	166.65
El Centro E-W, 2x0.2148g	5119	186.55	40.525	1437.8
El Centro U-D, 0.2148g	190.1	89.71	2.169	Nil
El Centro U-D, 2x 0.2148g	491.2	90.763	8.57	10.45

Table 5.21: Distribution of input seismic energy for twenty story 2D frame

Earthquake ground motions	Input Energy kNm	Strain Energy kNm	Kinetic Energy kNm	Hysteretic Energy kNm
Northridge E-W, 0.5165g	3375	11.277	1.37	Nil
Northridge E-W, 2x0.5165g	13070	11.48	5.4	Nil
Northridge N-S, 0.4158g	2836	11.299	0.042	Nil
Northridge N-S, 2x 0.4158g	11310	11.571	0.169	Nil
El Centro E-W, 0.2148g	814.8	11.815	4.17	Nil
El Centro E-W, 2x0.2148g	3226	11.636	16.7	Nil
El Centro U-D, 0.2148g	68.53	11.23	0.057	Nil
El Centro U-D, 2x 0.2148g	240.5	11.267	0.237	Nil

Table 5.22: Energy dissipated among beams and columns of nine story 2D frame

Input Seismic Energy (kNm)	Story No	Inner beams (kNm)	External beams (kNm)	Inner Columns (kNm)	External Columns (kNm)
135800	1	3154.5	3141	3996.8	9796.6
	2	1705.3	1476.3	0	0
	3	1100.8	1052.6	0	0
	4	907.65	843.94	0	0
	5	694.17	673.89	0	0
	6	510.28	508.74	0	0
	7	173.48	195.12	0	0
	8	0	7.58	0	0
	9	0	0	0	0

Table 5.23: Energy dissipated among beams and columns of nine story 2D frame.

Input Seismic Energy (kNm)	Story No	Inner beam (kNm)	External beam (kNm)	Inner Columns (kNm)	External Columns (kNm)
14580	1	124.77	400.89	0	477.42
	2	85.172	151.75	0	0
	3	107.68	143.64	135.78	0
	4	99.668	117.07	0	0
	5	43.762	64.305	0	0
	6	3.9466	12.654	0	0
	7	0	0	0	0
	8	0	0	0	0
	9	0	0	0	0

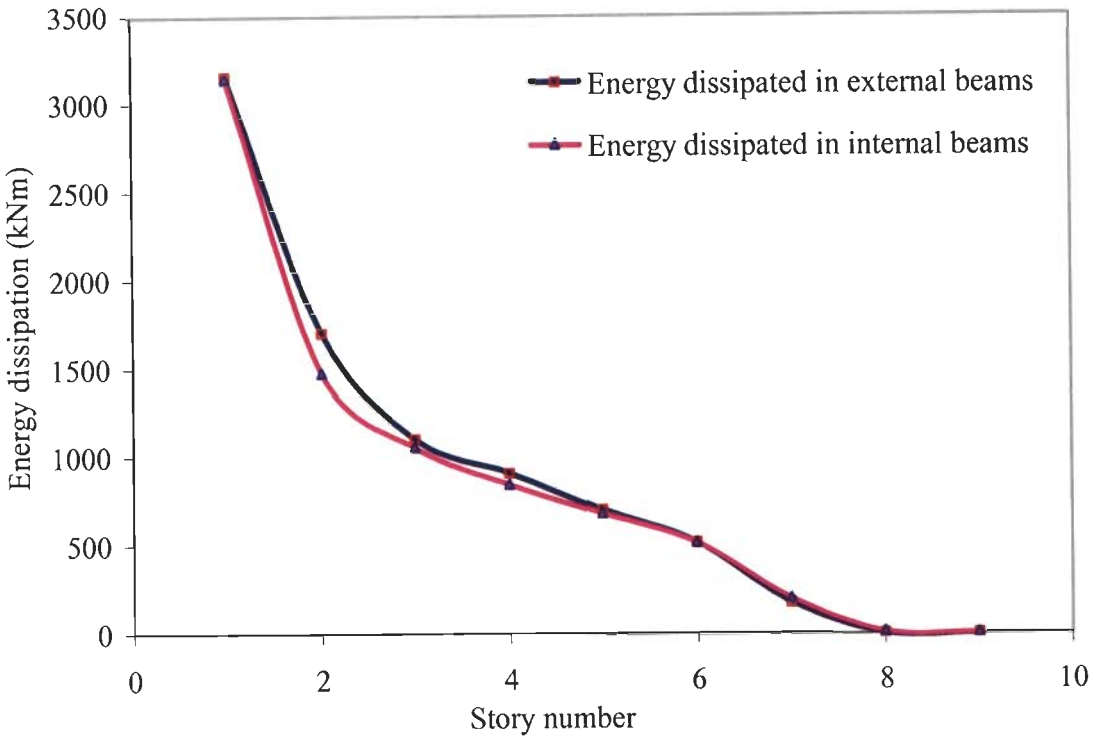

Figure 5.20: Energy dissipated in beams along the building height of nine story 2D frame

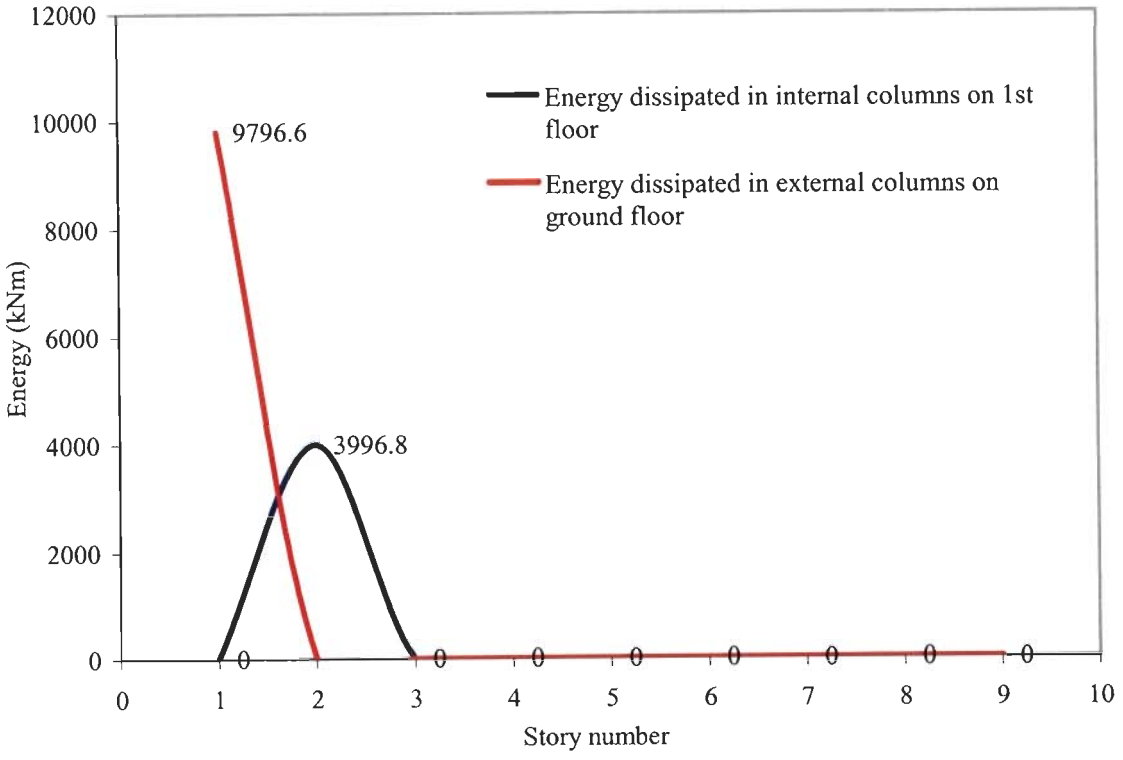

Figure 5.21: Energy dissipation in columns of nine story frame for input seismic energy =135800 kNm

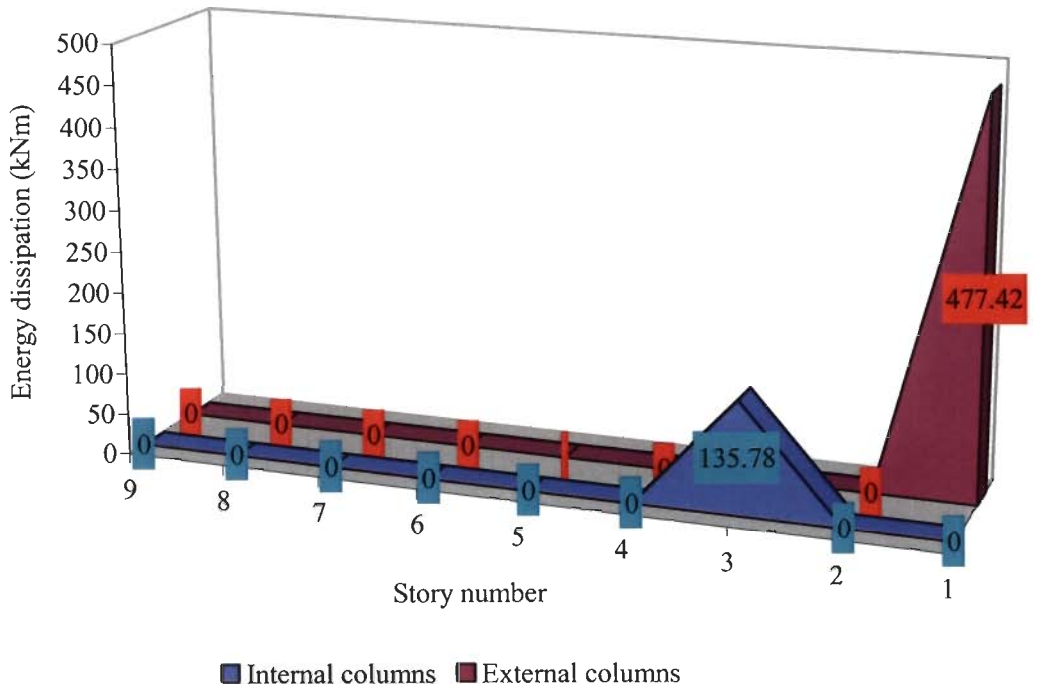

Figure 5.22: Distribution of energy among external and internal beams of nine story frame for input seismic energy =14580 kNm

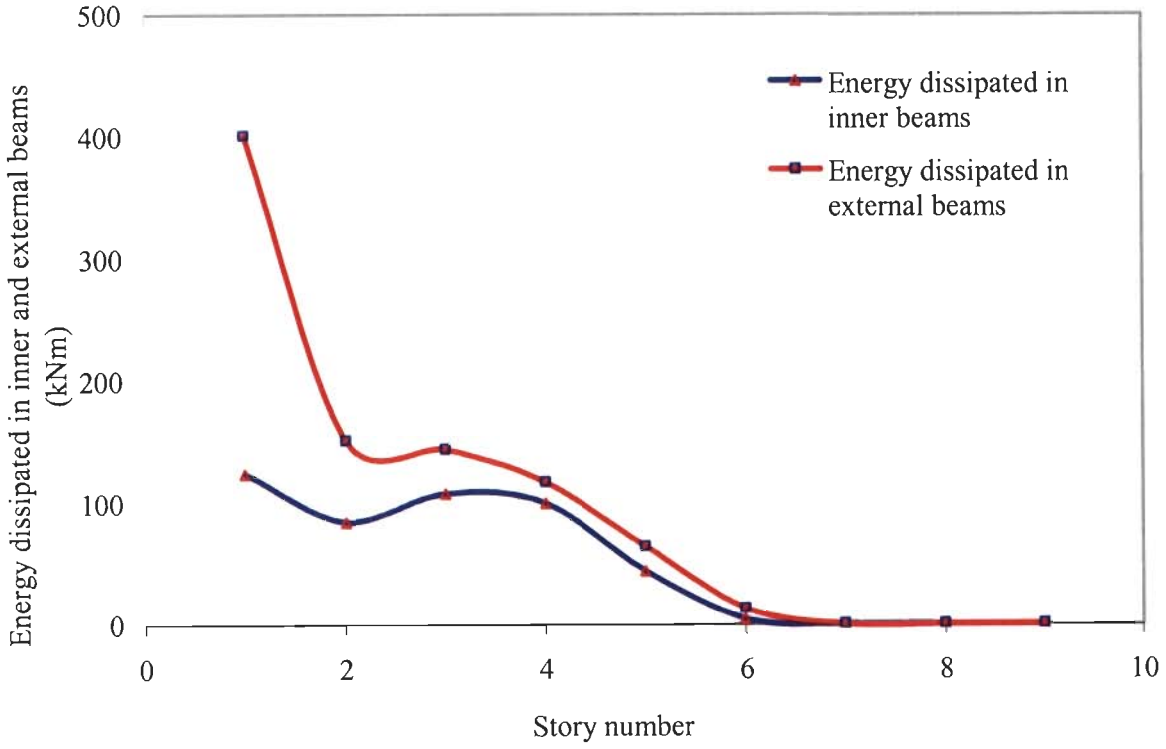

Figure 5.23: Distribution of energy among external and internal beams a of nine story frame for input seismic energy =14580 kNm

Distribution of input energy among hysteretic, strain and kinetic energy.

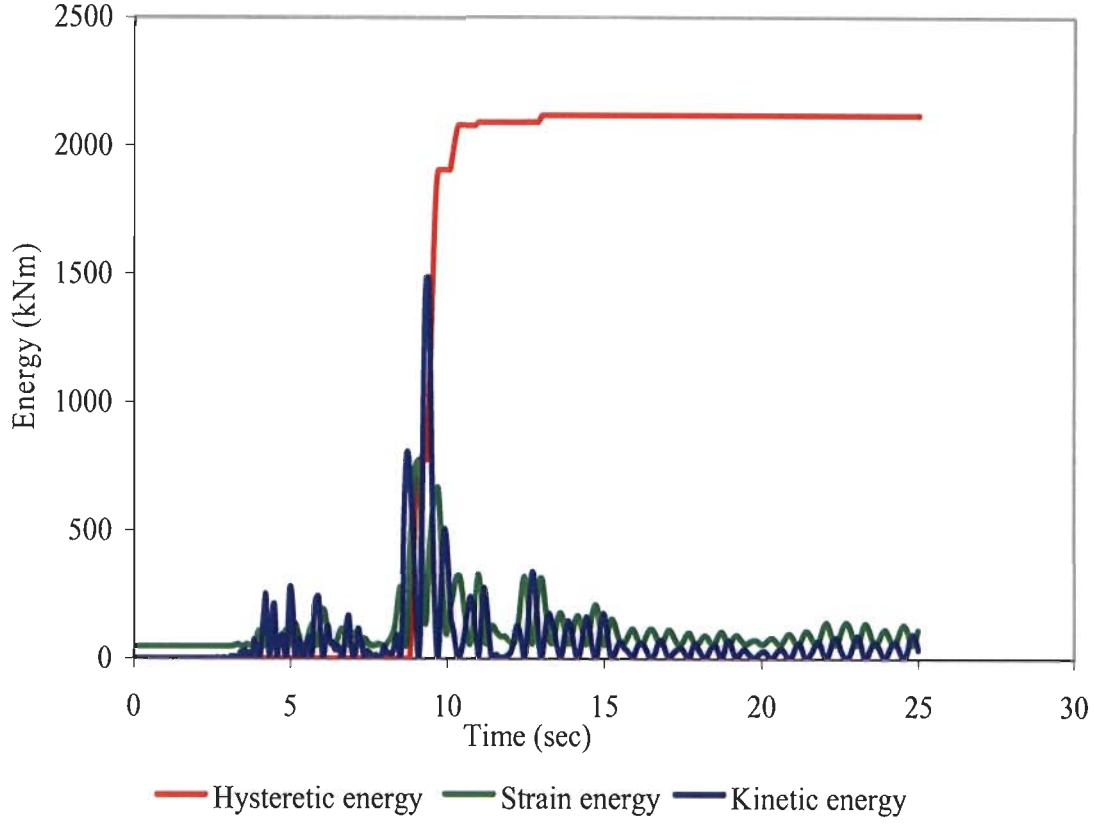

Figure 5.24: Energy distributions for table 5.17, 3 story 3D frame (Northridge: 0.5165g)

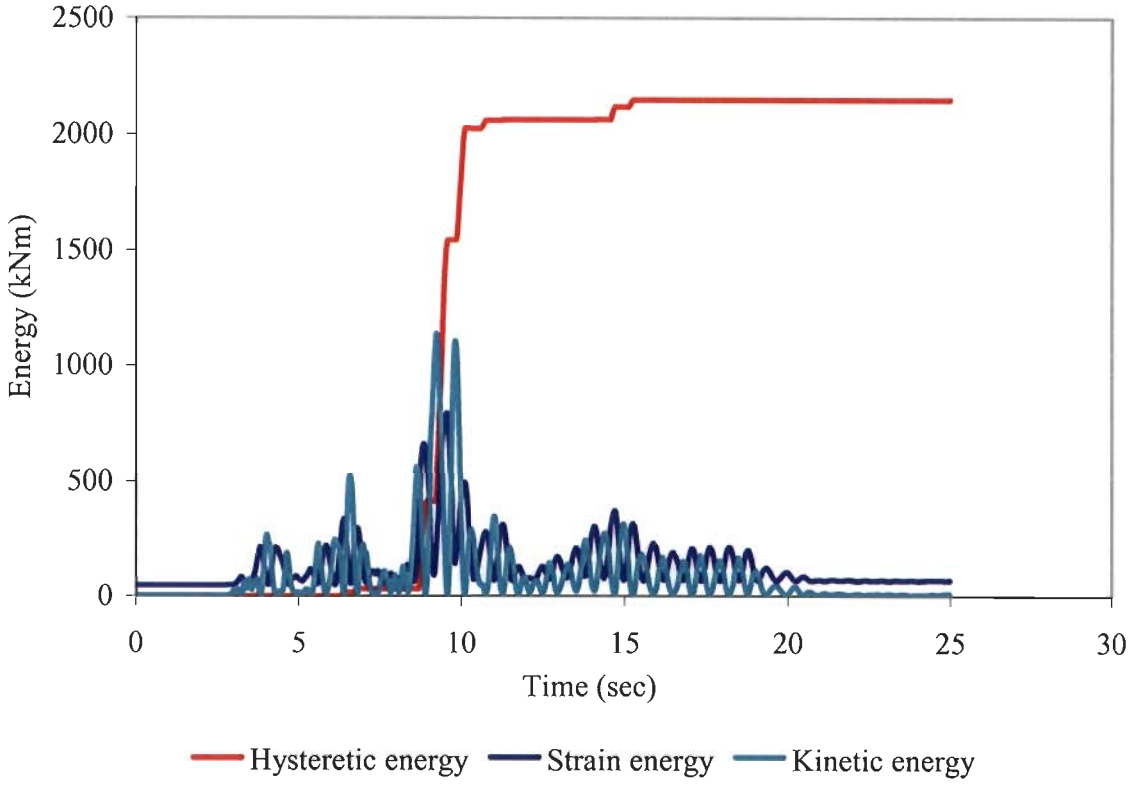

Figure 5.25: Energy distributions for table 5.17, 3 story 3D frame (Northridge: 0.4158g)

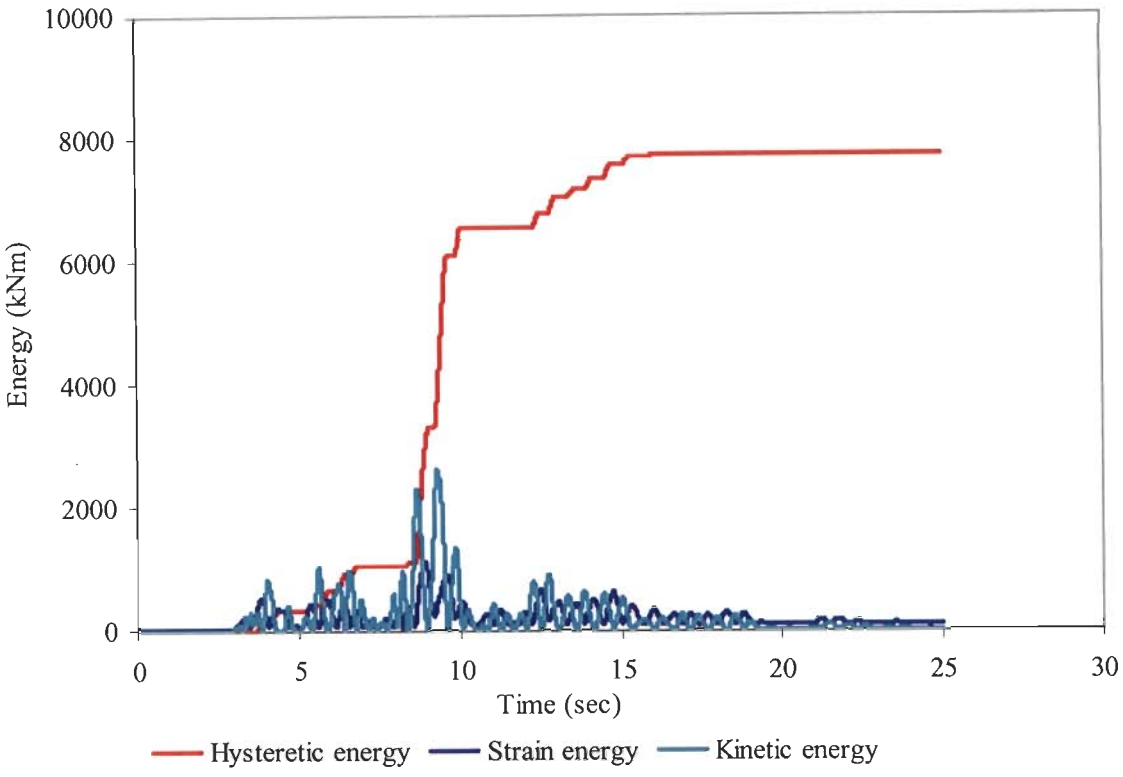

Figure 5.26: Energy distributions for table 5.17, 3 story 3D frame (Northridge: 2x 0.4158g)

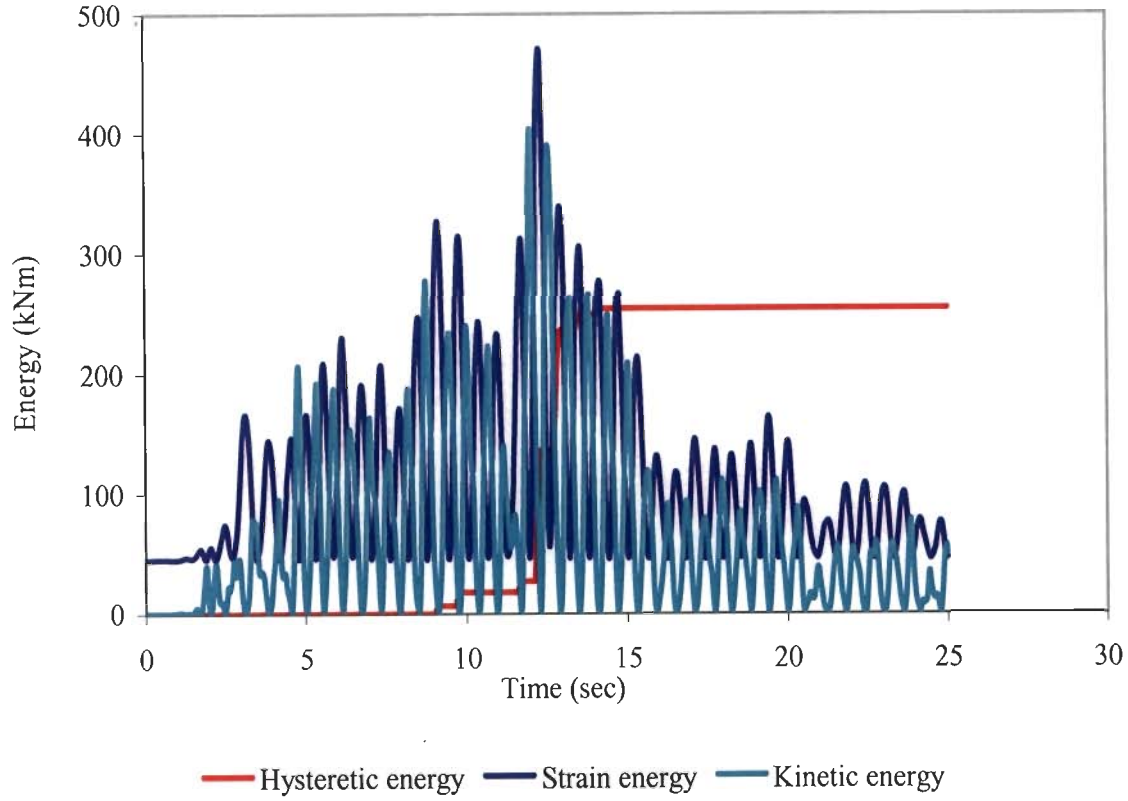

Figure 5.27: Energy distributions for table 5.17, 3 story 3D frame (El Centro: 0.2148g)

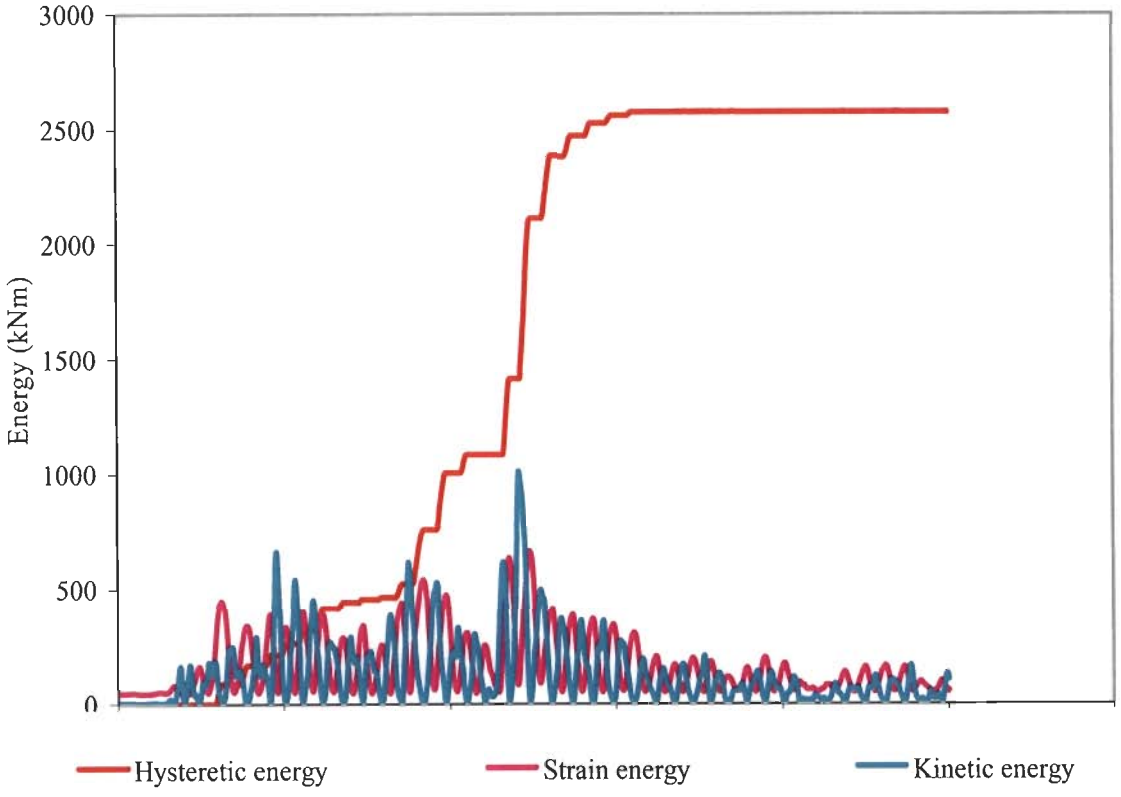

Figure 5.28: Energy distributions for table 5.17, 3 story 3D frame (El Centro: 2x0.2148g)

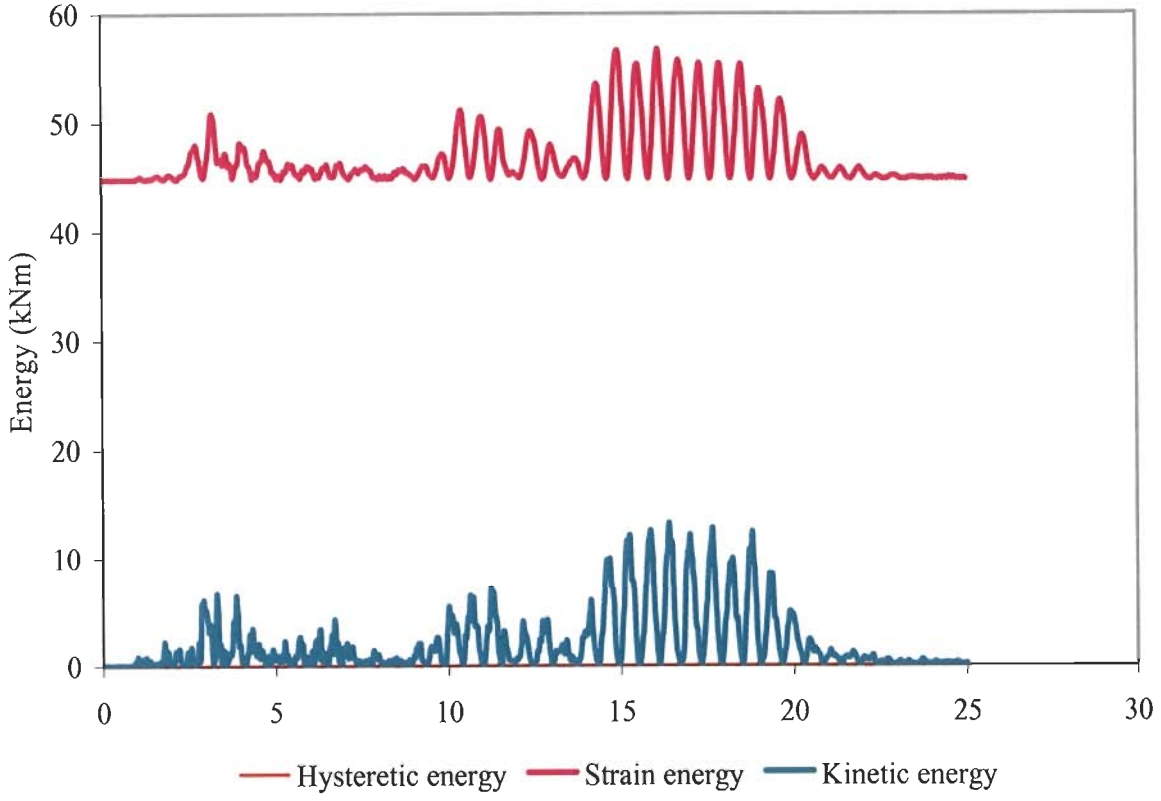

Figure 5.29: Energy distributions for table 5.18, 3 story 2D frame (Centro: 0.2052g)

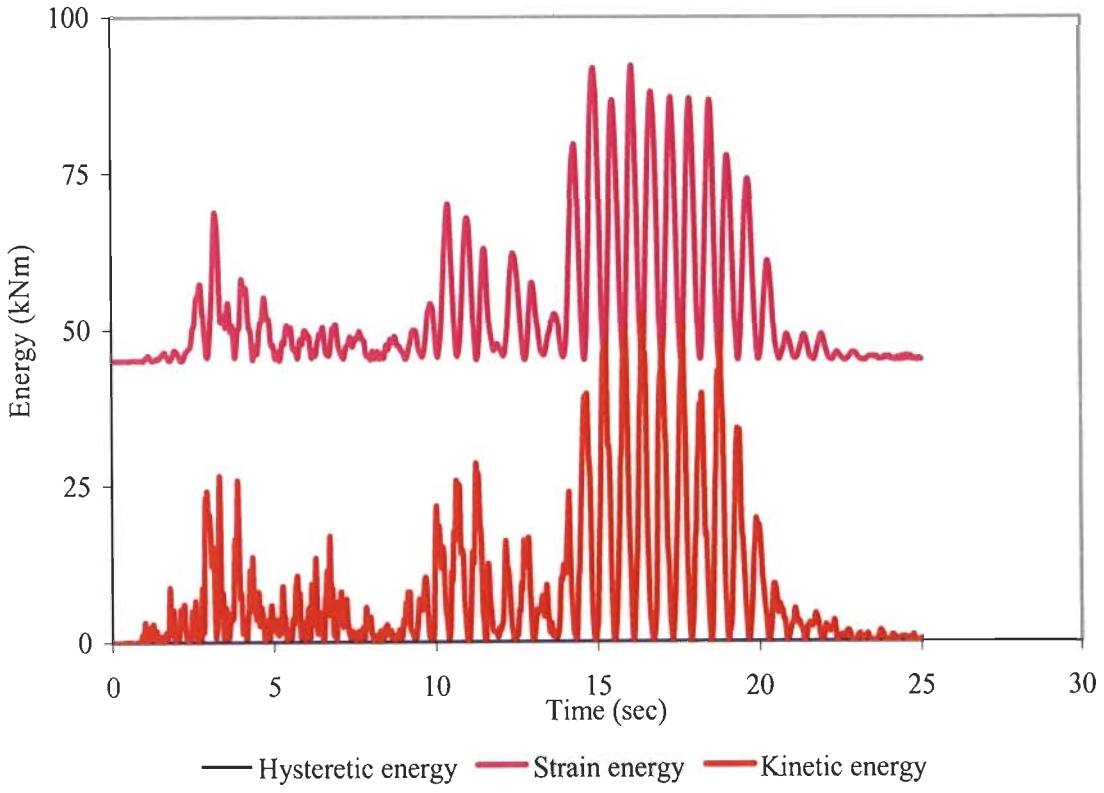

Figure 5.30: Energy distributions for table 5.18, 3 story 2D frame (El Centro: 2x0.2052g)

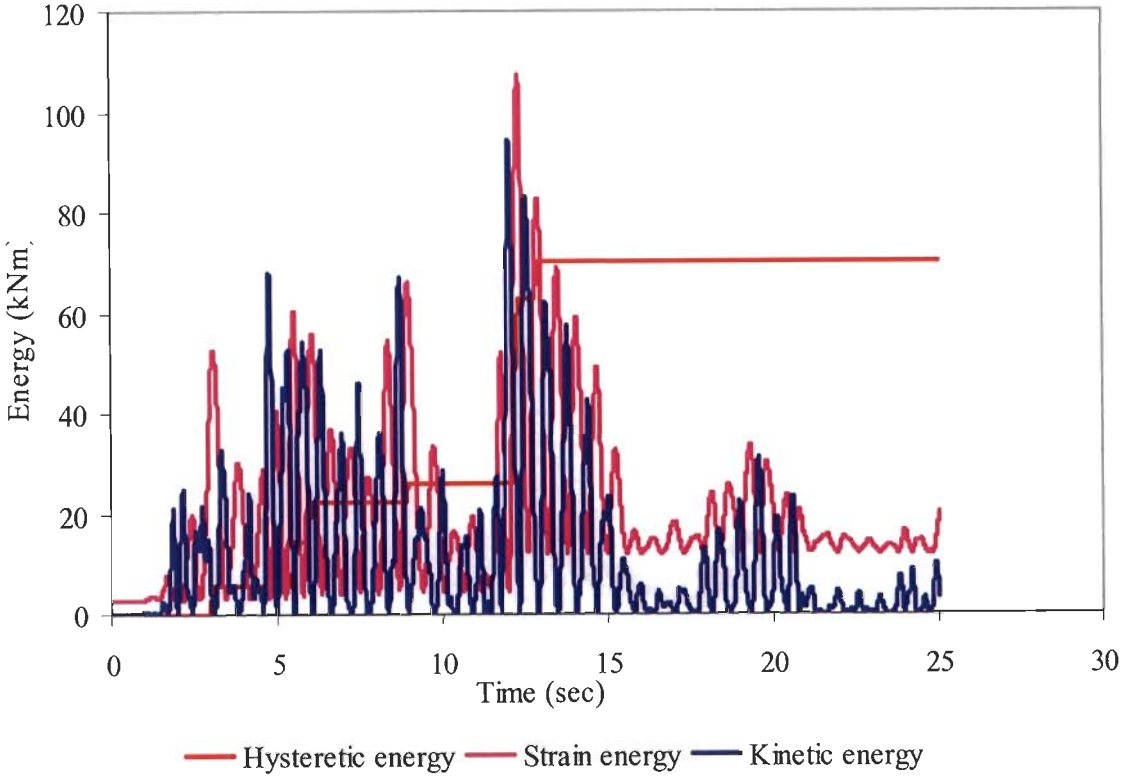

Figure 5.31: Energy distributions for table 5.18, 3 story 2D frame (El Centro: 0.2148g)

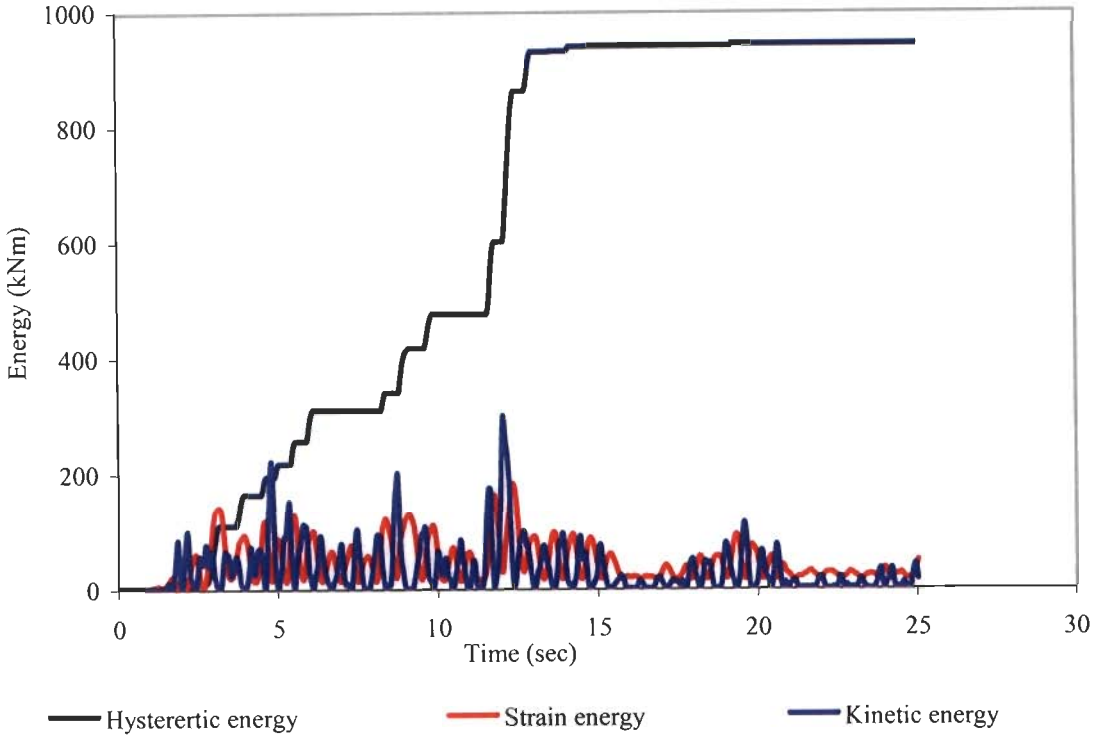

Figure 5.32: Energy distributions for table 5.18, 3 story 2D frame (El Centro: 2x0.2148g)

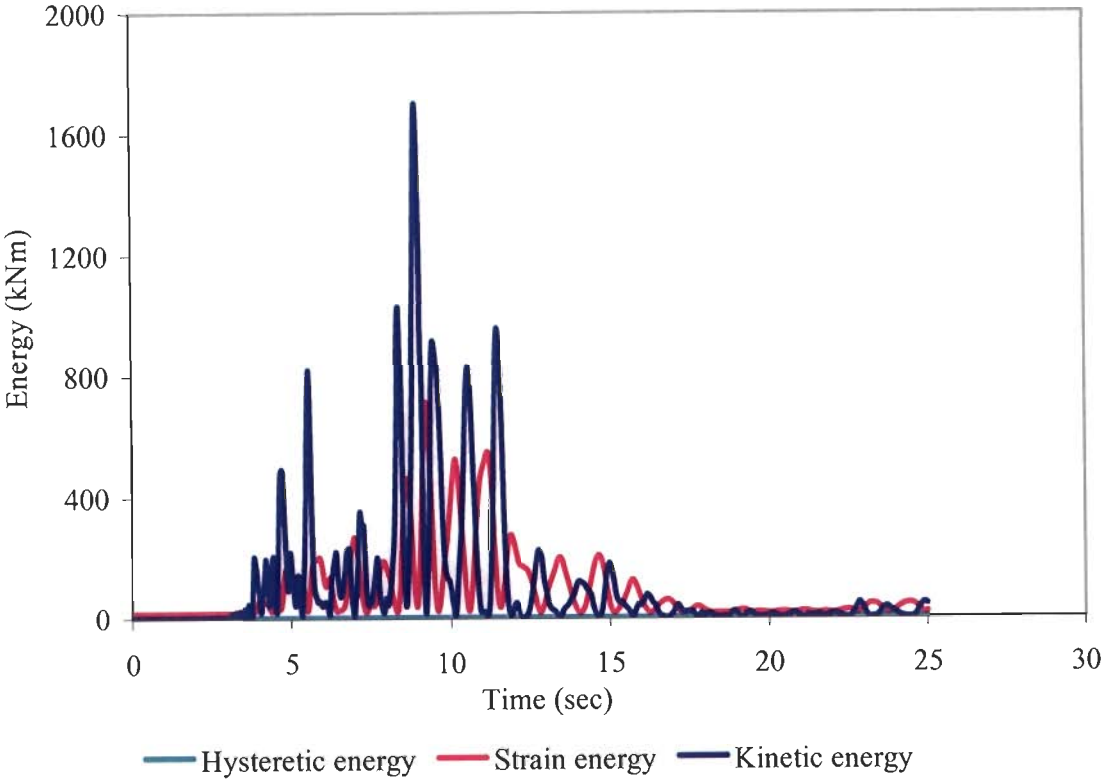

Figure 5.33: Energy distributions for table 5.19, 9 story 2D frame (Northridge: 0.5165g)

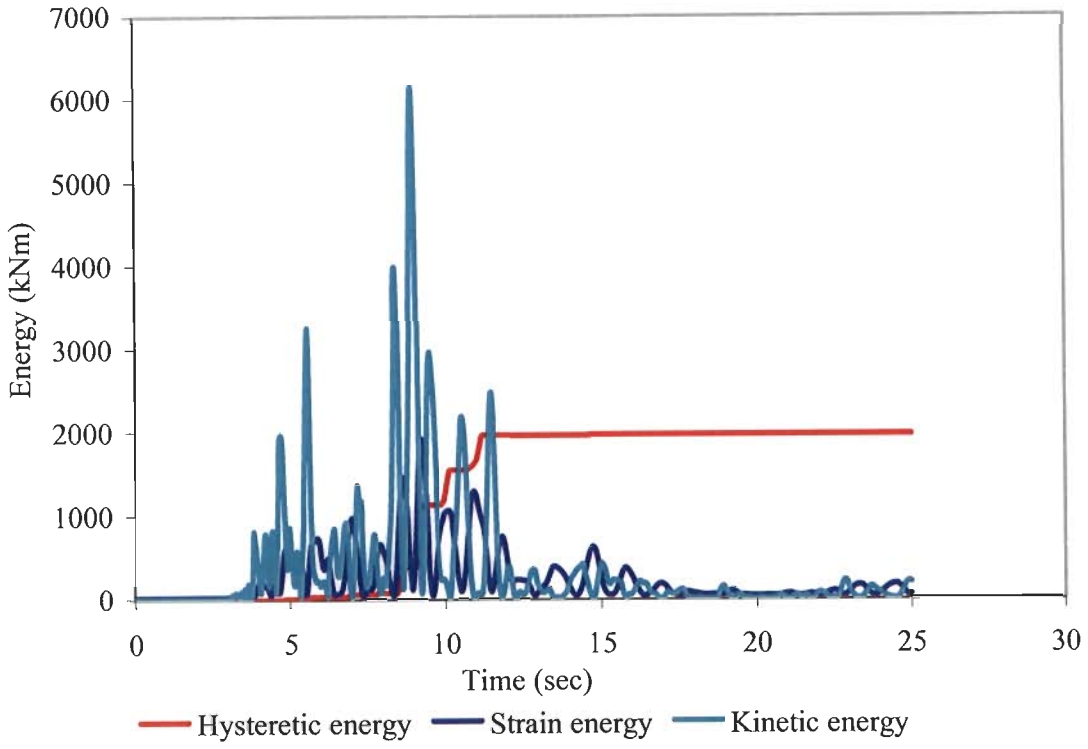

Figure 5.34: Energy distributions for table 5.19, 9 story 2D frame (Northridge: 2x 0.5165g)

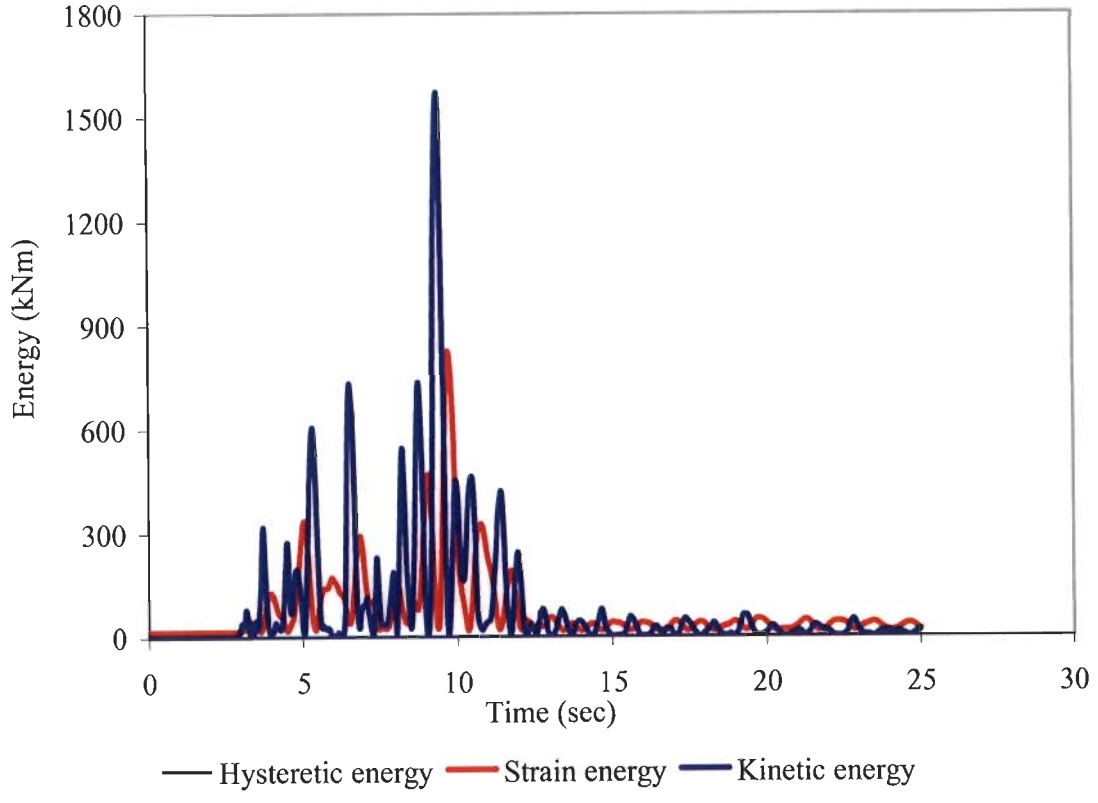

Figure 5.35: Energy distributions for table 5.19, 9 story 2D frame (Northridge: 0.4158g)

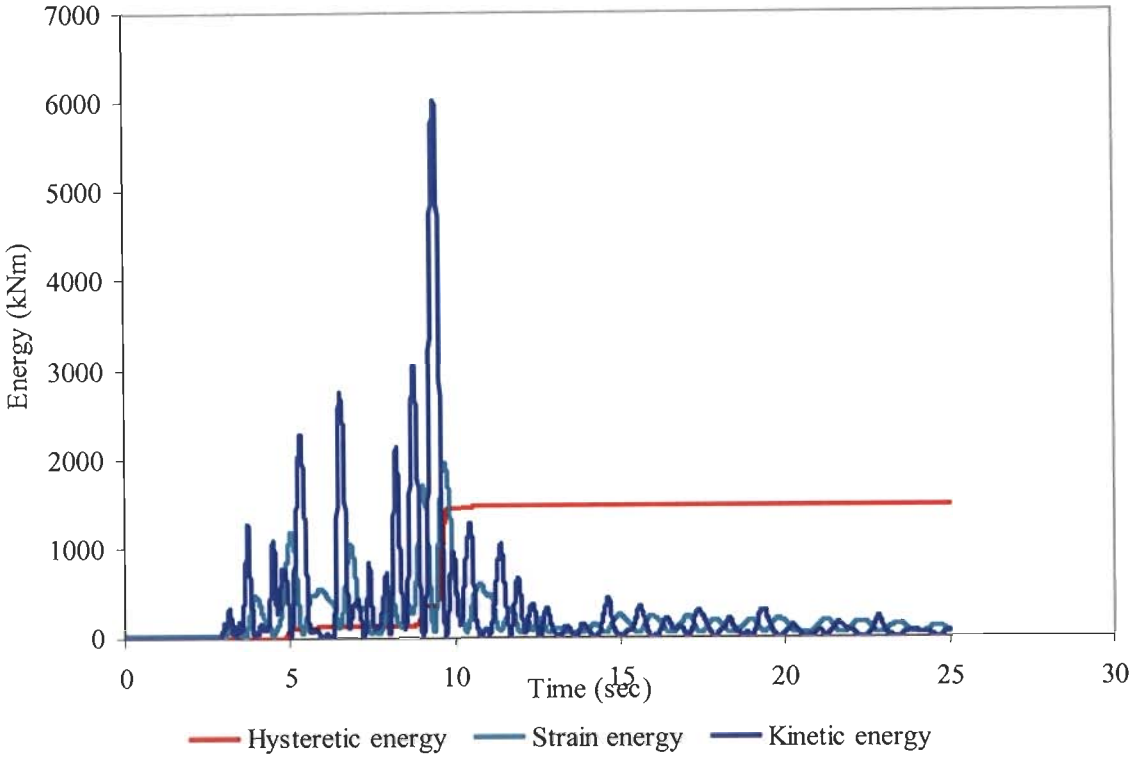

Figure 5.36: Energy distributions for table 5.19, 9 story 2D frame (Northridge: 2x 0.4158g)

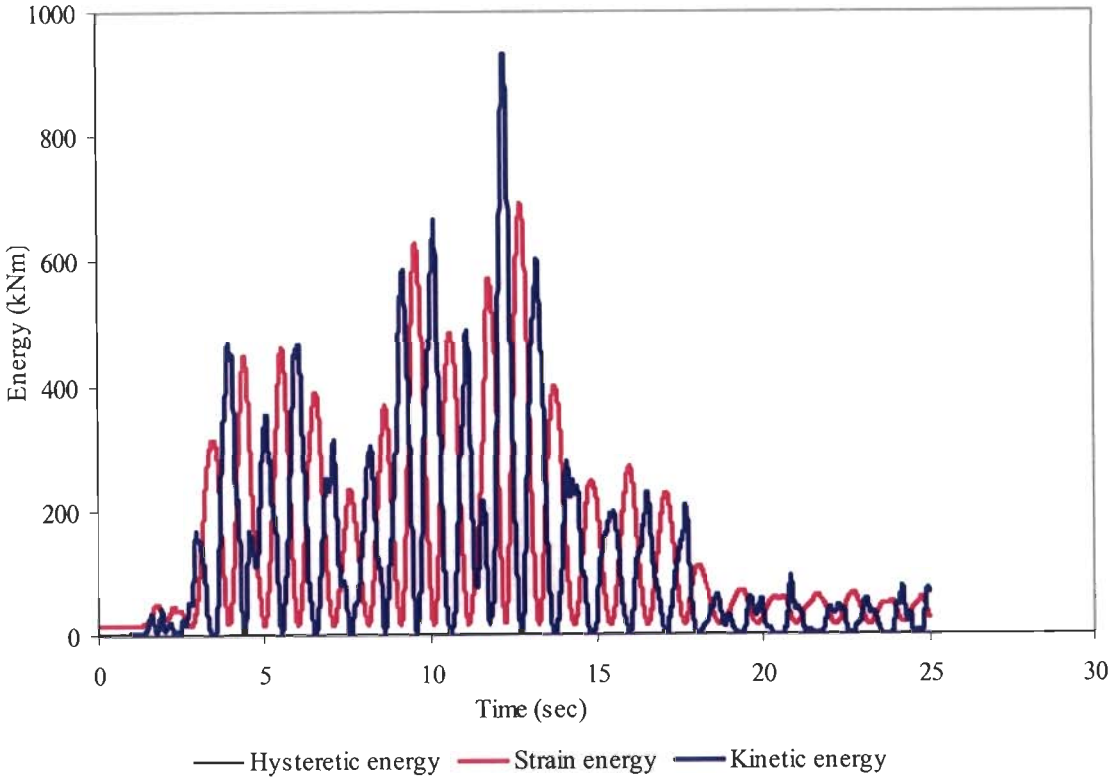

Figure 5.37: Energy distributions for table 5.19, 9 story 2D frame (El Centro 0.2148g)

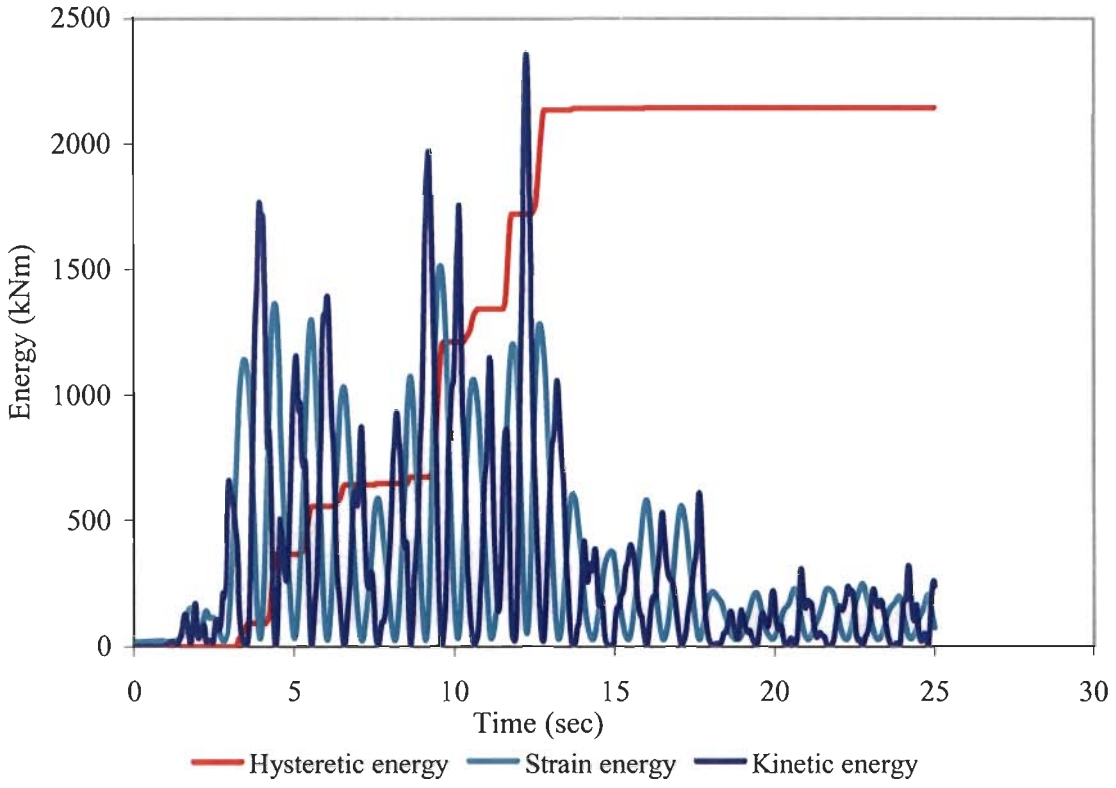

Figure 5.38: Energy distributions for table 5.19, 9 story 2D frame (El Centro:2x 0.2148g)

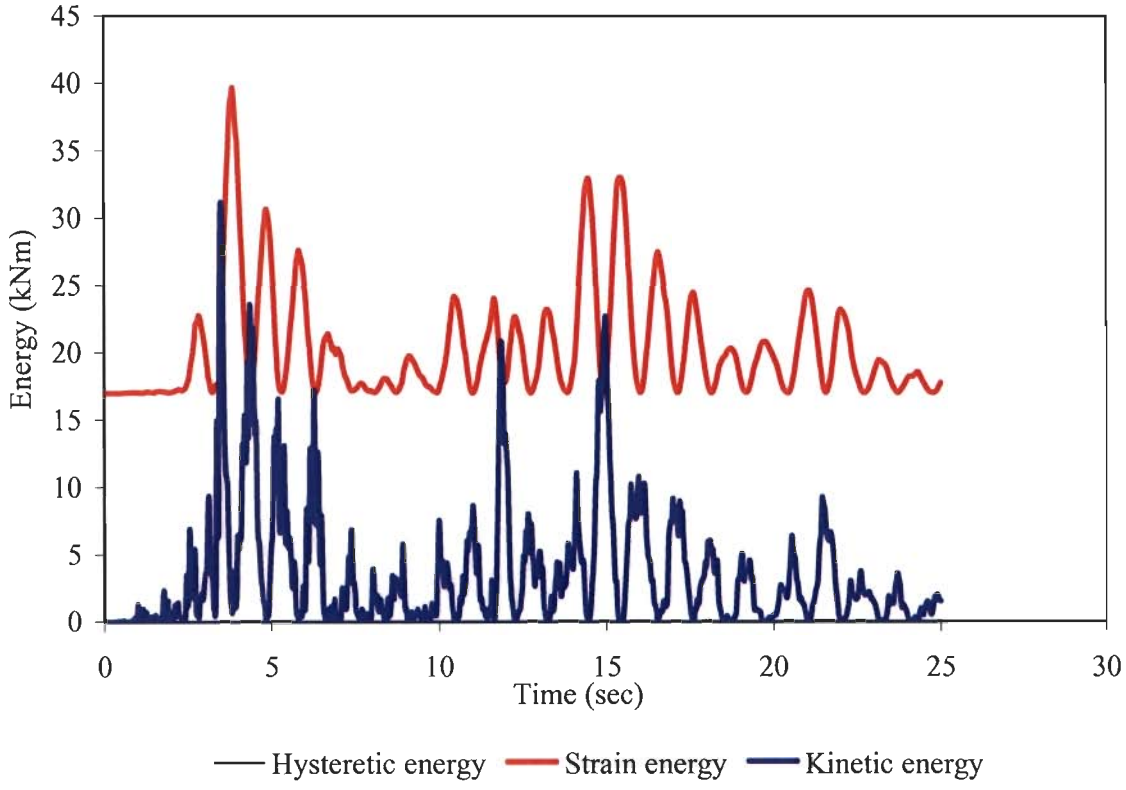

Figure 5.39: Energy-distributions for table 5.19, 9 story 2D frame (El Centro: 0.2052g)

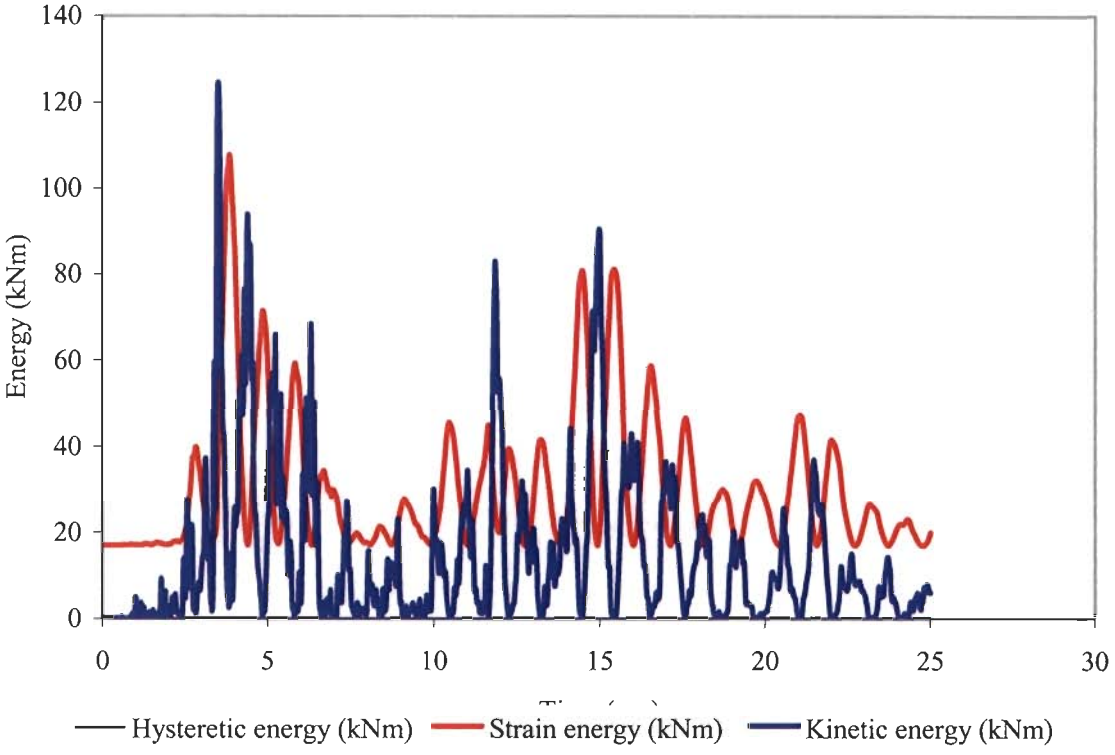

Figure 5.40: Energy distributions for table 5.19, 9 story 2D frame (El Centro: 2x0.2052g)

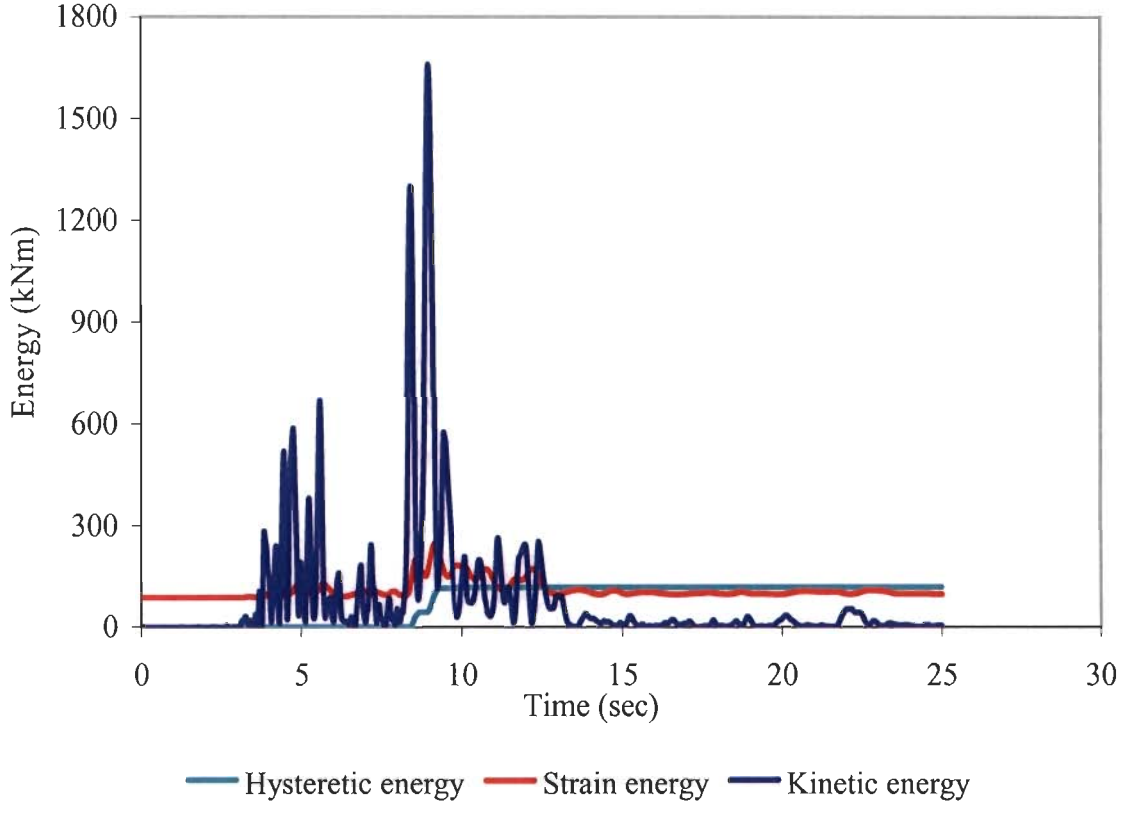

Figure 5.41: Energy distributions for table 5.20, 15 story 2D frame (Northridge: 0.5165g)

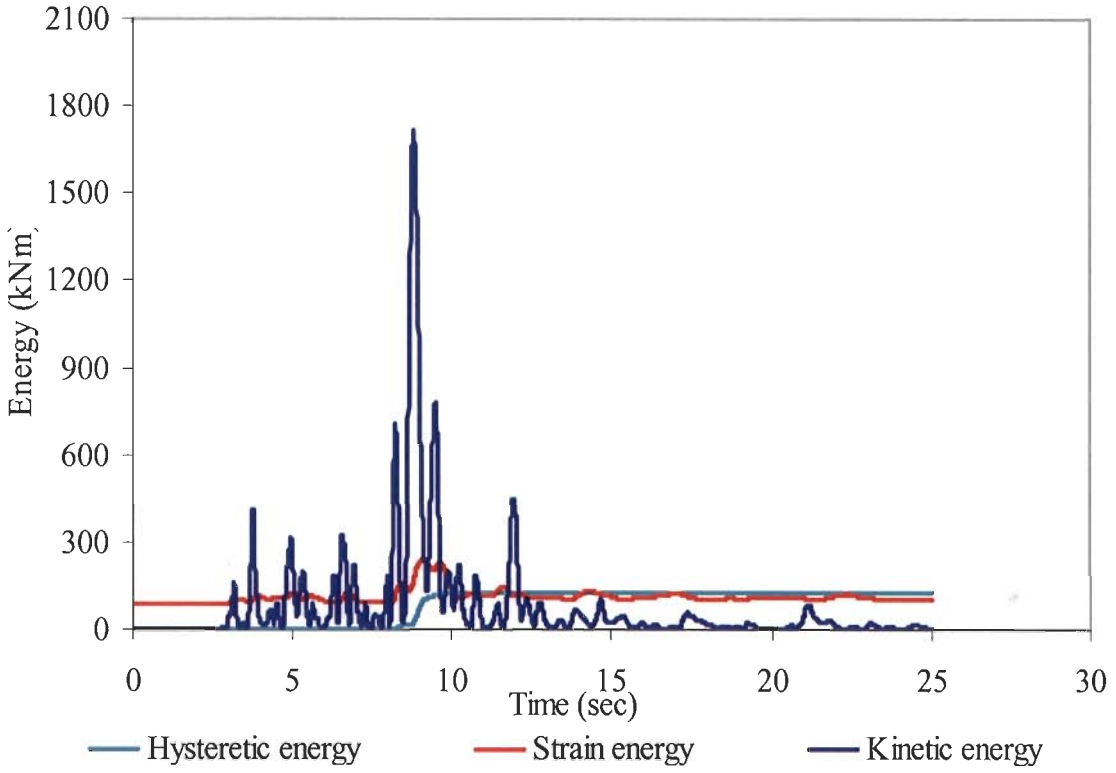

Figure 5.42: Energy distributions for table 5.20, 15 story 2D frame (Northridge: 0.4158g)

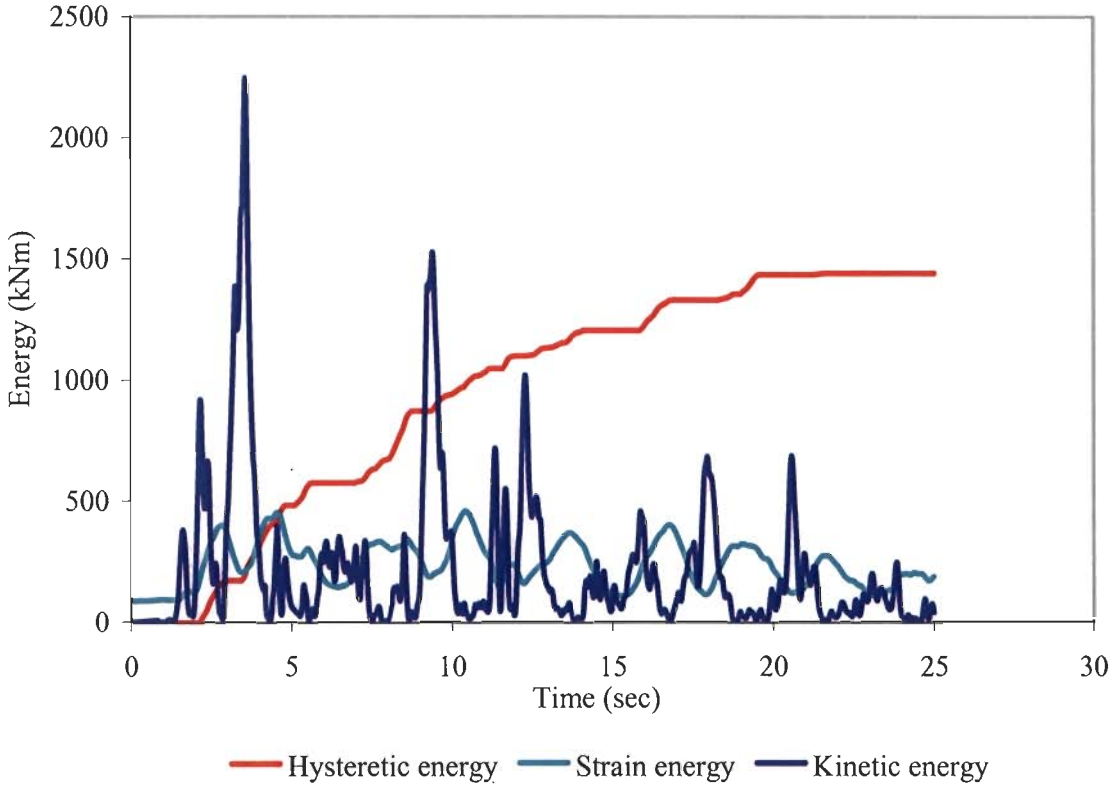

Figure 5.43: Energy distributions for table 5.20, 15 story 2D frame (El Centro: 2x0.2148g)

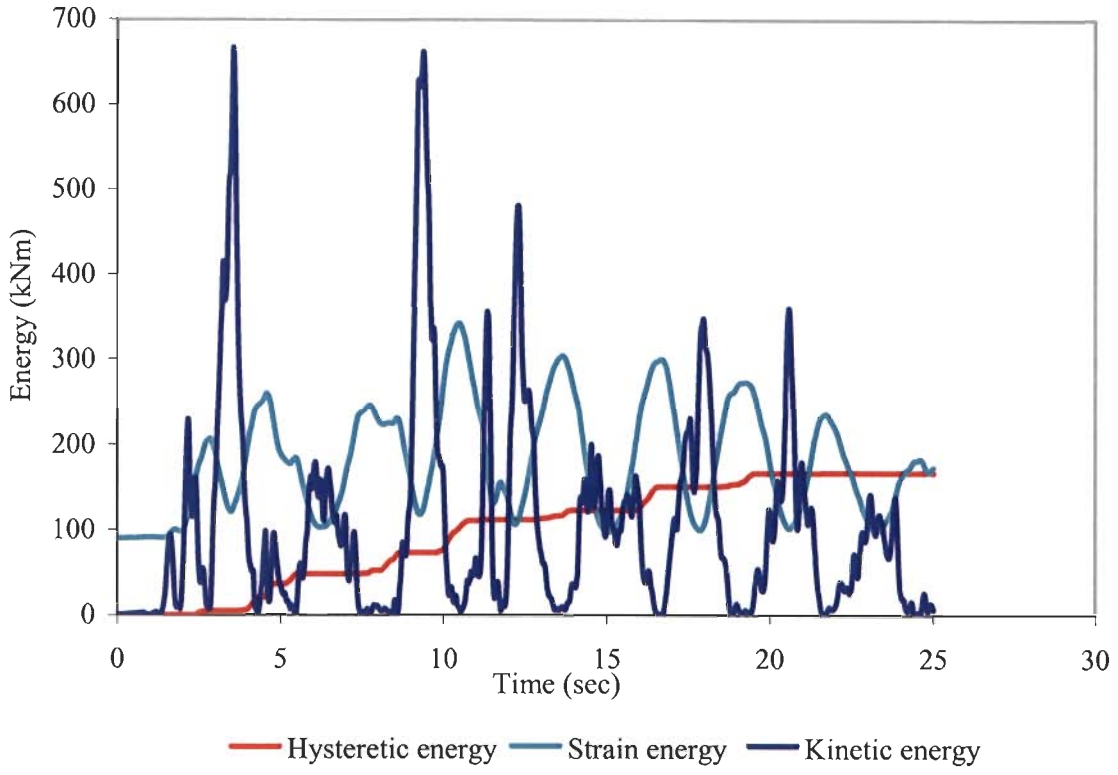

Figure 5.44: Energy distributions for table 5.20, 15 story 2D frame (El Centro: 0.2148g)

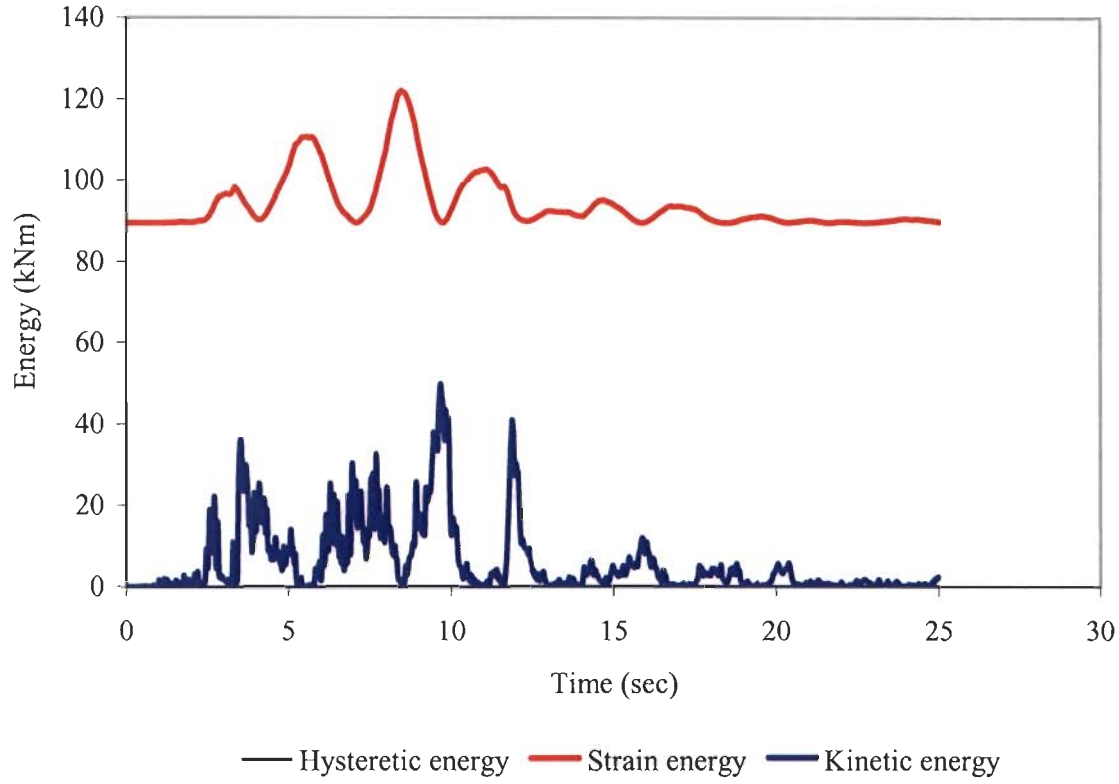

Figure 5.45: Energy distributions for table 5.20, 15 story 2D frame (El Centro: 0.2052g)

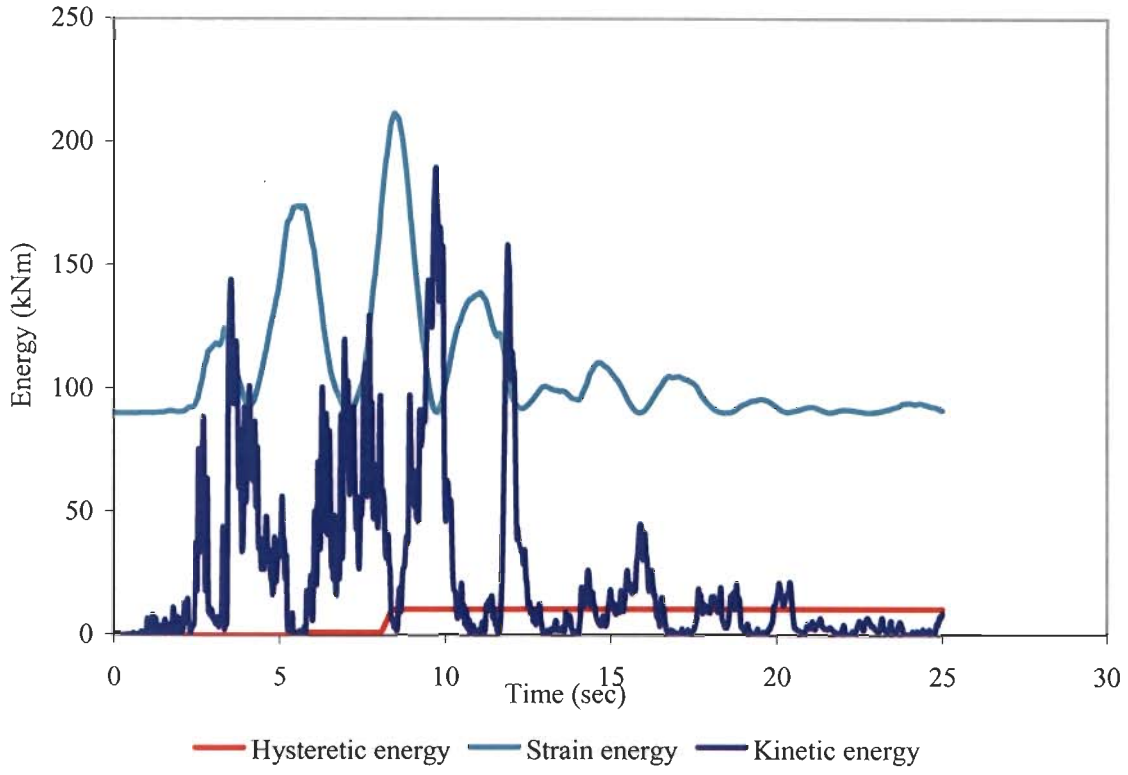

Figure 5.46: Energy distributions for table 5.20, 15 story 2D frame (El Centro:2x 0.2052g)

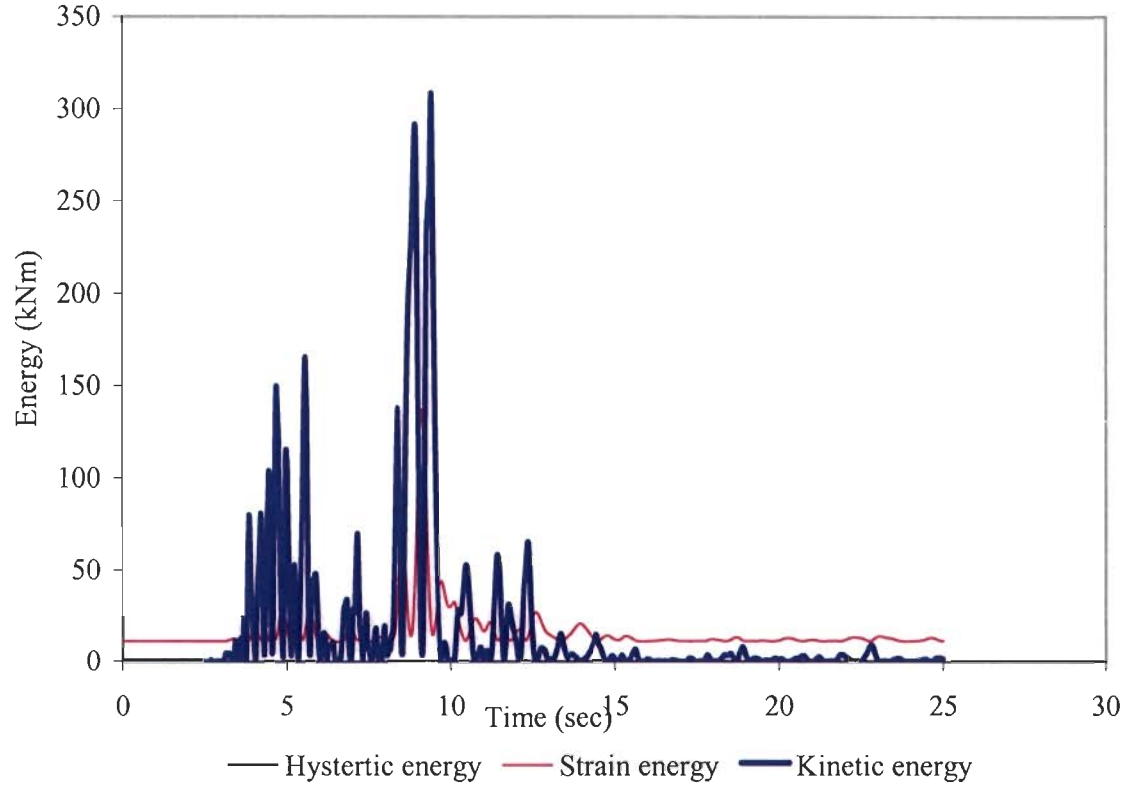

Figure 5.47: Energy distributions for table 5.21, 20 story 2D frame (Northridge 0.5165g)

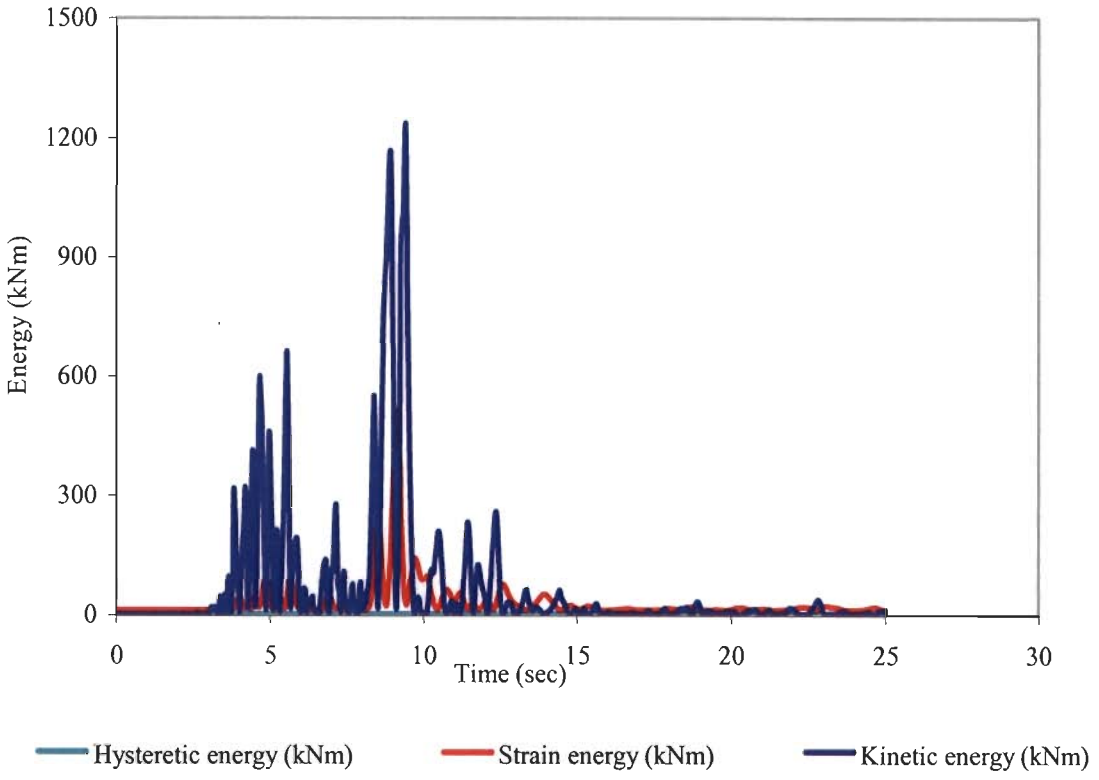

Figure 5.48: Energy distributions for table 5.21, 20 story 2D frame (Northridge: 2x0.5165g)

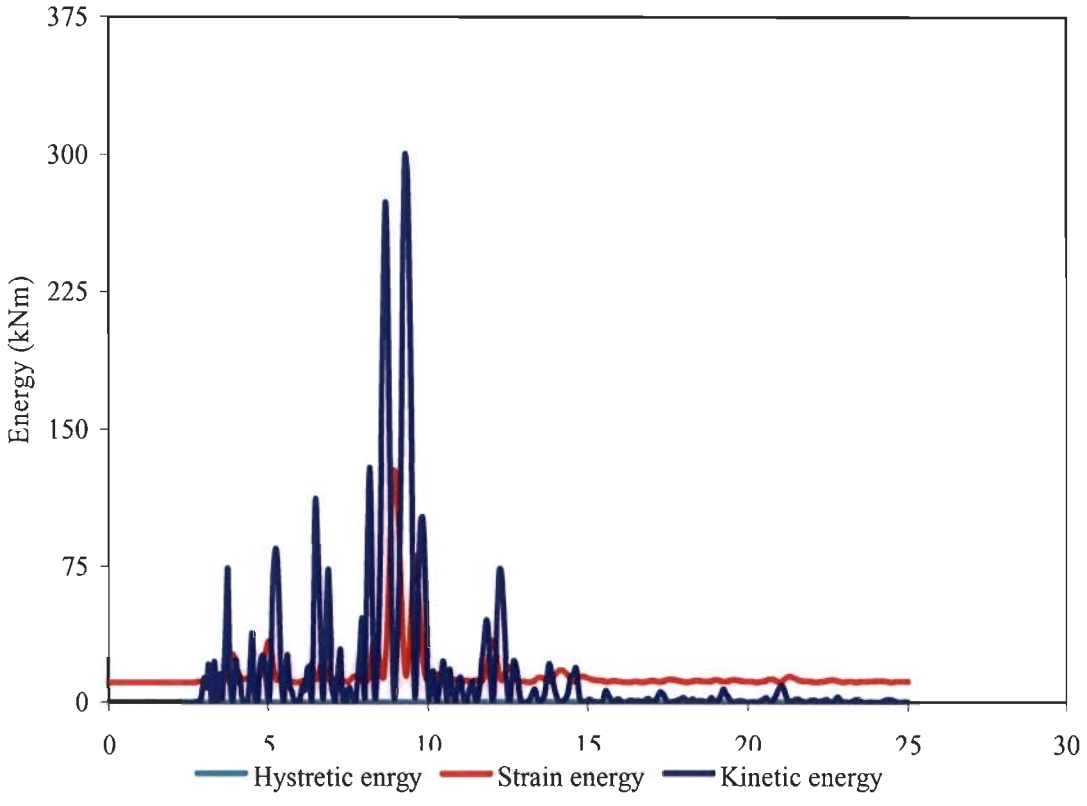

Figure 5.49: Energy distributions for table 5.21, 20 story 2D frame (Northridge 0.4158g)

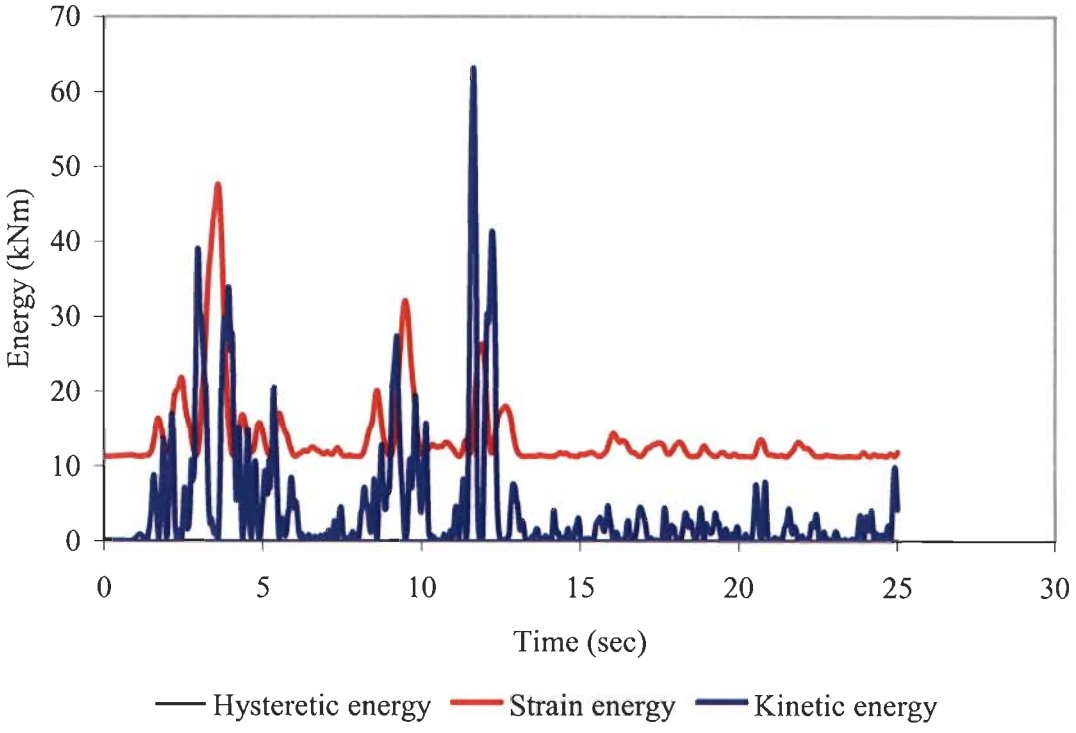

Figure 5.50: Energy distributions for table 5.21, 20 story 2D frame (El Centro 0.2148g)

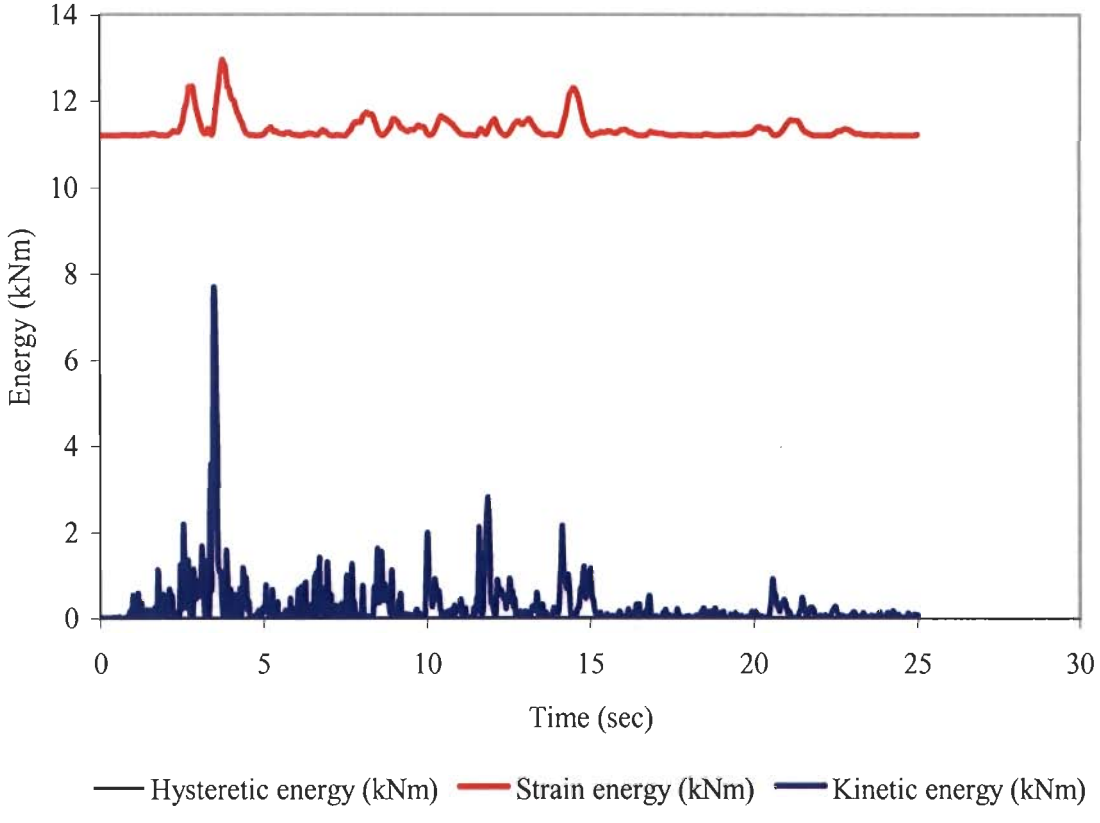

Figure 5.51: Energy distributions for table 5.21, 20 story 2D frame (El Centro 0.2052g)

5.5 Normalized Hysteretic Energy

Result: Tables 5.24 and 5.25 display the normalized hysteretic energy. The value of hysteretic energy and strain energy are known from the response history for energy fro the building frames in the study for a set of earthquakes. Tables 5.24 to 5.26 contain the hysteretic energy normalized with the strain energy for the building frameworks. Table 5.24 gives details of normalized hysteretic energy for the varying ground motions with higher peak ground accelerations. Tables 5.25 and 5.26 have the lower values of normalized energy due to the reason that the severity of the ground motions applied are smaller than the table 5.24.

5.5.1 Result Discussions: The major task of performance based seismic design is to incorporate stiffness, strength and ductility degradation under the severe earthquake ground motions in analytical expressions. Hysteretic energy in the normalized forma consists of this entire factor into a single equation. As found the data for normalized hysteretic energy in the table. 5.24, the value is nearly constant for varying ground motions. The next attribute of performance based seismic design is to consider the stable parameter or such attribute which can be stable when any drastic change takes place. Normalized hysteretic energy where the base is strain energy and the numerator is hysteretic energy is useful for such design development. Objective of this research program remained to identify the critical parameters for developing algorithm of promising PBSD. One of the problem formulations of Chapter 3 is normalized hysteretic energy in terms of hysteretic energy and normalized yield strength as a content of the research program. The elements at the component levels have been identified through the analysis results in terms of hysteretic energy. For those elements having significant hysteretic energy, the analytical expression derived in chapter 3 for normalized hysteretic energy has been used for further interpretation. Tables 5.25 to 5.26 have been used for the interpretation of normalized hysteretic energy for those frames which have dissipated significant amount of input seismic energy through yielding of beams/columns at various floors reveal the pattern of energy consumed by the structures as strain, kinetic and hysteretic energy. Hysteretic energy as the major source of consumption of input seismic energy under severs earthquake ground motions provides stable and promising response while a structure has no other alternatives for fail safe design.

Future recommendations: Normalized hysteretic energy using the mechanical characteristics having degrading values needs further investigation through explicit analytical function requires further experimental programs.

Table 5.24: Energy distributions (%) for three story 3D building framework.

Input Energy (kNm)	Strain Energy (kNm)	Kinetic Energy (kNm)	Hysteretic Energy (kNm)	% E_S	% E_K	% E_h	Earthquake ground motions
3379.83	51.69	157.66	2098.86	1.53	4.67	62.1	Northridge, (0.5165g)
10730.48	89.89	57.86	7598.12	0.84	0.54	70.8	Northridge(2x0.5165g)
21684.70	142.75	31.83	15142.00	0.66	0.15	69.8	Northridge(3x0.5165g)
32860.40	333.16	54.13	24667.90	1.01	0.16	75.1	Northridge(4x0.5165g)

Table 5. 25: Normalized hysteretic for three story 2D building frame.

Sl No	Elastic strain energy	Hysteretic Energy	Ratio of hysteretic and elastic strain energy	Earthquake ground motions
1	50.57	389.70	7.71	Northridge E-W,(0.5165g)
2	40.20	381.34	9.48	Northridge E-W,(2x0.5165g)
3	38.66	635.92	16.45	Northridge N-S,(2x0.4158g)
4	39.06	1326.80	39.96	El Centro E-W,(0.2148g)
5	36.84	943.72	25.61	El Centro E-W,(2x 0.2148g)

Table 5. 26: Normalized hysteretic for three story 3D building frame.

Sl No	Elastic strain energy	Hysteretic Energy	Ratio of hysteretic energy and elastic strain energy	Earthquake ground motions
1	104.1	2120.45	20.37	Northridge E-W, (0.5165g)
2	70.85	3179.37	44.87	Northridge E-W,(2x0.5165g)
3	177.87	7727.84	43.45	Northridge N-S,(2x0.4158g)
4	133.00	254.15	1.91	El Centro E-W,(0.2148g)
5	160.70	2571.43	16.02	El Centro E-W,(2x 0.2148g)

5.6 Hysteretic Energy (E_D) and Strain Energy (E_s)

Equation (3.40) as derived in the chapter 3, relates the total hysteric (E_D) and strain energy (E_S) i.e., $E_D = 8n \times \frac{(n+1)}{2} E_s$, Where E_D is the total energy dissipated, n is the total number of loops and E_s is the elastic strain energy. For performance based criteria the above equation is an important equation since, elastic strain energy (E_s) presents IO/OP performance levels and the successive values of total hysteretic energy reveals the other performance levels(LS, CP etc). E_D represents damage, which has the relation with elastic

strain energy through the number of loops, when a component yields and dissipates energy during reversal of stresses arising due to earthquake loadings. For single hysteretic loop, hysteretic energy is related with the strain energy through cumulative ductility. Since displacement approach for performance evaluation is poorly rated because the cumulative ductility is not easily accessible. However, for the known values of successive loop, the hysteretic energy is related with the cumulative ductility and can be estimated through the simple relation. Equation (3.40) derived in chapter 3 for normalized hysteretic energy, which relates the hysteretic energy with the cumulative ductility. Further, the same expression has been used for finding total energy dissipated (H_i) during reversal of stresses due to varying earthquake ground motions. (Table 5.27).

Table 5.27: Hysteretic energy of the successive loop

Sl No.	μ_i	1	2	3	4	5	6	7
01	$E_{ih}=\frac{\mu_i-1}{\mu_i}\times\mu_i E_s$	0	E_s	$2E_s$	$3E_s$	$4E_s$	$5E_s$	$6E_s$
02	$H_i=\sum_{i}^{2} E_{ih}$	0	E_s	$3E_s$	$6E_s$	$10E_s$	$15E_s$	$21E_s$

Table 5.28: Damage index

Sl. No.	μ_i	1	2	3	4	5	6	7
01	Damage Index $(DI)=\frac{\sum_{1}^{n} E_{ih}}{H_i}$	0	1/21 =0.067 Immediate Occupancy	3/21 0.2 Damage	6/21 0.4	10/21 0.47 Control	15/21 0.71 Life Safety	21/21 1.0 Collapse

With the known value of strain energy used for Operational occupancy, the relation of various performance objectives on the continuous spectrum of damage spectrum. Such a kind of relation in between the hysteretic energy and the strain energy is unique in its characteristics and can be used for the simplest formulation of performance levels, even without making much more computation.

Table 5.29: Hysteretic energy for elasto-plasto loop for successive displacement ductility

Sl. No	Displacement Ductility (μ)	(μ-1)	4(μ-1)/(μ)	E_h =.....Eso E_{so} =μ x E_s	Remarks
01	1	0	0	0	Algebraic sum of the hysteretic energy for successive cycles may be economically used for prediction of energy to be dissipated during continuous spectrum of damages
02	2	1	2	4	
03	3	2	8/3	8	
04	4	3	3	12	
05	5	4	16/5	16	
06	6	5	20/6	20	

Successive values of hysteretic energy will be controlled by the amount of hardening effect. Strain energy being a stable for the structure having the first mode dominancy, with the background that it is the first attributes of the capacity to come forward to meet the demand. The reason behind this truth is that input seismic energy is controlled by the time period of the structure, therefore, being associated with the stiffness, which is a stable mechanical characteristic during the linear behavior of the structures. Deformation being controlled by the dominancy of the first mode, hence, the strain is more stable capacity. Variation of stiffness for higher demands, when the structure yields are known as stiffness degradation, however, deformation elongates with certain strain degradation. The product of the degraded stiffness and elongated deformation maintains a stable style through the mechanical characteristics, ductility. Cumulative ductility during reversals of stresses arising during severe earthquake has been addressed by research community and sufficient literature is available on this topic [10]. Under the displacement based design as it directly represents the probable damages and are the contents of ongoing performance based seismic design. Displacement in the inelastic region, when the structure is continuously yielding, is related with the deformation at the yielding through the ratio of both displacements and ductility. Ductility under the condition of loading changes from element to element and at the structure levels [5].

Table 5.30: Theoretical and experimental damage ratio for three story 3D under Northridge (0.6g)

Sl No	Displacement Ductility	Cumulative Ductility	Theoretical damage ratio	Experimental damage ratio
1	1	1	0	0
2	2	3	0.2	0.06
3	3	6	0.4	0.33
4	4	10	0.67	0.42
5	5	15	1.00	1.00

Table 5.31: Theoretical and experimental damage ratio for three story 3D, El Centro (0.6g)

Sl No	Displacement Ductility	Cumulative Ductility	Theoretical damage ratio	Experimental damage ratio
1	1	1	0	0
2	2	3	0.06	0.02
3	3	6	0.13	0.29
4	4	10	0.22	0.34
5	5	15	0.33	0.43
6	6	21	0.47	0.52
7	7	28	0.62	0.81
8	8	36	0.80	0.96
9	9	45	1.00	1.00

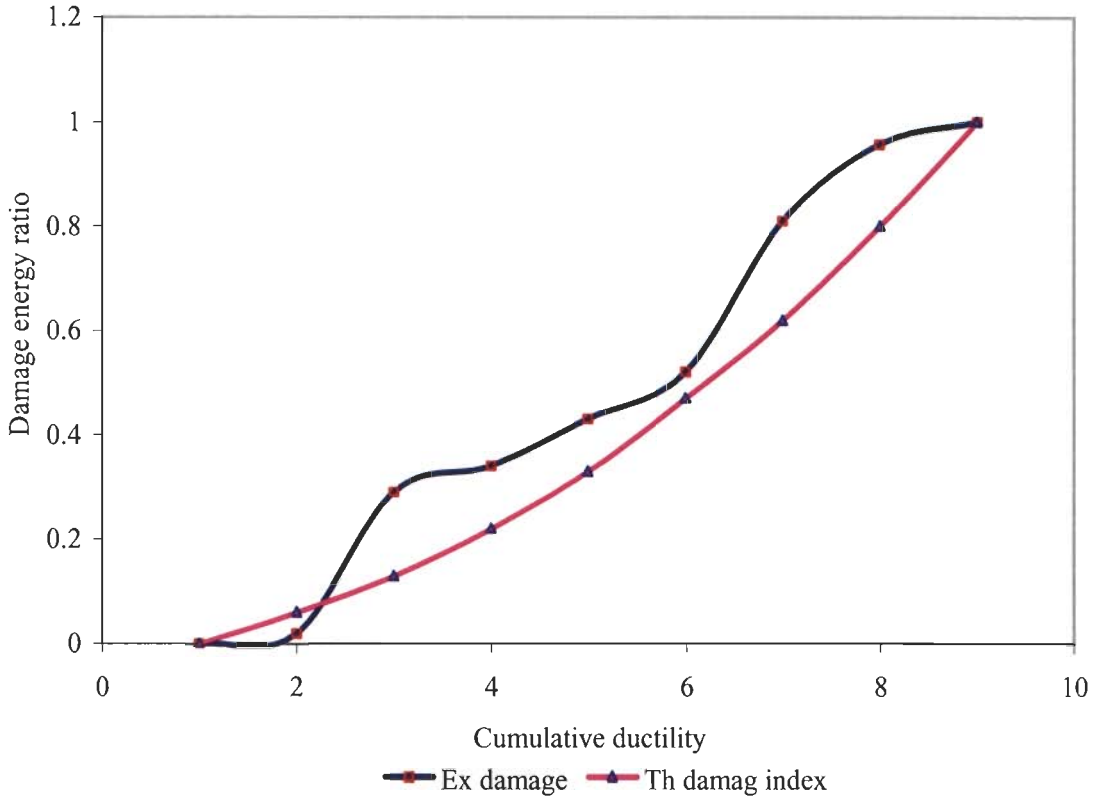

Figure 5.52: Theoretical and experimental damage ratio: cumulative ductility

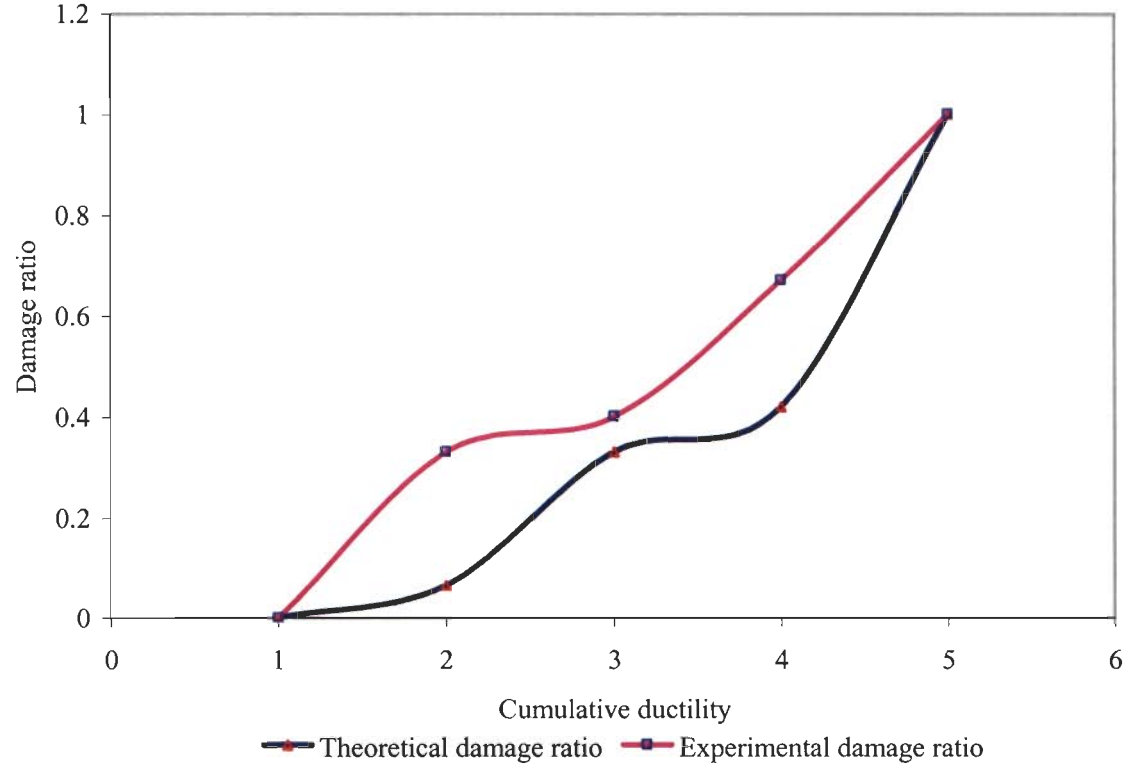

Figure 5.53: Theoretical and experimental damage ratio vs. cumulative ductility

5.6.1 Result discussions

Calculation of theoretical and experimental damage ratio

Cumulative ductility corresponding to the displacement ductility is estimated. Say displacement ductility is 10. Its corresponding cumulative ductility is 55. The first ordinate of ductility is 2, corresponding to the displacement ductility =2. Theoretical damage is the ratio of cumulative ductility corresponding to the displacement ductility divided by the equivalent largest available cumulative ductility.

Experimental damage ratio is ratio of hysteric energy corresponding to the displacement ductility to the highest hysteretic energy capacity. For three story 3D story steel building frame under varying earthquake ground motions, figures 5.53 and 5.54 represent theoretical and experimental damage ratio for the three story 2D and three story 3D building frames under the equivalent displacement ductility obtained from pushover analysis and the hysteretic energy under the varying earthquake loadings.

5.7 Simplified Park and Ang Damage Model

Chapter 3, equation (3.51) is the simplified expression (derived as the content of the present study) for Park and Ang damage index [1985] for estimation for over all damage indexes in terms of the component damage (local). Knowing the damage index at component levels, a strategy for overall damage (D_{Tn}) index can be easily known using the equation (3.51)

The generalized expression for overall damage index (D_{Tn})

$$D_{Tn} = \frac{D_{1e}^{\ 2} + D_{2e}^{\ 2} + D_{3e}^{\ 2} + D_{4e}^{\ 2} + \ldots\ldots - 0.6(D_{1e} + D_{2e} + D_{3e} + \ldots.)}{D_{1e} + D_{2e} + D_{3e} + \ldots\ldots - (0.6 + 0.6 + 0.6 + \ldots..).} \qquad (3.51)$$

The above expression of damage index is the extension of Park and Ang damage index for overall damage which includes the damage index at the element level to the global level. D_{ie} is the damage index at the element level. Damage contribution due to uni-axial deformation is 0.6 [Park and Ang, 1987]; therefore the above expression will give only the maximum value as 0.4. Let D_{1e}=0.3 and D_{2e}=0.4 for another set D_{1e}=0.3 and D_{2e}=0.4, D_{3e}=0.1, D_{4e}=0.2

Then find the overall damage index is 0.34, 0.214

5.7.1 Simplification for Damage Index for Monotonic Displacement

From the equation (3.52), it is concluded that the amount of strain energy increases the ductility times the initial strain energy.

Normalizing the inelastic strain energy with the elastic strain energy is the damage index for the first part of the damage index of the Park and Ang damage model.

$$\text{Damage} - \text{index} - \text{for} - \text{uniaxial} - \text{deformation} = \frac{E_{s2} - E_{s1}}{E_{s2}} \times 0.6 \tag{3.53}$$

0.6 implies for the total part of the damage, which is contributed by the direct deformation. The damage index will tend to 0.6 for maximum value of direct inelastic energy. The above

$$\text{equation (3.53) in terms of ductility} = \frac{\mu_i - 1}{\mu_i} \times 0.6 \tag{3.54}$$

5.7.2 Result Discussions

Park and Ang damage model when is modified for simplification takes the form of the equation (3.51). The advantages of this format of damage model are that overall damage index can be known if the damage index at component level is known. The first part of the Park and Ang damage can be simplified as the equation (3.54).

Adding the normalized damage index of equation (3.51) and (3.54), total damage index is known. Various values of the overall damage index corresponding to seismic hazards can be used as a design aid of PBSD.

Conclusion: The simplified equation for damage index can be used for practical design aid.

Recommendation: The validation of the simplified damage format for the simplified equations (3.51) and (3.54) of Park and Ang for any interim conclusion must be supported by experimental programs under earthquake loadings.

5.8 Number of Yield Excursion Cycles (NYEC) and PBSD

The number of yield excursion cycles under reversals of stresses is defined as the number of times a structural system yields in one direction and subsequently yields in the opposite direction in the following cycle. The number of yielding reversals is more for strong motion, while for low ground motion, the NYR is smaller. NYR spectra indicate that low cycle fatigue may be the problem for structures subjected to long duration earthquake if they are designed for only C_y resulting from the use of the assumed ductility ratio μ. The severity of the ground motions is reflected though the number of yielding in positive and negative. Locking and unlocking of hinges analysis for the assessment of the critical damages for collapse prevention may be through the values of NYEC, followed by the cross section behavior.

5.8.1 Result Discussions

For nine stories building frames critical beams and columns have been demonstrated for number of yield excursion cycles as these components have contributed significant amount of hysteretic energy during varying Northridge E-W (0.5165g) ground motions to the example 2D nine story steel building framework. Figures 5.55 to 5.77 show the pattern of number of yield excursions through the time history and hysteretic loops. The damage can be identified through the time history as well as hysteretic loop. Equation 3.41 derived as the content of the study gives the number of loops for the estimated values of hysteretic and strain energy. Table 5.34 contains the number of hysteretic loop, number of yield excursions, and the cumulative ductility of selected structural components under the severe earthquake ground motions. Theoretical values of these three parameters have been evaluated from the equation 3.41 derived in the chapter 3. Both values (theoretical and experimental) are close.

Conclusions: If the mode of seismic resistant designs control is through the inelastic deformation (yielding), behavior of structural components changes due to reversal of stresses, even a ductile material becomes brittle. Such in formations of number of loops, and the number of yield excursions (NYEC) directly provides the damages to the components.

Future recommendations:

Number of yield excursions directly give the status of damage and represent the severity of ground adverse effects on the structure. Damage corresponding to each yielding is non reversible, therefore, the residual life of the structure can be known. However, such type of results validity may require further investigation.

Cumulative Ductility and Plastic Ductility have close relations [10]

Cumulative ductility is commonly 4 times the plastic ductility due to monotonic loading. Normalized energy at component levels has also a stable quantity [14]. Coefficient of yielding, which is the ration of yield force and the weight has larger value of ductile structure than from the brittle structures [10]. In the lack of sufficient data, the cumulative ductility can be estimated from the ultimate plastic ductility μ_u obtained from monotonic test by $\eta u = \mathbf{4}\ \mu_u$ or more conveniently by $\eta u = \mathbf{3}\ \mu_u$ **for** ductile members and $\frac{\delta_{max}}{\delta_u} \leq 0.7$

where δ_{max} and δ_u are the maximum and ultimate displacement.

Table 5.32: Number of loops, number of yield excursions, and cumulative ductility for three story steel building.

Input Seismic Energy (kNm)	Strain Energy kNm	Hysteretic Energy kNm	Number of Loops	NYEC	Cumulative Ductility
3379.83	51.70	2098.86	2.72	5.00	6
10730.48	89.89	7598.35	4.12	8.00	10
21684.70	142.75	15139.74	4.67	9.30	15
32860.40	333.16	24665.64	3.83	7.66	10

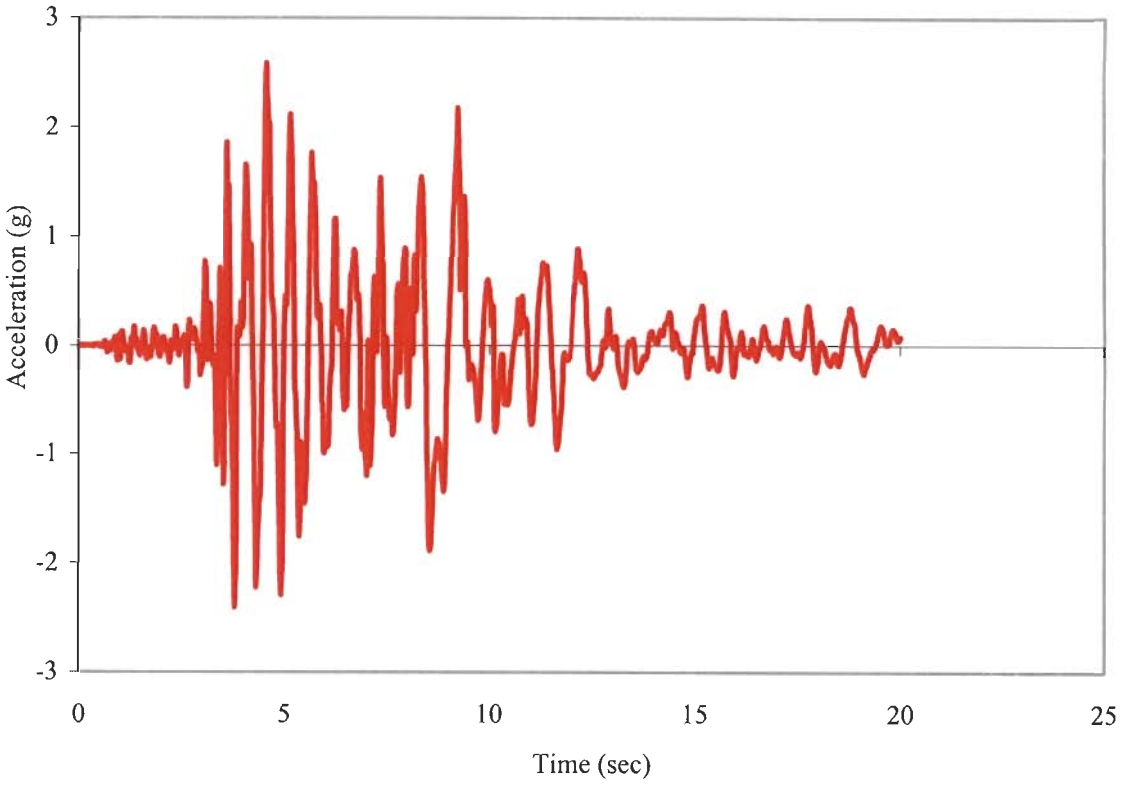

Figure 5.54: Accelerogram of Northridge E-W (0.5165g) with scale factor 5

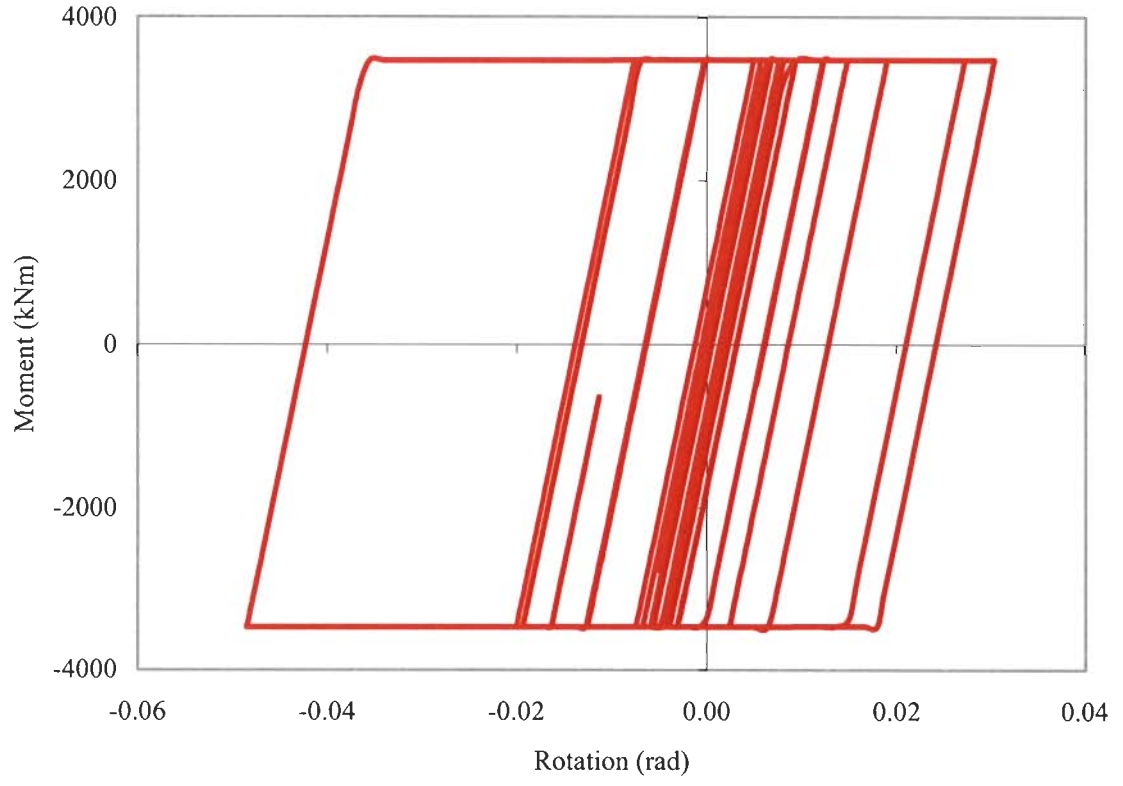

Figure 5.55: Time history of beam one on nine story 2D frame

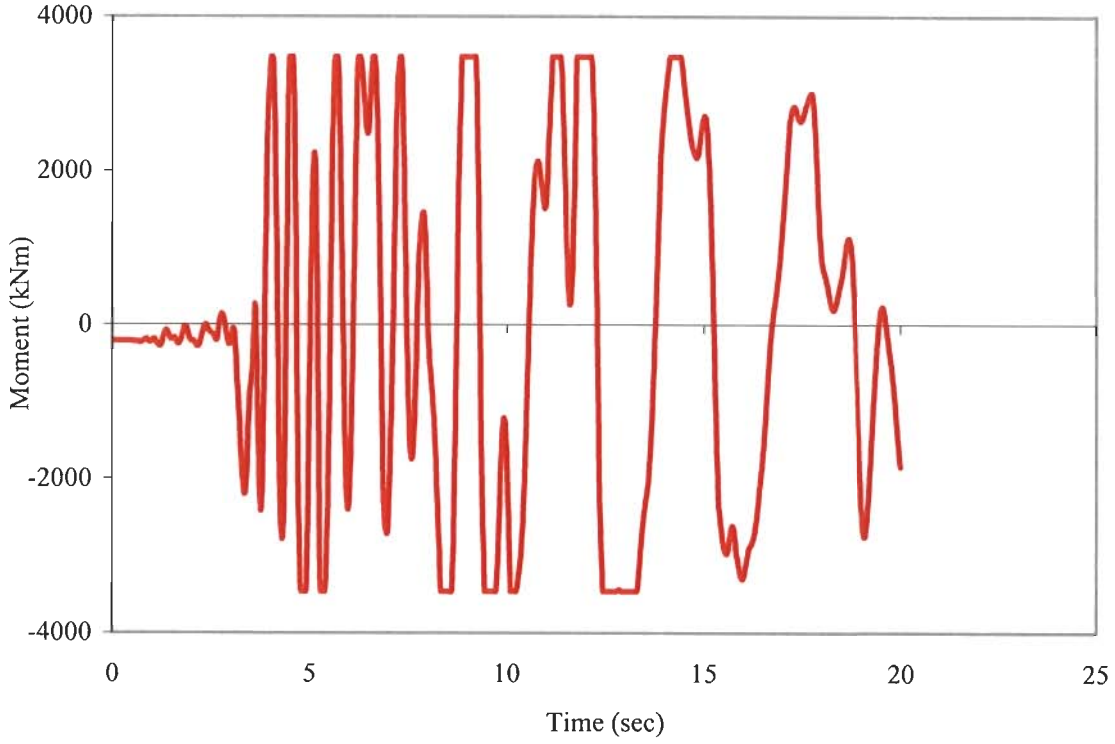

Figure 5.56: Time history of beam two on ground floor of nine story 2D frame

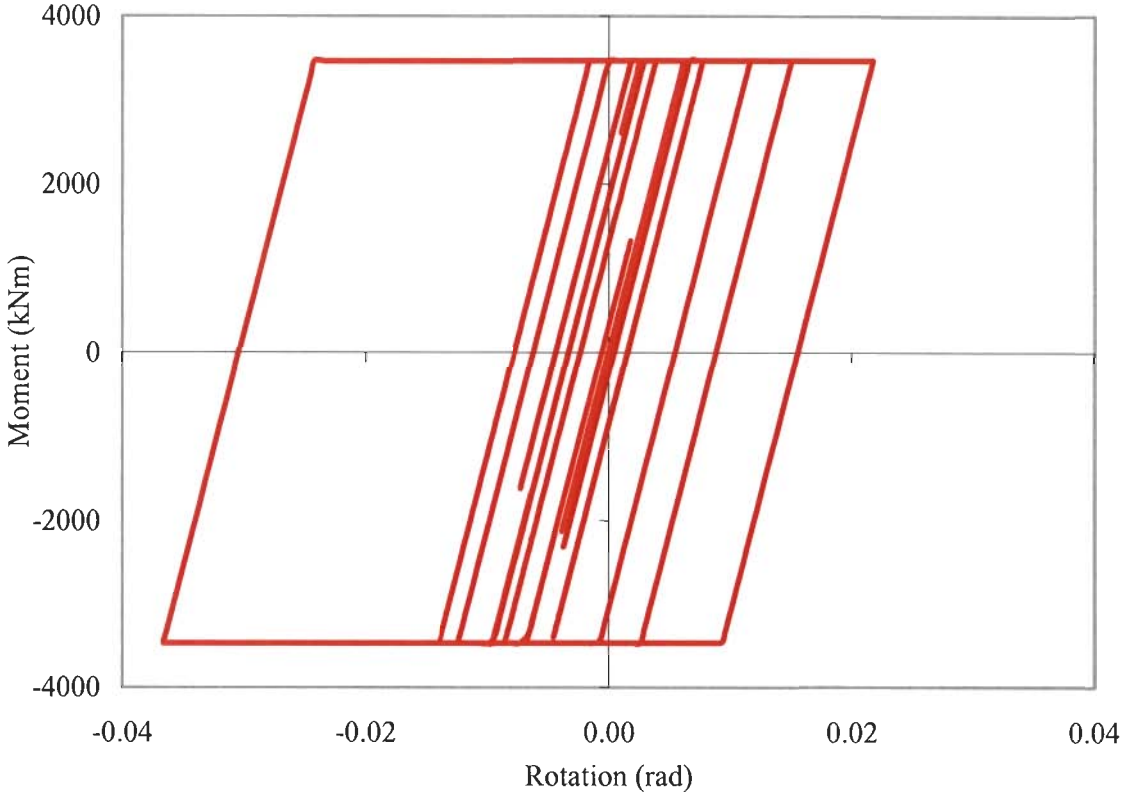

Figure 5.57: Hysteretic loop of beam two on ground floor of nine story 2D frame

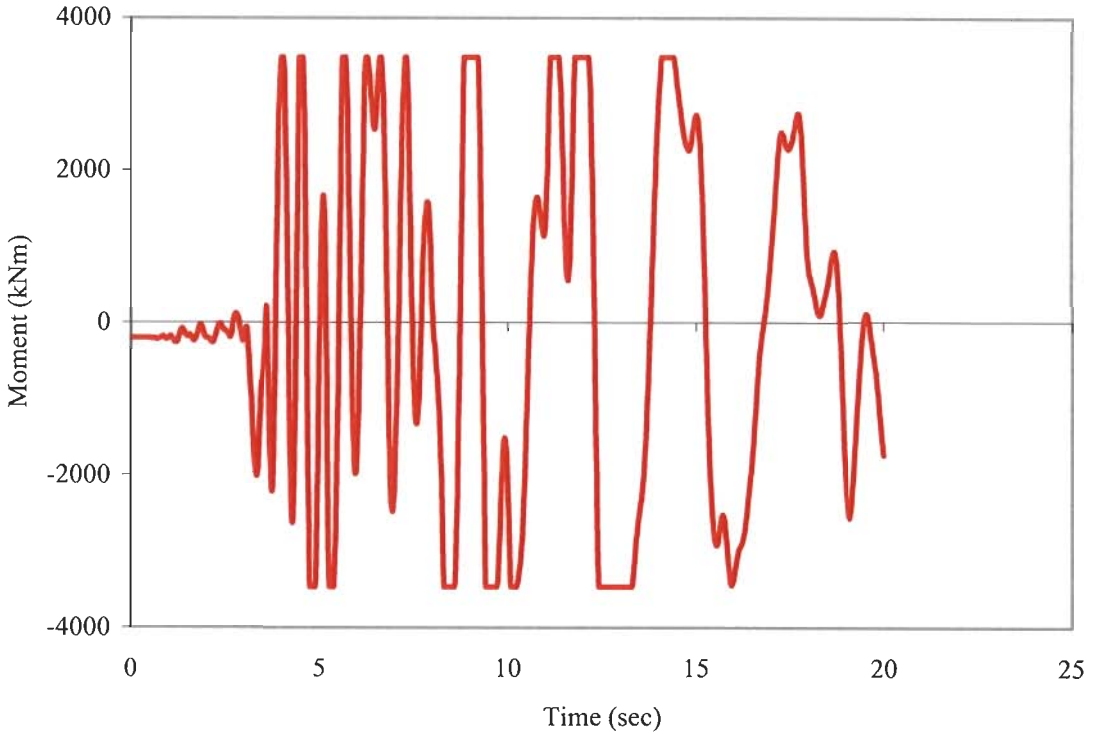

Figure 5.58: Time history of beam three on ground floor of nine story 2D frame

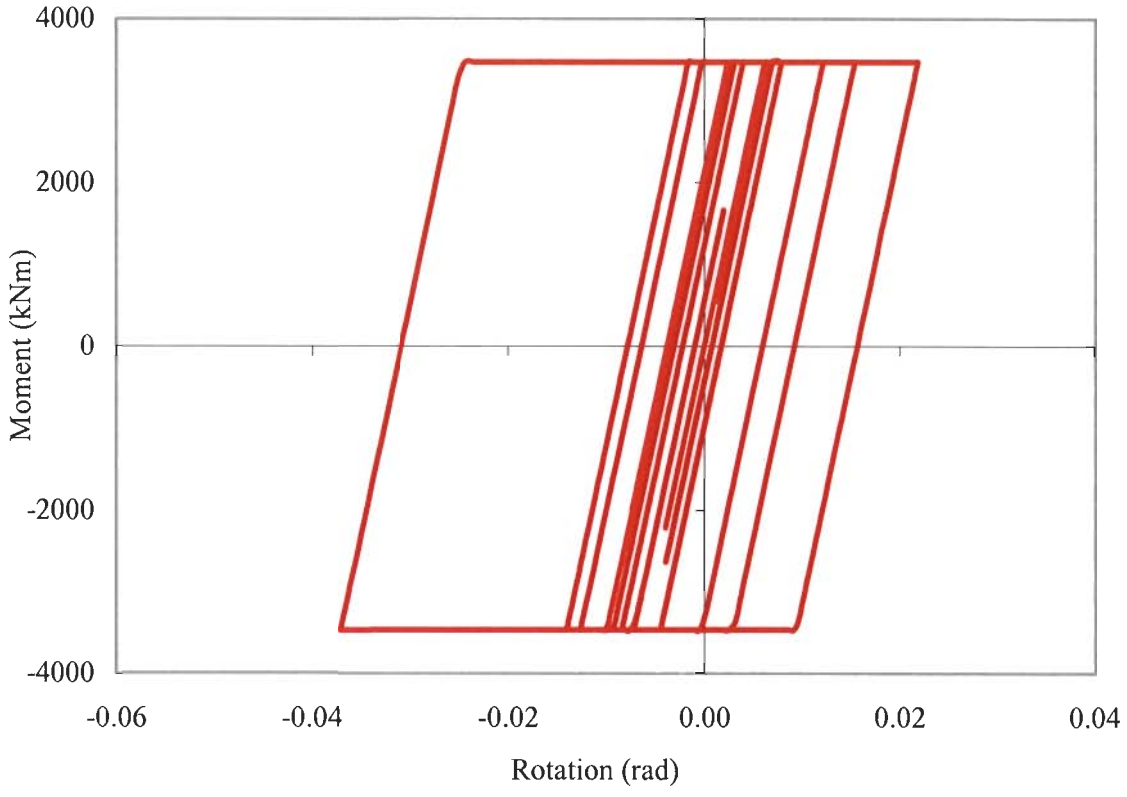

Figure 5.59: Hysteretic loop of beam three on ground floor of nine story 2D frame

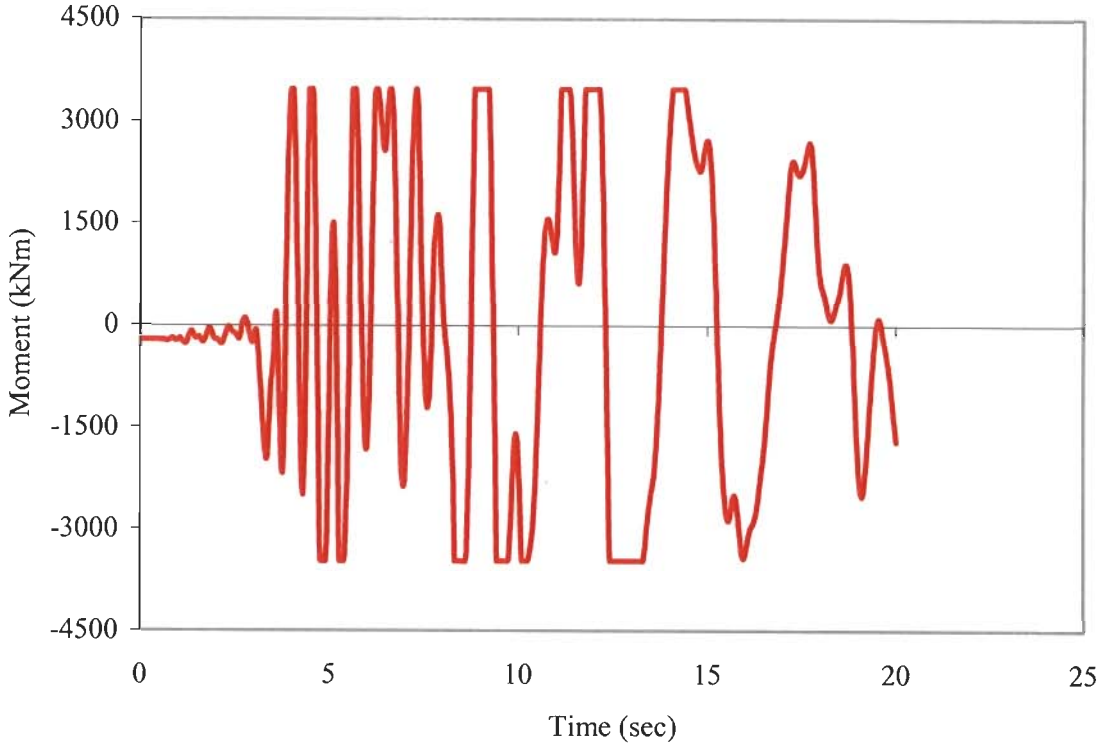

Figure 5.60: Time history of beam fourth on ground floor of nine story 2D frame

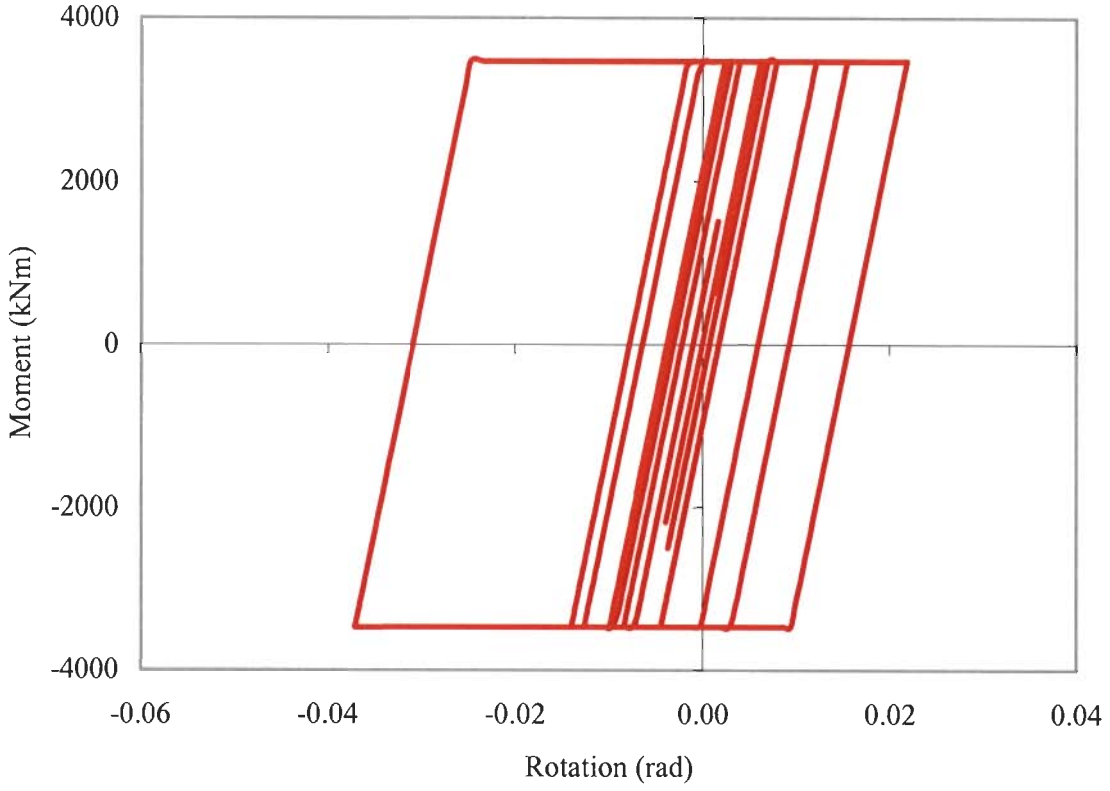

Figure 5.61: Hysteretic loop of beam fourth on ground floor of nine story 2D frame

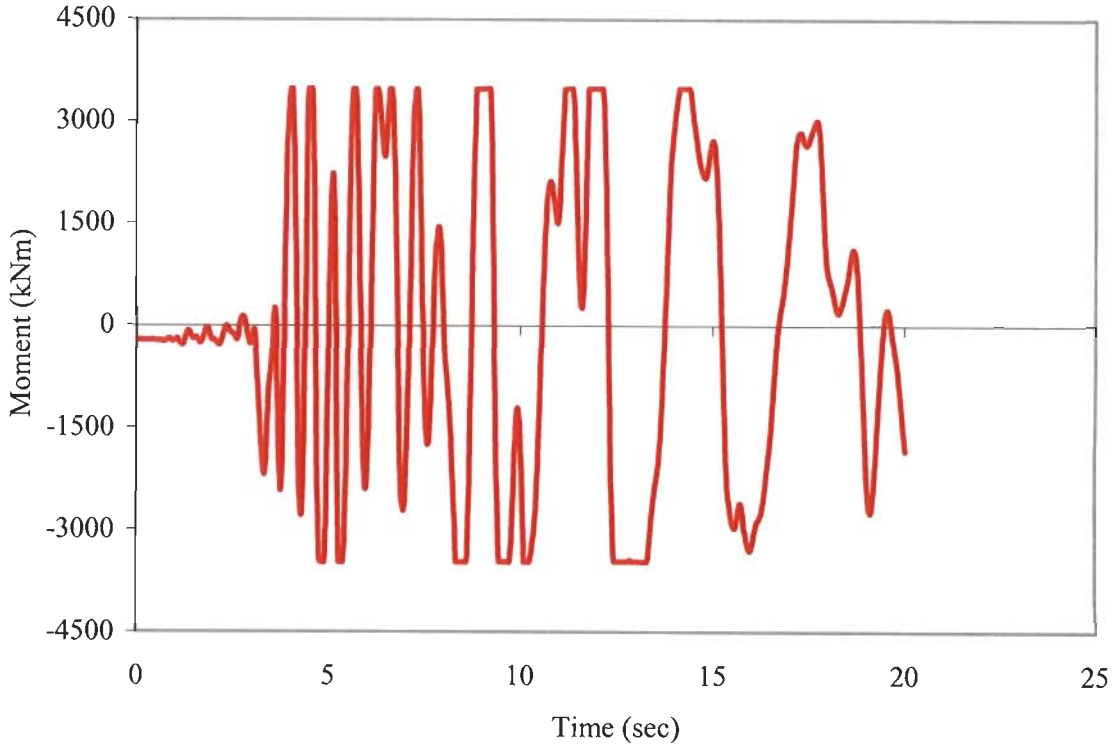

Figure 5.62: Time history of fifth beam on ground floor of nine story 2D frame

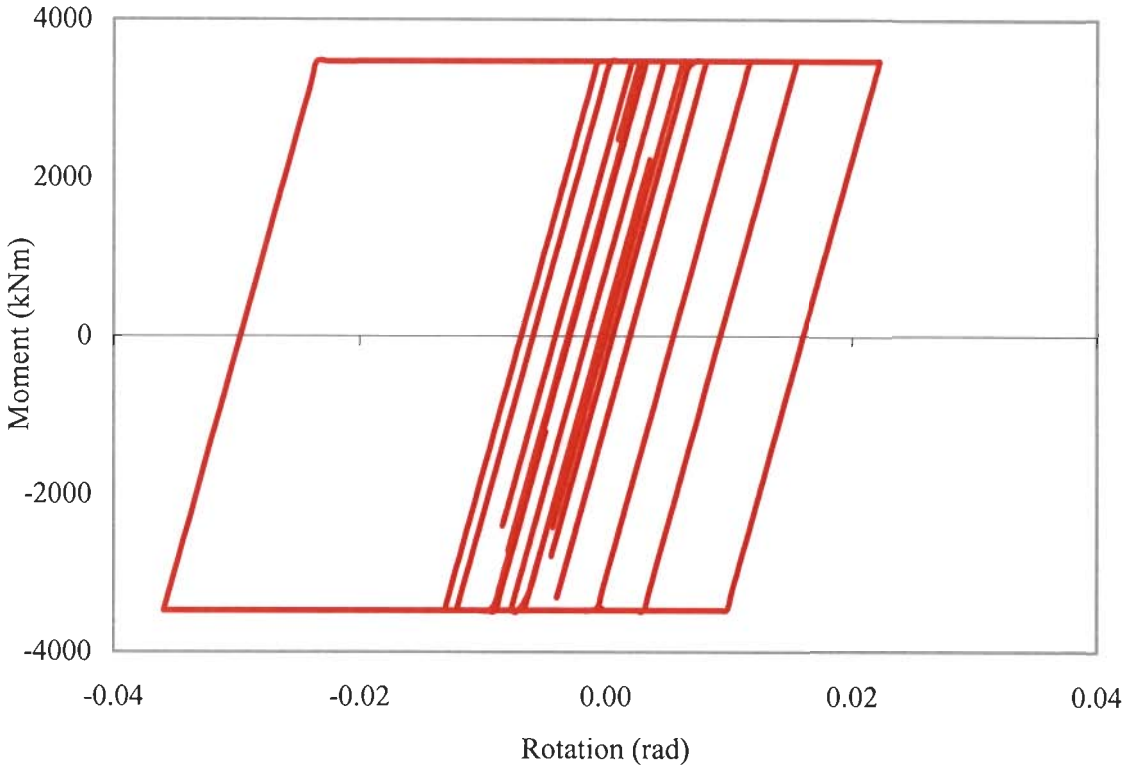

Figure 5.63: Hysteretic loop of fifth beam on ground floor of nine story 2D frame

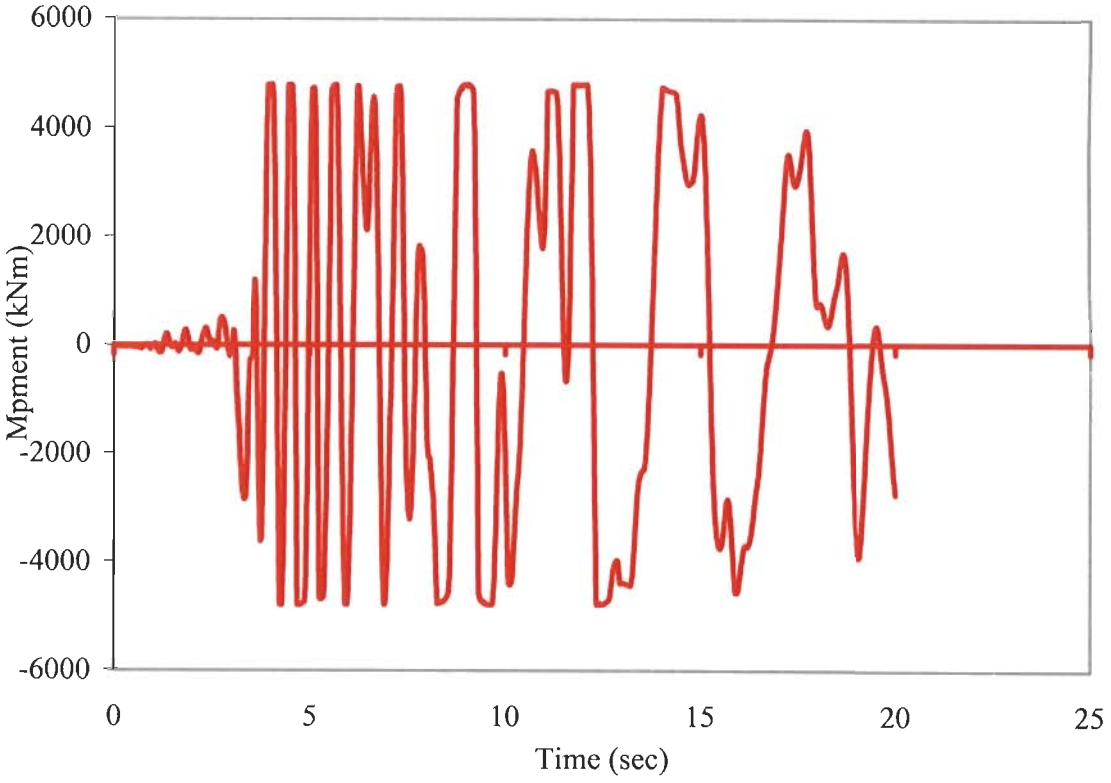

Figure 5.64: Time history of 1st column on ground floor of nine story 2D frame

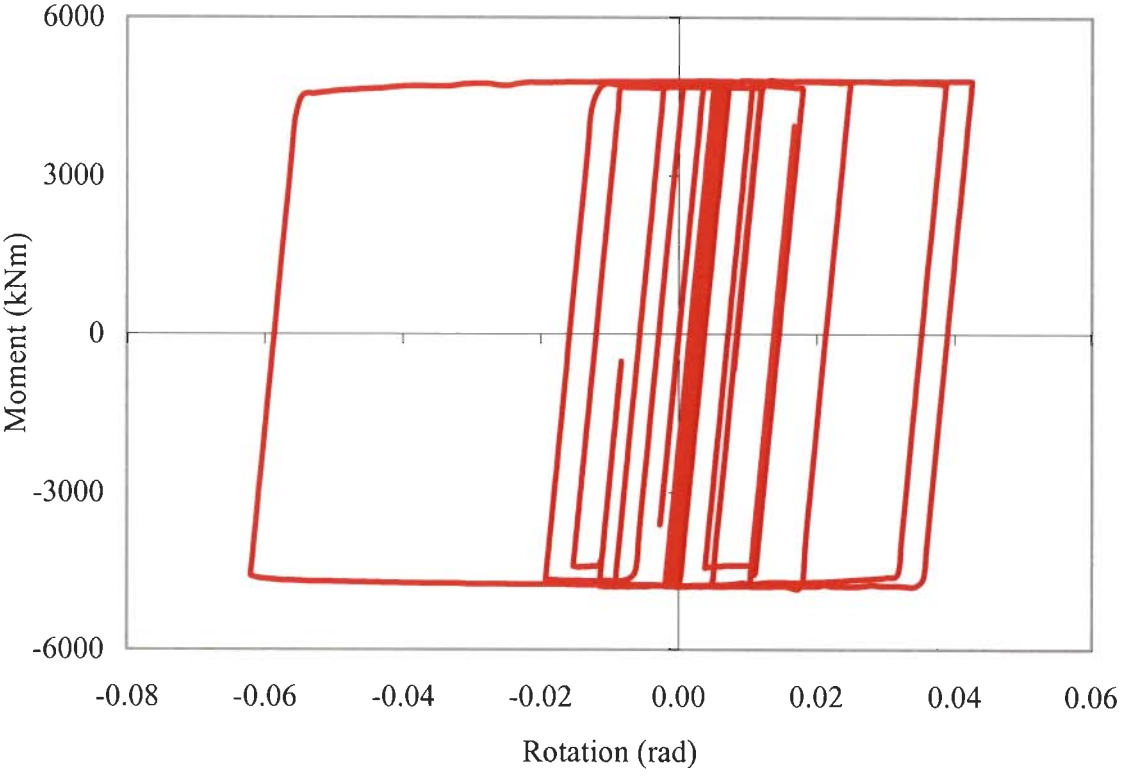

Figure 5.65: Hysteretic loop of 1st column on ground floor of nine story 2D frame

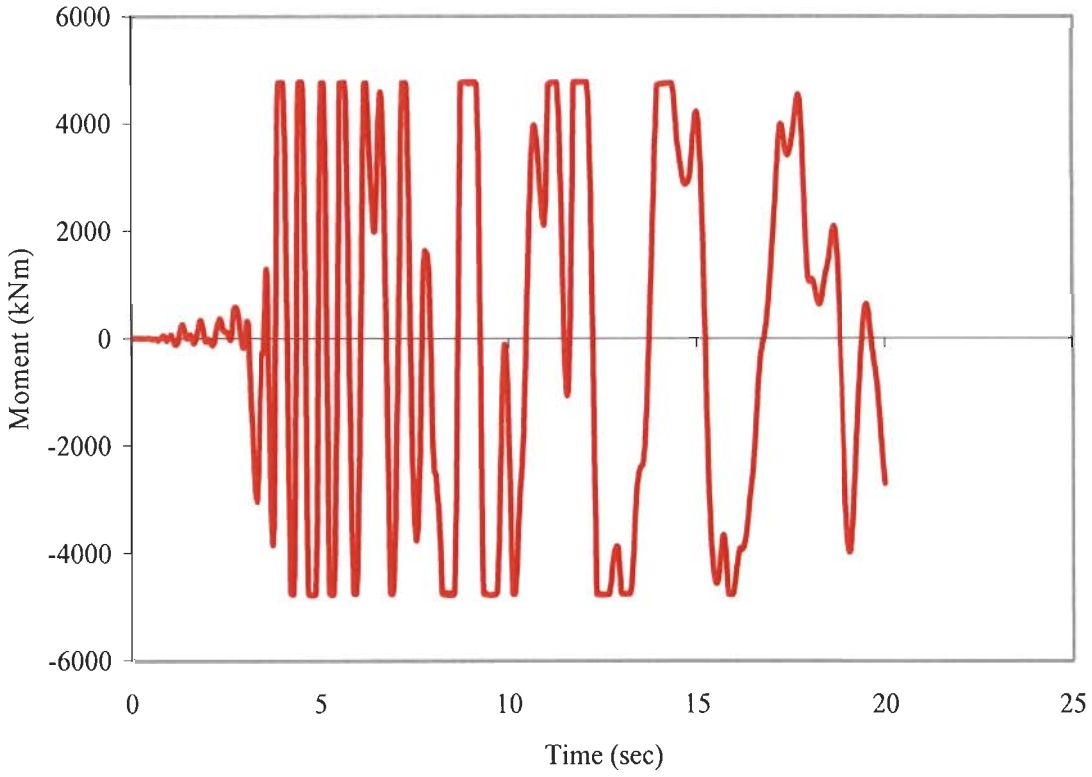

Figure 5.66: Time history of 2nd column on ground floor of nine story 2D frame

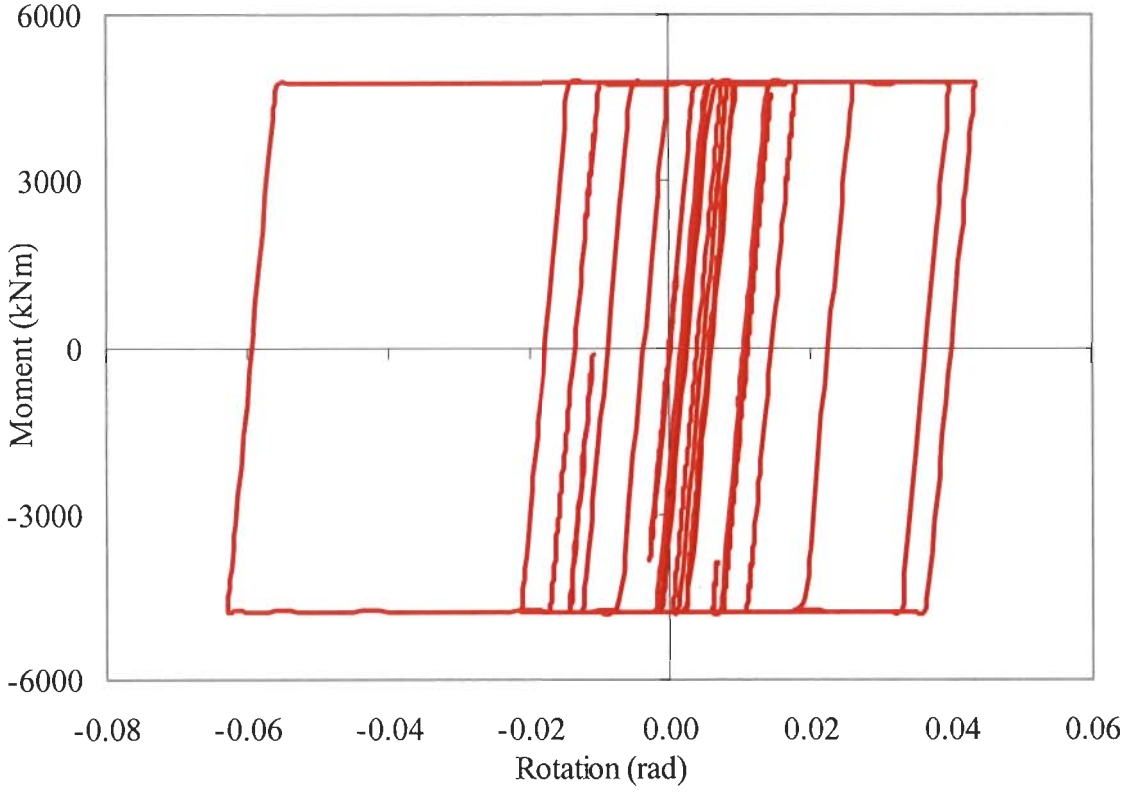

Figure 5.67: Hysteretic loop of 2nd column on ground floor of nine story 2D frame

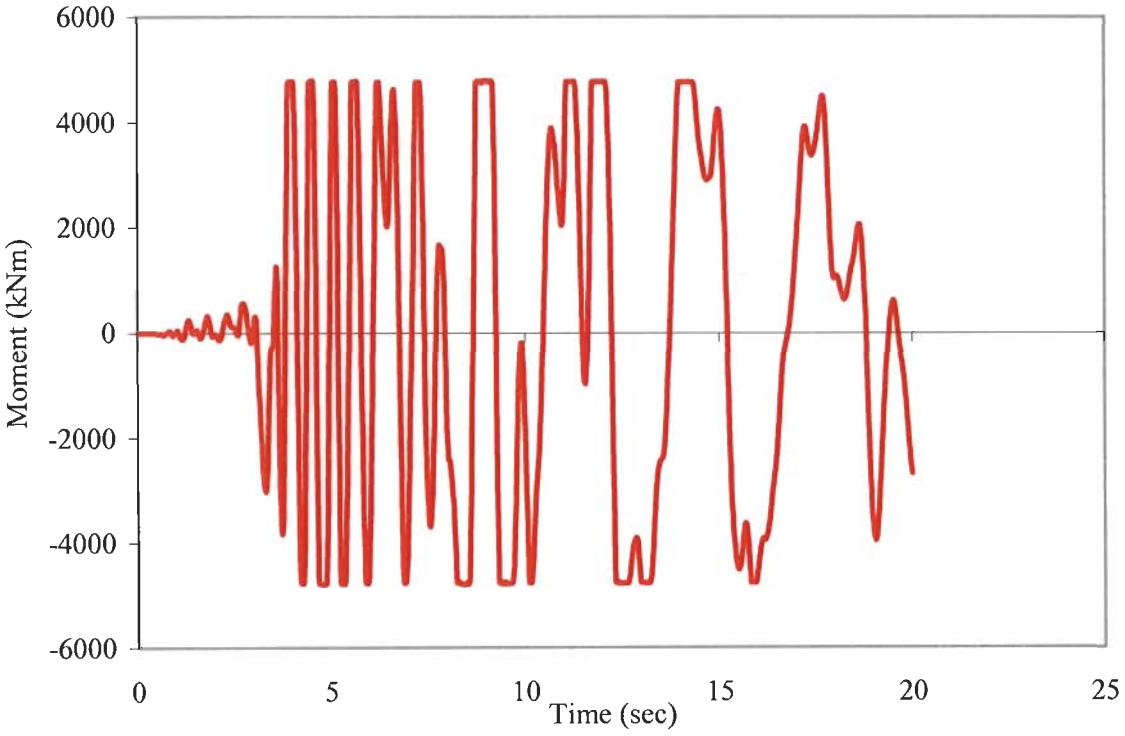

Figure 5.68: Time history of 3rd column on ground floor of nine story 2D frame

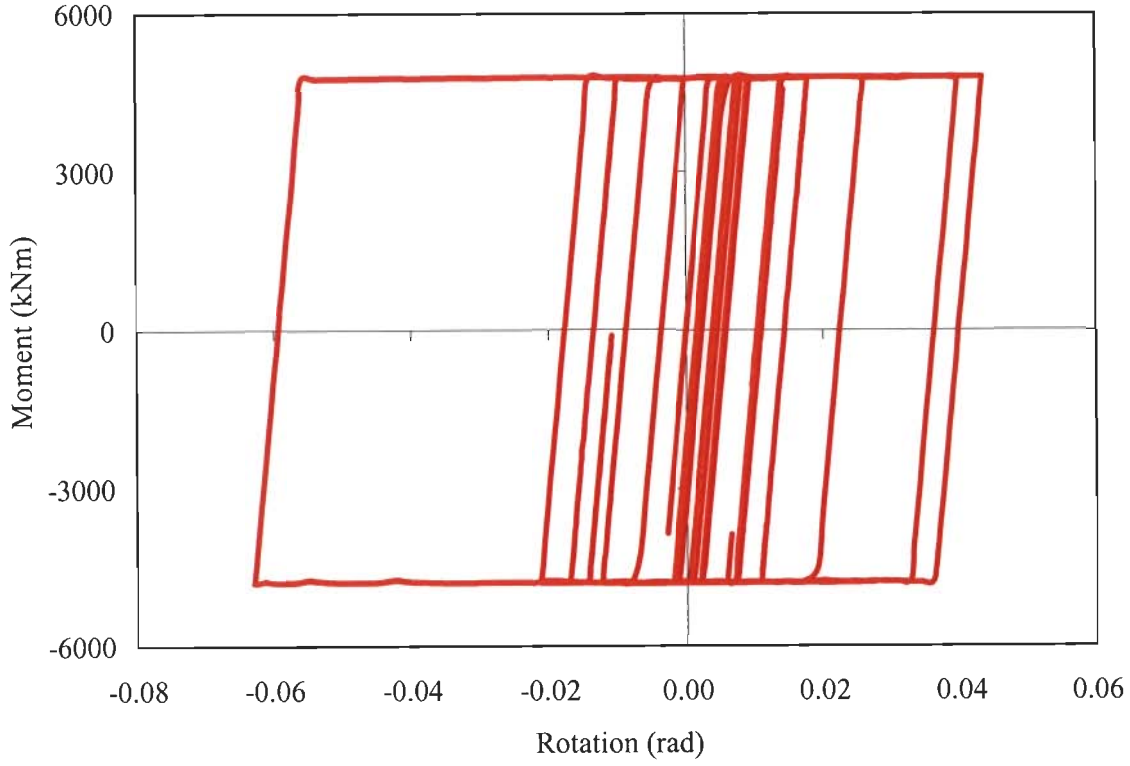

Figure 5.69: Hysteretic loop of 3rd column on ground floor of nine story 2D frame

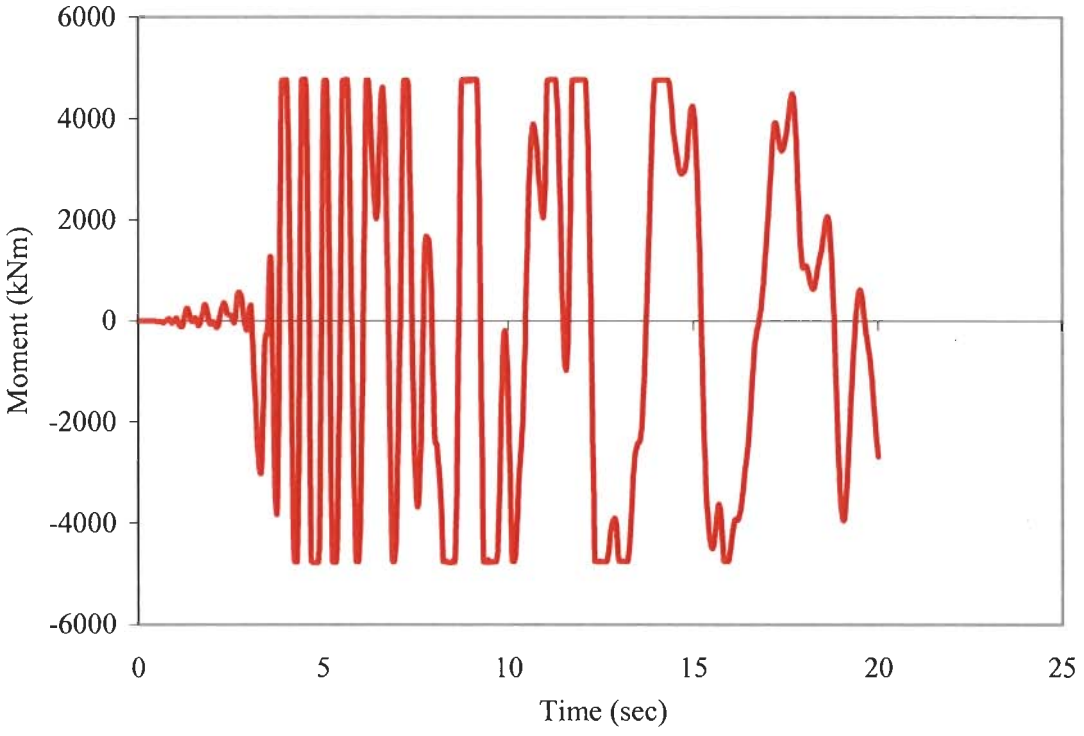

Figure 5.70: Time history of 4th column on ground floor of nine story 2D frame

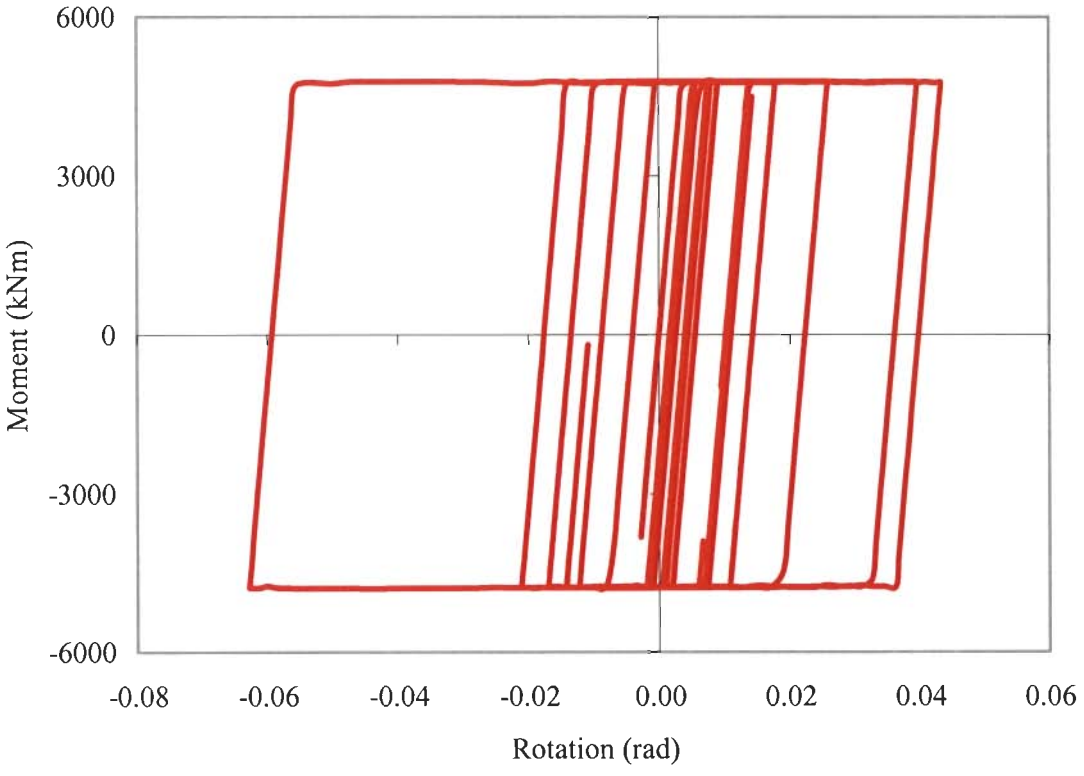

Figure 5.71: Hysteretic loop of 4th column on ground floor of nine story 2D frame

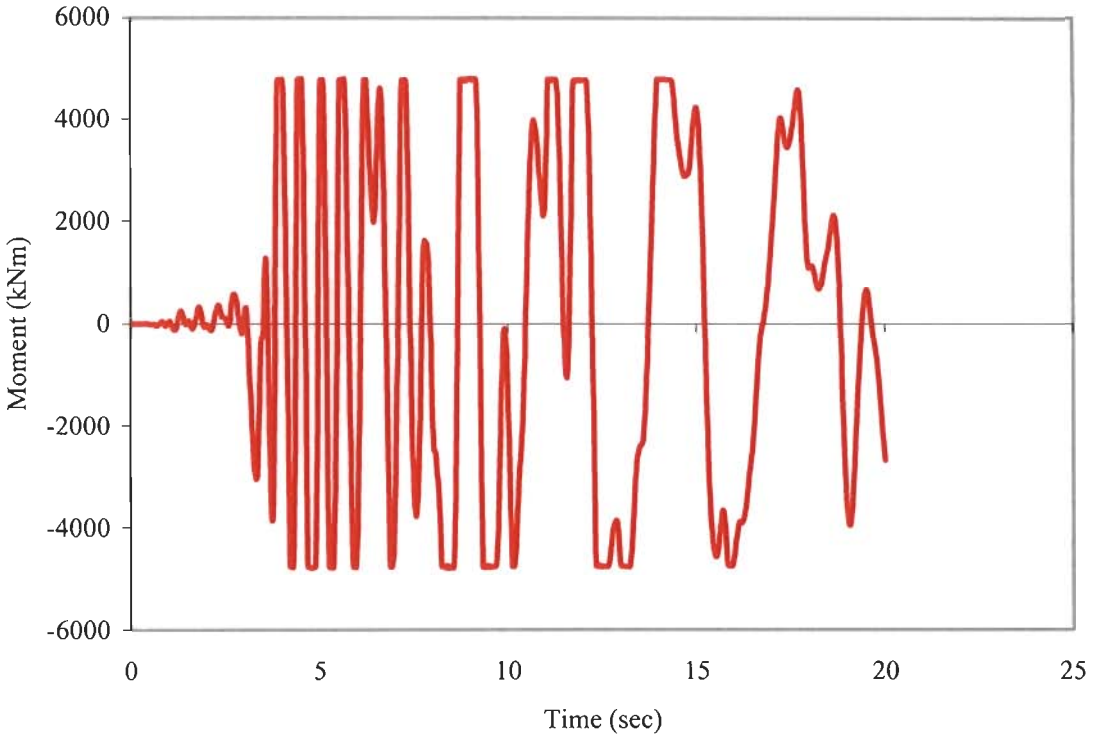

Figure 5.72: Time history of 5th column on ground floor of nine story 2D frame

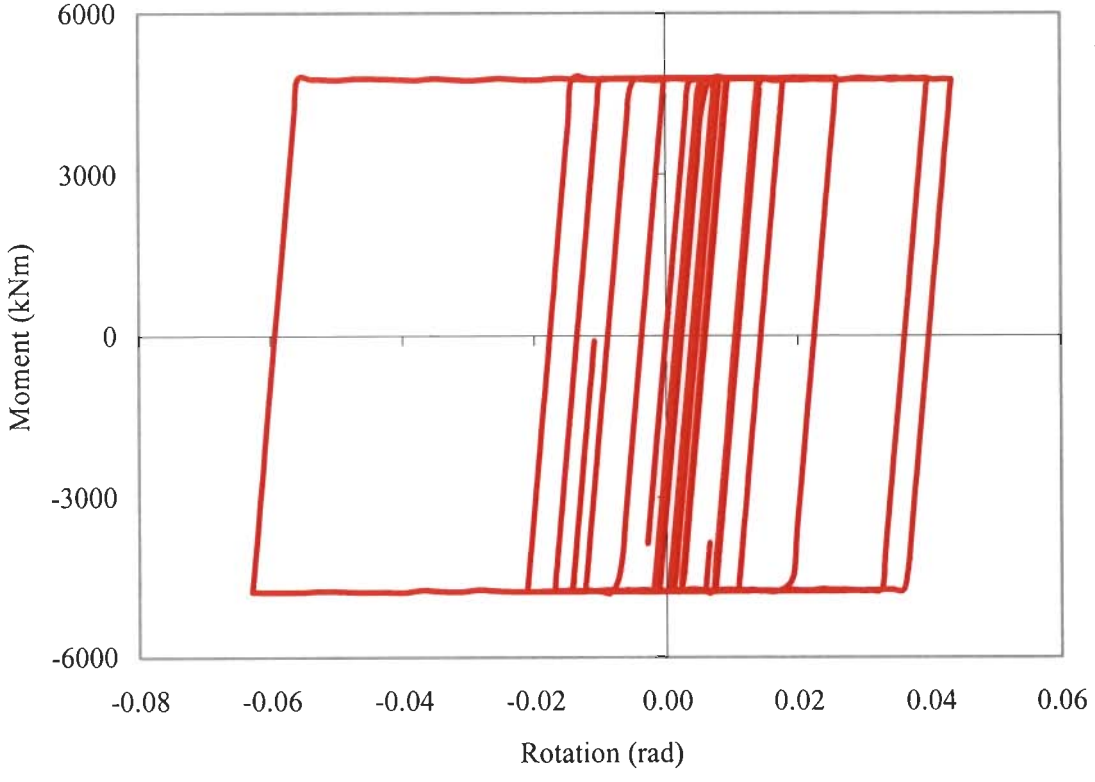

Figure 5.73: Hysteretic loop of 5th column on ground floor of nine story 2D frame

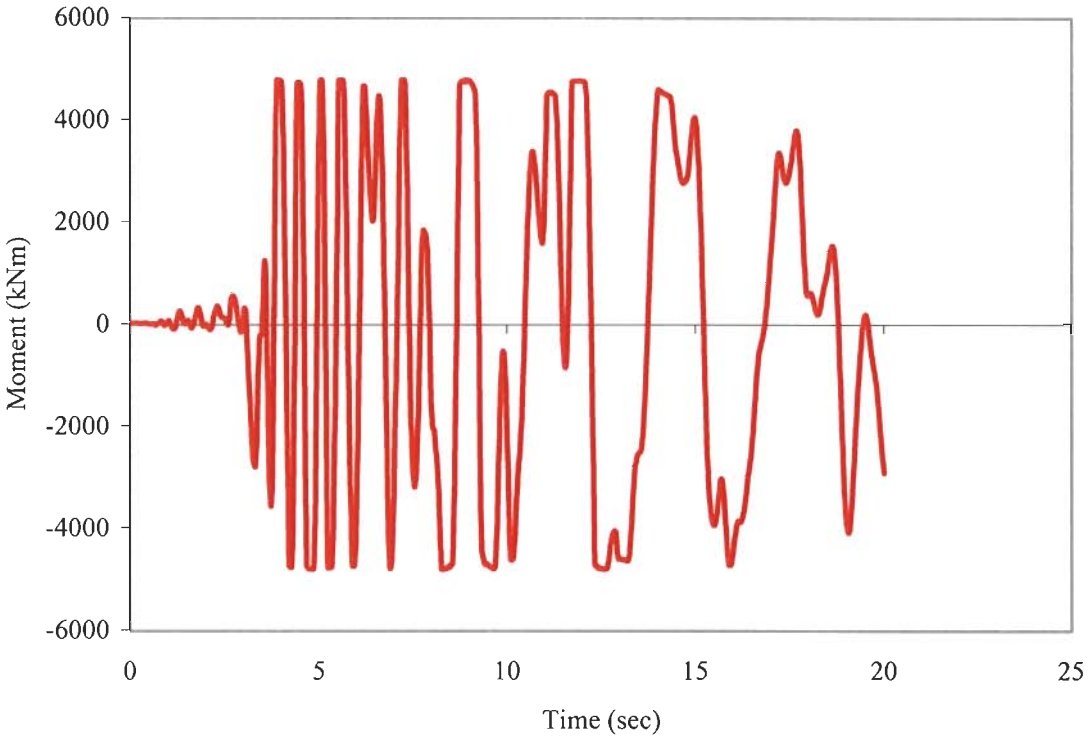

Figure 5.74: Time history of 6th column on ground floor of nine story 2D frame

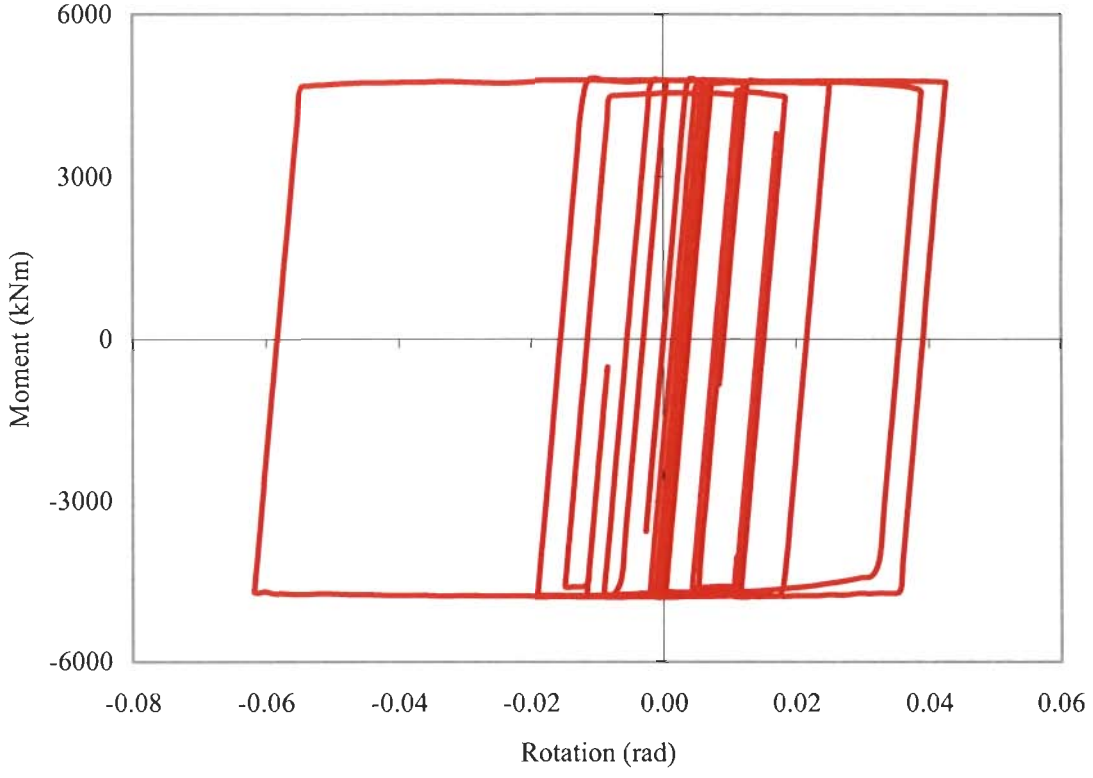

Figure 5.75: Hysteretic loop of 6th column on ground floor of nine story 2D frame

Table 5.33: Hysteretic energy, number of loops, NYEC, and cumulative ductility for nine story framework.

Sl .No	$E_{H\xi}$	E_S	No. of loops	NYEC (Theoretical)	NYEC (Experimental)	Ratio of Experimental and (Theoretical)	Cumulative ductility
01	1632.78	18.80	6.1	13	18	1.385	21
02	999.2	17.18	7	15	17	1.133	28
03	1051.5	16.5	6.3	13	18	1.385	21

5.9 Nonlinear Analysis of Critical Sections

Few critical beam and column components were identified. Sections of the identified components were modeled using Section Builders. From time history analysis of these components maximum moment, maximum shear, maximum pull or push were noted down and were applied to the modeled cross section in Section Builder. After analysis, the corresponding sections were investigated for their linear and nonlinear behavior.

5.9.1 Result Discussions

Figures 5.76 to 5.83 have been plotted for the response of cross sections of beam and column sections used for investigation of performance objectives in this study. These information's at the cross section levels reveal the relationship of the behavior under the seismic loading to the member characteristics at component levels. In order to check the progressive failure, this is likely under reversal of structures during severe earthquake ground motions. Figure 5.83 represents the cross section normal stresses of beam due to bending moment. The information's during the investigations for the loading under seismic action on the building frames are clear enough for performance objectives assessment since it is the point where from failure starts. Number of yield excursions for the critical members analyzed for cross section behavior is accordingly high.

Future Recommendations: Progressive failure at the cross sections are likely due to stresses developing randomly as happens during reversal of stresses due severe earthquake loading The study reveals the trend of deterioration of the cross section resistance. However, such kind of the issues needs further investigation if possible experimental demonstration through varying sections or loadings for getting more and more inside of such kind of behavior of cross section.

Critical sections behavior of beam and column sections on the ground floor of nine story frame for hysteretic energy = 999.2 kNm for beam and hysteretic energy = 1682 kNm for external and internal columns sections. The cross section of beam is $W_{920x238}$, external section is $W_{360x551}$ and internal column is $W_{360x744}$.

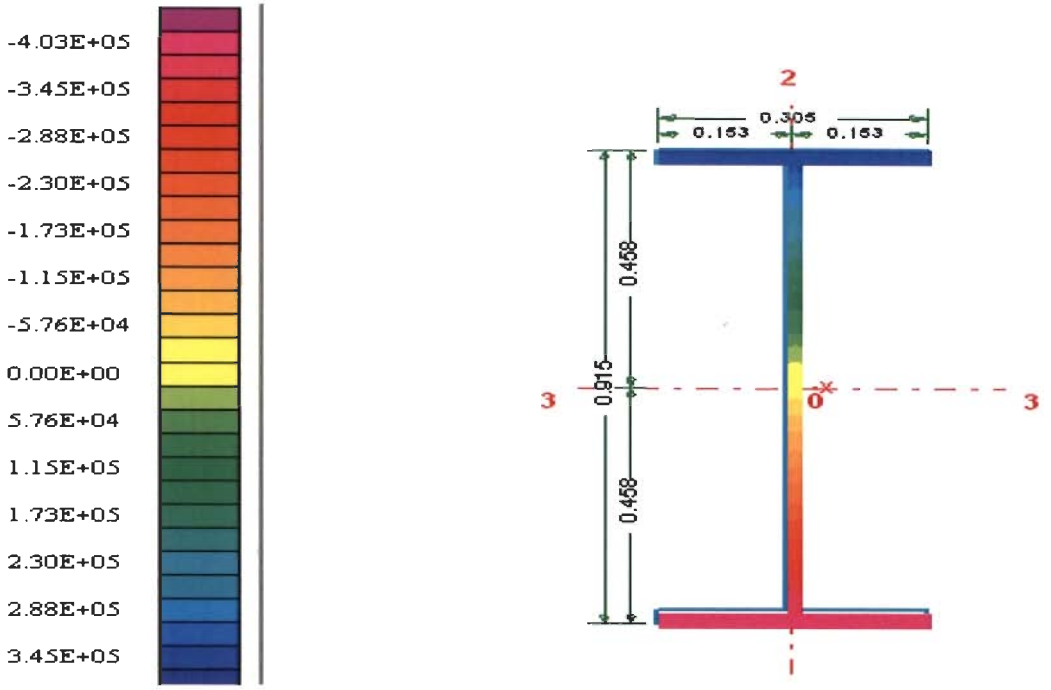

Figure 5.76: Normal stresses for beam on first floor of nine story frame $W_{920x238}$, Maximum moment =3483 kNm (Time history analysis)

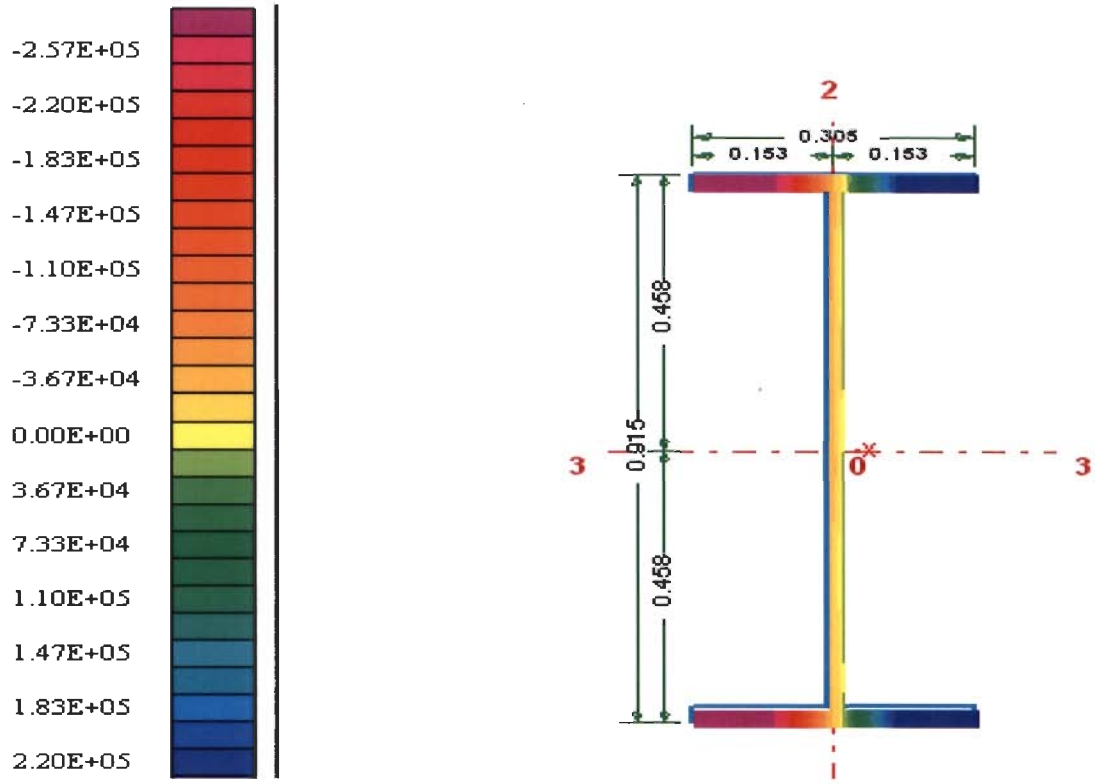

Figure 5.77: Crack section stress axial stress for beam on first floor of nine story frame

$W_{920x238}$, Maximum moment =3483 kNm

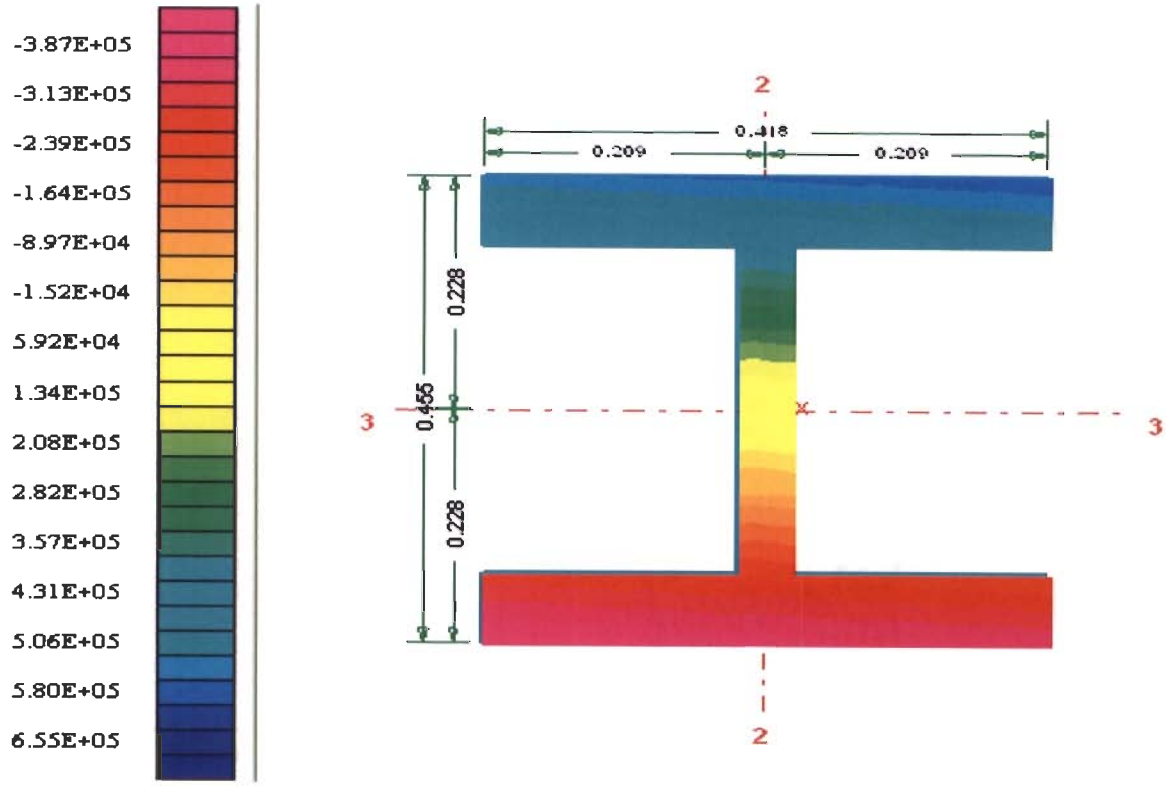

Figure 5.78: Axial stress for external column on first floor of nine story frame$W_{360x551}$, Maximum moment =4795 kNm, Minimum M =106.5 kNm Axial force = 8528 kN

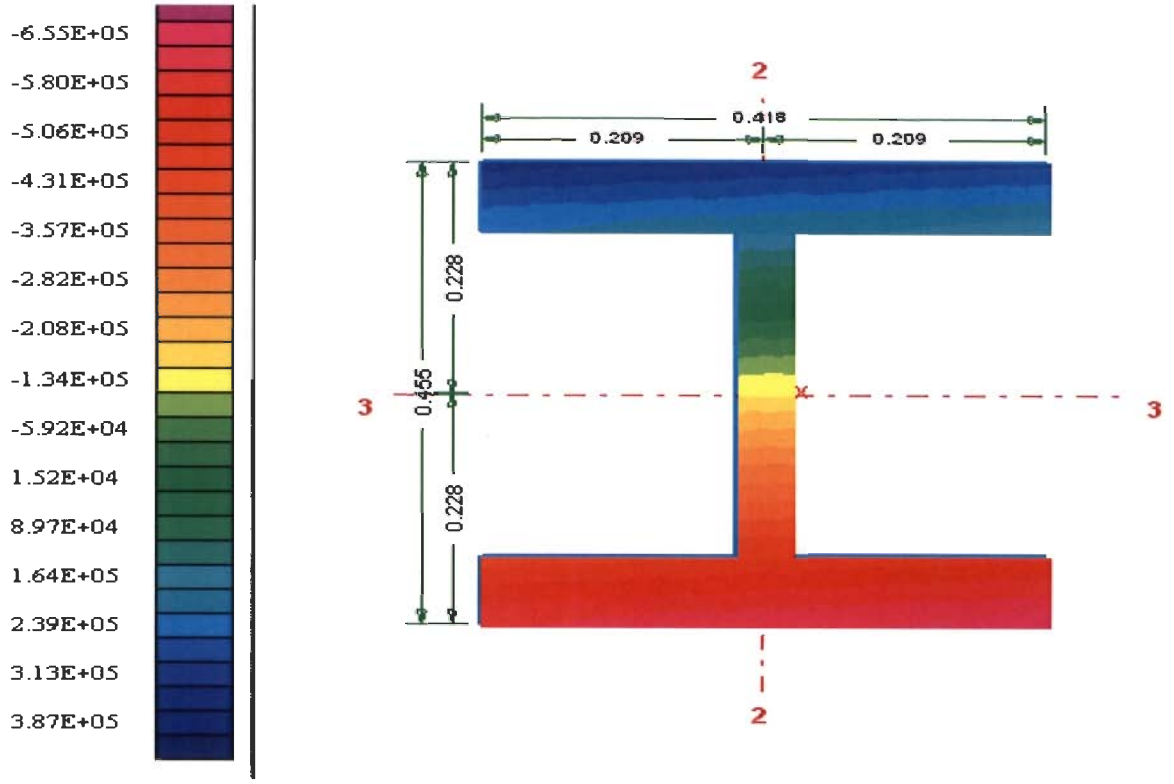

Figure 5.79: Normal stress for external column on first floor of nine story frame $W_{360x551}$, Maximum moment =4795 kNm, Minimum Moment =106.5 kNm Axial force = 8528 kN

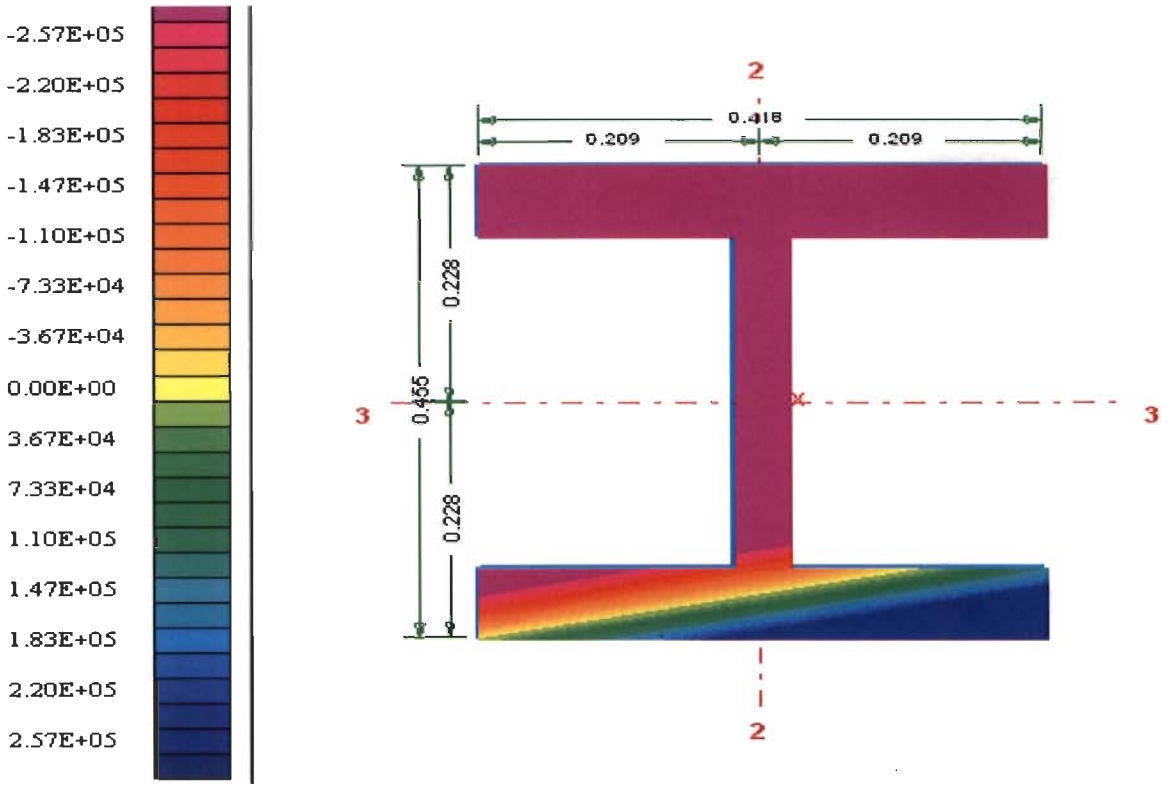

Figure 5.80: Normal stress for external column on first floor of nine story frame $W_{360x551}$, Maximum moment =4795 kNm, Minimum Moment =106.5 kNm Axial force = 8528 kN

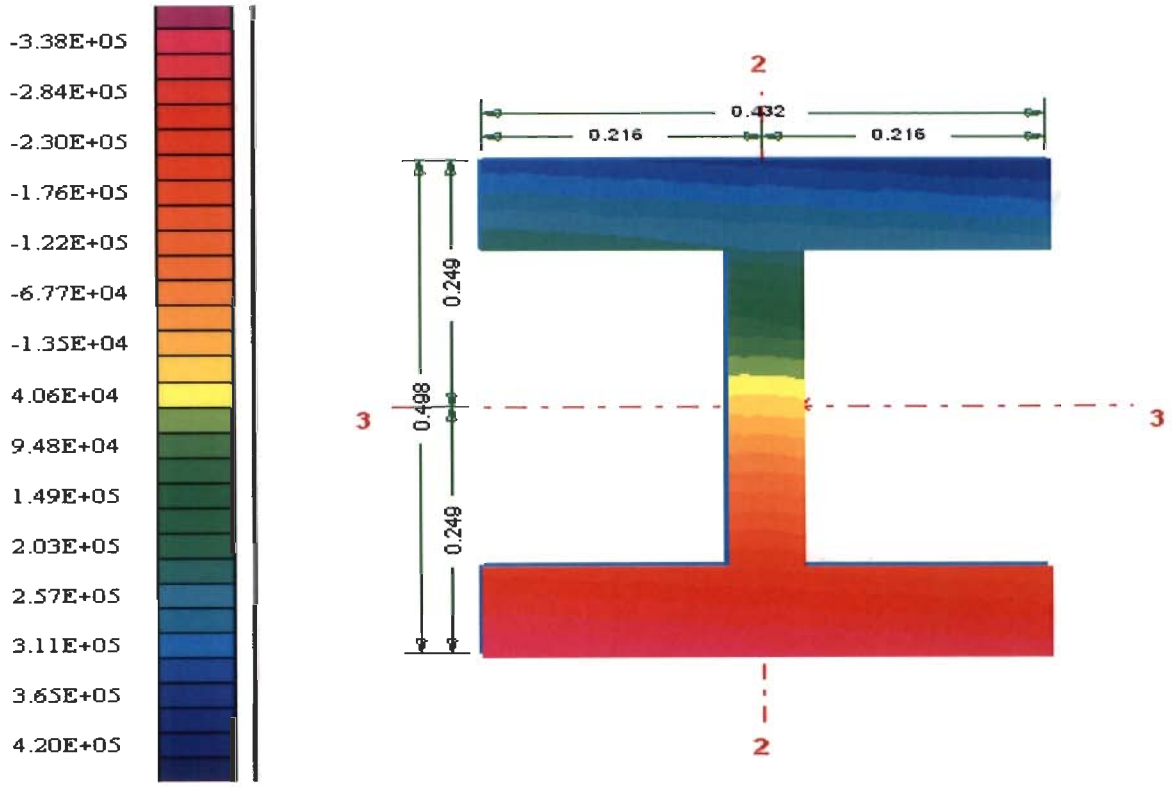

Figure 5.81: Cracked section - stress for internal column on first floor of nine story frame W360x744, Maximum moment =4795, Minimum M =106.5 kNm, Axial force = 3500 kN

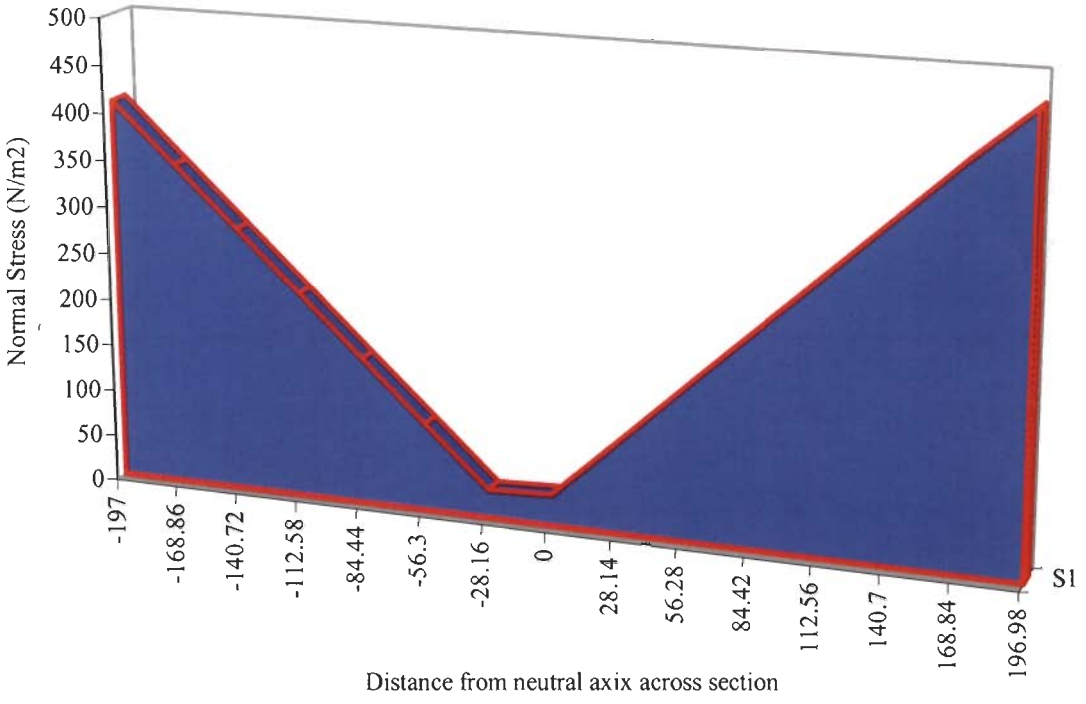

Figure 5.82: Normal stress distributions along depth of the column section $W_{360x551}$ of three story 3D

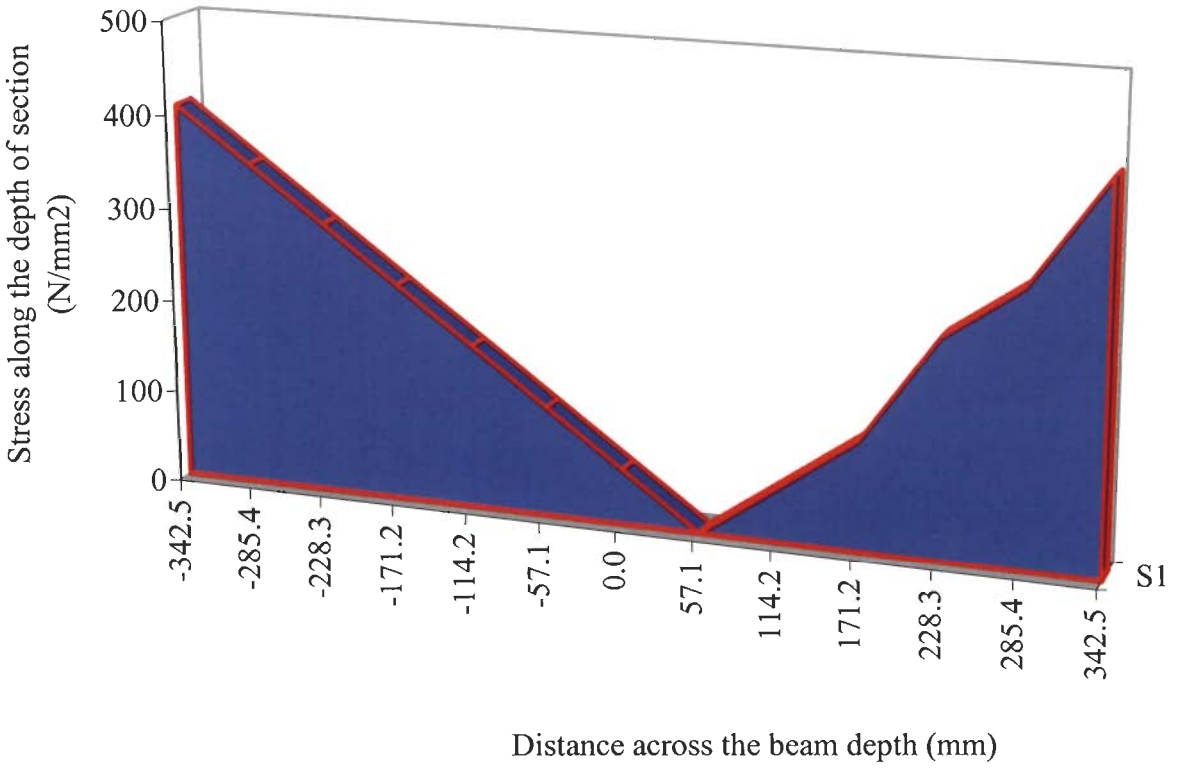

Figure 5.83: Normal stress distributions along depth of the beam section $W_{590x140}$ of three story 3D frame

5.10 Usage Ratio

5.10.1 Usage Ratio at Component Levels

Usage ratio is the ratio of demand and capacity. RAM Perform 3D [17] calculates the value using the limit states extension as per the constraints of performance objectives. A series of frames analyzed for input seismic energy and corresponding distribution of energy. The response parameters are employed for estimating demand and capacity simultaneously. Limit states of deformations are used for executing the demand and capacity at component levels. The results are used in the ratio of demand and capacity, which is known as usage ration at component level. For performance requirement the. ratio must be less than one, otherwise, redesign is carried till the ratio does not become less than one. Many times it has been found economical to find the ration using many components

5.10.2 Usage Ration at Global Level

Using the combination principle and normalization procedures, RAM Perform 3D has the option for evaluating the usage ration at structure level using the limit states.

Figures (5.85 to 5.91) have been plotted for the demand capacity ratio (usage ratio) for the three story 3D building frame under the varying earthquake ground motions. The building frames have been modeled at component levels by giving their individual identification number. The advantages of such numbering are that performance levels of individual members can be known through the response analysis. Any damage concentration is easy to identify. For fail safe design, some components are allowed to yield severely, however, with the intention to take full capacity without articulation of collapse procedures.

The aim of the usage ratio is to diagnose the actual capacity demand ratio so that performance of the particular components may be given in a format.

5.10.3 Result Discussion for the Usage Ratio

The main objectives of performance based seismic design are to incorporate limit states design since extension of limit states in terms of energy parameters provide a stable analysis tool. Perform 3D analysis automates the results through the combination of limit states in terms of usage ratio. Variation of usage ratio for the components of the building frames are clearly shown in the figures from 5.84 to 5.90. The analysis results of this building frame has been used for energy based evaluation for damage indices as well as for the capacity curve formulation as an analytical tool as the content of this study. A well behaved in formations: pushover curve, floor spectra, drift, hysteretic loop, time history results, along with the cross section response at the critical sections reveal consistency in between the conventional performance based seismic design procedures and the energy based response parameters.

Conclusions

Usage ratio since is based on the capacity, demand and takes care of the extension of limit states, which conveys the performance of the structure during varying seismic demand into the format of performance, based seismic design. Therefore, usage ratio is an effective response tool for the further new development.

Recommendations

Checking performance through usage ratio further requires to be clubbed with the degrading mechanical characteristics through explicit expression. Validity of such index must be investigated through experimental programs.

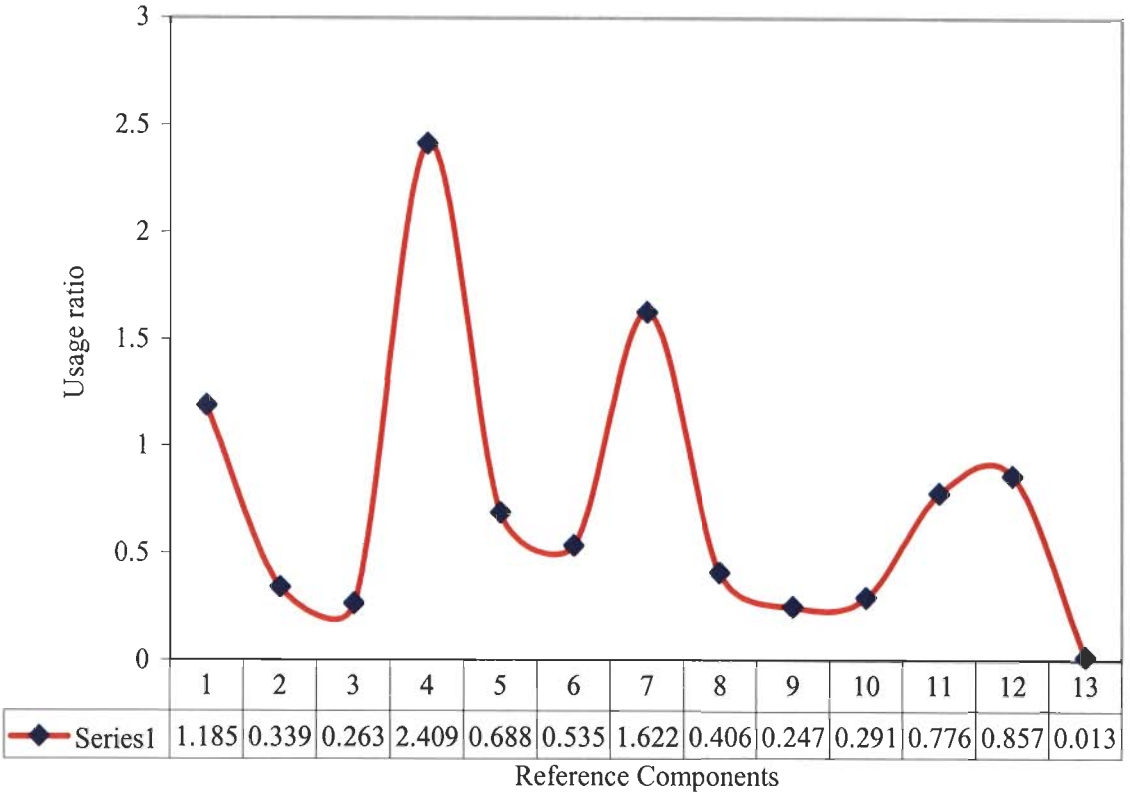

Figure 5.84: Usage ratios for 3story 3D frame under Northridge E-W (0.5165g)

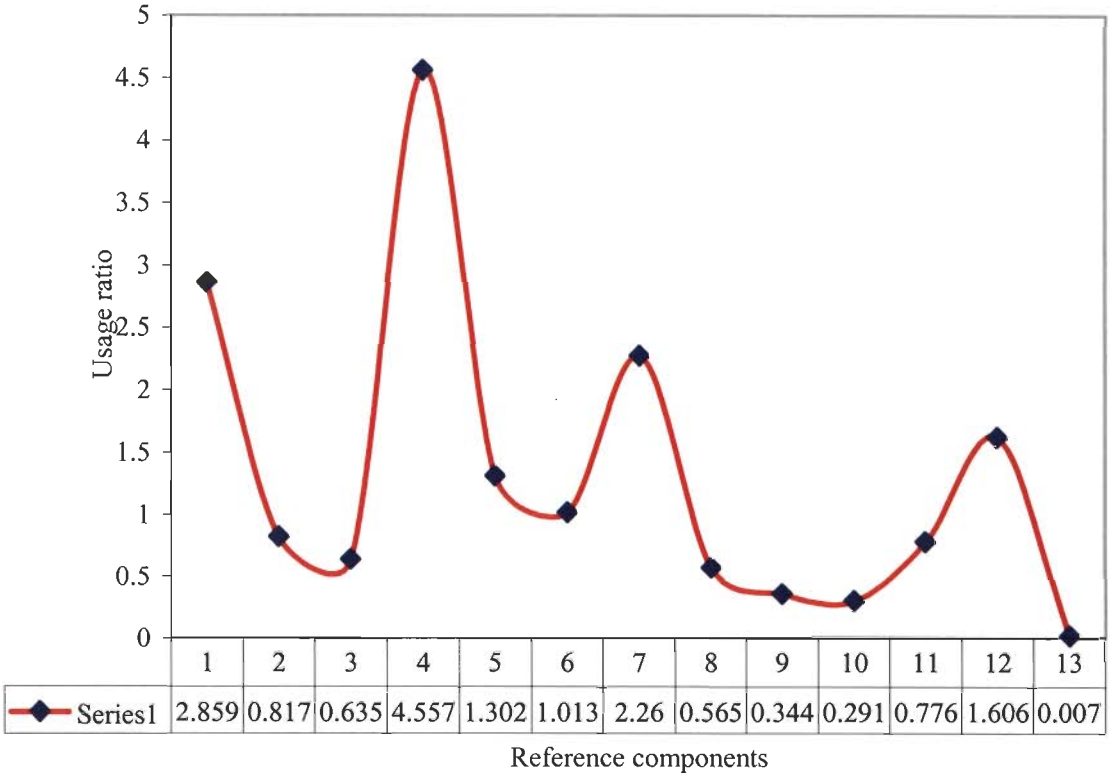

Figure 5.85: Usage ratios for 3story 3D frame under Northridge E-W (2x0.5165g)

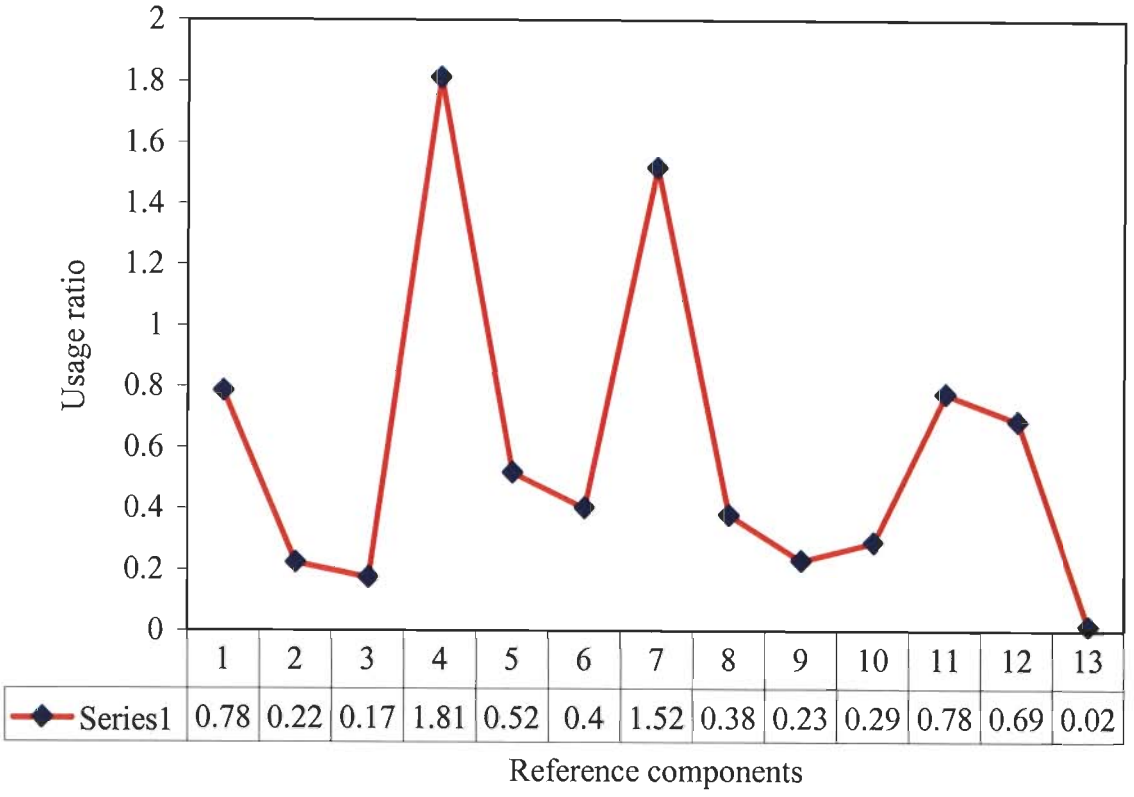

Fi

gure 5.86: Usage ratios for 3story 3D frame under Northridge N-S (0.4158g)

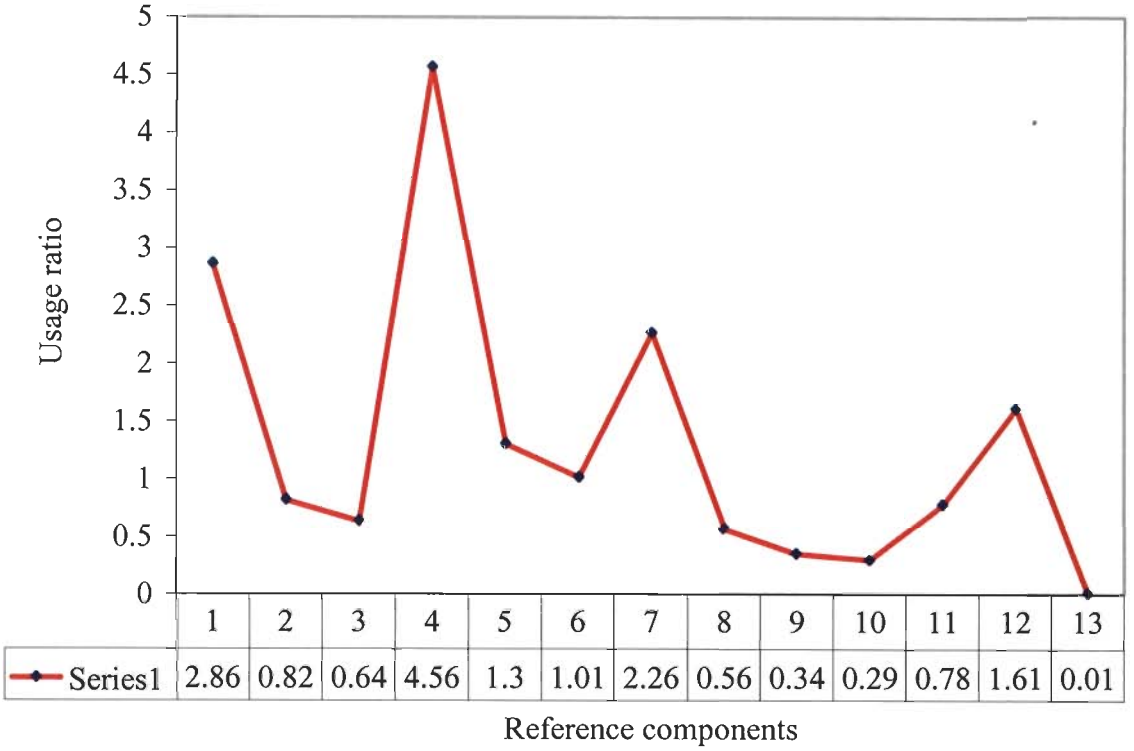

Figure 5.87: Usage ratios for 3story 3D frame under Northridge N-S (2x0.4158g)

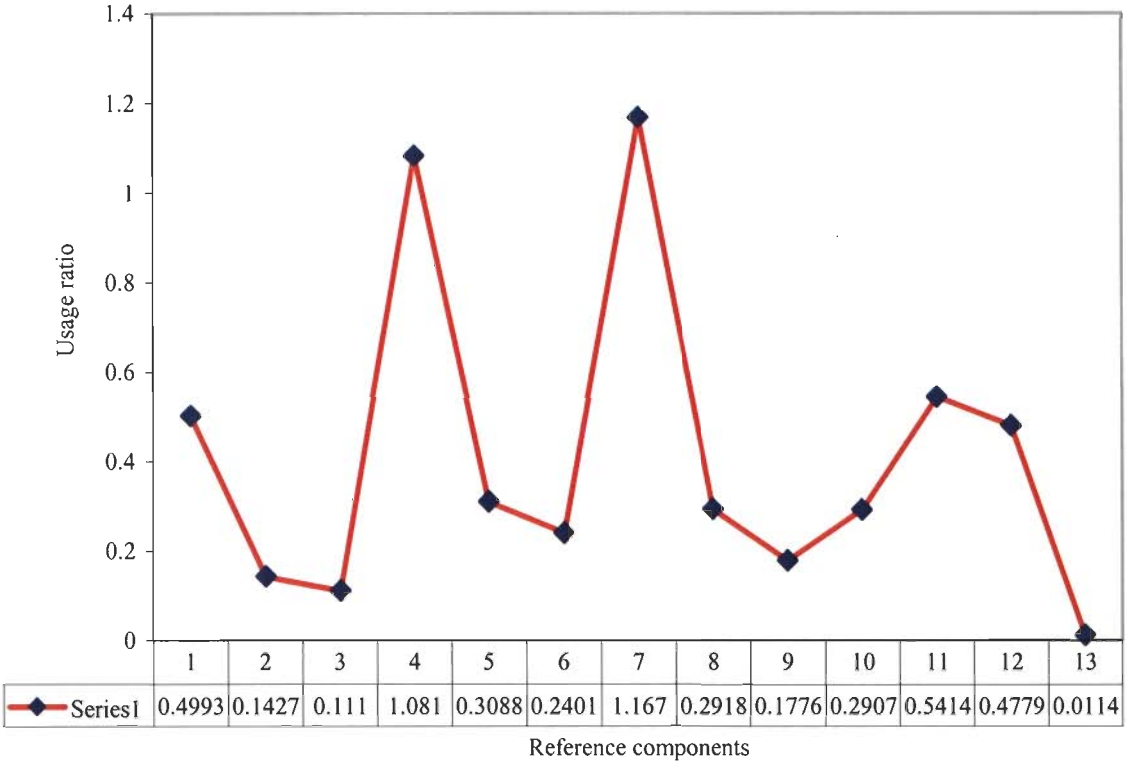

Figure 5.88: Usage ratios for 3story 3D frame under El Centro E-W (0.2148g)

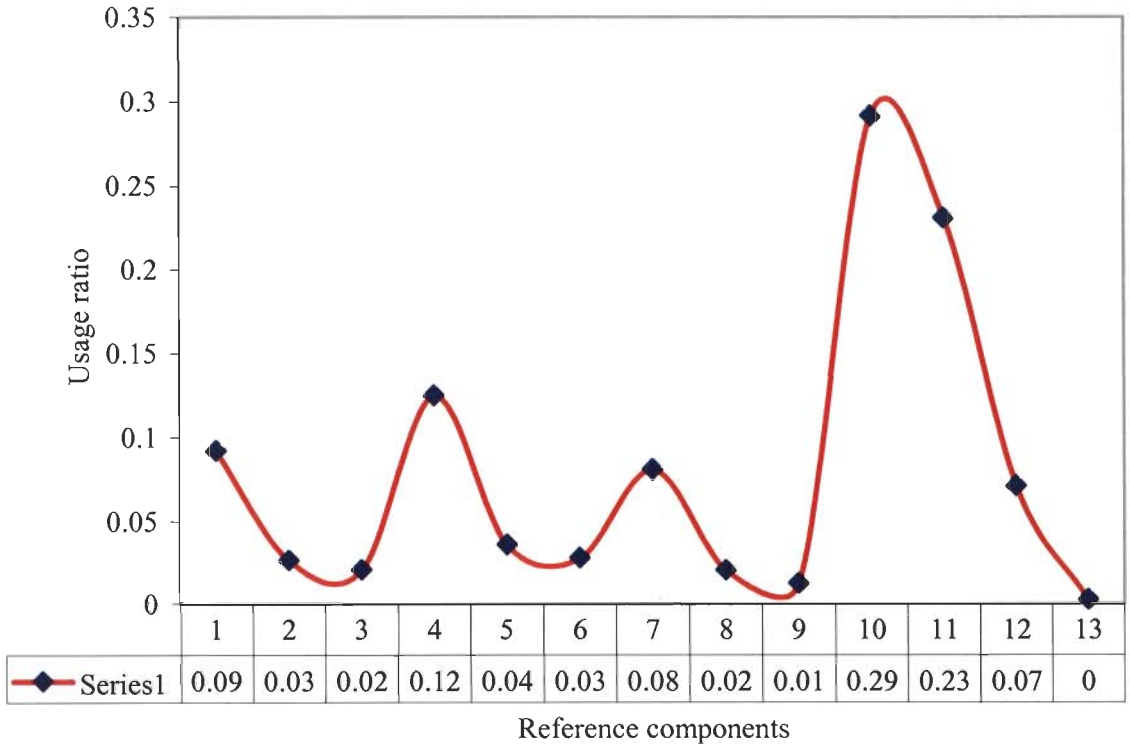

Figure 5.89: Usage ratios for 3story 3D frame under El Centro Up-Down (0.2052g)

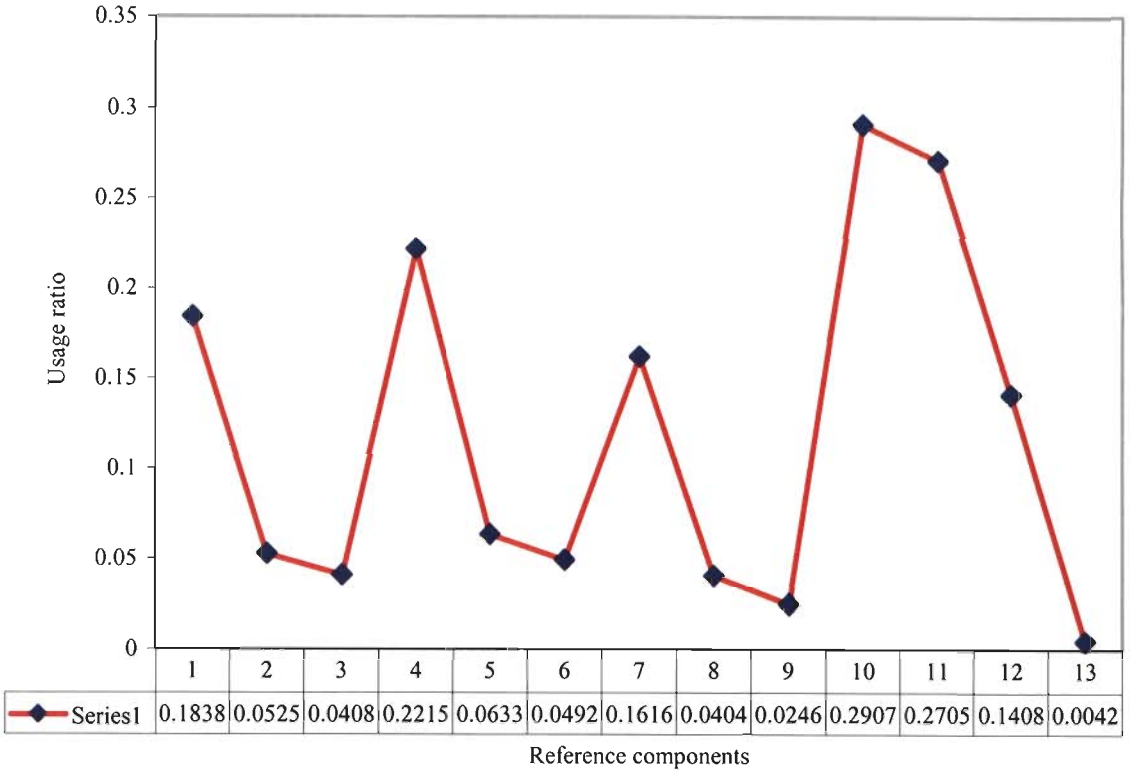

Figure 5.90: Usage ratios for 3story 3D frame under El Centro Up-Down (2x0.2052g)

Building frames used in the above reference have been modeled as components explained below:

Components 1: Usage ratio for perimeter column rotation, IO; **Components 2**: Usage ratio for perimeter column rotation, LS; **Components 3**: Usage ratio for perimeter column rotation, CP **Components 4**: Usage ratio for perimeter beam rotation, IO; **Components 5**: Usage ratio for perimeter beam rotation, LS; **Components 6**: Usage ratio for perimeter beam rotation, CP **Components 7**: Usage ratio for panel zone shear deformation, IO; **Components 8**: Usage ratio for panel zone shear deformation, LS; **Components 9**: Usage ratio for panel zone shear deformation, CP; **Components 10**: Usage ratio for beam bending strength; **Components 11**: Usage ratio for connector bending strength; **Components 12**: Usage ratio for H_1; **Components 13**: Usage ratio for H_2

Chapter 6

CONCLUSIONS AND RECOMMENDATIONS

6.1 Summary and Conclusions

The present study included the energy based seismic evaluation along with nonlinear static pushover procedures and recommended a set of results in terms of damage indices to assist performance based design procedures for moment resistant building frames in seismic regions. The research program was executed in four stages. The existing literature was reviewed (Chapter 2) and a gap was found for the formulation of the present study (Chapter 3). Chapter 4 discussed the modeling and analysis procedures used in the study. Investigation of the analysis results was the content of chapter 5. The following text summarizes each phase of study.

Assessment of performance based seismic design procedures with the conventional pushover curve was studied through developing capacity curve (Energy vs. displacement) using the response (Base shear vs. displacement). Evaluation of input seismic energy was given priority through steel building frameworks. Distribution of input seismic energy (demand) among its components (strain, kinetic and inelastic energy) along with flow of this energy at component levels was further investigated, since with the change of strain energy, the internal configuration of structural component is changed and became the source of disorderness of the structural system and hence the damages were likely for the higher values of such energy limit. Therefore, quantification of strain energy (elastic and as well as inelastic) remained the major task for a structural system during earthquake loading. Since energy approach has been recognized as more stable as the other methods, in spite of high randomness of ground motions. Incorporating normalized strength for normalization of hysteretic energy has been the main objective of performance identification as required for PBSD. Normalized yield strength with its further relation with ductility and strength reduction factor revealed the effect of higher ground motions which can be adjusted through the higher ductility with lower yield strength (Normalized SDOF system has been used in this regard), ductility was controlled through natural frequency, damping coefficient and normalized yield strength.

Chapter1 Introduced a general view of this study with the emphasis that energy based seismic evaluation would overcome many existing shortcoming procedures of performance based seismic design under the current practices.

Previous research on this subject was presented in Chapter 2. Motivation for the present study emerged during the study of the recent past developments in performance based design development. Thus, background of chapter 3 was based on the issues of PBSD, enumerated during the literature review in the chapter 2. Major documents [1, 2, 3, 38, 56, and 63] providing know how techniques of PBSD have been overviewed for the study during various stages of the present work. The main shortcomings of these two credentials are based on the components levels damage evaluation, [33, 64, and 65]; however, PBSD requires the damages at global levels. Emerging the new trends of PBSD to incorporate the damages in terms of death, damage and downtime payments, require explicit damage function in these parameters. While developing the background of chapter 3, a lot of consideration of this new situation has been kept into consideration in terms of demand and capacity evaluation under varying earthquake ground motions. Serviceability or functionality of a structure during and post earthquake evaluation are the main parameters, which control the overall performance of a structure in earthquake ground motions. Advantages of energy based seismic design approaches have been identified through the response analysis of steel building frames as the content of the present study. Modeling of building frameworks for nonlinear analysis were carried using the various elements available in Perform 3D and a set of the accelerograms in-built of this software. Nonlinear static pushover analysis for the prescribed base shears corresponding to varying performance levels were conducted on the building frames: 4.3.1, 4.3.2, 4.3.3, 4.3.4, and 4.3.5. The building frames considered for input seismic energy evaluation in the present study have been evaluated first for their seismic performance for assigned performance objectives from the guidelines of FEMA 273 [3]. The pushover analysis data have been used for energy based capacity curve formulations. Displacements corresponding to various performance levels have been used for estimation of energy ductility and energy correction factor for the consideration of the post-inelastic influence on the input seismic energy. Sequential hinge formation is identified through the energy displacement relation. Evaluation of input seismic energy (Tables 5.01 to 5.05, Figures 5.01 to 5.05) using some representative pseudo velocity spectra and energy correction factors takes into consideration of inelastic response building frames during severe earthquake ground motions. Input seismic energy among the structural components is identified through analysis results. A clear trend of energy dissipation in the desirable components is possible through nonlinear modeling (Tables 5.22 and 5.23). Hysteretic energy through yielding of columns and beams are employed for normalization, number of hysteretic loop determination using the

expressions derived in this study. Numbers of yield excursion cycles have the relation with severity of damages under the earthquake loadings as concluded from the observations of hysteretic loop and the time history analysis (Tables 5.32 to 5.33, Figures 5.55 to 5.75) are also investigated. The similarity of the input accelerogram, characteristics of hysteretic loop and the number of NYEC are found compatible. The severity of the ground motions through the structural behavior is clearly visible from their relations. Cross section of the critical members of the building frames, analyzed for nonlinear behavior, are observed for the adverse effects for severe demands arising due to severe ground motions (Figures 5.76 to 5.83). Effects on cross section under severe demand due to earthquake analysis predict the cross section characteristics for the progressive failure in terms of fiber behavior from the neutral axis of the section. Finally the applicability and practicality of the developed performance based seismic procedure for the steel building frameworks under seismic loading is shown through various damage indices. Usage ratio is found to satisfy the performance objectives assigned to the building frames. The following specific conclusions can be drawn from this study:

1. The developed expression for input seismic energy using the spectral velocity, energy correction factor is able to simultaneously account of medium building frame for post elastic effects, while a structure is under large earthquake.

2. Energy capacity curve derived from the conventional nonlinear static pushover is capable to reflect the sequential hinge formation. The curve reflects amount of released energy due to sequential formulations of hinge.

3. Energy distribution among the energy components (strain, kinetic and hysteretic energy) provides the characteristics of structure and structural components.

4. Energy distribution among structural components provides the basis of component design and the damage assessment at component levels. Distributed energy in normalized form are comparatively easy to diagnose the damage, therefore, identification and quantification of damages are possible.

5. Relations developed for floor spectra and inter story drift using the absolute energy concept are possible.

6. Relations developed for elastic strain energy and the hysteretic energy have the validation through the analysis results for the referred structural components.

A major contribution of this study is the development of energy based algorithm for performance base design of steel building framework under earthquake loading. In this regard, the study examines the influences of ground motion characteristics and structural properties on earthquake input energy and its distribution among energy components for five sets of building frames, using 8 accelerograms

The developed relation is capable to identify damage and damage based relations in terms of energy parameters at various performance levels. Investigation of input seismic energy, formulations of energy capacity curve, distribution of input seismic energy, normalization of the hysteretic energy with respect to input seismic energy and elastic strain energy, development of hysteretic and elastic strain energy relation, number of yield excursions, simplification of Park and Ang damage assessment through the introduction of local damage for global damage and assessment of the critical section under earthquake loadings have been investigated.

Conventional nonlinear static pushover analysis developed in the literature, load - control and displacement-control pushover analysis technique applicable for seismic loading for generation of significant data, for further use for plotting energy capacity curve. Energy capacity curve under the prescribed performance objectives formulated is compared with the conventional base shear plot in the same graph. While yielding takes place the base shear and displacement relation becomes almost elasto-plastic for steel structure. Sequential hinge formulations accompanied by strain hardening are not visible from base shear-displacement relations. However, energy-displacement relation is much more informative for the inelastic behavior including strain hardening with addition of hinges during the sequential loading.

Input seismic energy distribution among various energy components and among structural components is feasible in the present state of art. Identification of critical members through energy distributions including the quantum of energy is easy to control. Design algorithm or its further development using the energy at component levels is useful tool as identified in literature and the finding of this research program.

6.2 Recommendations for Future Work

Physical interpretation of performance levels corresponding to their specified seismic hazards through energy dissipation is the base of the present study. Energy based seismic design parameters have been found numerous applications in solving large scale damage identification through response analysis in the recent past. Considering how much computational techniques for evaluating energy demand and capacity through computer modeling and simulation to impact the seismic design procedures under earthquake loadings in future will be in practice, the design philosophy of PBSD is an integration of multidisciplinary knowledge of earthquake resistant design using the seismic risk and its corresponding acceptable damages in prescribed design format in order to take care of possible damages during varying ground motions to minimize socio economic (mitigation of seismic risk) post earthquake adverse impact. The following recommendations for future research are proposed to enhance or extend the capability of the developed technique for the seismic design under varying earthquake ground motions.

1. Development of realistic model of seismic demand evaluation. i.e., methods of input seismic energy must consider the soil-structure interaction, input energy attenuation with the dynamic condition of building frames.
2. Development of energy based capacity spectrum for the evaluation of performance check.
3. Explicit expression for identification of hinge development and the deterioration of the mechanical characteristic due to severity of the ground motions.
4. Sensitivity analysis of capacity curve (energy vs. displacement) through more conditions, since capacity curves are capable to quantify damages as sensitivity analysis to assist and to identify deterioration of mechanical characteristics evaluation (stiffness, strength and ductility).
5. Simplicity for identification and quantification of capacity of structure and structural components in terms of strain, kinetic and hysteretic energy.
6. Hysteretic energy distribution in terms of normalized formats taking the degradation of stiffness, strength and ductility are the various constraints or conditions for further investigation of performance based seismic design.
7. Investigation of number of yield excursions cycles for crack development at macro and micro levels. Hinge locking and opening during yield excursions require further

investigation for micro cracking, as the issue is more close to the fracture mechanics under inertial loading.

8. Development of explicit expression for energy based damage indices and performance attributes for using concrete or masonry structure.
9. Exchange of strain and kinetic energy is solely responsible for floor spectra and inter story drift interaction. During this research program limited response parameters have been used for the assessment of the typical issues related to PBSD. The issue of floor spectra may be studied exhaustively and a detailed study is still required with more and more types of the building structures.
10. Residual life of a structure after earthquakes may be estimated using the energy based evaluation, since hysteretic energy are cumulative and deducted from the energy capacity of the concerned structure. End condition of a structure after an earthquake becomes the initial condition of another event. Such boundary conditions formulations are easy from the energy based evaluation; however, it needs further investigation/study.

BIBLIOGRAPHY

[1] H. Krawinkler and G.D.P.K Seneviratna (1998), Pros and cons of a pushover analysis of seismic performance evaluation, Engineering Structures; Vol.20, No.4-6, pp.452-464.

[2] FEMA-283 (1996), Federal Emergency Management Agency, Performance Based Seismic Design of Buildings-An Action Plan for Future Studies, prepared by the Earthquake Engineering Research Centre, Washington DC, U.S.A.

[3] F. Naeim (2000), The Seismic Design Hand Book, Second Edition, Kluwer Academic Publishers, Boston, U.S.A, 2000.

[4] FEMA-349 (2000), Federal Emergency Management Agency, Action Plan for Performance Based Seismic Design, prepared by the Earthquake Engineering Research Centre, Washington DC, U.S.A.

[5] H. Krawinkler (1998), Issues and challenges in performance-based seismic design, Paper Reference: T178-3, Elsevier Science Ltd.

[6] P. Fajfar, Trends in seismic design and performance evaluation approaches. In: Proceedings of 11th European Conference on Earthquake Engineering, AA Balkema

[7] P. Fajfar, P. Gaspersic, D. Drobnic (1997), A simplified nonlinear method for seismic damage analysis of structures, in seismic design methodologies for the next generation of codes, Balkema, Rotterdam..

[8] P. Khashaee, B. Mohraz., F. Sadek., H.S.Lew and J.L. Gross (2007), Energy-based approach for seismic design: Energy spectra 2001 NISTIR 6599, Washington, D.C., U.S.A.

[9] M. Bruneau, N. Wang. (1996), Some aspects of energy methods for the inelastic seismic response of ductile SDOF structures, Engineering. Structure, Vol. 18, No1, pp. 1-12.

[10] IS:1893 (Part 1): 2002, Criteria for Earthquake Resistant Design of Structures, B.I.S. 2002, Manak Bhawan 9, Bahadur Shah Zafar Marg New Delhi 110002.

[11] P. Fajfar and H. Krawinkler (1997), Seismic Design Methodologies for Next Generation of Codes, Balkema, Rotterdam.

[12] FEMA-440 (2006), Federal Emergency Management Agency, Improvement of Nonlinear Static Seismic Analysis Procedures, Washington D.C, U.S.A.

[13] E. Rosenblueth (1980), Design of Earthquake Resistant Structures, Pentech Press, London, U.K.

[14] A. Hadjan (2002), A general framework for risk-consistent seismic design. Earthquake Engineering and Structural Dynamics, 31:601-626.

[15] A. Gregory. MacRae (99), Report No. SAC/BD-99/01, Parametric Study on the Effect of Ground Motion Intensity and Dynamic Characteristics on Seismic Demands in Steel Moment Resisting Frames, Department of civil Engineering, University of Washington, Seattle, Washington 98195-2700.

[16] FEMA-274 (1997), Federal Emergency Management Agency, NEHRP Commentary on the Guideline for the Seismic Rehabilitation of Buildings, Building Seismic Safety Council, Washington DC.

[17] AISC (1997), Seismic Provisions for Structural Steel Buildings, One East Wacker Drive Suite 3100, Chicago, Illinois 6060-2001

[18] PERFORM 3D (August 2006), Nonlinear Analysis and Performance Assessment of 3D Structures, User Guide, Version 4, Computers and Structures, Inc. 1995 University avenue Berkley, California 94704 USA.

[19] Chen W F, "Seismic Design of Steel Structures", Handbook of Structural Engineering", (C) 2003 by CRC Press LLC.

[20] Uniform Building Code (1985), International Conference of Building Officials, Whittier, California, USA.

[21] IS: 800(2007), Code of Practice for General Construction in Steel.

REFERENCES

[1] SEAOC Vision 2000 (1995), Performance-Based Seismic Engineering of Buildings, Vols. I and II: Conceptual Framework, Structural Engineers Association of California, Sacramento CA, U.S.A.

[2] ATC-40 (1996), Seismic Evaluation and Retrofit of Concrete Building. Volume 1, California, U.S.A.

[3] FEMA-273 (1997), Federal Emergency Management Agency, NEHRP Guideline for the Seismic Rehabilitation of Buildings, Building Seismic Safety Council, Washington DC, U.S.A.

[4] P. Fajfar (2000), A nonlinear analysis method for performance based seismic design, Earthquake Spectra, 2000; Vol. 16, No.3, pp. 573-592.

[5] M.M. Mazzolani (2002), Ductility of Seismic Resistant Steel Structures, Spon Press, New York, U.S.A.

[6] D.C. Rai (2000), Future trends in earthquake-resistant design of structures, Current Science, Vol. 79, No.9, 2000 (Special Section: Seismology 2000, pp. 1291-1300.

[7] Y. Gong (2003), Performance-based design of steel building frameworks under seismic loading. Ph.D. Thesis. Department of Civil and Environmental Engineering, University of Waterloo, Octario, Canada.

[8] H. Akiyama (1985), Earthquake-Resistant Limit State Design for Buildings, University of Tokyo Press, Tokyo, Japan.

[9] Y.J. Park and A.H. Ang (1985), Mechanistic seismic damage model for reinforced concrete, Journal of Structural Engineering, ASCE; 111:740-757.

[10] A. Surahman (2006), Earthquake resistant structural design through energy demand and capacity, Earthquake Engineering and Structural Dynamics; 36:2099-2117.

[11] S. Leelataviwat, W. Saewon, and S. C. Goel (2007), Energy based method for seismic evaluation of structures, SEAOC Convention 2007, September 26-29, Squaw Creek California, USA, 2007; pp. 21-31.

[12] G.W. Housner (1956), Limit design of structures to resist earthquakes, 1st World Conference on Earthquake Engineering, Berkley, California, U.S.A., pp. 5-1 to 5-13.

[13] Y. Bozorgnia and V.V. Bertero (2004), Earthquake Engineering from Engineering Seismology to Performance-Based Engineering, CRC Press, Washington DC, U.S.A.

[14] P. Prahlad, M. Shrikhande and P. Agarwal (2007), Performance-based seismic design using normalized hysteretic energy, 2007 SEAOC CONVENTION, September 26-29 Squaw Creek, California, USA, 2007; pp 473-487.

[15] P. Fajfar, T. Vidic, M. Fischinger (2005), On energy demand and supply in SDOF systems, Nonlinear seismic analysis and design of reinforced concrete buildings by P.Fajfar, Department of Civil Engineering University of Ljubljana, Slovenia and H. Krawinkler, Department of Civil Engineering Stanford University, U.S.A, Elsevier Applied Science London and New York.

[16] F.M. Mazolani (2000), Moment Resistant Connection of Steel Frames in Seismic Area. E and FN Spon, London, U.K.

[17] RAM Perform 3D, Version 4 (2006), Nonlinear Analysis and Performance Assessment for 3D Structures, Berkeley, Computer & Structures Inc., CA, U.S.A., 94704.

[18] A. Ghobarah, N.M. Aly and M. El-Attar (1997), Performance level criteria and evaluation. In: P. Fajfar and H. Krawinkler, Editors, Seismic Design Methodologies for the Next Generation of Codes, AA Balkema, Rotterdam; pp. 207–215.

[19] A. Gupta and H. Krawinkler (1999), Seismic demands for performance evaluation of steel moment resisting frame structures (SAC 5.4.3), John A. Blume Earthquake Engineering Research Center Rep. No. 132. Department of Civil Engineering, Stanford University.

[20] A. Whittaker, M. Constantinou, and P. Tsopelas (1998), Displacement estimates for performance-based seismic design, Journal of Structural Engineering, ASCE; pp.905-912.

[21] M. Saiidi and M.A. Sozen (1981), Simpler nonlinear seismic analysis of R/C structures, Journal of Structural Engineering Division, ASCE, 107, 937-952.

[22] J.R. Blume (1960), A reserve energy technique for the earthquake design and rating of structures in the inelastic range, Proceeding, World Conference on Earthquake Engineering, Tokyo, Vol. II.

[23] MJN. Priestly (2000), Performance-based seismic design 12th World Conference on Earthquake Engineering, Auckland, New Zealand; pp. 325-346.

[24] C.-M. Uang, V.V. Bertero (1990), Evaluation of seismic energy in structures, Earthquake Engineering and Structural Dynamics; 19(1), pp. 77-90.

[25] A.K. Chopra (2001), Dynamics of Structures: Theory and Applications to Earthquake Engineering, Second Edition, PHI Learning Pvt. Ltd, new Delhi, India.

[26] Y.J. Park, Ang, A.H., and Y.K Wen (1987), Damage-limiting a seismic design of buildings. Earthquake Spectra; 3(1), pp. 1-26.

[27] F. Zahrah and J. Hall William (1984), Earthquake energy absorption in SDOF structures. Journal of Structural Engineering, Vol. 110, No. 8, pp. 1757-1772.

[28] D.E. Hudson (1956), Response spectrum analysis in engineering seismology, 1st World Conference on Earthquake Engineering, Berkeley, California, U.S.A., pp. 4.1 to 4.12.

[29] G. Manfredi (2001), Evaluation of seismic energy demand. Earthquake Engineering Structural Dynamics, 30, pp. 485-499.

[30] A.K. Chopra and R.K. Goel (2002), A modal pushover analysis procedure for estimating seismic demands for buildings. Earthquake Engineering and Structural Dynamics, Vol.31, pp.561-582

[31] H. Krawinkler [1999], Challenges and progress in performance based earthquake engineering, International Seminar on Seismic Engineering for Tomorrow-In Honor of Professor Hiroshi Akiyama Tokyo, Japan, November 26, 1999, Department of Civil and Environmental Engineering, Stanford University, Stanford, CA 94305, U.S.A.

[32] D. Raul and V. Bertereo (2002), Performance-based seismic engineering: the need for a reliable conceptual comprehensive approach, Earthquake Engineering and Structural Dynamics, 31:627-652.

[33] ATC-58, Applied Technology Council, Framework for Performance Based Seismic Design of Nonstructural Components. Washington D.C., U.S.A.

[34] D. H. Lang, S. Molina-Palacios and C. D. Lindholm (2008), Towards near-real-time damage estimation using a CSM-based tool for seismic risk assessment, Journal of Earthquake Engineering; 12(S2):199–210.

[35] Y.A. Al-Salloum and T.H. Almusallam, (1995), Optimality and safety of rigidly and flexibly jointed steel frames, Journal of Constructional Steel Research, Vol. 35, No. 2, pp. 189-215.

[36] E. Cosenza, G. Manfredi and G. M. Verderame (2002), A new strategy for the seismic assessment of existing RC buildings, Annals of Geophysics, Vol. 45, No 6, pp 817-831.

[37] FEMA-445 (2006), Federal Emergency Management Agency, Next-Generation Performance-Based Seismic Design Guidelines, Program Plan for new Existing Buildings, Washington DC, U.S.A.

[38] FEMA 356 (2000), Federal Emergency Management Agency, Pre-stressed and Commentary for the Seismic Rehabilitation of Buildings Federal Emergency Management Agency, U.S.A. (2000).

[39] S.K. Jain, R. Sinha., D.C. Rai, J.N. Arlekar and R. Metzger (2002), Reinforced concrete structures, 2001 Bhuj, India earthquake reconnaissance Report, Earthquake Spectra July 2002, :Vol 18 Supplement A, pp.149-185.

[40] D.C. Rai, A. M. Prasad, S. K. Jain, G. Rao, P. Patel (2002), Hospitals and School. 2001 Bhuj, India earthquake reconnaissance Report, Earthquake Spectra, July, 2002: Vol 18 Supplement A, pp.265-277.

[41] S.K. Deb and D.K. Paul (1996), Simplified nonlinear analysis of base isolated building. Proc. of 11th World Conference on Earthquake Engineering, Acapulco, Mexico, 1996. Paper No. 1344 (CDROM).

[42] N. Subramanian (2008), Design of Steel Structures, Oxford University Press, Chennai, India.

[43] H.M. Enrique, O-S. Kwon, and M.A. Aschheim (2004), An energy-based formulation for first and multiple-mode nonlinear static pushover analysis, Journal of Earthquake Engineering; Vol 8, No. 1, 69-88.

[44] Extended 3D Analysis Building Systems (ETABS), Nonlinear Version 9.1, Berkley, Computer & Structures Inc., CA, U.S.A., 94704.

[45] K.J.Bathe (1997), Finite Element Procedures, Prentice Hall of India Pvt. Ltd. New Delhi-110001.

[46] P. Khasaee (2005), Damaged based seismic design of structures, Earthquake Spectra Volume 21, No. 2, pp.371-387.

[47] Powell, G.H. and Allahabadi, R. (1987), Seismic damage prediction by deterministic methods: concepts and procedures, Earthquake Engineering and Structural Dynamics 16, 719-734.

[48] R.S. Jangid and T.K. Datta (1996), Dissipation of hysteretic energy in base isolated structure, Journal of Shock and Vibration, Vol. 3, No. 5, pp. 353-359

[49] Fajfar P. (1992), Equivalent ductility factors, taking into account low-cycle fatigue. Earthquake Engineering and Structural Dynamics, 21(10):837-848.

[50] Lybas J. and Sozen M.A. (1977), Effect of Beam Strength and Stiffness on Dynamic Behavior of Reinforced Coupled Walls, Civil Engineering Studies, SRS No. 444, University of Illinois, Urbana, IL.

[51] W.E. McKevitt, D. Anderson, and S. Cherry (1980), Hysteretic energy spectra in seismic design, Proc. of the 2nd World Conference on Earthquake Engineering; Vol. 7, pp. 487-494.

[52] P. Prahlad, M. Shrikhande and P. Agarwal (2005), Performance-based seismic design using energy method, Earthquake Disaster: Technology and Management MN NIT, Allahabad, February, 11-12, pp. III-18 -21.

[53] P. Prahlad, M. Shrikhande and P. Agarwal (2005), Issues and challenges of performance-based seismic design of steel building framework, International Conference on Earthquake Engineering, SoCE, SASTRA, Deemed University Thanjavur Taminadu, India, February 25-26, pp. 110-123.

[54] R.W. Clough, J. Penzien (1975), Dynamics of Structures, McGraw-Hill, New York, U.S.A.

[55] FEMA-350 (2000), Federal Emergency Management Agency, Recommended Seismic Design Criteria for New Steel Moment-Frame Building, Federal Emergency Management Agency, Washington D.C. U.S.A.

[56] R. Hassan, L. Xu, and D.E. Grierson (2002), Pushover Analysis for Performance-Based Seismic Design, Computers and Structures, Vol.80, Issue 31 December, pp.2483-2493.

[57] Englekirk (2003), Steel Structures Controlling Behavior through design, John Wiley and Sons, Inc., New York, U.S.A.

[58] Velestos A.S., Newmark N. M., and Chelapati C.V. (1965). Deformation Spectra for Elastic and Elastoplastic Systems.

[59] Newmark N. M, and Hall W.J. (1982). Earthquake Spectra and Design, EERI, Berkley, CA, USA.

[60] P. Prahlad, M. Shrikhande and P. Agarwal (2006), Performance-based seismic design of steel building framework using parametric study, STESSA2006, held at Yakohama, Japan, 14-17th August 2006; pp. 79-84

[61] A. Rutenberg, P.C. Jennings and G. W. Housner (2006), The response of veteran hospital building 41 in the Sab Fernado earthquake, Earthquake Engineering and Structural Dynamics; Vol.10 issue 3, pp. 359-379.

[62] P. Prahlad, M. Shrikhande and P. Agarwal (2005), Performance-based seismic design of steel building frameworks, The Structural Engineering Convention (SEC 2005), IISc. Bangalore, Dec. 14-16, 2005, pp. CD ROM-420.

[63] S. Leelataviwat, S.C. Goel, and B. Stojadinovic (1999), Toward performance-based seismic design of structures, Earthquake spectra; 15(3), pp. 435-461.

[64] P. Prahlad, M. Shrikhande and P. Agarwal (2005), Performance-based seismic –An Overview, The Structural Engineering Convention (SEC 2005), IISc. Bangalore, Dec. 14-16, 2005, pp. CD ROM-421.

[65] P. Prahlad, M. Shrikhande and P. Agarwal (2007), Parametric study of performance-based seismic design National Seminar on Infrastructure Development in Jharkhand, 28th October, 2007, MECON Community Hall Shyamli, Ranchi, pp. 27-33.

List of Publications of Author Related to the Thesis Work

International Conferences

1 Prasad Prahlad, Shrikhande Manish and Agarwal Pankaj, "Performance-Based Seismic Design of Steel Building Framework Using Parametric Study", STESSA2006, held at Yakohama, Japan, 14-17th August 2006, pages 79-

2 Prasad Prahlad, Shrikhande Manish & Agarwal Pankaj, "Performance-Based Seismic Design Using Normalized Hysteretic Energy", 2007 SEAOC CONVENTION, Sptember 26-29 Squaw Creek, California, USA, pages 473-487.

3 Prasad Prahlad, Shrikhande Manish & Agarwal Pankaj, Issues and Challenges Performance-Based Seismic Design of Steel Building Frameworks", International Conference on Earthquake Engineering, February 25-26, SoCE, SASTRA, Deemed University Thanjavur Taminadu, India, February 25-26, pages 110-123.

4 Two Abstracts accepted for European Conference, 2010,

(i) Performance Based Seismic Design Using Normalized Hysteretic Energy,

(ii) Performance Based Seismic Design of Steel Building Frameworks in India.

National Conferences/ workshops/symposiums, etc.

1 Prasad Prahlad, Shrikhande Manish & Agarwal Pankaj, Performance-Based Seismic Design of Steel Building Frameworks, The Structural Engineering Convention (SEC 2005), IISc. Bangalore, Dec. 14-16, 2005, pages CD ROM-420.

2 Prasad Prahlad, Shrikhande Manish and Agarwal Pankaj, Performance-Based Seismic –An Overview", The Structural Engineering Convention (SEC 2005), IISc. Bangalore, Dec. 14-16, 2005, pages CD ROM-421.

3 Prasad Prahlad, Shrikhande Manish and Agarwal Pankaj, Performance-Based Seismic Design Using Energy Method, Earthquake Disaster: Technology and Management" MN NIT, Allahabad, February, 11-12, pages III-18 -21.

4 Prasad Prahlad, Parametric Study of Performance-Based Seismic Design National Seminar on Infrastructure Development in Jharkhand, 28th October, 2007, MECON Community Hall Shyamli, Ranchi, pages 27-33.